Characterization of the Multidomain Nsp2 Replicase Protein of Porcine Reproductive and Respiratory Syndrome Virus

A DISSERTATION

SUBMITTED TO THE FACULTY OF THE GRADUATE SCHOOL

OF THE UNIVERSITY OF MINNESOTA

BY

Jun Han

IN PARTIAL FULFILLMENT OF THE REQUIREMENTS

FOR THE DEGREE OF

DOCTOR OF PHILOSOPHY

Kay S. Faaberg, Ph.D., Advisor

Mark S. Rutherford, Ph.D., Co-advisor

December 2008

Acknowledgements

This thesis would not have been possible without the help and support of my advisors Dr. Kay S. Faaberg and Dr. Mark S. Rutherford. I owe a great deal of gratitude and appreciation to them for their guidance, patience, encouragement and generosity throughout my graduate career. I am fortunate to have such great mentors in my life, and they taught me not only how to conduct thoughtful research, but also critical thinking. They granted me much freedom to do the research I am very interested in. They are so open and supportive, and they allowed me to make mistakes and learn lessons from these mistakes, which in turn makes me into a better independent researcher. I also would like to extend my gratitude to my thesis committee members: Dr. Thomas Molitor, Dr. Peter J. Southern and Dr. Kathleen Conklin. They all contribute greatly to the success of my dissertation research.

I thank members from Faaberg/Rutherford lab and appreciate their helpful academic discussions and great friendship: GongPing Liu, Yue Wang, Hong Liu, Yin Jiang, Julie Hendrickson, Kyra Martins, Jin Liu, Shinichiro Enomoto, Cheryl Lancto, and Mary Mauzy.

I'd like to thank my grandmother, parents and sisters for their unwavering support of me these years. Without them, I would not be here today. In addition, I thank my wife, Dan Zhang, for her support and understanding throughout my Ph.D study. Finally, I thank my daughter Nancy for bring me so much fun and joy besides science.

Abstract

This dissertation focused on understanding the biology of the nonstructural protein 2 (nsp2) of porcine reproductive and respiratory syndrome virus (PRRSV), the etiological agent of porcine reproductive and respiratory syndrome (PRRS). PRRSV nsp2 is a multidomain protein, containing a putative N-terminal cysteine protease PL2 domain, a 500-700aa middle region of unknown function, a transmembrane domain and a C-terminal tail with uncertainty. In this dissertation, we report the following. (i) PRRSV nsp2 is undergoing rapid evolution in field strains exemplified by viral isolates MN184A and B. (ii) We showed that PRRSV nsp2 hypervariable regions aa12-35 and aa324-813 were not essential for viral replication in MARC-145 cells by using a reverse genetics system based on strain VR-2332. In contrast, deletion of the cysteine protease PL2 core domain, the PL2 downstream flanking sequence (aa181-323), the predicted transmembrane domain and the C-terminal domain were lethal to the virus. (iii) We provided evidence that the nsp2 protein encodes an active PL2 protease and mediates nsp2/3 processing in CHO cells with a substrate preference for the dipeptide $G^{1196}|G^{1197}$. The PL2 protease possessed both *trans*- and *cis*-cleavage activities, which could be distinguished by point mutations. Site-directed mutagenesis studies revealed that mutations that caused a specific loss of *trans* function of the PL2 protease, but not *cis* activity, were detrimental to the virus. In addition, we showed that the conserved aspartic acid residues (e.g., Asp^{89}) played an important role in the PL2 *trans*-cleavage activity. (iv) We investigated the proteolytic processing of nsp2 in MARC-145 cells using recombinant PRRSV expressing foreign epitope-tagged nsp2 protein. We showed the presence of the nsp2 protein as different isoforms in PRRSV-infected cells, which appeared to share the same N terminus but differed in their respective C-termini. The nsp2 species emerged almost simultaneously in the early stage of PRRSV infection, were stable and had low turnover rates. Deletion mutagenesis suggested that the smaller nsp2 species (e.g. nsp2d, e and f) were not essential for viral replication in cell culture. Lastly, a cellular protein, heat shock 70kDa protein 5 (HSPA5), was identified as a coimmunoprecipitate of nsp2.

Table of Contents

Chapter III: Identification of Nonessential Regions of the Nsp2 Replicase Protein of PRRSV Strain VR-2332 for Replication in Cell Culture

Chapter IV: Characterization of the Putative Cysteine Protease PL2 Domain Encoded in the N-terminus of PRRSV Nsp2 Replicase Protein

List of Tables

List of Figures

Chapter I

General Introduction

PRRS problem

Porcine reproductive and respiratory syndrome (PRRS) is currently one of the most economically devastating swine diseases in the U.S. and other swine-producing countries in the world. Reproductive failure (e.g., mummy, stillborns and abortions) in sows and respiratory distress (e.g., interstitial pneumonias) in young pigs are the most common clinical manifestations (65, 66, 193). The disease emerged almost simultaneously in Europe and North America in the late 1980's, initially termed as mystery swine disease (MSD), swine infertility respiratory syndrome (SIRS) and porcine epidemic abortion and respiratory syndrome (PEARS) (17, 41, 70, 99, 110, 247, 249, 264), and then spread quickly to other parts of the world.

The etiological agent of PRRS is porcine reproductive and respiratory syndrome virus (PRRSV) (37, 41, 151, 248), a small, enveloped, positive-stranded RNA virus with a genome size of ~15.4kb (3, 42, 152, 162). The virus belongs to the family *Arteriviridae* along with equine arteritis virus (EAV), murine lactate dehydrogenase elevating virus (LDV), and simian hemorrhagic fever virus (SHFV), and is classified as part of the newly established order *Nidovirales* together with the coronaviruses (29). Two genotypes of PRRSV strains have been categorized based on genetic differences: European PRRSV (Type I) and North American PRRSV (Type II). The Lelystad strain (LV) is the prototype of European PRRSV and strain VR-2332 is the foremost representative of the North American lineage (3, 148, 151, 162). PRRSV has a limited host range and pigs are the only natural host. The virus replicates predominantly in porcine macrophages (50, 100, 157, 215, 278). PRRSV infection mainly occurs through direct contact, aerosol, semen or vertical dissemination (38, 55, 78, 86, 117, 119, 149, 165, 173, 174, 225, 230, 243, 255).

The past 20 years have seen numerous PRRS endemic and pandemic outbreaks worldwide. Particularly, the virulent strains exemplified by Type II JA142 strains, MN184 strains and Type I European-like PRRSV caused severe disease in the swine

farms in the U.S. Midwest (75, 77, 192). In Asia, PRRSV contributes to large-scale outbreaks of swine high fever disease that swept throughout China in 2006-2007, leaving more than 300 million pigs affected with a high fatality rate of 20-30% (80, 222, 224, 275). The disease, called atypical PRRS, differed from conventional PRRS in clinical symptoms that are manifested as high fever (40-42°C), petechiae and erythematous blanching rash in ears, mouth, snout, back and inner thigh, and pregnant sows and adult pigs died as a result of the infection (80, 222, 224, 275).

Properties of PRRSV Infection

(i) *Persistent infection.* Following an acute infection of about one month, PRRSV successfully establishes a persistent infection with durations of 3-6 months that mainly reside in secondary lymphoid tissues (2, 10, 121, 160, 198, 254). Pigs infected with PRRSV can be long-term carriers and shed the virus at a low level to infect naïve pigs (2, 10, 121, 198, 254, 256). It is becoming clear that subclinical persistent infection of a herd contributes considerably to the uncontrolled spread of PRRSV and is the major impediment to the successful control of PRRS disease.

(ii) *Disregulation of host immunity*. PRRSV appears capable of subverting or evading host immunity. PRRSV infection fails to trigger a strong innate immune response that is always the key for successful control or clearance of pathogens (1, 135, 155, 236), resulting in severe suppression of genes involved in intrinsic immunity. The induction of INFα/β expression, a characteristic response to viral infection, is usually minimal in PRRSV infection both *in vivo* and *in vitro* (1, 135, 155, 236). The production of inflammatory cytokines such as IL-1 and IL-6 is also low (34, 236, 237). As for adaptive immunity, antigen specific antibodies are generated in the early stages of virus infection, usually at about 7-10 days post-infection, but are non-protective (163, 266). Neutralizing antibodies begin to appear only slowly 4-8 weeks post-infection with considerably low titers, a time point that the virus titer in peripheral blood has already begun going down at the end of the acute infection (83, 146, 146, 180, 265). The role of neutralizing antibodies in eliminating or preventing PRRSV infection has been in debate although some protective effects were observed against homologous infection by passive transfer (62, 133, 134, 171). In terms of cell-mediated immunity, the interferon gamma

(INF-γ) production is delayed and maintained at a low level, and T cell responses have not been convincingly linked to short term immune responses, but rather to eventual clearance of the virus from host tissues (11, 11, 13, 61, 62).

(iii) *Genetic variation*. The PRRSV genome has been undergoing broad genetic variation since it was first characterized (51, 109, 147, 159, 181). The North American PRRSV strains (NA) differ from European PRRSV strains (EU) by a 30-40% difference at the nucleotide level (3, 162). Even within genotypes, the difference may range from 0 to 20% percent. In particular, the coding regions for segments of the genome known as nonstructural protein (nsp) 1β, nsp2 and ORF5 have considerably high mutation rates (3, 75, 80, 101, 181, 192, 206). The continuous evolution of the PRRSV genome has led to the emergence of new strains with different antigenicity that might increase the fitness of the virus *in vivo*. The mutations in ORF5 that encodes the viral attachment molecule might change the antigenicity of the protein and help the virus escape neutralizing antibodies. Extensive naturally occurring mutations are the bottleneck for traditional vaccines, especially against heterologous PRRSV infection (20, 26, 120, 142, 170, 203, 204).

PRRSV Genome Structure

PRRSV shares the common features of nidoviruses in terms of genome organization, transcription and gene expression strategies (84, 208)**.** The virus genome contains a cap structure and a poly(A) tail at the respective 5' and 3'end (162, 177). The genome includes untranslated regions at 5' and 3' termini that contain *cis*-acting signals for genome replication and transcription (35, 177, 241). The open reading frames (ORFs) vary in and between the families of the *Nidovirales*. The two 5' largest ORFs, ORF1a and lb coding for the viral replicase, occupy two-thirds to three quarters of the PRRSV genome. ORF1b is translated by a -1 ribosomal frameshift mechanism directed by a ribosomal frameshift signal (RFS) at the overlap area of ORF1a and ORF1b (208). The translated multidomain precursors polyprotein 1a and lab (pp1a, pp1ab) undergo a maturation process that generates multiple nonstructural protein subunits (208, 277). Structural proteins are encoded by ORF2-7s in the 3'-end of viral genome. The order for the structural proteins of arteriviruses is GP2/E-GP3-GP4-GP5-M-N, while in

coronaviruses is S-E-M-N. Several accessory genes are located between S and E or between M and N protein in coronaviruses (84).

PRRSV virions are spherical particles with a diameter of 50-60nm consisting of a putative icosahedral core surrounded by an envelope (17, 53, 138). The capsid is formed by the 14kD nucleocapsid protein (N) subunits that package the 15kb viral genome via interaction with a yet unidentified packaging signal located in ORF1a coding region (52, 272). In the envelope, up to seven structural proteins including GP2a, E (GP2b), GP3, GP4, GP5, M and N have been identified and shown to be the components of the virions of European PRRSV (153) (52, 154, 235, 259, 260). The 17kD M protein is a non-glycosylated Type III membrane protein with a N-terminal ectodomain of 16aa, three transmembrane domain helices and a 78aa C-terminal endodomain (154). The 25kD glycosylated GP5 is predicted to have a N-terminal signal sequence of approximately 30aa, followed by a 35aa ectodomain, a hydrophobic region of about 60aa and a 70aa endodomain (52). M, N and GP5 constitute the major structural proteins, which are abundant in viral particles. The remaining proteins, GP2a, E, GP3 and GP4, are minor constituents at low abundance in virions, of which only E is non-glycosylated (52, 154). GP3 occupies a unique position and is a component of EU PRRSV virions (235), whereas for NA strains the protein was reported to be a soluble, secreted protein (82, 139).

GP5 and M proteins form a disulfide-linked heterodimer, presumably occurring between cysteine residues at positions 50 and 8 respectively (140), which has been demonstrated to be crucial for viral assembly, whereas the minor glycoproteins are not necessary (257). However, Type I PRRSV is noninfectious without the incorporation of the minor structural proteins (257), consistent with an earlier report that ORF2a/b or ORF4 products are essential for a North American strain of PRRSV since mutant genomes from which the ORFs have been deleted did not generate infectivity (246). A similar situation was observed in EAV, where incorporation of either of the minor proteins depended on all the other minor proteins, suggesting that these proteins interact with each other (251-253).

PRRSV Replication

PRRSV has a restricted host range and replicates predominantly in porcine

macrophages *in vivo* (50, 100, 157, 215, 278). Several cell lines, including the African green monkey kidney cell line MA-104 and its subclone MARC-145, as well as hamster cell line BHK-21 support PRRSV replication *in vitro*, however the latter does not support virus entry (12, 111, 150). Virus entry involves an initial nonspecific attachment to cells, which brings into close proximity the virion particles and specific receptors. Heparin sulfate on the surface of macrophages was shown to serve as the initial attachment molecule and sialoadhesin appeared to be the viral receptor (56-59, 239, 240). However, a different group demonstrated that porcine CD163 conferred susceptibility of nonpermissive cells to PRRSV infection (25). It has been postulated that the GP5-M heterodimer is involved in the receptor recognition. Neutralizing epitopes were mapped to the ectodomain of GP5, and some in GP4 (172, 183, 184, 258). However, chimeric viruses using EAV as backbone with the ectodomain of GP5 coming from PRRSV or LDV were viable and still could infect BHK-21 and RK-13 cells but not by PRRSV or LDV (7, 262), suggesting that GP5 might not be the only determinant for viral tropism and questioning a decisive role of GP5 in the virus invasion. Similarly, replacement of the ectodomain of PRRSV M protein by that of other arteriviruses also did not change PRRSV tropism (7, 262).

PRRSV binding to its receptor triggers viral penetration. The subsequent endocytosis appears to be clathrin-mediated (116). Several pieces of evidence showed that PRRSV entry is pH-dependent and requires acidification, suggesting that the entry most likely occurs through the endocytic secretory pathway (116, 161). Following membrane fusion and capsid disassembly, the PRRSV genome is released into cytoplasm and initiates immediate translation of ORF1a/b to generate pp1a and pp1ab. The subsequent proteolytic processing of replicase polyproteins is essential to the PRRSV replication. The polyproteins have to be correctly and efficiently cleaved and regulated in order to generate mature nonstructural protein subunits (nsp), which are critical for correct trafficking and assembly of viral replication complexes, and maybe for antagonizing host anti-viral responses. Arterivirus replicase maturation is fulfilled by virus-encoded proteases located in nsp1, nsp2 and nsp4 (277), and has only been extensively investigated in EAV (212, 245). Processing of PRRSV pp1a starts with the N-terminal

auto-processing of nsp1 by papain-like cysteine protease α and β (PCPα and PCPβ) while the PCPα domain is inactive in EAV (60, 210). A cysteine protease PL2 is predicted in the N terminus of the nonstructural protein 2 (nsp2) of PRRSV. In EAV, the PL2 counterpart has been shown to cleave at the site between nsp2 and nsp3 (213), and the picornavirus 3C-like protease (3CLpro) encoded by nsp4 is responsible for processing the remainder of ORF1a and ORF1b into nsp3-12 (214, 233, 234). In coronaviruses, nsp3 codes for papain-like proteases (PLP1, PLP2). Papain like protease 1 (PLP1) is responsible for processing nsp1 and nsp2 and PLP2 is believed to cleave the site at nsp3|nsp4 to release main protease 3CLpro, while SARS-CoV and group 3 coronaviruses encode only one accessory protease (PLP2) responsible for the maturation of the N-terminal nsp1, nsp2 and nsp3 (66, 215).

Processing of arterivirus ORF1b generates four putative domains which are conserved and have been found in all nidoviruses (84, 277): RNA dependent RNA polymerase (RdRp) (14), zinc binding domain (ZBD) (14, 143), helicase (HEL) and endoribonuclease U (XendoU) (103, 186, 205). Another two recently identified domains, 3'-to-5' exoribonuclease (ExoN) and the ribose-2'O-methyltransferase (O-MT) (32, 54, 156), are only present in coronaviruses and indispensable for viral RNA synthesis and the production of virus progeny in HCoV-229E and SARS-CoV.

The mature nsps from proteolysis are transported to proper intracellular compartments to form what are referred to as viral replication complexes. Viral replication carried out through cytoplasmic RNA-dependent RNA synthesis involves virus-modified host intracellular membranes that could be of many origins. Characteristic double membrane vesicles (DMVs) are always seen in nidovirus-infected cells (208). Cryoimmunoelectron microscopy of EAV and mouse hepatitis virus (MHV) infected cells revealed structures consisting of typical DMVs containing nonstructural proteins and *de novo* made viral RNAs (85, 179, 231). EAV DMVs probably originate from paired endoplasmic reticulum membranes and could be induced by heterologous expression of nsp2-nsp3, independent of RNA synthesis (179, 209). EAV nsp2 is also involved in targeting viral replication complexes to endoplasmic reticulum (ER) and the hydrophobic membrane domain may serve as membrane anchor, along with nsp3 and

nsp5, which have several hydrophobic domains (209, 232). MHV DMVs are derived from endosomal membranes and viral replicase proteins were found on the surface of DMVs (231). Similar DMV-like structures of unknown origin were also found in PRRSV infected cells (208).

Expression of PRRSV structural protein genes is fulfilled through a discontinuous transcription mechanism (135), which generates a 3' coterminal nested set of subgenomic RNAs containing a short 5' leader sequence derived from the 5' end of the viral genome (208). The transcriptional regulatory sequences (TRSs) located both upstream of ORF1a and immediately upstream of each of structural ORFs, are thought to regulate transcription of the subgenomic RNAs (sgRNAs) (177, 228, 229). The leader TRS is joined at a body TRS by a discontinuous transcription mechanism, taking place during the synthesis of negative-stranded sgRNAs (176, 177, 177, 229). The subgenomic RNAs are polycistronic but only the first ORF is translated, except in the case of GP2 and E (177). It is not clear how the viral RdRp differentiates viral subgenomic RNA synthesis from genomic RNA replication, and coordinates these two events.

In the late stage of replication cycle, PRRSV assembles itself from simple subunits to complex structures to ensure reproductive success. The crucial steps include formation of multi-subunits of capsid from individual nucleocapsid protein molecules, packaging of the nucleic acid genome, acquisition of a lipid bilayer, incorporation of viral structural proteins and release of newly assembled progeny virions, which are done in a very delicate and coordinated order. PRRSV budding appears to occur in ER (52, 53, 138). Release of PRRSV virions into extracellular space involves a process of exocytosis and/or direct lysis of virus-infected cells.

Virus-Encoded Proteases of Positive-Stranded RNA Virus

Proteolytic maturation of virus-encoded polyproteins is a critical step in the replication cycle of positive-stranded RNA viruses, and usually involves one or more proteases that could be of host or virus origin. In most cases, virus-encoded proteases function in the early stage of the virus replication cycle and carry out the proteolysis by either *cis* or *trans*-cleavage, or both. Four classes of proteases have been classified based on the nature of catalytic sites (68): serine (Ser, S), cysteine (Cys, C), or aspartic (Asp, D)

(acidic) proteases, and metalloproteinases, the last of which has not been identified in viruses.

The retrovirus proteases are located either in the C-terminus of the *gag* polyprotein precursor or at the N terminus of the *pol* precursor, and possess the typical Asp-Thr (Ser)-Gly catalytic motif (68, 69). One prominent feature for retroviruses to differ their cellular counterparts is that the retrovirus proteases must form a homodimer to be active rather than formation of a two-domain protein by single polypeptide chain folding (188). Many positive-stranded RNA viruses, on the other hand, encode serine and serine-like proteinases as the main proteinases with a signature catalytic triad of His-Asp-Ser/Cys (199, 200, 220, 276, 277). These enzymes include the capsid protease of alphaviruses, the NS3 proteases from *Flaviviridae*, the 2A and 3C proteases from *Picornaviridae* as well as the 3C-like proteases from *Nidovirales*. Although the catalytic triad of serine proteinases is conserved among viruses, a wide range of variability in cleavage site specificity and cofactor requirements have been shown [for reviews, see references (68, 199, 200, 220, 277)]. The cysteine proteinases are another large class of enzymes found in viruses, which have a catalytic dyad composed of Cys and His residues in close proximity. Examples include alphavirus nsp2, aphthoviruses leader protein, potyvirus HC-pro, pestivirus p20, coronavirus papain-like proteinase PLP1 and PLP2, and arterivirus PCPα and PCPβ as well as cysteine proteinase 2 (PL2).

Positive-stranded RNA viruses utilize different strategies to regulate viral gene expression. Picornaviruses encode all of their proteins in a single long ORF. The proteolytic processing is mediated by three different viral proteinases, with some activities encoded by only a subset of the different viruses. The 3C has two forms: 3C and 3CD. Complete processing of the poliovirus capsid protein P1 requires 3CD whereas the P2 and P3 are processed by either 3C or 3CD (107, 267, 268). However, 3CD is not needed for P1 processing in encephalomyocarditis virus, foot-and-mouth disease virus and hepatitis A virus in which the 3C proteinase alone could fulfill the requirement (40, 96, 175). The 2A protein of enteroviruses and rhinoviruses cleaves at its own N terminus to release the P1 from the P1-P2-P3 polyprotein precursor (199), which is shown to be very rapid and cotranslational (226). In contrast, the 2A protease equivalent of

cardiovirus and aphthovirus subgroup cleaves at its C terminus to generate a P1-2A polyprotein intermediate, and the 3C protease then cleaves at the N terminus of the 2A protein to generate the P1 polyprotein.

Proteolytic processing of alphavirus polyproteins entails the nsp2 protease, a multidomain protein with a size of about 90kDa (63, 95). The nsp2 encodes a helicase and a cysteine protease in its N-terminus and middle region, respectively (81, 95, 191). The sindbis virus nsp2 protease has been characterized in some detail (46, 49, 94, 122, 123, 201, 202, 207, 244). The nsP123 polyprotein is the major translation product from the incoming genome RNA while the nsP1234 polyprotein exists at a minor mount generated by a frameshift mechanism. The kinetics of cleavage of the nsP123 polyprotein is variable for each site, and the processing pathways are quite complicated. Basically, initial processing at the nsP3/4 junction site prompts the synthesis of negative-stranded genome RNA, while further processing at the nsP1/2 junction ensures genomic RNA synthesis. A complete processing of polyprotein nsP1234 is critical for subgenomic RNA transcription, which in turn inhibits the negative-stranded RNA synthesis. Expression of the nsPs of Semliki Forest virus (SFV), a closely related alphavirus, is a little bit different from that of Sindbis virus. The stop codon between nsP3 and nsP4 is replaced with a sense codon, and an nsP1234 polyprotein is synthesized (216). Takkinen *et al*. proposed that nsP4 has an aspartic-type proteolytic activity and is responsible for releasing the nsP4 protein from the polyprotein (217). The remaining cleavage of nsP123 is mediated by the nsp2 cysteine- proteinase (218).

Viruses within the *Flaviviridae* (the flavi-, pesti- and hepatitis C viruses) use a combination of host and viral proteases to process the polyproteins (200). The host cell signalases act on multiple sites within both the structural protein and nonstructural protein coding regions while the remainder of the cleavages is fulfilled by the viral NS3 protein (200). The cleavage activities of the flavivirus NS3 protease depend upon a hydrophobic NS2B cofactor, which could be provided in either *cis* or *trans* (4, 24, 30, 31, 74, 128). The viral NS2B-NS3 protease cleaves at the junction sites of NS2A/NS2B, NS2B/NS3, NS3/NS4A, and NS4B/NS5 as well as at the internal sites within NS2A, NS3, and NS4A (200). However, for pestiviruses and hepatitis C virus, an enhanced NS3

activity requires NS4A instead of NS2B (71, 72, 104, 114, 127, 166, 219, 223). The cofactor activity of NS4A is mapped to a short oliopeptide sequence within the center of NS4A (23, 223).

Unlike other positive-stranded RNA viruses, the structural proteins of nidoviruses are expressed via individual subgenomic RNAs and do not need further maturation via proteolytic processing (277). The processing of the replicase polyproteins of nidoviruses is mediated by virus-encoded accessory and main proteinases (277). Although the accessory proteases among nidoviruses share a similar catalytic signature of a Cys-His dyad, there are some differences between coronavirus and arterivirus papain-like proteinases: (i) The arterivirus PCPα and PCPβ cotranslationally process their immediate downstream sites in *cis* and don't possess *trans*-cleavage activity (60, 60, 210), whilst the coronaviruses PL1 and PL2 possess both *cis*- and *trans*-cleavage activity and process at distant upstream sites (6, 18, 67, 98, 93, 108, 126). (ii) The arterivirus papain-like proteinases are much smaller than the coronavirus counterparts and the region separating the Cys-His dyad for coronaviruses is twice as long as that of arterivirus papain-like proteinases. In addition, the C-terminal domain of the coronavirus papain-like proteinase has additional ubiquitinating enzymatic activity and has the capability to target the proteins for proteosomal degradation (9, 129). The proteolytic activities of coronaviruses papain-like proteinases (PL) have been extensively studied *in vitro* and crystal structures have been resolved (190, 277), while the processing of replicase polyprotein was only carried out in the arterivirus family member EAV (277).

Arteriviruses also encode a unique and highly conserved PL2 cysteine protease with a core size of about 100aa near the N terminus of the nsp2 protein (277). The arterivirus PL2 proteases combine the properties of both papain-like proteinases and chymotrypsin-like proteases (277). (i) The PL2 proteases carry the hallmark of papain-like proteinases, namely the catalytic motif Cys-His dyad. However, the arterivirus PL2 protease also has features different from papain-like proteinases in that the putative catalytic Cys is always followed by Gly, instead of a conserved aromatic amino acid Trp or some other bulky amino acids seen in papain-like proteinases (277). In EAV, a reversion of Gly to canonical Trp inactivated the EAV PL2 active *in vitro* (213). Most noticeably, the Cys-

Gly dipeptide is the hallmark of chymotrypsin-like cysteine proteases. (ii) The PL2 protease does not cleave immediately downstream site as shown in EAV (212, 214). There is a huge distance between the PL2 domain and the putative cleavage sites. In EAV, this distance is about 500 residues, while this distance can even extend to more than 700 residues in PRRSV strain VR-2332. Currently, only the EAV PL2 has been studied *in vitro* and shown to be active in *trans* and perhaps *cis* (212, 213).

The Putative PRRSV Nsp2 Replicase Protein

The putative PRRSV nsp2 replicase protein was initially predicted to contain ORF1a aa384-1363 (3), and later projected to include aa384-1578 (nsp2 aa1-1196) of PRRSV strain VR-2332 ORF1 protein through genetic analysis of both *Coronaviridae* and *Arteriviridae* (277). PRRSV nsp2 is a multidomain protein, containing a N-terminal putative cysteine protease (aa47-147) (CP2, newly named as PL2) (213), a middle hypervariable region with unknown function, a three to four transmembrane spanning domain (876-878, 911-930, 963-979 and 989-1018) and a C-terminal tail.

The downstream cleavage site of PRRSV nsp2 is poorly understood. In EAV, the cleavage at the nsp2/3 junction is mediated by the PL2 protease, which appears to prefer the dipeptide G|G (213). Mutagenesis of the putative P1 residue (Gly-831 to Pro) abolished the processing of nsp2/3 (214). Several conserved G|G dipeptides have been discerned in PRRSV nsp2, including 647G|G, 828G|G|G, 981G|G, 1117G|G and 1196G|G|. Processing of EAV nsp2 is the key step for the downstream processing of pp1a and pp1ab. Two alternative pathways have been proposed for processing the carboxyl terminus of ORF1a in EAV after nsp2 cleaves the site between nsp2|nsp3 (245). Nsp4|5 site processing represents the major pathway in which nsp2 serves as the cofactor of nsp4 for cleavage of the nsp4|5 site by the nsp4-encoded $3CL^{pro}$, while processing of the nsp5|6 and nsp6|7 sites represents the minor pathway when nsp2 is not associated with nsp3-8 precursor (245, 277). It is generally believed that cleavage at either of these sites will render the alternative sites inaccessible.

The available data show that PRRSV nsp2 is heterogeneous and highly variable (3, 75, 162, 192). Amino acids 160-844 in PRRSV nsp2 is the key region for size difference between Type I and Type II PRRSV strains (3, 162). Insertion or, most notably, deletions

are commonly seen in this region. The PRRSV North American SP isolate has a unique insertion of 36aa relative to the position between aa811 and aa812 of PRRSV strain VR-2332 nsp2 (206), while NA strain HB-2(sh)/2002 possesses a 12aa deletion at the position aa470-482 of nsp2 (80). A similar deletion is observed in a newly identified European PRRSV strain, with a 17aa deletion corresponding to the position aa734-751 of Type I strain ORF1a (75, 192). In addition to deletions, extensive mutations are also observed, mainly centered in the middle region of nsp2. Comparison of the predicted nsp2 protein of different PRRSV strains revealed that the similarity of nsp2 within genotype could range from 60% to 99% but differed greatly between genotypes (<50% similarity), exhibiting moderate to extensive sequence divergence (Chapter II). The significance of broad genetic variations in nsp2 and its relationship to the biological fitness of PRRSV remain to be defined.

The PRRSV nsp2 protein is rich in B cell epitopes and highly antigenic and immunogenic. Oleksiewicz *et al.* (168) used phage display libraries of PRRSV protein fragments with sera from experimentally infected pigs to identify linear B-cell epitopes that are commonly recognized during infection *in vivo*. Six out of ten linear epitope sites (ES) 11 to 53 amino acids in length are localized to nsp2 (168). These epitopes are 456-469, 691-722, 752-807, 839-849, 913-940 and 1032-1065 corresponding to the ORF1a residues of European PRRSV LV strain, antibody responses to which could be detected as early as one week post-infection. The antibodies to nsp2 have also been detected in boar semen and their presence was correlated with the duration of PRRSV secretion in semen (167). In addition, in a DNA vaccination with a plasmid encoding ORF1a, the humoral immune responses are mainly against nsp2 (8), and the antibodies to nsp2 ES-7 showed up as early as 14 days post-infection as demonstrated by a peptide-based ELISA (8, 169). Similar observations were also reported in North American strains (48, 105, 158). Overall, the early antibody response to nsp2, which could be detected at a similar time as the antibodies to PRRSV N protein, has proven nsp2 to be one of the most immunodominant proteins. These studies may imply an important immunological role for nsp2 in PRRSV infection *in vivo*, which remains to be resolved.

Objectives

The aim of this dissertation was to elucidate the biological aspects of the multidomain nsp2 replicase protein of PRRSV. Chapter II focused on monitoring the evolution of nsp2 proteins in field PRRSV stains. Chapter III described assembly of a PRRSV infectious cDNA clone of PRRSV strain VR-2332 and identification of essential and nonessential domains of the nsp2 protein for viral replication in cell culture. In Chapter IV, the biological aspects concerning the enzymatic activities of the putative PL2 protease domain and its role in the PRRSV replication cycle were explored. Finally, the proteolytic processing of PRRSV nsp2 in virus-infected MARC-145 cells was investigated in Chapter V.

Chapter II

Complete Genome Analysis of RFLP 184 Isolates of Porcine Reproductive and Respiratory Syndrome Virus

Modified from Jun Han, Yue Wang and Kay S. Faaberg. 2006. *Virus Res*. **122**, 175-182

Abstract

Two full-length genomes of recently emerged virulent isolates of porcine reproductive and respiratory syndrome virus (PRRSV) were sequenced and compared to other PRRSV strains. The results revealed that these two isolates (named MN184), of North American lineage, represented the shortest PRRSV genomes sequenced to date with a nucleotide length of 15019 bases. Genetic analysis demonstrated that the two isolates were not identical and shared approximately 87 and 59% nucleotide identity with prototype North American strain VR-2332 and European strain Lelystad, respectively. Three quite variable regions were identified, corresponding to putative nsp1β, putative nsp2 and ORF5. Nsp2, the most variable region, shared only 66-70% amino acid similarity to other sequenced North American-like PRRSV nsp2 proteins. Further study revealed that the nsp2 protein of the MN184 isolates contained three discontinuous deletions when compared to strain VR-2332 nsp2 protein, with the sizes of 111, 1, and 19 amino acids corresponding to strain VR-2332 positions 324-434, 486 and 505-523, respectively. Taken together, these data suggest PRRSV nsp2 replicase protein is undergoing rapid evolution in field.

Introduction

Porcine reproductive and respiratory syndrome virus (PRRSV) is a positive-sense single-stranded RNA virus that is the cause of an often severe and an economically important swine disease worldwide. As a member of the family *Arteriviridae* of the order *Nidovirales*, PRRSV has been shown to be subject to remarkable evolution, perhaps related to its inherent ability to undergo high frequency viral recombination (238, 271-274). There are two major PRRSV genotypes, based on the genetic differences seen in the prototype strains Lelystad (151) and VR-2332 (162). The European-like strains (Type 1; prototype Lelystad) are about 60% similar to North American-like strains (Type 2; prototype VR-2332) on the nucleotide level. Each of these genotypes contains individual PRRSV isolates that can vary in nucleotide sequence up to approximately 20%. The broad genetic and antigenic variation in PRRSV and the presence of multiple viral genotypes circulating on swine farms have made control of PRRSV infection extremely difficult.

Primarily to gain a better understanding of the structural basis for PRRSV virulence/attenuation, we have previously completed full-length nucleotide sequence analysis of several PRRSV genomes (162, 192, 271). However, in late 2001, a severe form of PRRS disease appeared in the State of Minnesota, USA, that was attributed to Type 2 viral isolates that were significantly different from previous isolates, based on ORF5 nucleotide sequence analysis and comparison to the PRRSV database (http://prrsvdb.org).

In the present study, the full-length sequence generation and genome analysis of two of these new isolates, named MN184 for the U.S. state of origin and defined ORF5 restriction fragment length polymorphism (RFLP; (250)) was completed. The two MN184 isolates were the same genome length but were different from each other, as detailed in this report. In addition, nucleotide alignment to other sequenced genomes revealed that the MN184 isolates were the shortest PRRSV isolates identified to date, and the length difference was again mapped to the putative nsp2 region. Nsp2 size variation in both genotypes has been previously documented but sequencing studies had indicated that Type 1 strains were approximately 300 nucleotides shorter in length in the nsp2

genomic region, compared to Type 2 strains (75, 80, 151, 192, 206). This study provided clear evidence that nsp2 size cannot be used to differentiate between the two PRRSV genotypes. It was also noted that the MN184 length difference was due to three discrete deletions when compared to other Type 2 strains, not just a single genomic event as had been seen previously. These data strongly suggested that PRRSV nsp2 is a highly variable protein, and the importance to characterize the causes or consequences of nsp2 variability in future study.

Materials and Methods

Cells and viral strains. MA-104 cells (ATCC CRL-2621) were maintained in minimum essential medium (EMEM) (SAFC 56416C) supplemented with 10% fetal bovine serum (FBS) at 37 °C and 5% CO_2. Two PRRSV isolates, identified by an ORF5 restriction fragment polymorphism (RFLP) pattern of 1-8-4 at the Minnesota Veterinary Diagnostic Laboratory in 2002, were designated as MN184A (DQ176019) and MN184B (DQ176020) (250) and amplified once on porcine alveolar macrophages (PAM).

RT-PCR. Viral RNA (vRNA) was extracted from PRRSV infected cell supernatant with QIAmp® Viral RNA Mini Kit (Qiagen, Valencia, CA). RT-PCR was performed with the Qiagen® OneStep RT-PCR Kit according to the protocol provided (Qiagen). Primers (Table 1) were designed based on the published sequences of different strains of PRRSV deposited in GenBank as well as newly generated MN184 sequence (DQ217415, AY424271, DQ176019, DQ176020). To determine the 5′ nucleotide sequence of the two PRRSV isolates, rapid amplification of cDNA ends (RACE) was performed using the 5′-Full RACE Core Kit (TaKaRa Bio, Madison, WI). A 5′-end phosphorylated reverse primer 5′-788L15 was used to synthesize first-strand cDNA. After digestion of vRNA by RNaseH, the single strand cDNA was circularized with T4 RNA ligase and was followed by nested inverse PCR using primer set 5′-139U20/3′-729L18 for the first round and 5′-214U23/3′-608L20 set for the second round. 3′-RACE was performed with SMART™ RACE cDNA Amplification Kit (Clontech, Mountain View, CA). Briefly, the 3′-CDS primer targeting the polyA was used for the first strand cDNA synthesis and the PRRSV specific primer 5′-14923U21 and a kit supplied 3′-CDS specific primer universal primer

(UPM) were used for subsequent PCR amplification.

Sequence analysis. PCR products were gel purified with QIAquick® gel purification kit (Qiagen, Valencia, CA), cloned into the pGEM-T Vector (Promega, Madison, WI) and 3-5 clones for each RT-PCR product were chosen for sequencing. The nucleotide sequence determination was completed in both directions with the PCR specific primers or the vector encoded SP6 and T7 promoter primers. The products were submitted to the Advanced Genetic Analysis Center at the University of Minnesota for sequence determination with an ABI 377 automated DNA fragment analyzer. A quality sequence representing at least three-fold genome coverage was obtained. Sequence data was assembled and analyzed by using the GeneTool sequence analysis program (BioTools Inc., Edmonton, Alberta CA) and Lasergene (DNASTAR, Madison, WI). Multiple sequence alignments were generated with CLUSTALX (221) or Wisconsin Package Version 10.3 (Accelrys Inc., San Diego, CA). Editing of the multiple alignments was completed using Jalview (39) and Adobe® Photoshop® CS, version 8.0. The following GenBank full-length sequences were used for comparison: VR-2332 (U87392), Ingelvac MLV (AF066183), 01NP1.2 (DQ056373), PL97-1 (AY58524), PA -8 (AF176348), SP (AF184212), BJ-4 (AF331831), HN1 (AY457635), 16244B (AF046869), HB-1 (AY150312), HB-2 (AY262352), CH-1a (AY032626), P129 (AF494042), JA142 (AY424271), SDPRRS-01-08 (AY375474), EuroPRRSV (AY366525), Lelystad (M96262), IAF-93-653 (U64931), IAF-Klop (AY184209), 98-3298 (DQ306877), 98-3403 (DQ306878), 99-3584 (DQ306879).

Results

Genome characterization of MN184 isolates. Late in the year 2001, many virulent isolates of a seemingly novel PRRSV were identified in the State of Minnesota, USA. ORF5 nucleotide sequence analysis and comparison to the PRRSV database (>5000 isolates; http://prrsvdb.org/) revealed that the isolates were of Type 2 lineage, but were significantly different from previous isolates. Furthermore, they were most closely related to those isolates previously seen in Canada in the early 1990s (141) and in the State of Minnesota in 1998. Restriction fragment length polymorphism (RFLP) analysis of ORF5 also demonstrated that they belonged to the same group of viruses as these early cases,

known as 1-8-4 isolates (250) and were thus named MN184 isolates. Because of the striking dissimilarity with all but one previously isolated MN PRRSV isolate, we amplified two of these new isolates with a single passage on porcine alveolar macrophages (PAM), the host cell, and completed full-length genome analyses on the viruses, designated as MN184A (DQ176019) and MN184B (DQ176020). These two isolates were collected at different times from two separate farms.

Genomic alignment demonstrated that these two PRRSV were quite distinct (>14.5% nucleotide dissimilarity) from other NA Type 2 full-length sequenced genomes, yet comparison with Type 1 (European) full-length sequences confirmed that the isolates were solely of Type 2 genotype origin as they were only approximately 59% similar at the nucleotide level to both EuroPRRSV and Lelystad strains (data not shown). Strikingly, these Type 2 MN184 isolates represented the shortest PRRSV genomes detected to date (15019 nt, not including the poly A tail). In addition, no specific area was discerned that suggested that these isolates were derived from viral recombination between Type 1 and Type 2 strains (data not shown).

Full-length sequence analysis revealed that the two MN184 isolates were actually genetically distinct. They shared 98.0% nucleotide similarity or 2% difference. This percentage of dissimilarity was unexpected due to their sudden simultaneous appearance in Minnesota late in 2001, with no clear recent related isolate seen in our PRRSV database at that time. Table 2.2 represents the detailed nucleotide and amino acid comparison between the two isolates and Fig. 2.1 depicts the amino acid differences seen between these two strains. Both of these isolates possessed nucleotide degeneracy in several regions of the genome, predominantly in the predicted nsp2 region of ORF1 (Table 2.2). The fact that nucleotide degeneracy was seen in these isolates suggested that PRRSV may consist of several individual species, often referred to as a swarm of related but distinct viral sequences, within infected animals.

In order to more closely pinpoint the individual regions of these MN184 isolates that showed the most dissimilarity from other PRRSV strains and to assign the region(s) accounting for the difference in Type 2 viral genome length, these two isolates were compared to the sequence of the prototype Type 2 strain VR-2332. The differences

between the two isolates could again be discerned, with isolate MN184B possessing slightly increased similarity to strain VR-2332 than isolate MN184A (data not shown). The nucleotide and amino acid comparisons to VR-2332 showed individual MN184 isolate regions varied from 81.5 to 94.7 and 78.4 to 100%, respectively, but the regions corresponding to ORF5 (86.4–86.7 and 87.0–87.5%, respectively) predicted nsp1β (83.8–84.0 and 84.8–85.4%, respectively, and nsp2 (81.5–85.5 and 78.4–79.5%, respectively) were the most variable (data not shown). Most interesting was that only the predicted nsp2 genomic region showed a difference in nucleotide length and that both MN184 isolates possessed the same nsp2 deletion, detailed below. The comparison also revealed that the 5′- and 3′-UTR's were the most conserved regions of the genome (94.7 and 94.0%, respectively), indicating sequence conservation in important regions for viral replication and transcription (data not shown).

GP5 and nsp1β amino acid comparison ORF5 encodes a heterogeneous PRRSV structural protein (GP5) and is often used for PRRSV diagnostic identification (109). GP5 is a predicted three transmembrane protein with an endodomain and ectodomain. The 30 amino acid ectodomain is composed of a short highly conserved domain usually containing at least two *N*-glycosylation sites bounded by two hypervariable regions. The highly conserved domain of this 30 amino acid region has been shown to code for the viral attachment epitope in Type 2 strains (172, 182, 184). GP5 of the same set of full-length genomes, as well as the original RFLP184 isolates identified in Canada (IAF-93-653, IAF-Klop) and in 1998–1999 in Minnesota (98–3298, 98–3403, 99–3584) were aligned (Fig. 2.2). The alignment of PRRSV GP5 revealed amino acid identities ranging from 82.5 to 87.7% between the new MN184 isolates and other non-RFLP184 Type 2 strains (data not shown). Interestingly, the amino acid differences between the new MN184 isolates and the older RFLP184 isolates were quite large (5.7–12.2%, data not shown) and thus we detected no clear origin of the new RFLP184 virus. The limited alignment shows that most of the amino acid differences observed were found in the hypervariable regions (Fig. 2.2). The two conserved *N*-glycosylation sites were maintained in the MN184 isolates, except for detected nucleotide degeneracy coding for amino acid 44 in isolate MN184B.

Nsp1β encodes a papain-like cysteine protease (60). An amino acid alignment of the MN184 isolates with a non-redundant set of available Type 2 nsp1β sequences as well as Type 1 strains EuroPRRSV and Lelystad was completed (Fig. 2.3). The nsp1β protein possesses a number of completely conserved amino acids, and the proposed catalytic residues were maintained in all sequenced genomes (60). The alignment, ordered by amino acid similarity, indicates that the MN184 isolates are more similar to Type 1 strains than the other sequenced full-length Type 2 sequences. In particular, five amino acids (boxed in Fig. 2.3) directly mimic the Type 1 strains. However, the amino acids that were conserved in the other non-redundant Type 2 sequences were also mostly conserved in the MN184 isolates, but scattered amino acids and the amino acid similarity (84.8–85.4%) revealed a more divergent Type 2 protein than had been evidenced to date. Thus, the alignment further defines maintained residues of nsp1β that may be critical to the replication cycle of PRRSV.

Amino acid comparison of nsp2 An amino acid alignment of non-redundant sequences of nsp2, ordered by pairwise identity, is shown in Fig. 2.4. A highly conserved chymotrypsin-like cysteine protease (PL2) domain is present at the N-terminus, previously predicted by alignment with equine arteritis virus (EAV) nsp2 (208, 277). There are 3–4 predicted transmembrane domains near the C-terminus of this protein (145), but the exact C-terminal cleavage site has not been empirically determined. Two predictions of the C-terminal cleavage site have been proposed, one G|G at VR-2332 nsp2 amino acid 981 (3) and the other at amino acid 1197 (277), but there several completely conserved G|G doublets within this protein (VR-2332 nsp2 amino acids 647, 981, 1117, 1196, 1197; downward arrows in Fig. 2.4). Prior work had also shown that the predicted nsp2 protein is proline rich and contains multiple potential B-cell epitopes (75, 168, 192). The large middle region of PRRSV nsp2 (VR-2332 nsp2 amino acids 148–880) has no assigned function but is highly variable in length. Furthermore, the length difference between sequenced Type 1 and Type 2 strains of PRRSV has been mapped to this variable middle region of nsp2 (Fig. 2.4). Until now, sequenced Type 1 genomes have been shown to be 313–364 bases shorter than most Type 2 PRRSV (75, 151, 192). However, the multiple sequence alignment established that the MN184 genome contains

the shortest predicted nsp2 to date (2547 bp), 393 bp shorter than prototype Type 2 strain VR-2332. Furthermore, it contained three discontinuous deletions in the translated protein with deletion sizes consisting of 111, 1 and 19 amino acids, respectively, corresponding to the amino acid positions in PRRSV strain VR-2332 nsp2 of 324–434, 486 and 505–523, respectively (Fig. 2.4). The three deletions resulted in the loss of several proline residues and predicted B-cell epitopes (data not shown). Besides these deletions, significant alterations in nsp2 amino acid sequence from other Type 2 strains were also seen, sometimes corresponding to the Type 1 amino acid seen at the same relative position (Fig. 2.4). Comparison of the nsp2 predicted protein of the two PRRSV genotypes demonstrated that the amino acid identity within Type 2 viruses ranged from 66 to 99% and from 88 to 90% within Type 1 viruses, but differed greatly between genotypes (<45% similarity). In particular, the MN184 isolates displayed 66–80% amino acid identity to all Type 2 nsp2 predicted proteins and only 43–45% identity to Type 1 strains (data not shown). When surveying the multiple sequence alignment in Fig. 2.4, we also noted that all instances of insertion or deletion in both genotypes occurred in this hypervariable middle region. To this point, Shen *et al*. (2000) (206) first reported that PRRSV North American Type 2 strain SP has a unique insertion of 36 aa relative to the position between aa 813 and 814 of PRRSV VR-2332 nsp2. Another investigator found a unique 12 aa deletion at position 466–477 in PRRSV isolate HB-2(sh)/2002 nsp2 (80). A 17 aa deletion occurred in newly identified European-like PRRSV isolates when compared to strain LV (75, 192). The instances of mutation did not consistently occur along the same stretch of amino acids, although the deletions seen between the MN184 isolates and other Type 2 viruses encompass most of the largest deletion detected between Type 1 and other Type 2 PRRSV. All of these data suggested that the nsp2 ORF contains a conserved protease motif and predicted transmembrane spanning regions that may be necessary for replication of PRRSV, but is highly susceptible to mutation in the large middle section.

Discussion

The sudden appearance of field isolates of PRRSV in Minnesota reflecting the 184 RFLP pattern is still a mystery, but the consequences of this event are even now being

realized. The Minnesota Veterinary Diagnostic Laboratory now performs routine sequencing on similar 184 RFLP isolates from approximately one-fourth of the total number of ORF5 sequence requests. In addition, the 184 RFLP pattern has now been detected not only in Minnesota, but also in Iowa, Wisconsin, South Dakota, Kansas, Missouri, Illinois, Nebraska, Kentucky, Oklahoma and Wyoming. We chose to derive the full-length sequences from two isolates because of the need to understand if this could be more than a single virus type and the fact that the swine herd diagnosed with isolate MN184A presented with a milder case of PRRS than the herd infected with isolate MN184B, as reported by the attending pathologist (Kurt Rossow, personal communication). The strains have not been inoculated into naïve animals to verify the case presentations, but it is interesting to note that isolate MN184B had many more nucleotide degeneracies detected when analyzing the genome and this might reflect the severity of the disease reported.

This genome analysis increased our understanding of the immense nucleotide and amino acid sequence variation that exists in the field. Factors driving this variation may be related to the way swine are now managed, the interstate and international transport of swine and boar semen, the intermixing of different PRRSV isolates within herds and the nature of the virus itself. Full genome sequence generation also allows us to monitor where on the genome variation is tolerated and which regions are more conserved. As a result of this study, as well as a previous publication (192), a picture is emerging that indicates nsp2, nsp1β and ORF5 are extraordinarily versatile proteins.

This study has also provided clear evidence that nsp2 size can no longer be used to differentiate between the two PRRSV genotypes. The novel finding that nsp2 evolved to display a Type 2 genome with three discontinuous deletions, leading to the shortest genome to date (15,019 kb), suggests that PRRSV may be evolving to eliminate dispensable genomic regions and make the genome more compact. Finally, although the significance of genetic variation in PRRSV can only be surmised at present, the evolutionary change seen in ORF5, nsp1β and nsp2 should reasonably be related to the biological fitness of PRRSV during selection pressure.

Acknowledgement

The authors wish to acknowledge the efforts of the Minnesota Veterinary Diagnostic Laboratory, especially Carrie Wees and Linda Schuveiller, for continued ORF5 sequence generation. We would also like to thank Althea Faricy for review of the manuscript and Seth Baker and Shannon Whittet for technical help in generating the genome sequences of the MN184 strains. The support of the Minnesota Rapid Response Fund and Boehringer Ingelheim Vetmedica was greatly appreciated.

Table 2.1. Oligonucleotide primers used in this study. Forward primers are indicated by a slash (/) after the designator, reverse primers are preceded by a slash. Genome positions are based on GenBank Submission U87392 (VR-2332).

Primer	Position (nt)	Sequence
5′- and 3′-RACE Primers		
/3′-CDS primer		5′-AAGCAGTGGTATCAACGCAGAGTAC$(T)_{30}$VN
/3′-608L20	274-293	5′-GGAGGGACCGTGCACTGAGA
/3′-729L18	395-412	5′-CCCAGCAGGGGAGCACTC
5′-139U20/	607-626	5′-CGTTTTCGCCAACTCCCTAC
5′-214U23/	682-704	5′-CCCGCAGAGACCTAAGCCTGAAG
5′-788L15/	786-800	5′-PO_4-GCGGAGCCCAAGAGA
5′-14923U21/	14923-14943	5′-AGAAAGGGGACGGCCAGCCAG
Sequencing Primers		
vr131/	1-31	5′-TATGACGTATAGGTGTTGGCTCTATGCCTTG
5′-871/	871-888	5′-TCCTTCCCGCCCCACCAC
/3′-1000	981-1000	5′-GCAGTTGCCTTCAGGGACAG
1493U21/	1527-1547	5′-GGGAATTGCGGCTGGCACTGT
/3′-1800	1806-1824	5′-AGGCAGGCAGGGTCAAATC
5′-2087/	2084-2103	5′-CGGAGGAGGTCGCAGCAAAG
/2345L24	2677-2700	5′-AGGGAGGGGCCTGCTCTCTGGTAG
2844U25/	3242-3266	5′-CAAAGTACTCAGCTCAAGCCATCAT
3′-3264/	3264-3282	5′-GGGCCCACCTGAGTTAATG
839-5′-4229-P2/	4091-4116	5′-CTTTCGCTGTTGGTTTGTTC
/3′-4000	4153-4177	5′-GAGAAGCTCAAAAGAATGAAGGATG
4430U20/	4828-4847	5′-CGGTCCGGCTACTCCACCAC
839-5′-116-P2/	5123-5142	5′-AAGCGCTGTTAAAGGCAGAG
4976U20/	5374-5393	5′-GTGAACATGCCCTCAGGAAT
/5165L20	5563-5582	5′-AGCATGGTGCGGCCAGTCAA
/5744L17	5745-5761	5′-TGGCTGCCGACCTTCAC
5905U21/	6295-6315	5′-TGGACGCCCTTGGTTGCTGTG
6670U21/	7061-7081	5′-CGCCCGTTGGCAGCATCTTTG
/6839L21	7230-7250	5′-CAGGCACTGGGGCCGTTCTCT
5′-7550/	7524-7545	5′-GGTCCCCGTCAACCCAGAGAAT
/7539L21	7930-7950	5′-CGTCGGCACCGGAGATCAAGA
7851U21/	8248-8268	5′-CTAACGCCACCCCGGTGACTG
/3′-8500	8481-8500	5′-CATGGGCAAACAGGTATTTC
5′-9100/	9033-9056	5′-GGCCTGTCATCTGGTGATCCGATC
/8828L25	9225-9249	5′GCATGGTGGGAGACTCGGCATACAG
5′-10193/	10183-10200	5′-TCAACGTCCCGGCAGGCA
/3′-10310	10240-10261	5′-CCGCCGGCCAGGATGCGAACCC
10372U22/	10769-10790	5′-TGCAAAAAGCACGCCCGTCAAC
VRBP9/	10840-10859	5′-GAATGCACGGTTGCTCAGGC
/3′-10853	10841-10858	5′-TGGGCAACCGTGCATTCT
/11283L22	11680-11701	5′-CCCATGCAGGGGTCCAGGTACA
761P1/	12128-12144	5′-CTTCACGGAGTTCTTG
/712P6	12283-12301	5′-GGCCTCATAAGATCTTCTG
P41/	13213-13231	5′-GACGGCGGCAATTGGTTTC
/416P1	13633-13650	5′-CATGTTGGACGTAGCTGG
416P4/	14020-14039	5′-TATGGTGCCCTCACTACCAG
/05P4	14320-14339	5′-ACGGAACCATCAAGCACAAC
/P72	15341-15361	5′-CGCCCTAATTGAATAGGTGAC

Table 2.2. Detailed analysis of individual PRRSV genomic regions and translated proteins, and number of degenerate bases detected in each region

Region	Bases	Nucleotide length	% Nucleotide Similarity	% Nucleotide Identity	Number of Degenerate Bases (184A/184B)	Size (aa)	%Amino Acid Similarity	%Amino Acid Identity
5' UTR	1-190	190	99.5	98.9	1/0	-	-	-
ORF1A	191-7309	7119	98.5	96.7	16/109	2372	96.8	96.5
NSP1a	191-688	498	98.8	98.5	1/0	166	97.6	97.6
NSP1b	689-1339	651	98.3	97.5	2/3	217	97.2	95.9
NSP2	1340-3886	2547	98.0	94.6	10/76	849	94.2	94.2
NSP3	3887-5224	1338	98.7	98.7	0/0	446	99.3	98.9
NSP4	5225-5836	612	98.5	96.4	0/13	204	97.1	97.1
NSP5	5837-6346	510	99.2	95.3	3/17	170	97.1	97.1
NSP6	6347-6394	48	100.0	100.0	0/0	16	100	100
NSP7	6395-7171	777	99.3	99.3	0/0	259	99.6	99.2
NSP8	7172-7309	138	99.3	99.3	0/0	46	97.6	97.6
ORF1B	7306-11679	4374	99.2	98.9	5/4	1457	99.5	99.2
NSP9	7288-9225	1938	98.9	98.8	1/1	646	99.4	98.9
NSP10	9226-10548	1323	99.3	98.9	3/3	441	99.8	99.3
NSP11	10549-11217	669	99.3	99.3	0/0	223	99.5	99.5
NSP12	11218-11679	462	99.6	99.4	1/0	153	99.3	99.3
ORF2a/GP2	11681-12451	771	99.0	98.3	1/0	222	98.0	97.3
ORF2b/E	11686-11907	222	99.6	99.6	0/0	73	100	100
ORF3/GP3	12304-13068	765	98.6	98.6	0/0	254	97.6	97.6
ORF4/GP4	12849-13385	537	98.5	98.5	0/0	178	98.9	98.9
ORF5/GP5	13396-13998	603	97.8	97.7	1/0	200	96.5	96.5
ORF6/M	13983-14507	525	99.6	97.4	0/0	174	100	100
ORF7/N	14497-14868	372	98.9	98.9	0/0	123	97.6	97.6
3' UTR	14869-15019	151	100	98.0	1/1	-	-	-

Fig. 2.1. (A) Diagrammatic representation of the PRRSV genome. Putative non-structural protein cleavages are depicted above ORF1a and 1b, represented by downward arrows. Signature motifs are identified below ORF1a and 1b, indicating their placement in the PRRSV genome [papain-like cysteine protease and β (PL1); cysteine protease (PL2); serine/3C protease (3CL); polymerase (RdRp); helicase (Hel); *Xenopus laevis* homolog poly(U)-specific endoribonuclease (N)] (84, 102, 277). **(B)** Schematic diagram of the comparison of ORF1 protein (replicase) of MN184A and MN184B and putative processing. The degeneracy seen in nsp2 is included in the comparison. **(C)** Schematic diagram of the comparison of ORF2-7 proteins of MN184A and MN184B.

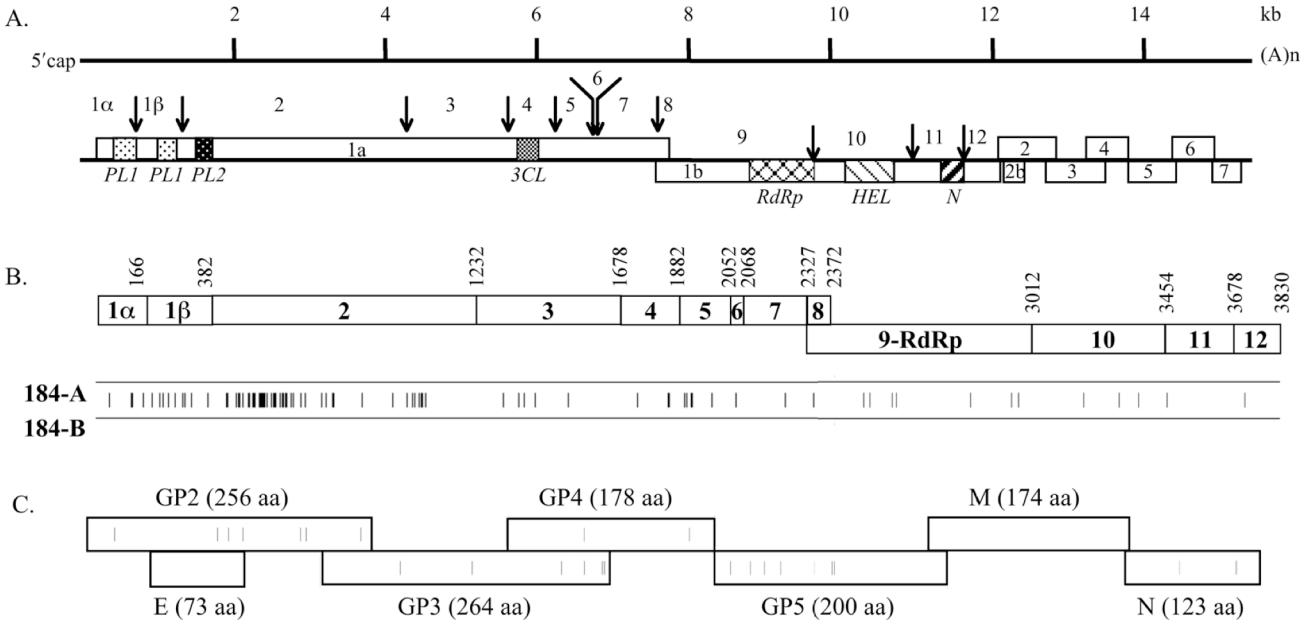
A.
2
4
6
8
10
12
14
kb
5′cap
(A)n
1α
1β
2
3
4
5
6
7
8
9
10
11
12
PL1
PL1
PL2
1a
3CL
1b
RdRp
HEL
N
2
4
6
2b
3
5
7
B.
166
382
1232
1678
1882
2052
2068
2327
2372
3012
3454
3678
3830
1α
1β
2
3
4
5
6
7
8
9-RdRp
10
11
12
184-A
184-B
C.
GP2 (256 aa)
GP4 (178 aa)
M (174 aa)
E (73 aa)
GP3 (264 aa)
GP5 (200 aa)
N (123 aa)

Fig. 2.2. ORF5 amino acid sequence alignment of divergent PRRSV. Multiple sequence alignments were generated with CLUSTALX (221) or Wisconsin Package Version 10.3 (Accelrys Inc., San Diego, CA). Full-length PRRSV sequences were aligned using ClustalX (Version 1.83.1; IUB DNA weight matrix, gap penalty 15.00, gap length penalty 6.66). The resulting alignment was further analyzed using the Wisconsin Package Version 10.3 Distances Program (Jukes-Cantor distance method, partial matches due to degenerate symbols considered). In figure dark grey boxes indicate high amino acid conservation (>80%), medium grey (>60%), lighter grey (>40%) and unshaded (<40%) boxes identify less conserved residues. The dashed region indicates the putative signal sequence, the boxed regions identify the proposed transmembrane regions, the hypervariable regions are indicated (HV-1 and HV-2), and the proposed orientation of the protein in the virion is identified in bold italics. The conserved cysteine residue that is proposed to interact with the M protein is identified by the downward arrow (↓). The two conserved putative *N*-glycosylation sites are identified by stars and hypervariable region 1 contains strain/isolate specific *N*-glycosylation sites (NxS/T). Sequences were aligned with the Pileup program of the Wisconsin Package (Blosum62 Scoring Matrix, gap weight =8, length weight =2, weighted ends). The alignment was scored for redundancy and colored for percent identity using Jalview (Clamp et al., 2004) and then transferred to Adobe® Photoshop® CS, Version 8.0, for grayscale transformation.

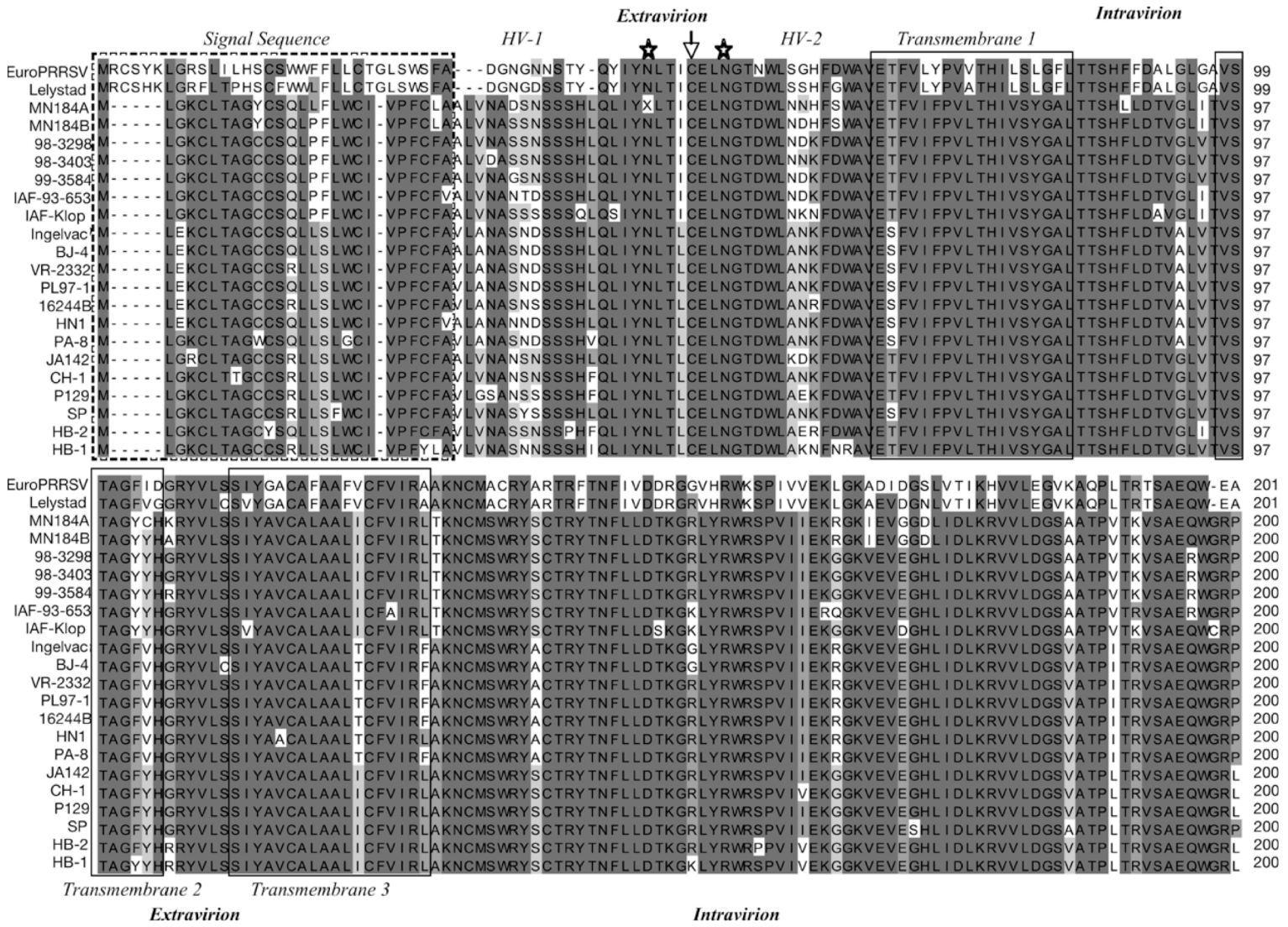
Extravirion
Intravirion
Signal Sequence
HV-1
HV-2
Transmembrane 1
Transmembrane 2
Transmembrane 3
Extravirion
Intravirion

Fig. 2.3. Nsp1β amino acid sequence alignment of divergent PRRSV. The figure derivation and color scheme was described in the Fig. 2 legend. The two completely conserved putative catalytic residues are identified by stars and the boxed amino acids identify MN184 sequence conservation with Type 1 isolates and EAV. The proposed cleavage site is identified by the downward arrow (↓). Sequences were aligned with the Pileup program of the Wisconsin Package (Blosum62 Scoring Matrix, gap weight=8, length weight=2, weighted ends)

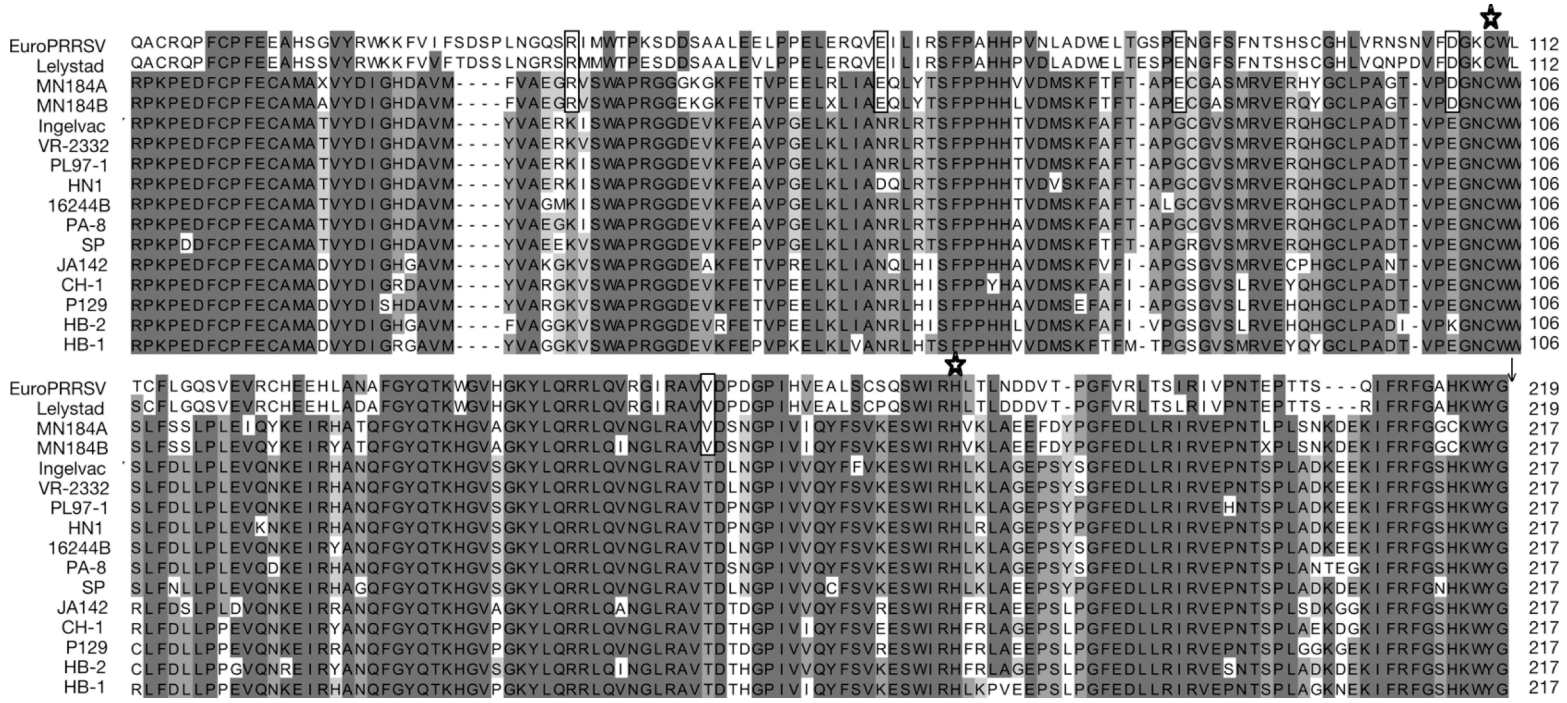
EuroPRRSV QACRQPFCPFEEAHSGVYRWKKFVIFSDSPLNGQSRIMWTPKSDDSAALEELPPELERQVEILIRSFPAHHPVNLADWELTGSPENGFSFNTSHSCGHLVRNSNVFDGKCWL 112
Lelystad QACRQPFCPFEEAHSSVYRWKKFVVFTDSSLNGRSRMMWTPESDDSAALEVLPPELERQVEILIRSFPAHHPVDLADWELTESPENGFSFNTSHSCGHLVQNPDVFDGKCWL 112
MN184A RPKPEDFCPFECAMAXVYDIGHDAVM----FVAEGRVSWAPRGGKGKFETVPEELRLIAEQLYTSFPPHHVVDMSKFTFT-APECGASMRVERHYGCLPAGT-VPDGNCWV 106
MN184B RPKPEDFCPFECAMAAVYDIGHDAVM----FVAEGRVSWAPRGGEKGKFETVPEELXLIAEQLYTSFPPHHLVDMSKFTFT-APECGASMRVERQYGCLPAGT-VPDGNCWV 106
Ingelvac RPKPEDFCPFECAMATVYDIGHDAVM----YVAERKISWAPRGGDEVKFEAVPGELKLIANRLRTSFPPHHTVDMSKFAFT-APGCGVSMRVERQHGCLPADT-VPEGNCWV 106
VR-2332 RPKPEDFCPFECAMATVYDIGHDAVM----YVAERKVSWAPRGGDEVKFEAVPGELKLIANRLRTSFPPHHTVDMSKFAFT-APGCGVSMRVERQHGCLPADT-VPEGNCWV 106
PL97-1 RPKPEDFCPFECAMATVYDIGHDAVM----YVAERKISWAPRGGDEVKFEAVPGELKLIANRLRTSFPPHHTVDMSKFAFT-APGCGVSMRVERQHGCLPADT-VPEGNCWV 106
HN1 RPKPEDFCPFECAMATVYDIGHDAVM----YVAERKISWAPRGGDEVKFEAVPGELKLIADQLRTSFPPHHTVDVSKFAFT-APGCGVSMRVERQHGCLPADT-VPEGNCWV 106
16244B RPKPEDFCPFECAMATVYDIGHDAVM----YVAGMKISWAPRGGDEVKFEAVPGELKLIANRLRTSFPPHHTVDMSKFAFT-ALGCGVSMRVERQHGCLPADT-VPEGNCWV 106
PA-8 RPKPEDFCPFECAMATVYDIGHDAVM----YVAEGKISWAPRGGDEVKFEAVPGELKLIANRLRTSFPPHHAVDMSKFAFT-APGCGVSMRVERQHGCLPADT-VPEGNCWV 106
SP RPKPDDFCPFECAMATVYDIGHDAVM----YVAEEKVSWAPRGGDEVKFEPVPGELKLIANRLRTSFPPHHAVDMSKFTFT-APGRGVSMRVERQHGCLPADT-VPEGNCWV 106
JA142 RPKPEDFCPFECAMADVYDIGHGAVM----YVAKGKVSWAPRGGDEAKFETVPRELKLIANQLHISFPPHHAVDMSKFVFI-APGSGVSMRVECPHGCLPANT-VPEGNCWV 106
CH-1 RPKPEDFCPFECAMADVYDIGRDAVM----YVARGKVSWAPRGGDEVKFETVPEELKLIANRLHISFPPYHAVDMSKFAFI-APGSGVSLRVEYQHGCLPADT-VPEGNCWV 106
P129 RPKPEDFCPFECAMADVYDISHDAVM----YVARGKVSWAPRGGDEVKFETVPEELKLIANRLHISFPPHHAVDMSEFAFI-APGSGVSLRVEHQHGCLPADT-VPEGNCWV 106
HB-2 RPKPEDFCPFECAMADVYDIGHGAVM----FVAGGKVSWAPRGGDEVRFETVPEELKLIANRLHISFPPHHLVDMSKFAFI-VPGSGVSLRVEHQHGCLPADI-VPKGNCWV 106
HB-1 RPKPEDFCPFECAMADVYDIGRGAVM----YVAGGKVSWAPRGGDEVKFEPVPKELKLVANRLHTSFPPHHVVDMSKFTFM-TPGSGVSMRVEYQYGCLPADT-VPEGNCWV 106
EuroPRRSV TCFLGQSVEVRCHEEHLANAFGYQTKWGVHGKYLQRRLQVRGIRAVVDPDGPIHVEALSCSQSWIRHLTLNDDVT-PGFVRLTSIRIVPNTEPTTS---QIFRFGAHKWYG 219
Lelystad SCFLGQSVEVRCHEEHLADAFGYQTKWGVHGKYLQRRLQVRGIRAVVDPDGPIHVEALSCPQSWIRHLTLDDDVT-PGFVRLTSLRIVPNTEPTTS---RIFRFGAHKWYG 219
MN184A SLFSSLPLEIQYKEIRHATQFGYQTKHGVAGKYLQRRLQVNGLRAVVDSNGPIVIQYFSVKESWIRHVKLAEEFDYPGFEDLLRIRVEPNTLPLSNKDEKIFRFGGCKWYG 217
MN184B SLFSSLPLEVQYKEIRYATQFGYQTKHGVAGKYLQRRLQINGLRAVVDSNGPIVIQYFSVKESWIRHVKLAEEFDYPGFEDLLRIRVEPNTXPLSNKDEKIFRFGGCKWYG 217
Ingelvac SLFDLLPLEVQNKEIRHANQFGYQTKHGVSGKYLQRRLQVNGLRAVTDLNGPIVVQYFFVKESWIRHLKLAGEPSYSGFEDLLRIRVEPNTSPLADKEEKIFRFGSHKWYG 217
VR-2332 SLFDLLPLEVQNKEIRHANQFGYQTKHGVSGKYLQRRLQVNGLRAVTDLNGPIVVQYFSVKESWIRHLKLAGEPSYSGFEDLLRIRVEPNTSPLADKEEKIFRFGSHKWYG 217
PL97-1 SLFDLLPLEVQNKEIRHANQFGYQTKHGVSGKYLQRRLQVNGLRAVTDPNGPIVVQYFSVKESWIRHLKLAGEPSYPGFEDLLRIRVEHNTSPLADKEEKIFRFGSHKWYG 217
HN1 SLFDLLPLEVKNKEIRHANQFGYQTKHGVSGKYLQRRLQVNGLRAVTDPNGPIVVQYFSVKESWIRHLRLAGEPSYPGFEDLLRIRVEPNTSPLADKEEKIFRFGSHKWYG 217
16244B SLFDLLPLEVQNKEIRYANQFGYQTKHGVSGKYLQRRLQVNGLRAVTDLNGPIVVQYFSVKESWIRHLKLAGEPSYSGFEDLLRIRVEPNTSPLADKEEKIFRFGSHKWYG 217
PA-8 SLFDLLPLEVQDKEIRHANQFGYQTKHGVSGKYLQRRLQVNGLRAVTDSNGPIVVQYFSVKESWIRHLKLAGEPSYSGFEDLLRIRVEPNTSPLANTEGKIFRFGSHKWYG 217
SP SLFNLLPLEVQNKEIRHAGQFGYQTKHGVSGKYLQRRLQVNGLRAVTDLNGPIVVQCFSVKESWIRHLKLAEEPSYPGFEDLLRIRVEPNTSPLADKDEKIFRFGNHKWYG 217
JA142 RLFDSLPLDVQNKEIRRANQFGYQTKHGVAGKYLQRRLQANGLRAVTDTDGPIVVQYFSVRESWIRHFRLAEEPSLPGFEDLLRIRVEPNTSPLSDKGGKIFRFGSHKWYG 217
CH-1 RLFDLLPPEVQNKEIRYANQFGYQTKHGVPGKYLQRRLQVNGLRAVTDTHGPIVIQYFSVEESWIRHFRLAGEPSLPGFEDLLRIRVEPNTSPLAEKDGKIFRFGSHKWYG 217
P129 CLFDLLPPEVQNKEIRRANQFGYQTKHGVPGKYLQRRLQVNGLRAVTDTDGPIVVQYFSVRESWIRHFRLAEEPSLPGFEDLLRIRVEPNTSPLGGKGEKIFRFGSHKWYG 217
HB-2 CLFDLLPPGVQNREIRYANQFGYQTKHGVSGKYLQRRLQINGLRAVTDTHGPIVVQYFSVKESWIRHFRLAGEPSLPGFEDLLRIRVESNTSPLADKDEKIFRFGSHKWYG 217
HB-1 RLFDLLPPEVQNKEIRHANQFGYQTKHGVPGKYLQRRLQVNGLRAVTDTHGPIVIQYFSVKESWIRHLKPVEEPSLPGFEDLLRIRVEPNTSPLAGKNEKIFRFGSHKWYG 217

Fig. 2.4. Nsp2 amino acid sequence alignment of divergent PRRSV. The completely conserved putative cysteine protease catalytic residues are identified by stars and the boxed amino acids signify protease sequence conservation within PRRSV and EAV. The proposed cleavage sites are identified by filled arrows (↓); additional possible cleavage sites are indicated by a hashed arrow. A signal peptide was predicted using the SignalP server (solid grey box; (16). Transmembrane regions, shown in hashed black boxes, were derived by PHDhtm (194) and potential *N*-glycosylation sites indicated by an asterisk (*) were identified by PROSITE (5) using the PredictProtein server (195). Sequences were aligned with the Pileup program of the Wisconsin Package (Blosum62 Scoring Matrix, gap weight = 8, length weight = 2, weighted ends). The figure derivation and color scheme were described in the Fig. 2 legend.

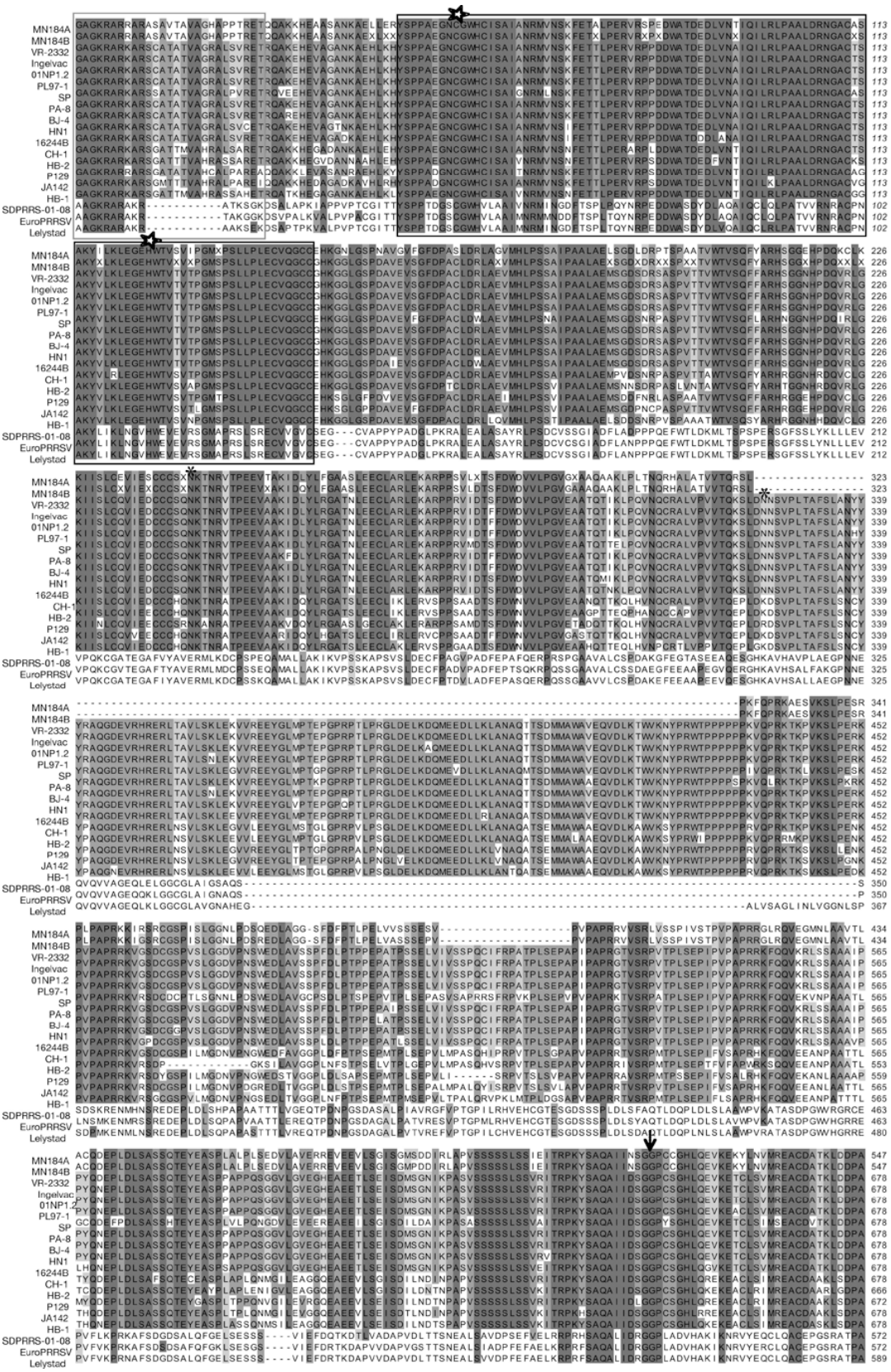
MN184A
MN184B
VR-2332
Ingelvac
01NP1.2
PL97-1
SP
PA-8
BJ-4
HN1
16244B
CH-1
HB-2
P129
JA142
HB-1
SDPRRS-01-08
EuroPRRSV
Lelystad

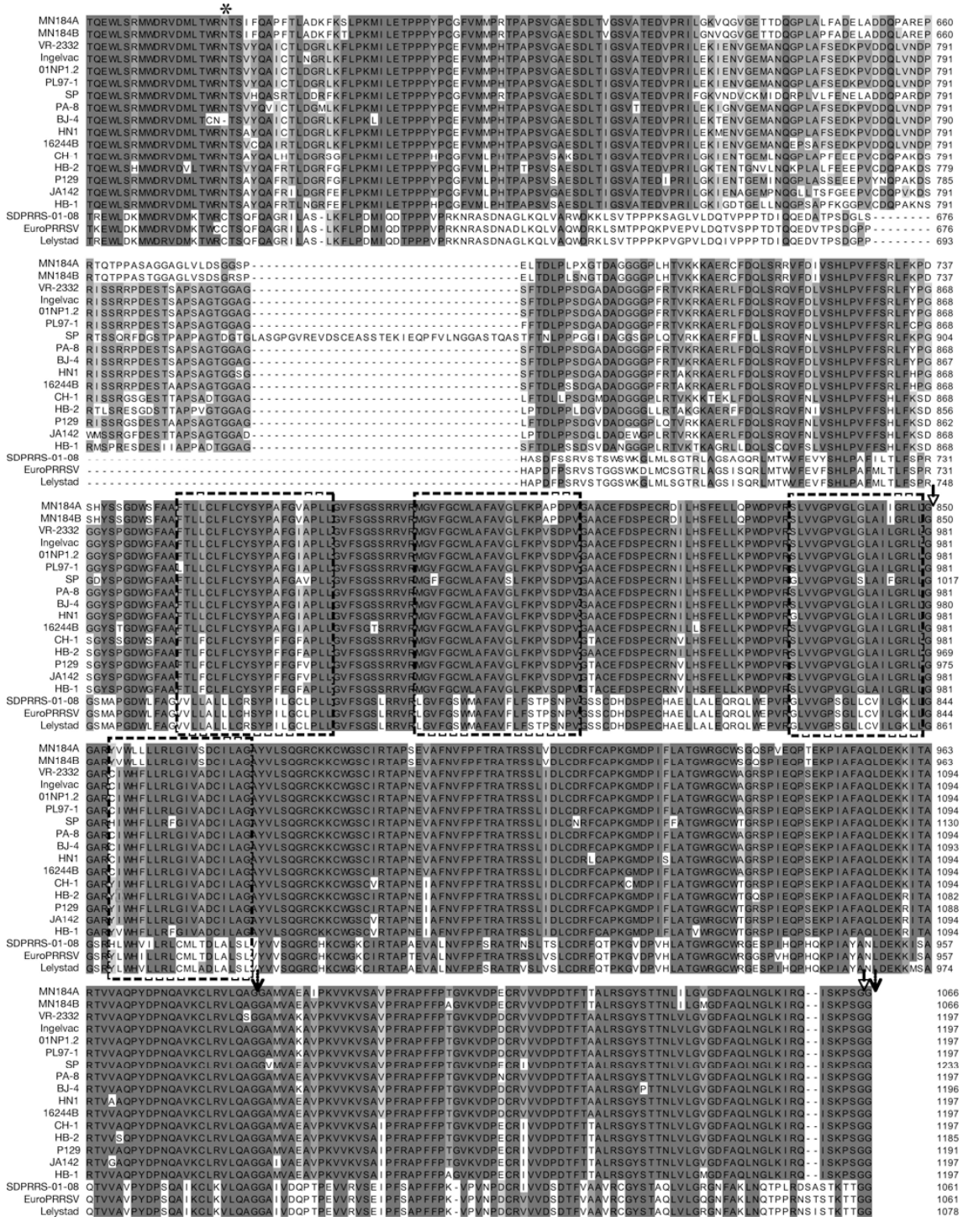
MN184A
MN184B
VR-2332
Ingelvac
01NP1.2
PL97-1
SP
PA-8
BJ-4
HN1
16244B
CH-1
HB-2
P129
JA142
HB-1
SDPRRS-01-08
EuroPRRSV
Lelystad

Chapter III

Identification of Nonessential Regions of the Nsp2 Replicase Protein of PRRSV Strain VR-2332 for Replication in Cell Culture

Jun Han, Gongping Liu, Yue Wang and Kay S. Faaberg. 2007. *J. Virol.* 81, 9878-90

Abstract

The nonstructural protein 2 (nsp2) of porcine reproductive and respiratory syndrome virus (PRRSV) is a multidomain protein and has been shown to undergo remarkable genetic variation, primarily in its middle region, while exhibiting high conservation in the N-terminal putative protease domain and the C-terminal predicted transmembrane region. A reverse genetics system of PRRSV North American prototype VR-2332 was developed to explore the importance of different regions of nsp2 for viral replication. A series of mutants with in-frame deletions in the nsp2 coding region were engineered, and infectious viruses were subsequently recovered from transfected cells and further characterized. The results demonstrated that the cysteine protease domain (PL2), the PL2 downstream flanking sequence (amino acids [aa] 181 to 323), and the putative transmembrane domain were critical for replication. In contrast, the segment of nsp2 preceding the PL2 domain (aa13 to 35) was dispensable for viral replication, and the nsp2 middle hypervariable region (aa324 to 813) tolerated 100-aa or 200-aa deletions but could not be removed as a whole; the largest deletion was about 400 aa (nsp2Δ324-726). Characterization of the mutants demonstrated that those with small deletions possessed growth kinetics and RNA expression profiles similar to those of the parental virus, while the nsp2Δ324-726 mutant displayed decreased cytolytic activity on MARC-145 cells and did not develop visible plaques. Finally, the utilization of the genetic flexibility of nsp2 to express foreign genes was examined by inserting the gene encoding green fluorescent protein (GFP) in frame into one nsp2 deletion mutant construct. The recombinant virus was viable but impaired and unstable and gradually gained parental growth kinetics by the loss of most of the GFP gene.

Introduction

Porcine reproductive and respiratory syndrome virus (PRRSV), the etiological agent of PRRS, is an enveloped, positive-stranded RNA virus belonging to the family *Arteriviridae* in the order *Nidovirales* (29) and contains a 15.1-to 15.5- kb long genome (151, 162). Two genotypes, represented by prototype viruses Lelystad and VR-2332, have been discerned based on a difference in nucleotide sequence by approximately 40%, and are referred to as European (EU or Type 1; Lelystad) (151) and North American strains (NA or Type 2; VR-2332) (3, 162). The 5' two-thirds of the viral genome is occupied by overlapping open reading frames (ORF) 1a and 1b, which generate the viral replicase proteins. Polyprotein 1a (pp1a) is encoded by ORF1a and the synthesis of pp1ab occurs through a ribosomal frameshift at the ORF1a/1b junction (21, 208). These polyproteins are immediately translated upon virus entry and then proteolytically processed by viral encoded proteinases into intermediate precursors and at least 12 mature nonstructural proteins, which appear to be responsible for forming membrane-bound replication complexes, called viral-induced double membrane vesicles, that are sites for viral RNA synthesis (208).

The processing of pp1a and pp1ab is believed to be mediated by accessory proteinases, located in nsp1 and nsp2, and the main serine proteinase in nsp4, 3C-like proteinase (3CLpro) (277). The catalytic sites of these enzymes and the corresponding cleavage sites are well conserved among arteriviruses (277). Processing of pp1a begins with the N-terminal nsp1, which is automatically cleaved by papain-like cysteine proteases (PCP1α and PCP1β) in PRRSV, while the PCP1α domain is inactive in equine arteritis virus (EAV) (60, 211). Arterivirus nsp2 contains a predicted cysteine protease (PL2) in its N terminus that was shown to cleave at the nsp2|nsp3 junction in EAV (213). The 3CLpro is responsible for processing the remainder of ORF1a and ORF1ab into several subunits (nsp3 to -12) (233, 277).

Among the nonstructural proteins, the multidomain protein nsp2 is the largest PRRSV replicative protein and was originally identified as spanning amino acids (aa) 384-1363 (nsp2 aa1-981) and then projected to include aa384-1578 (nsp2 aa1-1196) of strain VR-2332 ORF1a through genetic analysis of both *Coronaviridae* and *Arteriviridae*

(3, 277). PRRSV nsp2 protein has a similar organization as the arterivirus family member EAV nsp2 counterpart (213, 277). Three major domains could be discerned through the alignment of arterivirus nsp2 proteins: an N-terminal cysteine proteinase domain (PL2), a functionally unspecified middle region and a hydrophobic transmembrane (TM) region near the C-terminus (92, 277). In addition, the exact C-terminal cleavage sites have yet to be determined. PRRSV PL2 is predicted to act on the potential substrates at the nsp2|nsp3 junction and two potential cleavage sites have been proposed: 981G|G and 1196G|G|G (3, 277), according to the knowledge obtained from nsp2 of EAV, which prefers G|G dipeptides (213). The function of PRRSV nsp2 in the virus replication cycle is currently not known, while EAV nsp2 has been shown to be involved in the generation of double-membrane vesicles together with nsp3, and to serve as a cofactor for the nsp4 protein (209, 245).

Although PRRSV nsp2 possesses potential enzymatic function, it has been shown to be highly heterogeneous and variable. It is well documented that PRRSV nsp2 accounts for the major genetic differences between Type 1 and Type 2 PRRSV strains, sharing less than 40% similarity at the amino acid level (3, 162). In addition, nsp2 is also the key region for length difference between PRRSV Type 1 and Type 2 strains. Natural mutations, insertions or most notably, deletions are always seen in the middle region or near the N-terminal region of the nsp2 protein in field strains, while the putative PL2 domain, predicted transmembrane domain as well as the predicted cleavage sites remain well conserved (3, 75, 80, 92, 162, 192, 206).

Reverse genetics provides a very valuable tool to explore the function of viral proteins by targeted gene manipulation. In this study, we explored the genetic flexibility of the PRRSV nsp2 protein and sought to identify critical and nonessential regions in PRRSV VR-2332 nsp2 for viral growth in cell culture. We first developed an infectious clone of Type 2 prototype strain VR-2332 and then created mutant constructs by deletion mutagenesis. The mutant viruses were rescued and their growth properties and RNA synthesis capacities were then evaluated. The results suggested that PRRSV nsp2 contains several nonessential regions for viral replication, while the conserved PL2 domain and transmembrane domain are critical to maintain nsp2 function. In addition, we

assessed the flexible nature of nsp2 by expressing the green fluorescent protein in one of the nsp2 deletion mutants. We found that the GFP recombinant virus was viable and induced typical CPE, but displayed an impaired growth rate. In addition, the GFP recombinant virus was unstable and gradually gained fitness, shown by increased growth kinetics through the loss of part of the GFP gene.

Materials and Methods

Cells and viral strains. MA-104 cells or a subclone (MARC-145 cells; ATCC CRL-11171), an African green monkey kidney epithelial cell line which supports PRRSV replication, were maintained in EMEM (SAFC Biosciences) supplemented with 10% fetal bovine serum (FBS) at 37 °C with 5% CO_2. PRRSV North American prototype strain VR-2332 (U87392) was used as a wild type (*wt*) control in all experiments. The derived vaccine strain of VR-2332, Ingelvac PRRS® MLV (AF066183), was utilized for genome comparison only.

Construction of PRRSV full-length cDNA clone of VR-2332. cDNA synthesis was performed with Enhanced Avian HS RT-PCR Kit (Sigma). Eight PCR primers (Table 1) were used to amplify four overlapping cDNA fragments covering the complete VR-2332 genome (Fig. 1). Each PCR fragment was purified with the QIAEX II Gel Extraction Kit (Qiagen) and cloned into pCR®2.1-TOPO® vector with TOPO TA Cloning® Kit (Invitrogen). Plasmids representing each fragment were submitted for nucleotide sequence analysis. QuikChange®Multi Site-Directed Mutagenesis Kit (Stratagene) was used to modify all cDNA clones. The fragments with the minimum nucleotide mutations compared to parental VR-2332 sequence (GenBank no. U87392) were used to assemble the full-length cDNA, as shown in Fig 3.1. In each overlap region, a unique restriction enzyme site was utilized to join flanking fragments. Four digested fragments, representing full-length genomic sequence, were precisely assembled stepwise into a modified low copy plasmid vector pOK12HDV-PacI (Genbank no. EF486278). The vector was modified to include the HDV ribozyme by inserting a 244 bp *SmaI* to *SalI* fragment containing the HDV antigenome ribozyme and a T7 RNA polymerase terminator sequence from Transcription vector 2.0 into the corresponding sites in pOK12 (GenBank No: AF223639) (106, 178, 242). The NcoI restriction enzyme site in this 244

bp fragment was replaced with unique SphI and PacI by PCR method and a linker including FseI, AvrII and BsrGI restriction sites was then inserted into the site between SphI and PacI by restriction enzyme digestion. Thus, the modified new vector pOK12HDV-PacI contains five unique restriction sites: SphI, FseI, AvrII, BsrGI and PacI. In the full-length cDNA clone, viral genomic sequence was preceded by the T7 RNA polymerase promoter, 2 G residues and a T residue, and followed by a polyadenylic acid tail of 50 nucleotides. Assembled clones were propagated in the *Eschericia coli* DH1 cells and then submitted for full-genome nucleotide sequence confirmation (GenBank no. DQ217415).

Deletion mutagenesis of PRRSV VR-2332 nsp2. Fragment I (bases 1-4545) was digested with SphI and FseI and cloned into the modified pOK12HDV-PacI vector. The subsequent plasmid was named pOK-I. Similarly, fragment II (bases 4545-7591) was removed to generate shuttle plasmid pOK-II. To delete VR-2332 nsp2 nucleotides, overlapping extension PCR was performed on pOK-I or pOK-II. Briefly, one primer pair was used to generate fragment A and the other primer pair was used to obtain fragment B. Second round PCR was performed to generate the final full-length deletion fragment with the upstream primer from the first primer set and downstream primer from the second primer pair and the described overlapping fragments A and B as templates. The PCR product was next gel purified, digested with proper enzymes and cloned into pOK-I or pOK-II cut with the same enzymes. After confirmation by sequencing, mutated fragment I or II was inserted into the infectious clone backbone to construct the final full-length deletion mutant clone.

To make a recombinant virus expressing green fluorescent protein (GFP), the GFP gene minus the stop codon (714 bp) was inserted into the exact position where nsp2 aa324-434 was previously deleted. The insertion of GFP into the nsp2 deletion site was accomplished via three separate PCR reactions. Two flanking fragments were PCR amplified from pVR-V7-nsp2Δ324-434 by primer sets dVR-67U22/dVR-189L33 and dVR-903U33/dVR-1307L24 and one middle fragment from GFP using primer set dVR-189U33/dVR-903L33. The overlapping extension PCR was completed using all three fragments as templates and primer pair dVR-67U22/dVR-1307L24 to derive the GFP

fusion fragment, which was then excised with MluI and EcoRV and cloned back into pOK-I to generate the new plasmid pOK-I-nsp2Δ324-434-GFP. The fragment I-nsp2Δ324-434-GFP was then inserted into the infectious clone backbone as described above to result in full-length clone pVR-V7-nsp2Δ324-434-GFP.

***In vitro* transcription and transfection.** The full-length cDNA clone was linearized by cleavage with PacI. Capped RNA transcripts were produced using the mMESSAGE MACHINE^{TM} Kit (Ambion) with an optimized 2:1 ratio of methylated cap analogue to GTP. The RNA was then purified by the RNeasy mini kit (Qiagen). RNA was evaluated for quality on 1% native agarose gel, and quantified by spectrophotometry at OD_{260}. For transfection, a modified procedure was generated based on the approach described by Nielsen et al (164). Briefly, MA-104 or MARC-145 cells were seeded onto six-well plates (2-3 x 10^5 cells/well) in 3 ml of complete medium EMEM supplemented with 10% fetal bovine serum (FBS) and then incubated at 37°C, 5% CO_2 for 20-24 hours until approximately 80% confluent. Three microgram of *in vitro* transcribed RNA and 2 µl of DMRIE-C (Invitrogen) diluted in 1 ml Opti-MEM® medium were combined and vortexed briefly. The cells were washed once with Opti-MEM® medium and then immediately overlaid with the lipid:RNA complex solution. After 4 h of exposure to the lipid:RNA complexes, the monolayers were washed and fresh complete medium was added. The transfected cells were monitored daily for appearance of cytopathic effect (CPE).

Detection of progeny viral RNA. To detect progeny viral RNA, cell culture supernatants from transfected and viral infected cells were harvested. RNA was isolated with QiaAmp viral RNA minikit (Qiagen). One-step RT-PCR was performed with selected primer pairs (Table 1) to detect parental virus and PRRSV nsp2 mutant viruses.

Immunofluorescence assay. MARC-145 cells grown on coverslips and infected with virus were fixed in 3.7% paraformaldehyde at room temperature for 10 min, permeabilized and blocked for 20 min with 0.1% Triton/2% BSA/PBS. The cells were incubated for 60 min with PRRSV nucleocapsid protein specific monoclonal antibody SDOW17 (137) and then stained with goat anti-mouse immunoglobulin G (IgG) conjugated with Alex fluor 568 (Molecular Probes) for another 60 min. The nuclear DNA

was stained with DAPI (4', 6-diamidino-2-phenylindole; Molecular Probes). The images were collected under an Olympus IX-70 inverted microscope.

Viral growth assays. MA-104 cell monolayers in T-25 flasks were infected with either parental or mutant viruses at an multiplicity of infection (MOI) of 5×10^4 PFU. After 1 h attachment at room temperature with gentle mixing, the inocula were removed and the monolayers were washed three times with serum-free EMEM. After washing, 7 ml complete medium was added and the flasks were then incubated for up to 5 days at 37°C, 5% CO_2. Samples were collected from medium at different hours post-infection (hpi) and titrated by viral plaque assay. For recombinant virus V7-nsp2Δ324-726 and VR-V7, MARC-145 cells were infected with 10^3 $TCID_{50}$ of the viruses. The viral infected supernatants were taken every 12 hpi and titrated by an endpoint dilution assay, and the titers were expressed as 50% tissue culture infectious doses ($TCID_{50}$)

Northern Blot Analysis. Intracellular RNAs of viral infected cells were extracted using an RNeasy Mini kit (Qiagen) and electrophoresed (15μg/sample) on a glyoxal denaturing gel as described previously (162, 272). After RNA transfer to 0.45 micron MagnaGraph Nylon Transfer Membrane (Osmonics), the membrane was probed with an oligonucleotide against ORF7 end labeled with γ-32P-ATP (Amersham) using polynucleotide kinase (Promega) as described previously (272)**.**

Results

Construction of full-length cDNA clone of VR-2332. Four overlapping genome fragments were amplified from purified strain VR-2332 viral RNA by RT-PCR using the primer pairs indicated (Figure 3.1, Table 3.1). Each fragment was individually cloned to generate intermediate plasmids pCR-SphI-FseI (segment I), pCR-FseI-AvrII (segment II), pCR-AvrII-BsrGI (segment III), and pCR-BsrGI-PacI (segment IV). The fragments were sequenced and the mutations corrected by site-directed mutagenesis. The cDNA clones were then digested with two unique restriction enzymes, as indicated by the clone name. Four fragments were gel-purified and ligated stepwise into low copy vector pOK12HDV-PacI to generate a full-length cDNA clone of PRRSV (pVR-V7). The infectious clone pVR-V7 contains 11 nucleotide and no amino acid changes from *wt* strain VR-2332, besides those also seen in Ingelvac MLV (Table 3.2).

Growth properties of recombinant virus VR-V7. The recombinant virus induced typical CPE, characterized by cell clumping, detachment and lysis at 72-96 hours post-transfection. At 108 hours post-transfection, most of the cells had undergone lysis and detached from the plate (data not shown). In order to rule out the possibility of contamination by *wt* VR-2332, we sequenced the recombinant virus at passage 3 (P3). The sequencing results confirmed that the exact nucleotide mutations at residues at 7329 and 7554 were detected in virus resulting from pVR-V7 (Table 3.1). Corresponding mutations were not seen in P3 virus from *wt* vRNA transfections (data not shown). Direct immunofluorescence assays were used to detect the expression of PRRSV nucleocapsid protein in infected MARC-145 cells. All cells infected by recombinant virus (P3 and on) as well as *wt* VR-2332 were positive. Massive nucleolar accumulation of the nucleocapsid protein was readily apparent, as previously reported by Rowland et al (197) (data not shown). The recombinant virus VR-V7 displayed a similar growth rate to *wt* VR-2332, which also correlated with the viral genomic and subgenomic RNA synthesis. The plaque size of VR-V7 is slightly smaller than *wt* VR-2332 (Fig. 3.4B and C).

Generation and recovery of nsp2 mutant viruses. EAV and PRRSV N-terminal ORF1 proteins and their cleavage patterns are depicted in Fig. 3.2. To determine the functional importance of different regions of nsp2, pVR-V7 fragment I or II was digested with SphI and FseI or FseI and AvrII, respectively, and cloned into the pOK12HDV-PacI adaptor plasmid treated with the same enzymes to generate the shuttle plasmid pOK-I or pOK-II for subsequent nsp2 mutagenesis. The deletions were designed to maintain the ORF1a translational reading frame. Some deletions were based on the deletions seen in the nsp2 region of PRRSV MN184 strains (92), which contained three discontinuous deletions with a total size of 131aa, compared to strain VR-2332, corresponding to the amino acid positions in PRRSV strain VR-2332 nsp2 of 324-434, 486 and 505-523, respectively. In order to evaluate the importance of other regions in nsp2, a series of ~100aa stepwise deletions were created by overlapping PCR (Fig. 3.3). Each mutated PCR product was digested by appropriate restriction enzymes and cloned back into pOK-I or pOK-II. After sequence confirmation, mutated fragment I or II was then digested and placed into the infectious clone backbone. After assembly of the full-length cDNAs, at

least three clones each were chosen to test downstream viability. The procedures for in vitro transcription and transfection were the same as for VR-V7. The viral induced CPE was monitored daily after transfection.

Deletions of the PL2 domain and the region immediately downstream are lethal. The PL2 domain is predicted to have a size of about 100aa (PRRSV Y47 to C147) and is highly conserved among all arteriviruses, especially for the putative active catalytic sites at PRRSV C55 and H124, and has been proposed to be responsible for processing its downstream substrate between nsp2 and nsp3 (213, 277). To test the importance of the PRRSV PL2 domain, an in-frame deletion of nsp2 (Y47 to S180) was engineered and transferred to the infectious clone. The deletion of the PL2 core domain was lethal to the virus, defined as failure to detect extracellular or intracellular replication evidence by RT-PCR or immunostaining after supernatant passage to new cell monolayers and 5-6 days subsequent incubation. Next, we examined the core enzyme domain flanking sequences, which might play a role in maintaining the secondary and tertiary structure of the PL2 domain. For PRRSV nsp2 PL2, its upstream sequence is about 45aa and highly variable either within or between Type 1 and Type 2 strains, except the N-terminal first 7aa, which are highly conserved and perhaps needed for recognition by PCP1β. Since a natural deletion was seen in MN184 isolates corresponding to the position N324 to P434 in VR-2332, the flanking sequence downstream of PL2 to be examined included residues up to L323. To determine the importance of the regions immediately upstream and downstream of the PL2 domain, either the upstream flanking sequence (A13 to V35; V7-nsp2Δ13-35) or downstream sequence (S180 to L323; V7-nsp2Δ181-323) were deleted. Transfection of MARC-145 cells with transcript RNA from these constructs indicated that V7-nsp2Δ13-35 resulted in viable virus, while V7-nsp2Δ181-323 was lethal, as confirmed by negative RT-PCR and immunostaining results (data not shown). To rule out the suggestion that the deletion of aa180-323 might have affected the PL2 activity, since the deletion was close to the enzyme domain, another deletion mutant (S241 to L323; V7-nsp2Δ241-323) was made. This deletion also turned out to be lethal to virus replication. To negate the possibility that the deletion of these sequences could affect the processing of nsp1, the mutant full-length RNAs were *in vitro* translated. The results

established that nsp1 was correctly processed into nsp1α and nsp1β (data not shown). Taken together, our data revealed that an intact PL2 domain and its immediately downstream flanking sequence were essential for PRRSV replication, but the upstream region of nsp2 aa13-35 was dispensable for viral growth.

The hypervariable region of nsp2 aa324-813 tolerated deletions. The region encompassing nsp2 aa150-850, between the PL2 domain and the predicted transmembrane domain, is highly divergent among PRRSV strains and especially between genotypes (3, 162). Several reports have documented that deletions, mutations and insertions occur in this region (75, 80, 192, 206). We recently reported that nsp2 of MN184 strains contained the largest natural deletions ever found in Type 2 field isolates (92). To determine whether the deleted regions seen in the MN184 isolates were required for strain VR-2332 replication, full-length infectious clone pVR-V7 was engineered to lack nsp2 residues D324 through P434 (V7-nsp2Δ324-434) and D324 through A523 (V7-nsp2Δ324-523). Virus-induced cytopathic effect (CPE) was readily detected at 4-5 days post-transfection in cells transfected with these nsp2 truncation mutants. Clarified supernatants harvested from MARC-145 cells transfected with VR-V7 nsp2 mutant RNAs were capable of initiating a productive infection in freshly inoculated MARC-145 cells, demonstrating the presence of viable virus. These results indicated that the deletions seen in MN184 strains were also dispensable for strain VR-2332 replication *in vitro*.

In order to determine whether the entire downstream hypervariable region was dispensable for viral replication, a large deletion mutant (V7-nsp2Δ324-845) from D324 to Q845 was produced but found to be lethal for virus replication. This suggested a detailed stepwise mutagenesis was needed for defining the nonessential region boundaries. Four approximately 100aa or 200aa deletion constructs were produced as shown in Fig. 3.4: V7-nsp2Δ543-632 (I543 to R632); V7-nsp2Δ633-726 (I633 to P726), V7-nsp2Δ543-726 (I543 to P726) and V7-nsp2Δ727-845 (C727 to Q845). The transfection results suggested that only V7-nsp2Δ727-845 produced a non-replicating PRRSV genome; all others resulted in viable virus. Further bioinformatics analysis suggested that V7-nsp2Δ727-845 might have affected the structure or stability of the juxtaposed hydrophobic

domain. Thus, a smaller deletion (C727 to G813, V7-nsp2Δ727-813) was also made, and this deletion allowed the rescue of viable virus. Thus, the region of nsp2 aa324-813 did tolerate several 100 - 200aa deletions. To determine if the whole region could be deleted, two additional deletion constructs (D324 to P726, V7-nsp2Δ324-726 and D324 to G813, V7-nsp2Δ324-813) were generated. The 403aa deletion (V7-nsp2Δ324-726) allowed viable virus recovery, while the construct V7-nsp2Δ324-813 did not. The combined data suggested that VR-2332 nsp2 harbors a large nonessential region for viral replication in cell culture.

The TM region and C-terminal tail are critical for nsp2 function. The carboxyl region of nsp2 is highly conserved among all PRRSV strains and has been predicted to contain 3-4 putative hydrophobic transmembrane domains (TM; aa876-898, 911-930, 963-979 and 989-1009) (92). This is consistent with the nsp2 counterpart of PRRSV arterivirus family member EAV, which also has TM domains in the respective C termini (213, 277). According to EAV, PL2 prefers G|G dipeptides (213). Thus, a carboxyl-terminal tail was predicted for PRRSV nsp2 that harbors two potential cleavage sites (981G|G and 1196G|G|G) (3, 277). Since the hydrophobic domains are responsible for targeting the nonstructural proteins for intracellular membranes to form viral replication complexes as demonstrated in EAV (209, 232), a complete deletion (W876 to Q1009, V7-nsp2Δ876-1009) of the TM domain was made as an attempt to determine if the hydrophobic region was required for PRRSV replication. The result indicated that the deletion was lethal to the virus. Since a potential cleavage site (981G|G) lay between the third and four transmembrane helices (92), a truncated TM (A880 to A937, V7-nsp2Δ880-937) was subsequently constructed to maintain the potential cleavage site. However, the deletion again resulted in nonviable virus. Similarly, deletion mutagenesis (S1072 to A1162, V7-nsp2Δ1072-1162) between the two potential cleavage sites (981G|G and 1196G|G|G) also did not allow virus rescue. Thus, the TM regions and carboxyl terminal tail appeared to be critical for nsp2 function.

Characterization of nsp2 mutant viruses. First, the possibility of contamination by parental virus was ruled out. Two sets of primers were employed to identify each mutant virus: one primer set targeting the sites across the deletion region was to detect

the mutant viruses while the other set primer was used for parental virus detection by targeting the deletion region with one primer. There was no evidence of cross-contamination by VR-V7 virus (Fig. 3.4A). The nsp2 mutated region integrity of the recombinant viruses was also examined by RT-PCR after four or five passages. All the viruses maintained the respective engineered deletion with expected size (Fig. 3.4A) and had no other mutations within nsp2 (data not shown). The entire genomes of V7-nsp2Δ324-726 P1, 3 and 6 were sequenced to confirm that there were no other compensatory mutations.

To determine the effect of the respective nsp2 deletions on PRRSV growth, the ability to form plaques was first examined. All the mutants except V7-nsp2Δ324-726 formed viral plaques within 5 days, the sizes of which were either comparable or smaller than the parental virus VR-V7 (Fig. 3.4B). Further growth curve analysis showed that all the small deletion mutants had similar growth kinetics as parental VR-V7 recombinant virus, slightly reduced from *wt* strain VR- 2332 (Fig. 3.4C). To determine if the nsp2 deletions had any effect on viral genomic and subgenomic RNA synthesis, the intracellular RNAs of viral infected cells at 30 hours postinfection (hpi) with 10^3 $TCID_{50}$ of P3 viruses were extracted and subjected to northern blot analysis with a probe against ORF7. Most of these mutants had similar viral RNA expression profiling compared to parental virus VR-V7, except V7-nsp2Δ727-813, which exhibited a decrease in RNA accumulation at 30 h (Fig. 4D, lanes 1 through 9).

Plaque assay results showed that V7-nsp2Δ324-726 could not develop visible plaques even the incubation time was extended to 8-10 days (Fig. 3.4B). Close microscopic investigation of infected cells suggested that the viral infection did cause CPE foci characterized by vacuolization, but the cell walls mostly remained intact and the virus failed to cause complete cell lysis (Fig. 3.5A). The impaired ability of V7-nsp2Δ324-726 to form visible plaques suggests that some differences exist in the viral replication cycle when compared to VR-V7, since plaque development is a consequence of differences in yield, rate of synthesis, viral release as well as cytolytic activity (189). On initial transfection of the *in vitro* derived transcript RNA, the V7-nsp2Δ324-726 mutant exhibited a 2-3 day delay and only sporadic CPE. The virus grew slowly in the

first two passages and then reached a titer of around 10^5 $TCID_{50}$/ml at P3 and $10^{5\sim6}$ $TCID_{50}$/ml at P6 (data not shown). To examine the basis of the defect, growth kinetics of V7-nsp2Δ324-726 mutant virus at P2, P3 and P6, monitored by end point dilution assay instead of plaque formation, were determined with an initial inoculum of 10^3 $TCID_{50}$. The V7-nsp2Δ324-726 mutant showed several differences as compared to the parental virus VR-V7. First, V7-nsp2Δ324-726 had a slower growth rate than VR-V7 at early times of infection and exhibited a 12-24 h delay in peak titer compared to VR-V7. VR-V7 reached a peak titer around 36 hpi while V7-nsp2Δ324-726 P6 reached a similar titer at 60 hpi (Fig. 3.5B). The increase in V7-nsp2Δ324-726 P6 titer at later times in infection may be a consequence of the decrease in cell cytolysis (discussed below). Northern blot analysis, monitoring genomic and subgenomic viral RNA expression levels at 30 hpi for V7-nsp2Δ324-726 P2 to P6 as well as VR-V7, revealed a comparable result (Fig. 3.4D). Secondly, V7-nsp2Δ324-726 was impaired in cytolytic activity. The investigation of virus-induced CPE revealed that VR-V7 induced rapid CPE and displayed very rigorous cytolysis, as almost all of the cells were rounded and detached at 55-60 hpi, while V7-nsp2Δ324-726 virus caused milder cytolysis (Fig. 3.5C). V7-nsp2Δ324-726 induced CPE was seen as cell clustering and clumping, with only a portion (30%-50%) of the cells lysed and detached at both 84 and 120 hpi (Fig. 3.5C). In order to examine if the decreased cytolysis was due to inefficient infection, an immunofluorescence assay (IFA) was employed to monitor the infection process at 24, 48 and 60 hpi. There was no apparent defect in cell infection, since more than 90% of the cells were infected by V7-nsp2Δ324-726 at 60 hpi (Fig. 3.5C), suggesting delayed but typical viral spread. In addition, virus release and the amount of virus produced appeared normal since the mutants reached a comparable titer to VR-V7 at 60 hpi (Fig. 3.5B). Therefore, the difference in cell viability was most likely due to the decreased cytolytic activity of V7-nsp2Δ324-726. Taken together, it appeared that decreased cytolytic activity played an important role in impairing the ability of V7-nsp2Δ324-726 to form viral plaques (Fig. 3.4B).

Nsp2 is functionally competent with internal insertion of GFP. The identification of several nonessential regions suggests that nsp2 is genetically flexible. To evaluate if

nsp2 could accept foreign genes in these nonessential regions, the green fluorescence protein (GFP) gene was inserted into one of the viable mutants (V7-nsp2Δ324-434), in frame, in the position where the region of MN184 nsp2 (aa324-434) was deleted compared to VR-2332. To test the effect of this nsp2 modification on virus viability, MA-104 cells were transfected with *in vitro* transcribed RNA of pVR-V7-nsp2Δ324-434-GFP. Viral induced CPE was observed 5-6 days after transfection. Thus, nsp2 was functionally competent with internal insertion of GFP gene, as shown recently for an infectious clone of type 1 PRRSV (76). At passage 2, GFP expression was examined under an inverted fluorescence microscope. GFP was successfully expressed and the fluorescence was associated with the foci of observed CPE (Fig. 3.6A and B). Since GFP was expressed as part of the nsp2 protein, the localization of GFP also might reflect the distribution of nsp2 in recombinant virus infected cells. The visualization of the GFP protein, near the nucleus stained with DAPI, thus suggested that the nsp2 protein was localized in the perinuclear region of the MA-104 cells, a similar distribution pattern to EAV nsp2 counterpart (Fig. 3.6C) (179, 232).

Growth, stability and nsp2-GFP processing of the GFP recombinant virus. To evaluate the growth properties of the GFP recombinant virus, titers were determined from different passages. As shown in Fig. 3.6D, the GFP insert diminished viral growth, as the GFP recombinant virus grew to very low titers in the first three passages. However, after three passages, the GFP recombinant virus reached a much higher titer of 10^5TCID$_{50}$/ml, similar titers to VR-V7. To investigate the basis for the change in growth, the GFP recombinant virus was propagated for five generations. RT-PCR was performed with a primer set (dVR-67U22/dVR-1307L24) amplifying nsp2 across the GFP gene (2 kb). As shown in Fig. 3.6E, two products were detected in P3 (2kb and 1.4 kb) and from P4 on, only the smaller 1.4 kb band was detected. The smaller PCR product correlated with the size of the amplicon without GFP. To determine if the virus spontaneously lost the GFP gene and in this manner acquired growth advantage over the original GFP virus, we determined the nucleotide sequence of the two PCR products. The 2 kb band indeed represented the full-length GFP product while the 1.4 kb band indicated that splicing had occurred during viral growth, resulting in deletion of all but the first 30nt of the GFP

gene (data not shown). Green fluorescence was also monitored for P1-5 of GFP recombinant virus. The loss of GFP gene from P4 and on correlated with the RT-PCR results (data not shown). Thus, the increase in the virus titer at P4 and the concomitant loss of fluorescence indicated a gain in replication fitness upon deletion of the GFP gene.

Discussion

In this study, we described the construction of a full-length infectious cDNA clone of North American prototype VR-2332, which differed from the one reported earlier (164). VR-V7 coded for 6 nucleotides (5 amino acids) of the related vaccine Ingelvac PRRS® MLV, whereas the previously published clone was derived independently and possessed 14 nucleotides (9 amino acids) of Ingelvac PRRS® MLV besides 2 additional amino acid mutations in ORF1. More importantly, nine disparate nucleotides located in nsp9-12, coding for crucial polymerase and helicase regions, were of *wt* VR-2332 origin in pVR-V7. We also utilized VR-V7 to examine the genetic flexibility of the nsp2 replicase protein as well as its potential use as an expression vector. PRRSV VR-2332 nsp2 was found to contain several nonessential regions including aa13-35 before the PL2 domain and aa324-813 in the middle hypervariable section. We also found that the PL2 domain and its immediate downstream sequence as well as the putative transmembrane region were essential for viral replication, suggesting their critical role in maintaining nsp2 function in the cell culture. Finally, we reported the successful insertion of the GFP gene in the nonessential region, but found that the recombinant virus is impaired and unstable.

The N terminus of the nidovirus replicase protein has been shown to exhibit considerable genetic variability (84), despite its likely crucial function in viral replication. The variability includes size variation and genetic mutation. In coronaviruses, the N terminus amino sequence identity varies from less than 30% to over 60% among different groups, with the most variability occurring in the protein domains upstream of the nsp3 orthologs (87, 187). The C terminus of the nsp1 protein of murine hepatitis virus (MHV) and the nsp2 protein of MHV and severe acute respiratory syndrome coronavirus (SARS-CoV) have all been shown dispensable for viral replication (22, 87). Very similarly, broad genetic variation in the N terminus of the PRRSV replicase protein has also been observed, especially in nsp2 and to a lesser degree in nsp1 (3, 75, 80, 92, 162, 192, 206).

With the continuing emergence of viral strains during the past 18 years, the nsp2 replicase protein with noted mutations, insertions and deletions, has become a vital region for monitoring the rapid evolution of PRRSV. The earliest report concerning nsp2 variation is from the full genome comparison of North American prototype VR-2332 and European prototype Lelystad (LV) strain (3, 162). The nsp2 of PRRSV LV strain is 119 amino acids shorter than that of VR-2332, and the amino acid similarity is under 40%. Since then, several other cases have been reported. PRRSV Type 2 SP strain had an unique insertion of 36 aa relative to the position between aa813 and 814 of VR-2332 nsp2 (206), and Type 2 isolate HB-2(sh)/2002 nsp2 protein contained a unique 12aa deletion at relative positions aa466-477 (80). Similarly, a 17aa deletion was identified in the newly identified European-like PRRSV field isolate when compared to strain LV (75, 192). Our recent report of two virulent MN184 strains of North American lineage revealed a further truncated PRRSV nsp2 gene, which is 131aa shorter than Type 2 prototype VR-2332 and contains three discontinuous deletions with the total size of 131aa, leading to the shortest genome detected to date (15,019 kb) (92). The immense genetic variability of nsp2 protein suggests that the hypervariable regions in nsp2 may play a very limited role for viral replication. Accordingly, we demonstrated this hypothesis was correct in that PRRSV nsp2 contained a vast redundant region, at least for viral replication in cell culture. In contrast, the entire region of the nsp2 protein of EAV was found to be crucial for nsp2/3 processing in the vaccinia virus-T7 system (213). Even small deletions were not tolerated in EAV nsp2 even though it has a similar organization as PRRSV nsp2, possessing a large middle region (500aa) that separates PL2 from its cleavage site. This may reflect a uniqueness of PRRSV nsp2 amongst arteriviruses.

We also reported that small deletions in the region of VR-2332 nsp2 aa324-812 did not affect virus viability. However, the deletion of the whole region appeared to be lethal to the virus. We have tried at least five clones (V7-nsp2Δ324-812) but the attempts were not successful. The largest deletion that resulted in viable virus is 402aa (V7-nsp2Δ324-726). One possible explanation is that there might be a size limit for the middle hypervariable region to maintain the correct folding of functional domain of nsp2, and too large of a deletion could interfere with the interaction of PL2 domain and its

substrates. Given that regions of nsp2 are highly heterogeneous, the whole region of nsp2 aa324-812 may be dispensable in PRRSV strains besides VR-2332. In other strains, mutations elsewhere in nsp2 might have a compensatory effect in maintaining a proper structure for the nsp2 functional domains.

Although the nsp2 hypervariable region (aa324-726) is dispensable for viral replication, the mutant virus was severely crippled in its ability to form plaques and did not cause complete cell lysis in the final stages of replication. The decreased cytolytic activity appeared to be most likely linked to the defect in plaque formation. Therefore, this may indicate that the long hypervariable region of nsp2 might play an important role in regulating maximal cytotoxicity through an undescribed mechanism. In addition, the nsp2 hypervariable region has been proposed to play an important role against host immune responses. Several reports have documented that the nsp2 hypervariable regions in both Type 1 and Type 2 PRRSV strains contained several highly immunogenic B cells epitopes, and the antibodies against these epitopes could be detected as early as one week (8, 48, 168). The hypothesis proposed states that linear sequences of the nsp2 protein are strongly antigenic and could serve as decoy epitopes, deflecting the host immune responses away from critical viral proteins (75, 168). Although only speculative, swine inoculation of recombinant viruses with variable length deletions in the nsp2 hypervariable region may lead to a clearer knowledge of the biological function of PRRSV nsp2 in *in vivo* infection.

PRRSV as a potential viral vector has been investigated previously, but the region of study was mainly focused on the 3' section of the genome and the size of insertion, if any, was limited to less than 10 amino acids when fused to viral structural proteins (88). Foreign genes have also been inserted into intergenic regions of PRRSV structural proteins and a transcription regulatory signal prior to the inserted genes was employed to generate subgenomic RNA (263). The exceptional genetic variability of PRRSV nsp2 suggested the likelihood of expressing a large foreign gene as a fusion protein in the viral replicase region. In this study, the identification of nonessential regions in the nsp2 replicase protein provided further guidelines for successful insertion of a foreign gene and increased the possibility of generating viable virus. To test this hypothesis, we

inserted the green fluorescent gene into one of the VR-2332 nsp2 deletion mutants (nsp2Δ324-434). The visualization of green fluorescence emitted from infected cells indicated that nsp2 was functionally competent to express a foreign gene in the hypervariable region. However, instability arose in later passages of the GFP mutant, consistent with another recent report (76). In that case, virus instability was seen when the insertion of GFP was attempted in a natural nsp2 deletion position that exists between Type 1 and Type 2 PRRSV. Many factors could contribute to the instability of GFP expression (19, 47). First of all, the GFP gene has a much larger size than the length of the deleted sequence. Thus it could potentially exert a strong structural influence on surrounding sequences, especially the nearby PL2 protease domain in its interaction with viral substrates, thereby effecting the efficiency of processing the nsp2|nsp3 cleavage. In addition, the nature of the gene insert and the precise position of insertion might influence virus stability. The stability of the firefly luciferase gene varied strongly on its location in MHV genome, whereas the *Renilla* luciferase gene was maintained in all of the positions tested (47). Given that PRRSV nsp2 harbors such a large hypervariable region, it is possible that stable insertion is position-dependent and that expression of a foreign gene will be successful when insertion is manipulated elsewhere in the coding sequence. Thus size, insertion position and the nature of a selected foreign gene appear important when considering nsp2 for gene fusion expression.

In summary, the identification of nonessential regions and successful expression of a foreign gene in nsp2 region by a reverse genetic approach further extends our knowledge concerning PRRSV nsp2 genetic flexibility. The successful recovery of the shortest self-replicating PRRSV (V7-nsp2Δ324-726, 14.2kb) also suggests that certain regions in this RNA virus are more flexible than previously thought. In addition, the attenuation of morphological phenotypes such as plaque appearance and cytolytic activity through modification of the viral replicase gene highlights a promising area for future PRRSV vaccine design.

Acknowledgement

The United States Department of Agriculture (award 206-01598) and Boehringer Ingelheim Vetmedica, Incorporated, provided funds for this study.

Table 3.1. Oligonucleotide primers used in this study.

Primer	Genome Position*	Sequence
pVR-V7 Construction		
T7Leader-VR long/	1-30	5' ACAT***GCATGC***TTAATACGACTCACTATAGTATGA CGTATAGGTGTTGGCTCTATGCCTTGG
/3'-4300	4617-4635	5' CTGGGCGACCACAGTCCTA
5'-4056-*AscI*/	4055-4080	5' CTTCTC***GGCGCGCC***CGAATGGGAGT
/3'-7579	7578-7603	5' TCATCATACCTAGGGCCTGCTCCACG
5'-7579/	7578-7603	5' CGTGGAGCAGGCCCTAGGTATGATGA
/P32	13293.13310	5' TGCAGGCGAACGCCTGAG
VR1509/	11938-11958	5' GTGAGGACTGGGAGGATTACA
/3'end-FL	15405-15411	5' GTC***TTTAATTAA***CTAG $(T)_{30}$ AATTTCG
Construction of GFP recombinant virus, identification of nsp2 mutants and northern analysis		
dVR-67U22/	2167-2187	5' CGCCCGCCACGCGTAATCGACA
/dVR-1307L24	3740-3763	5' CTGTGCCTGCGGACGGAGCTGATG
/dVR-191L30	GFP	5' GAGGTGCGGGAATTGGCAAGGACTTTTGAG
dVR-198U34/	GFP	5' GTCCTTGCCAATTCCCGCACCTCGCGGAACTGTG
dVR-192U30/	GFP	5' TCAAAAGTCCTTGCCAAAAGTTCAGCCTCG
/dVR-192L30	GFP	5' CGAGGCTGAACTTTTGGCAAGGACTTTTGA
VR-1051U27/	1051-1077	5' TCGCCATGCTAACCAATTTGGCTATC
VR-1371U18/	1371-1388	5' GTGGCGACTGCTACAGTC
/VR-1712L26	1712-1737	5' GACATCCCAGGGGTCACAGTGACAGT
VR-1824U24/	1824-1847	5' TTGACCGGCTGGCTGAGGTGATGC
/VR-2430L24	2430-2453	5' TTGGCATGAGCCCATATTCTTCTC
VR-2812U22/	2812-2833	5' CCCACCTGAGCCGGCAACACCT
VR-2393U22/	2393.2414	5' CTAACCGCCGTGCTCTCCAAGT
/VR-3080L37	3080-3116	5'CCCCGCTCTGCGGCGGTGCTGGGGGAGA GGCCTCATA
VR-3331U26/	3331-3356	5' GCGCGAGGCATGTGATGCGACTAAGC
/VR-3349L26	3349-3374	5' GCGTAGCAGGGTCATCAAGCTTAGTC
VR-3667U26/	3667-3692	5' CTCCGAGGATAAACCGGTAGATGACC
/VR-3847L34	3847-38880	5' CCGGGATCCTTGGTCAAAGAGCCTTTCAGCTTTT
/VR-4258L31	4258-4279	5' CCGGGATCCGCCCAGTAACCTGCCAAGAATG
/ORF7 probe	14904-14943	5' TGGCTGGCCATCCCCCTTCTTTCTCTTCTGCTGC TTGCCG

[a] Forward primers are indicated with a slash (/) after the designator, and reverse primers are preceded by a slash.

[b] Unless otherwise noted, genome position is based on GenBank submission U87392.

[c] Inserted restriction enzyme sites are shown in boldface.

Table 3.2. Amino acid changes detected in pVR-V7.

NT Position	ORF AA Position	Region	VR-2332	pVR-V7	MLV
309	40	nsp1a	Q	Silent	Q
642	151		P	Silent	P
1107	306	nsp1b	L	Silent	L
4407	1406	nsp3	P	Silent	P
4593	1468		Q	Silent	Q
4681	1498		S	A	A
4866	1559		V	Silent	V
5097	1636		R	Silent	Silent
5247	1686		V	Silent	V
6674	2162	nsp5	P	L	L
7329	2380	nsp7	K	Silent	K
7554	2455		V	Silent	V
11329	3739	nsp11	G	A	A
14336	183	ORF5	G	Silent	G
14404	10	ORF6	H	Silent	H
14735	121		R	G	G
14737	121		R	G	G

[a]Amino acid identity with Ingelvac PRRS MLV is shown in boldface.

Fig. 3.1. Assembly of full-length clone of PRRSV strain VR-2332. The 15.4-kb genome was amplified in four sections (I to IV) that incorporated unique restriction enzyme cleavage sites present in viral cDNA (FseI, AvrII, and BsrGI) or added to the PRRSV sequence at the 5' and 3' ends by insertion mutagenesis (SphI and PacI). A T7 polymerase promoter and two nontemplated G residues and a T residue preceded the viral sequence. The pOK12 vector was modified to include the above five enzyme restriction sites and an HDV ribozyme downstream of a polyadenosine tail of 50 nucleotides. Signature motifs are identified below ORF1a and -1b, with upwards arrows indicating their placement in the PRRSV genome. Abbreviations: PL2pro, chymotrypsin-like cysteine protease; 3CLpro, serine/3C-like protease; POL, RNA-dependent RNA polymerase; C/H, cysteine/histidine rich; HEL, helicase; XendoU, *Xenopus laevis* homolog poly(U)-specific endoribonuclease.

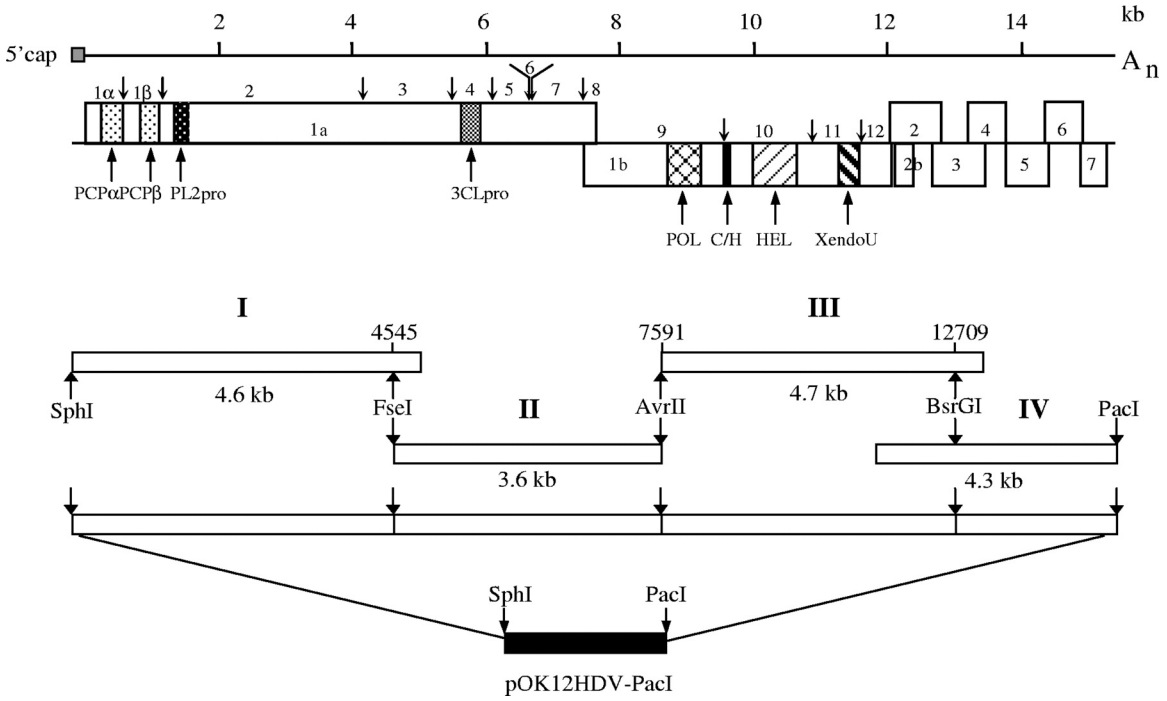
kb
2
4
6
8
10
12
14
5'cap
A n
1α
1β
2
3
4
5
6
7
8
1a
9
10
11
12
2
4
6
1b
2b
3
5
7
PCPαPCPβ
PL2pro
3CLpro
POL
C/H
HEL
XendoU

I
III
4545
7591
12709
SphI
4.6 kb
FseI
II
AvrII
4.7 kb
BsrGI
IV
PacI
3.6 kb
4.3 kb
SphI
PacI
pOK12HDV-PacI

Fig. 3.2. Schematic representation of the putative PRRSV nsp2 protein. The organization of the nsp1-to-nsp5 region of PRRSV and EAV is represented schematically. The cleavage sites are labeled by triangles, and the positions are annotated. The putative active enzyme domains are marked by dark boxes, while the inactive PCP1 domain in EAV is boxed gray. The putative TM domains (aa 876 to 898, 911 to 930, 963 to 979, and 989 to 1009) are also shown. Two hypervariable regions (HV) of unknown function are also discerned in the PRRSV nsp2 region.

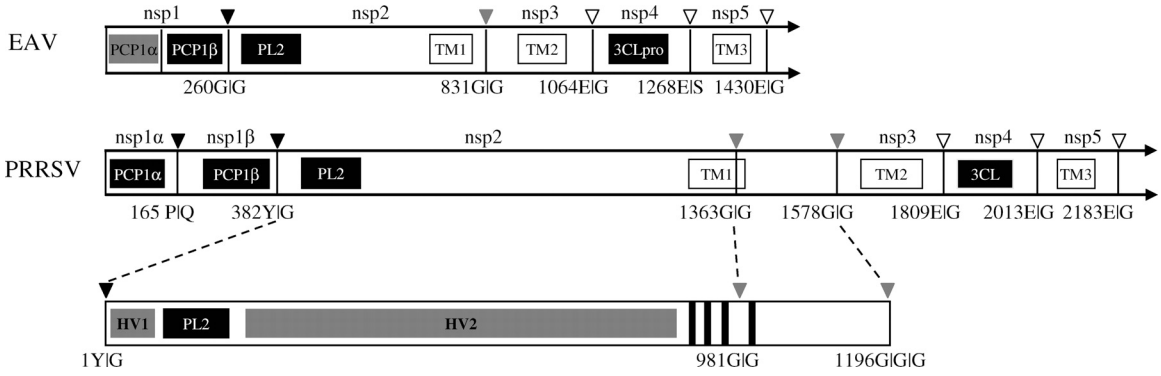
EAV
nsp1
nsp2
nsp3
nsp4
nsp5
PCP1α
PCP1β
PL2
TM1
TM2
3CLpro
TM3
260G|G
831G|G
1064E|G
1268E|S
1430E|G
PRRSV
nsp1α
nsp1β
nsp2
nsp3
nsp4
nsp5
PCP1α
PCP1β
PL2
TM1
TM2
3CL
TM3
165 P|Q
382Y|G
1363G|G
1578G|G
1809E|G
2013E|G
2183E|G
HV1
PL2
HV2
1Y|G
981G|G
1196G|G|G

Fig. 3.3. Construction of strain VR-2332 nsp2 mutants. Mutagenesis was completed to achieve products with in-frame deletions of the nsp2 region by overlapping PCR. The deleted amino acids are shown as a dashed line, and the relative positions are indicated in the individual mutant name. For the purpose of foreign gene expression, the GFP gene was inserted into the position where the region aa 324 to 434 of nsp2 was deleted to generate the mutant V7-nsp2Δ324-434-GFP. The putative enzyme domain and TM region as well as the predicated cleavage sites are shown. The viability for each mutant constructed is shown on the right: +, viable; –, nonviable

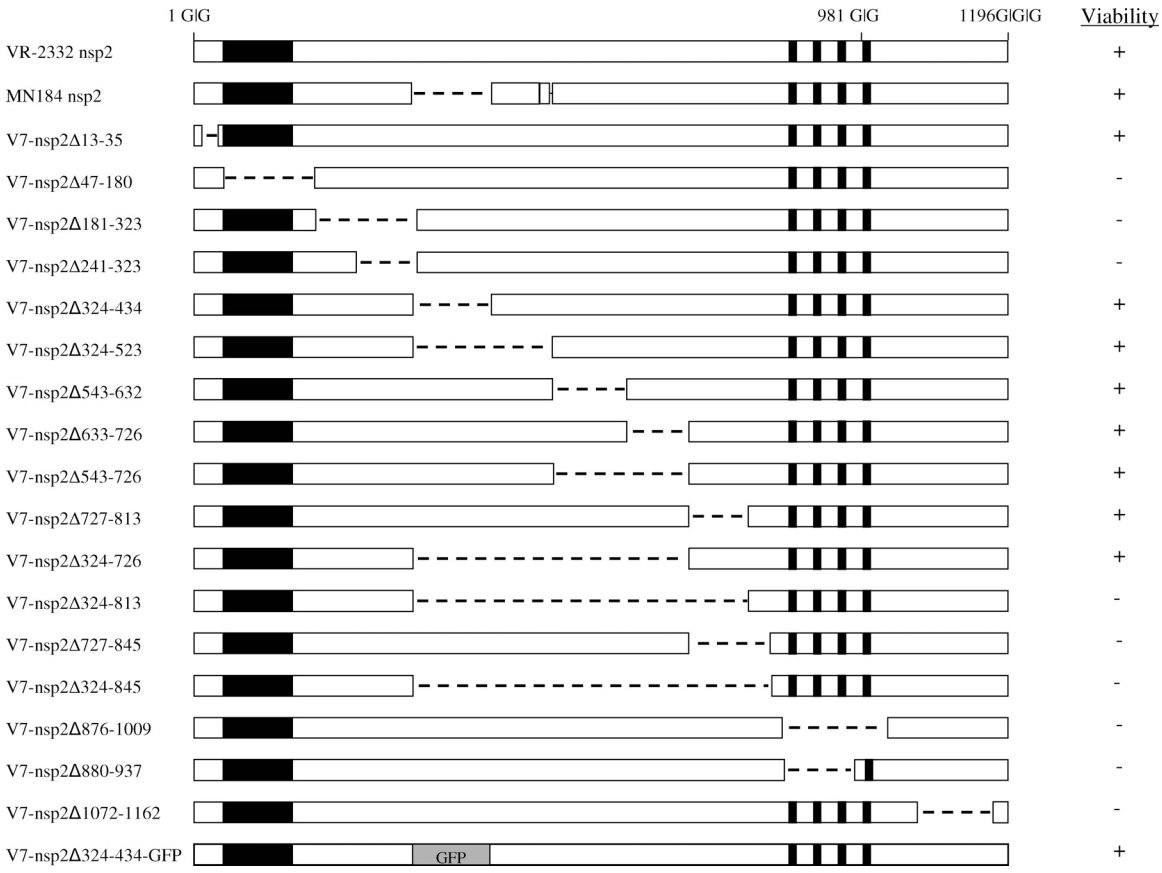
1 GlG
981 GlG
1196GlGlG
Viability
VR-2332 nsp2
MN184 nsp2
V7-nsp2Δ13-35
V7-nsp2Δ47-180
V7-nsp2Δ181-323
V7-nsp2Δ241-323
V7-nsp2Δ324-434
V7-nsp2Δ324-523
V7-nsp2Δ543-632
V7-nsp2Δ633-726
V7-nsp2Δ543-726
V7-nsp2Δ727-813
V7-nsp2Δ324-726
V7-nsp2Δ324-813
V7-nsp2Δ727-845
V7-nsp2Δ324-845
V7-nsp2Δ876-1009
V7-nsp2Δ880-937
V7-nsp2Δ1072-1162
V7-nsp2Δ324-434-GFP
GFP
+
+
+
-
-
-
+
+
+
+
+
+
+
-
-
-
-
-
-
+

Fig. 3.4. Characterization of nsp2 small mutants. **(A)** Identification of viable nsp2 mutant viruses by RT-PCR, as shown in the schematic. One primer set (a/b; indicated for each mutant below) was used to confirm the presence of a mutant virus in the odd-numbered lanes, while another primer set (c/d; indicated for each mutant below) was used to ensure there was no contamination with parental virus in the even-numbered lanes. The detection of mutants nsp2Δ13-35 (VR-1051U27/VR-1712L26 [618 bp]), nsp2Δ324-434 (dVR-67U22/VR-3349L26 [875 bp]), nsp2Δ324-523 (dVR-67U22/VR-3349L26 [608 bp]), nsp2Δ543-632 (VR-2393U32/VR-3349L26 [712 bp]), nsp2Δ633-726 (VR-2812U22/VR-3847L34 [787 bp]), nsp2Δ727-813 (VR-2812U22/VR-3847L34 [808 bp]), nsp2Δ543-726 (VR-2393U32/VR-3847L34 [936 bp]), and nsp2Δ324-726 (dVR-67U22/VR-38474258L31 [904 bp]) is shown in lanes 1, 3, 5, 7, 9, 11, 13, and 15, respectively, and the corresponding detection of wild-type or parental virus contamination is shown in lanes 2 (VR-1371U18/VR-1712L26), 4 (VR-1824U24/VR-2430l24), 6 (VR-2812U24/VR-3349L26), 8 (67U22/VR-3080L37), 10 (VR-3331U26/VR-3847L34), 12 (VR-3667U26/VR-4258L31), 14 (VR-3331U26/VR-3847L34), and 16 (VR-3331U26/VR-4285L31). M refers to a 1-kb DNA ladder (New England Biolabs). **(B)** Plaque assays for *wt* VR-2332, VR-V7, and nsp2 mutants were completed in parallel. MARC-145 cells were infected with viruses, and monolayers were stained with crystal violet at 4 days postinfection, while mutant V7-nsp2Δ324-726 was developed 8 to 10 days postinfection. **(C)** Viral growth curve analysis. MA-104 cells in T-25 flasks were infected with PRRSV nsp2 small deletion mutants and parental virus at an MOI of 10^4 PFU. The cell supernatants were collected for titration analysis by viral plaque assay at different time points. The virus was titrated on MA-104 cells. **(D)** Northern blot analysis of viral RNA (vRNA) synthesis. MARC-145 cells in T-75 flasks were inoculated with 10^3 $TCID_{50}$ of viruses, and the intracellular RNAs were extracted at 30 hpi. The viral genomic RNA and subgenomic mRNAs 2 to 7 produced by *wt* VR-2332 (lane 1), VR-V7 (lane 2), V7-nsp2Δ13-35 (lane 3), V7-nsp2Δ324-434 (lane 4), V7-nsp2Δ324-523 (lane 5), V7-nsp2Δ543-632 (lane 6), V7-nsp2Δ633-726 (lane 7), V7-nsp2Δ543-726 (lane 8), V7-nsp2Δ727-813 (lane 9), V7-nsp2Δ324-726 P2-6 (lanes 10 to 14), and mock-infected MARC-145 cell control (lane 15) are shown. The viral RNAs were probed with an oligonucleotide complementary to ORF7.

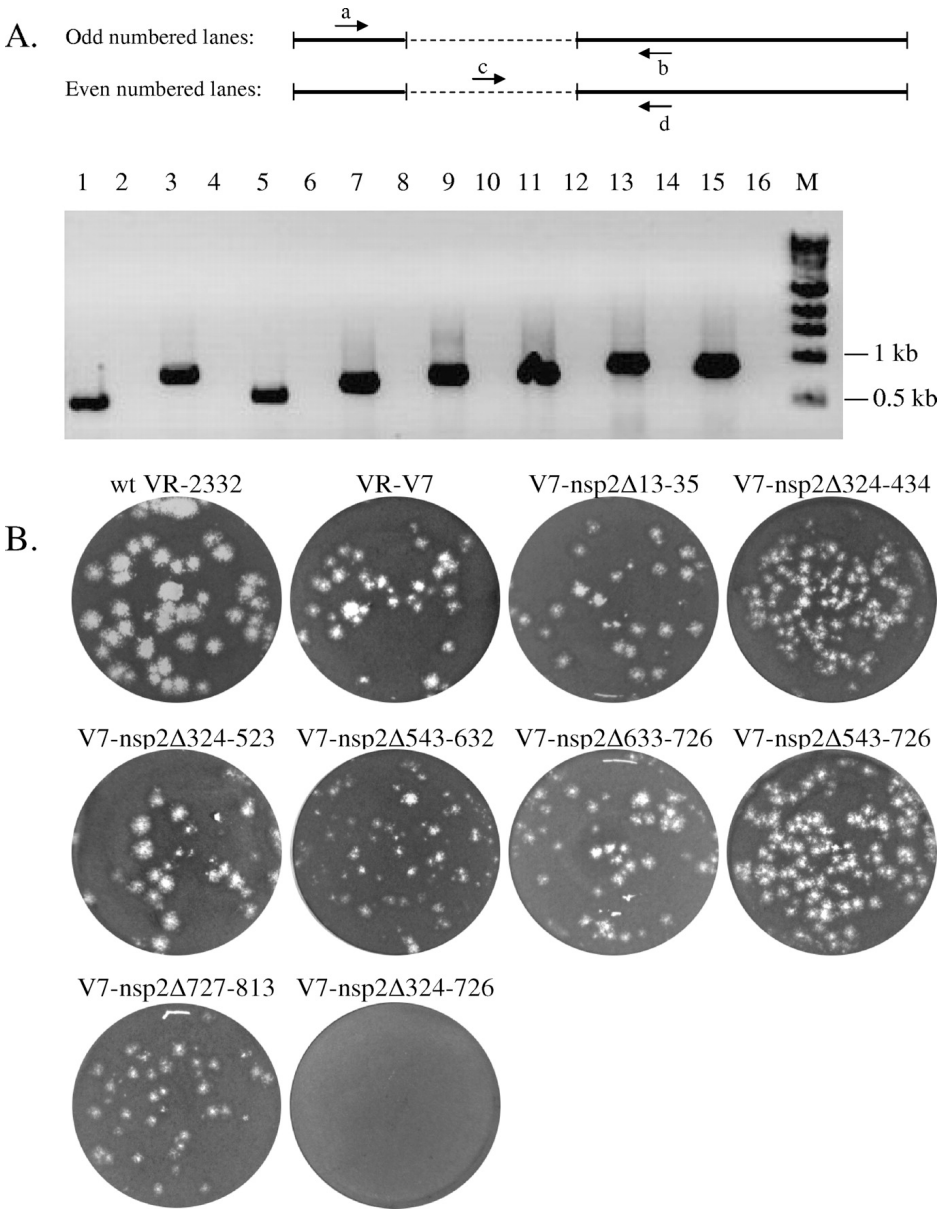
A.
Odd numbered lanes:
a
b
Even numbered lanes:
c
d
1 2 3 4 5 6 7 8 9 10 11 12 13 14 15 16 M
1 kb
0.5 kb
B.
wt VR-2332
VR-V7
V7-nsp2Δ13-35
V7-nsp2Δ324-434
V7-nsp2Δ324-523
V7-nsp2Δ543-632
V7-nsp2Δ633-726
V7-nsp2Δ543-726
V7-nsp2Δ727-813
V7-nsp2Δ324-726

C.

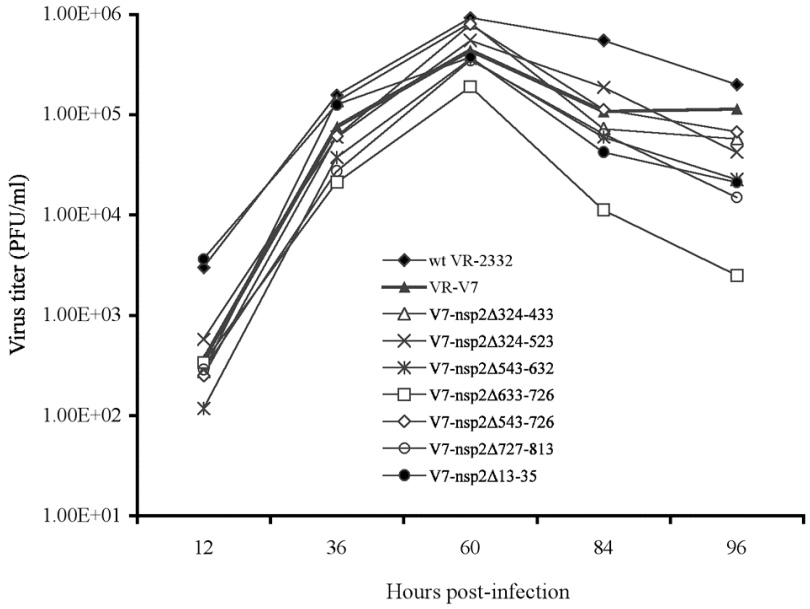
1.00E+06
1.00E+05
1.00E+04
1.00E+03
1.00E+02
1.00E+01
Virus titer (PFU/ml)
12
36
60
84
96
Hours post-infection
wt VR-2332
VR-V7
V7-nsp2Δ324-433
V7-nsp2Δ324-523
V7-nsp2Δ543-632
V7-nsp2Δ633-726
V7-nsp2Δ543-726
V7-nsp2Δ727-813
V7-nsp2Δ13-35

D.

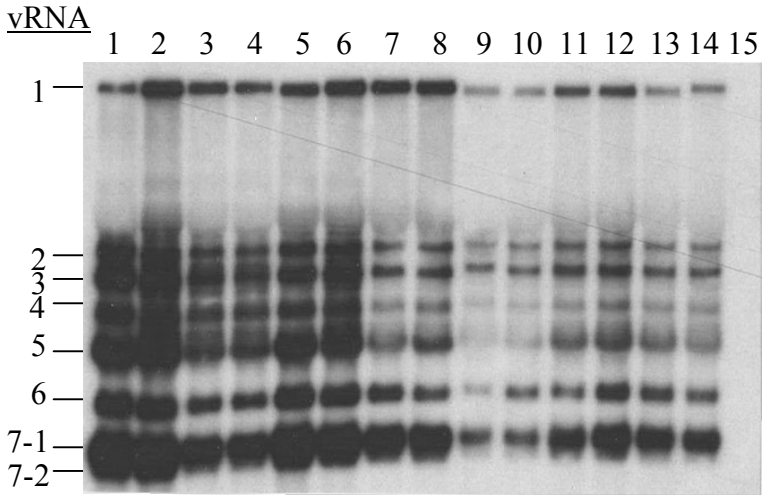
vRNA
1 2 3 4 5 6 7 8 9 10 11 12 13 14 15
1
2
3
4
5
6
7-1
7-2

Fig. 3.5. *In vitro* growth properties of V7-nsp2Δ324-726 mutant. (A) Six-well plates were infected with the mutant or left uninfected and incubated for plaque assay. After 9 days, the cells were observed before removal of agarose for virus-induced CPE foci under an inverted microscope. **(B)** Growth kinetics of V7-nsp2Δ324-726 P2, P3, and P6 as well as VR-V7 P3. The viruses were used to infect MARC-145 cells in T-25 flasks with an MOI of 10^3 $TCID_{50}$. The virus-infected cell supernatants were collected every 12 h and then titrated by using the $TCID_{50}$ assay. **(C)** Comparison of CPE development by VR-V7 and V7-nsp2Δ324-726 P6. MARC-145 cells in T-25 flasks were infected with VR-V7 P3 and V7-nsp2Δ324-726 P6 at an MOI of 10^3 $TCID_{50}$. Mock-infected cells served as a control. CPE was monitored daily under an inverted microscope (x20). The lower panel indicates the immunofluorescence detection of the viral nucleocapsid protein with monoclonal antibody SDOW-17 in V7-nsp2Δ324-726 P6-infected cells at 24, 48, and 60 hpi, respectively. DAPI was used to stain cell nuclei. The images (x20) were merged by the use of Adobe Photoshop.

A.

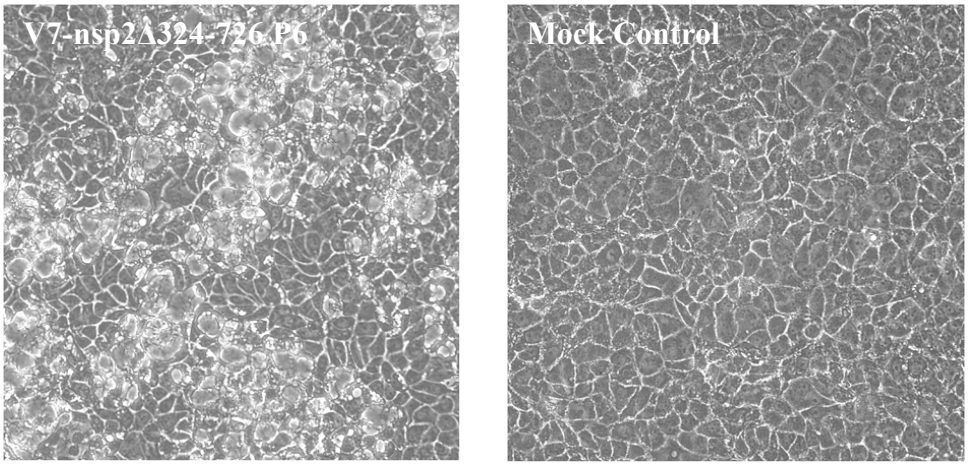
V7-nsp2Δ324-726 P6
Mock Control

B.

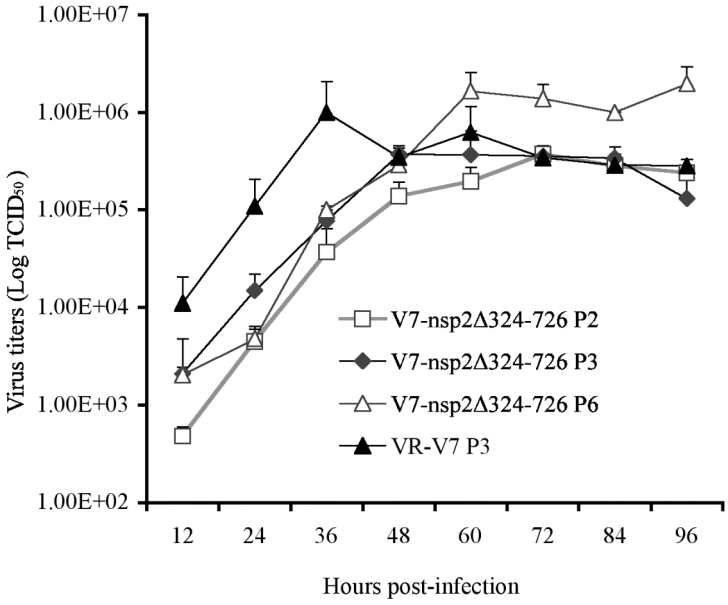
1.00E+07
1.00E+06
1.00E+05
1.00E+04
1.00E+03
1.00E+02
Virus titers (Log TCID50)
12
24
36
48
60
72
84
96
Hours post-infection
V7-nsp2Δ324-726 P2
V7-nsp2Δ324-726 P3
V7-nsp2Δ324-726 P6
VR-V7 P3

C.

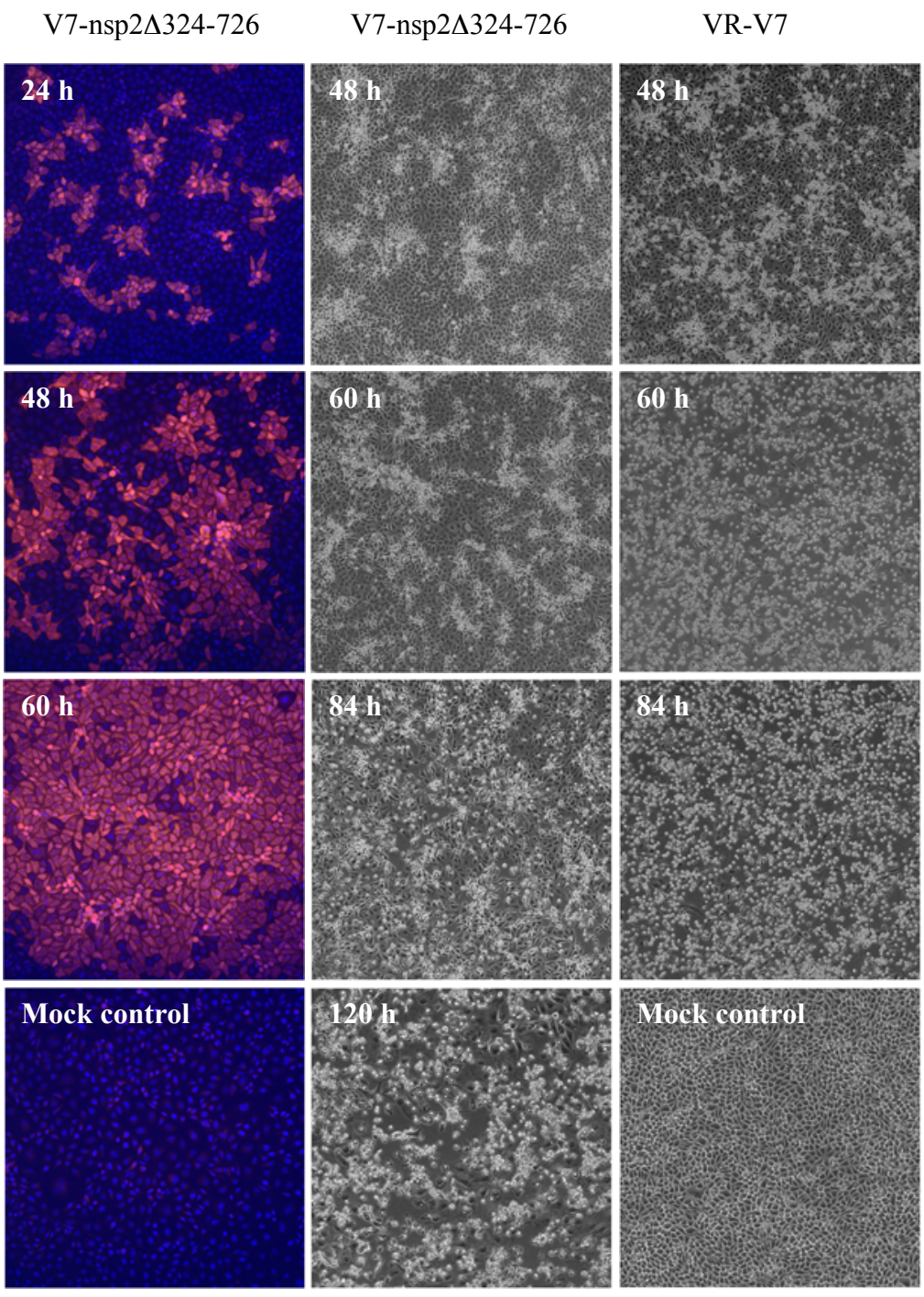
V7-nsp2Δ324-726
V7-nsp2Δ324-726
VR-V7
24 h
48 h
48 h
48 h
60 h
60 h
60 h
84 h
84 h
Mock control
120 h
Mock control

Fig. 3.6. Utilization of nsp2 to express foreign gene. Viable GFP recombinant virus was generated in MA-104 cells. (**A and B**) Light (A) and fluorescence (B) (x10) microscopy under the same field showed the fluorescence was associated with the virus-infected foci. **(C)** A similar field was stained with DAPI (blue) to visualize the cell nucleus (x100). **(D)** Titration of V7-nsp2Δ324-434-GFP P1 to -5. **(E)** Stability analysis of the GFP gene by RT-PCR with primers (dVR-67U22/dVR-1307L24) across the GFP gene. Lane M is a 1-kb DNA ladder (New England Biolabs), and lanes 1 to 5 represent V7-nsp2Δ324-434-GFP P1 to -5, respectively.

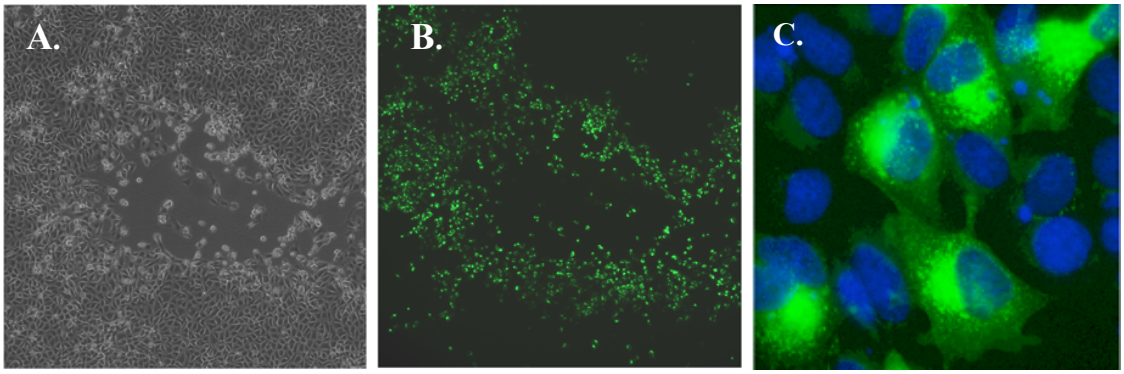
A.
B.
C.

D.

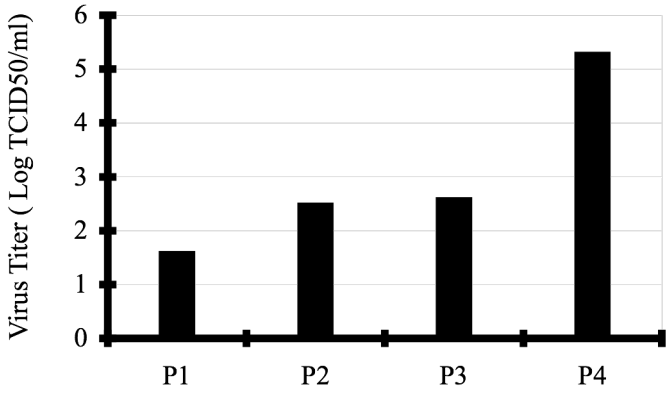
Virus Titer (Log TCID50/ml)
6
5
4
3
2
1
0
P1
P2
P3
P4

E.

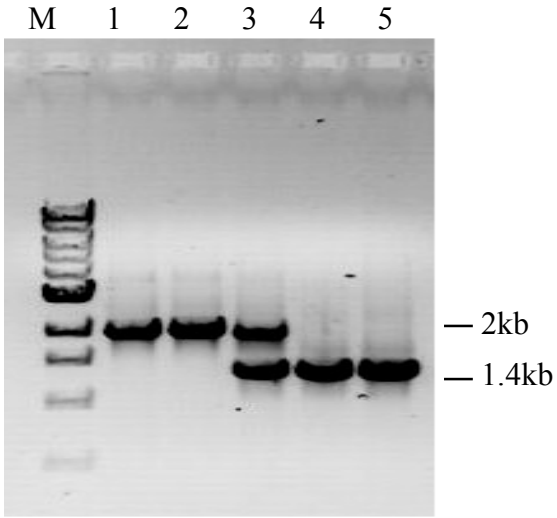
M
1
2
3
4
5
— 2kb
— 1.4kb

Chapter IV

Characterization of the Putative Cysteine Protease PL2 Domain Encoded in the N-terminus of the Nsp2 Replicase Protein of Porcine Reproductive and Respiratory Syndrome Virus

Abstract

The N-terminus of the nsp2 replicase protein of porcine reproductive and respiratory syndrome virus (PRRSV) contains a putative cysteine protease PL2 domain. In Chapter III, we showed that deletion of either the PL2 core domain or its immediate downstream region (aa181-323) was lethal to the virus. We now provide evidence that the PL2 domain encodes an active enzyme that mediates efficient processing of nsp2-3 in CHO cells. The PL2 protease possessed both *trans*- and *cis*-cleavage activities, which could be separated by point mutations in the protease domain. The minimal size required to maintain the respective enzymatic activity included the nsp2 region aa47-240 (Tyr^{47}-Cys^{240}) and aa47-323 (Tyr^{47}-Leu^{323}) correspondingly. Introduction of targeted amino acid substitutions in the protease domain confirmed that the putative Cys^{55}-His^{124} catalytic motif was important for nsp2/3 proteolysis, as were three additional conserved cysteine residues (Cys^{111}, Cys^{142} and Cys^{147}), and that the conserved aspartic acids (e.g. Asp^{89}) were essential for the PL2 protease *trans*-cleavage activity. Reverse genetics revealed that the *trans*-cleavage activity of the PL2 protease played an important in role in the PRRSV replication cycle in that mutations that impaired the *trans* function but not the *cis* activity of the PL2 protease were detrimental to viral viability. Last, the potential PL2 cleavage site was probed. We showed that mutations with the largest impact on *in vitro* cleavage were positions at the $G^{1196}|G^{1197}$ dipeptide, corresponding to previously predicted cleavage site.

Introduction

Porcine reproductive and respiratory syndrome virus (PRRSV) is the causative agent of porcine reproductive and respiratory syndrome (PRRS), a prevalent and devastating swine disease (17, 37, 41, 248, 249). PRRSV is a positive-strand RNA virus with a genome size of about 15.4kb (152, 162), and together with equine arteritis virus (EAV), murine lactate dehydrogenase-elevating virus (LDV) and simian hemorrhagic fever virus (SHFV), form the family *Arteriviridae* of the order *Nidovirales* (29). PRRSV shares similar genome organization with its family members and contains at least nine open reading frames (ORFs) (208). ORF1a and ORF1b encode the viral replicase proteins pp1a and pp1b at the 5'end, while ORF2-7s at the 3'end of the genome code for viral structural proteins expressed from subgenomic RNAs that are generated through a discontinuous transcription mechanism (177, 208). Replication of PRRSV involves translation of two precursor polyproteins pp1a and pp1ab. The subsequent proteolytic maturation is thought to be mediated by virally encoded proteases, which produce at least 12 mature nonstructural proteins required for viral RNA replication (84, 277).

The nonstructural protein 2 (nsp2) of PRRSV is a multidomain protein located immediately adjacent to nsp1 within ORF1a. It possesses a putative cysteine protease PL2 domain, a 500-700 amino acid middle hypervariable region with unknown function, a transmembrane domain and C-terminal tail (90, 92). The PL2 domain of PRRSV has a predicted core size of about 100aa (nsp2aa 47-147) and is believed to cleave the downstream nsp2|3 junction site similar to its EAV PL2 counterpart (212, 213). The PL2 protease core of PRRSV nsp2 is well conserved not only among PRRSV strains but also among the arterivirus family, especially for the putative Cys^{55}-His^{124} catalytic dyad (numbering according to the sequence of PRRSV strain VR-2333 nsp2). The arterivirus PL2 protease is a hybrid of papain-like cysteine proteases and chymotrypsin-like cysteine proteases (60, 68, 210, 211, 213, 277) in that it possesses both the signature Cys-His catalytic motif of viral papain-like proteases as well as the marker of chymotrypsin-like cysteine proteases in which the putative catalytic Cys^{55} is always followed by Gly^{56} instead of an amino acid with a large side chain as seen in papain-like proteases. Using a PRRSV reverse genetics system, we recently showed that deletion of either the predicted

PL2 protease core domain (aa47-180) or the immediate downstream region (aa181-323) is lethal to the virus (90).

In this report, we further characterized the nsp2 PL2 domain of PRRSV strain VR-2332. We showed that the putative PL2 protease possessed both *cis*- and *trans*-cleavage activities with a substrate preference for $G^{1196}|G^{1197}$ dipeptide for nsp2/3 proteolysis in CHO cells, and that the highly divergent C-terminal extension region (Ser^{181}-Cys^{240}) of the PL2 protease core domain (Tyr^{47}-Cys^{147}) was critical for the PL2 catalytic activity. In addition, mutagenesis studies identified specific residues important for PL2 protease activity including amino acids within the putative Cys^{55}-His^{124} catalytic motif, and revealed that the *trans*-cleavage activity of the PL2 protease could be distinguished from the *cis*-cleavage activity by point mutations, and played a very important role in the PRRSV replication cycle.

Materials and Methods

Antibodies. Antibodies used in this report include mouse monoclonal antibody to c-*myc* (9E10) (Developmental Studies Hybridoma Bank at the University of Iowa), rabbit polyclonal anti-c-*myc* antibodies (Abcam Inc., Cambridge, MA), mouse anti-hemagglutinin epitope (HA) antibodies (Covance Research Products, Denver, CO), mouse anti-FLAG epitope antibodies (M2, Sigma, St. Louis, MO) and HRP conjugated anti-mouse IgG or anti-rabbit IgG secondary antibodies (SouthernBiotech, Inc., Birmingham, AL). The rabbit polyclonal antibody V (Covance) was raised against a peptide contained within PRRSV VR-2332 nsp2 region aa1078-1094 (SEKPIAFAQLDEKKITA).

Plasmids. The constructs were made by standard recombinant DNA procedures. To create a HA-FLAG epitope tagged vector, a linker containing HA-FLAG epitopes was inserted into the position between *Xba*I and *Apa*I in the plasmid vector pcDNA3.0 (Invitrogen) to generate pcDNA3/HA-FLAG. The plasmid pV7-nsp2Δ324-433-GFP was reported previously (90). The GFP gene was replaced by 3 copies of the c-*myc* epitope (EQKLISEEDL) to generate plasmid pV7-nsp2dΔ324-433-*myc*. The constructs expressing specific regions of nsp2 were generated by PCR amplification from plasmid pV7-nsp2Δ324-433-*myc*. Briefly, the region coding for nsp2-3 (ORF1a nt1401-5618)

was amplified, digested with *Bam*HI and *Xba*I, and then cloned into pcDNA3/HA-FLAG to generate pNsp2-3. The nsp2-3 is in frame with the HA-FLAG tag. Similarly, the region of PRRSV VR-2332 nucleotides (nt) 2057-5618 was cloned to generate pNsp2-3Δ1-240. To generate pPL2 (12-323), the region of PRRSV VR-2332 genome nt 1371-2305 (nsp2 region aa12-323) was amplified and digested with *Hind*III and *Xho*I, and then cloned into pcDNA3. The PL2 truncation constructs including pPL2 (12-240), pPL2 (12-180), pPL2 (12-160), pPL2 (47-323), pPL2 (47-240), pPL2 (47-180) and pPL2 (47-160) were generated in a similar way. A 10 amino acid c-*myc* epitope was attached to the carboxyl terminus of all the PL2 truncation mutants. The plasmids pNsp2-3Δ181-323, pNsp2-3Δ241-323, and pNsp2-3Δ324-813 were generated from the infectious cDNA clone plasmids pV7-nsp2Δ181-323, pV7-nsp2Δ241-323, and pV7-nsp2Δ324-813 (90) respectively by insertion of the corresponding nsp2-3 deletion fragment into the vector pcDNA3/HA-Flag through PCR amplification. A c-*myc* epitope was added to the N terminus of the nsp2 protein. All the constructs included a Kozak core sequence GCCACCATGG for optimal translation. Primers utilized for construction of these clones are listed in Table 1.

Site-directed mutagenesis. The plasmids pPL2 and pNsp2-3 were subjected to site-directed mutagenesis by using the Quickchange XL Site-directed Mutagenesis Kit (Stratagene, La Jolla, CA) according to the manufacturer's instructions. For mutagenesis of the infectious cDNA clone pVR-V7, the mutations were first introduced in the shuttle plasmid pOK-I or pOK-II (12). After verification by sequencing, the digested fragment I or II was transferred to the PRRSV strain VR-2332 infectious clone backbone (pVR-V7) as described previously (90).

Cell culture and transfection. MARC-145 cells (ATCC CRL-11171) and CHO cells (Invitrogen) were maintained in EMEM supplemented with 10% fetal bovine serum (FBS) at 37°C with 5% CO_2. Transient plasmid transfections of CHO cells were carried out according to Invitrogen's transfection protocol. Briefly, 10μl lipofectamine 2000 (Invitrogen) and 8-10μg plasmid diluted in 1ml Opti-MEM were added onto CHO cell monolayers in 60mm petri dishes. The transfection medium was removed after 4h of incubation and fresh culture medium (1X EMEM with 10% FBS) was added. At 48h

post-transfection, the cells were lysed with RIPA buffer (50mM Tris-HCl PH 7.4, 1% NP-40, 0.5% Na-deoxycholate, 150mM NaCl, 1mM EDTA and cocktail protease inhibitors). For transfection of the monocistronic construct, 10μg of each nsp2-3 mutant were transfected into CHO cells in 60mm petri dishes. For the co-transfection, 6μg of each PL2 mutant was co-transfected with 5μg of the substrate plasmid pNsp2-3Δ1-240. For RNA transfection of MARC-145 cells, the full-length infectious clone plasmids were *in vitro* linearized, purified, transcribed and transfected as described previously (90, 164).

Detection and titration of mutant viruses. After transfection of full-length RNA transcripts into MARC-145 cells, virus-induced cytopathic effect (CPE) was monitored daily as characterized by cell rounding and detachment. For transfections that did not induce CPE by 72h, the cell supernatants were collected and blindly passaged onto fresh monolayers for three times. Total intracellular RNAs were extracted using the RNAeasy Mini Kit (Qiagen, Valencia, CA) and PRRSV was detected by RT-PCR using primers targeting ORF7 encoding viral nucleocapsid protein. For viable viruses, passage 1 mutants were titrated by the end point dilution assay and expressed as 50% tissue culture infective doses ($TCID_{50}$) (Reed and Muench, 1938). The parental infectious clone derived virus VR-V7 served as positive control (90).

Immunoprecipitation and western blot. Transfected CHO cells were rinsed twice with cold phosphate buffered saline (PBS; 0.14M NaCl, 2.7mM KCl, 10mM Na_2HPO_4, 1.5mM KH_2PO_4), and lysed with RIPA buffer on a platform shaker at 4°C for 30min. The cell debris was removed by centrifugation at 13,000 rpm for 25min. The supernatants were then precleared by protein G or A agarose, then incubated with proper antibodies as well as protein G PLUS-agarose (Santa Cruz Biotechnology, Santa Cruz, CA) or protein A agarose (Roche, Nutley, NJ) at 4°C overnight. Immunocomplexes were washed twice with cold RIPA buffer, once with 0.1% SDS RIPA buffer and once with PBS. After boiling for 5min in loading buffer (Invitrogen) with 5% β-mercaptoethanol, the proteins were separated by SDS-PAGE and then electrophoretically transferred to a nitrocellulose membrane. For western blot analysis, the membrane was blocked with 5% milk powder in PBST (20mM $NaPO_4$, 140mM NaCl, 0.1% Tween-20) for 1h, and then incubated with appropriate primary antibodies diluted in PBST-5% milk overnight at 4°C. After washing

three times for 30min with PBST, the blot was incubated with the appropriate secondary antibody in PBST for 1h. The membrane was then again washed and developed with the ECL Western Blotting Analysis System (Pierce Chemical, Rockford, IL).

Results

Nsp2 was efficiently processed from nsp2/3 precursor. Previously, we demonstrated the viability of PRRSV strain VR-2332 with an insertion of the green fluorescence protein gene (GFP) in place of nsp2 nonessential region aa324-434 (90). To facilitate the analysis of nsp2 processing *in vitro* and to bypass the need for generating nsp2-specific antibodies, the GFP gene was replaced with 3 consecutive c-*myc* epitopes to generate a new plasmid pV7-nsp2Δ324-434-*myc*. The c-*myc* tagged nsp2-3 fragment corresponding to ORF1a aa394-1809 (C^{394}-E^{1809}) was then cloned into the vector pcDNA3/HA-FLAG to generate the plasmid pNsp2-3, with the carboxyl terminus of nsp3 fused to the HA-FLAG tag (Fig. 4.1A).

To determine if nsp2 is processed from the nsp2-3 precursor, pNsp2-3 was transfected into CHO cells. At 48h post-transfection, the cells were lysed and subjected to immunoprecipitation and western blot analysis. As shown in Fig. 4.1B, a major band of about 120kDa of nsp2 was detected by anti-c-*myc* antibodies (Fig. 4.1B, lane 2), but not by anti-HA antibodies (Fig. 4.1C, lane 2), demonstrating that the nsp2-3 precursor is processed. To detect the processed nsp3 protein, the cell lysates were immunoprecipitated with the anti-HA antibodies and followed by western blot with anti-FLAG antibodies. A specific band about 29kDa that corresponded to the predicted size of nsp3-HA-FLAG (28.7kDa) was detected (Fig. 4.1D, lane 1). Thus, these results suggest that nsp2 was efficiently processed in transfected CHO cells.

The PL2 domain mediated the nsp2/3 proteolysis. The PRRSV cysteine protease PL2 domain (Fig. 4.2A) is predicted (92, 213) to have a core size of about 100aa (Y^{47} to C^{147}) and is highly conserved among all arteriviruses (Fig. 4.2B). The Cys^{55}-His^{124} is the putative catalytic dyad (213, 277). To determine if the putative PL2 domain mediates the nsp2 processing, we adopted two approaches. First, we mutated the putative catalytic residue His^{124} to Cys (pNsp2-3 H124C). The nsp2-3 H124C mutant had a slower migration rate than the unmodified nsp2 (Fig. 4.1B, lane 2; Fig. 4.1C, lane 2) and could

be detected by both anti-c-*myc* (Fig. 4.1B, lane 1) and anti-HA antibodies (Fig. 4.1C, lane 1), suggesting that the H124C mutation abolished nsp2 processing. We also deleted the region of nsp2 aa1-240 containing the PL2 domain (pNsp2-3Δ1-240; Fig. 4.1A). We hypothesized that if the PL2 domain mediates the processing of nsp2-3, deletion of the protease domain would render nsp2-3Δ1-240 uncleaved. Anti-c-*myc* and anti-HA antibodies detected the intact nsp2-3Δ1-240 precursor after transfection into CHO cells (Fig. 4.1E, lanes 1 and 3). Thus, the PL2 domain is responsible for the nsp2/3 proteolysis.

We also detected an additional nsp2-specific band with a molecular weight of around 70-80kDa (Fig. 4.1B, lanes 1 and 2). This is likely a product cleaved by a cellular protease since it could be detected under the condition in which the viral PL2 protease activity was blocked by a H124C mutation (Fig. 4.1B, lane 1) and after deletion of the PL2 domain (Fig. 4.1E, lane 1). The latter band possessed a smaller size (51kDa) due to truncation of the N-terminal PL2 domain (24kDa). Therefore, we conclude that the major band corresponding in size to nsp2 is processed by the PRRSV PL2 protease while the minor product (70-80kDa) is cleaved by an unknown cellular protease.

The PL2 domain possessed *trans*-cleavage activity. To test if the PL2 protease is *trans* active, the fragment corresponding to nsp2 aa12-323 (Cys^{12}-Leu^{323}) was cloned into pcDNA3 to generate construct pPL2 (Fig. 4.3A). The rationale for including downstream flanking sequence of the predicted PL2 core domain was that the nsp2 aa181-323 is critical for viral viability as previously demonstrated in a PRRSV reverse genetics system (90). To facilitate the detection of the encoded peptide, a c-*myc* epitope tag was added to the C-terminus of the protein (Fig. 4.3A). To test the *trans*-cleavage activity of the PL2 domain, the plasmid pPL2 was co-transfected along with pNsp2-3 H124C into CHO cells, and transfection of the single plasmid pPL2 or pNsp2-3 H124C served as control. At 48 hours post transfection, CHO cells were lysed and immunoprecipitated with anti-c-*myc* monoclonal antibodies (9E10), followed by western blotting with anti-c-*myc* polyclonal antibodies or anti-HA antibodies. As shown in Fig. 4.3B, when the PL2 domain was *trans* provided, the substrate nsp2-3 H124C underwent efficient proteolytic cleavage (Fig. 4.3B, lane 2; Fig. 4.3C, lane 2), and the processed nsp2 had a faster migration rate than the unprocessed nsp2-3 precursor (Fig. 4.3B, lane 3). In contrast,

when the H124C mutation was introduced into the *trans* provided PL2 domain (Fig. 4.3A), the PL2 H124C failed to cleave the substrate as shown by the detection of nsp2-3 precursor using anti-HA antibodies (Fig. 4.3D, lane 3). Thus, we conclude that the PL2 protease possesses *trans*-cleavage activity.

The PL2 *trans*-cleavage activity required nsp2 N-terminal region aa47-240. To identify the catalytic core for the PL2 *trans*-cleavage activity, a series of deletion mutants based on the parental plasmid pPL2 (12-323) were generated (Fig. 4.4A). Initially, three C-terminal truncation mutants [pPL2 (12-240), pPL2 (12-180) and pPL2 (12-160)] were cotransfected with the substrate plasmid pNsp2-3Δ1-240. Only PL2 (12-240) could effectively cleave the substrate nsp2-3Δ1-240 (Fig. 4.4B, lanes 8 and 9). Both the PL2 (12-180) and PL2 (12-160) truncated mutants lost the ability to cleave in *trans* (Fig. 4.4B, lane 6 and 7). This suggested that the residues between 181-240 were required for *trans* proteolytic activity. Our previous work showed that nsp2 aa12-35 is dispensable for nsp2 function (90). Alignment of the nsp2 PL2 domain revealed that the region of nsp2 aa12-46 is highly divergent among PRRSV strains (data not shown). Therefore, we made four N-terminal truncation mutants: pPL2 (47-323), pPL2 (47-240), pPL2 (47-180), and pPL2 (47-160) (Fig. 4.4A). We found that nsp2-3Δ1-240 was efficiently processed when cotransfected with either pPL2 (47-323) or pPL2 (47-240) (Fig. 4.4B, lane 4 and 5), but not when further truncations of the carboxyl terminus were tested. Increasing the amount of mutant PL2 domain plasmid did not result in observable cleavage of the substrate (data not shown). We did not make further N-terminal truncations since a C55A mutation inactivated the protease, described below (see Fig. 4.6A, lane 1).

The PL2 downstream flanking sequence aa181-323 was critical for nsp2/3 proteolysis in monocistronic condition. The above experiment demonstrated that the flanking sequence aa181-240 of PL2 core domain is critical for the PL2 protease activity in *trans*. To test if the similar region is important for nsp2/3 cleavage under monocistronic condition, we generated two constructs: pNsp2-3Δ181-323 and pNsp2-3Δ241-323. A c-*myc* epitope tag was fused to the N terminus of nsp2 (Fig. 4.5A). As shown in Fig. 4.5B, deletion of nsp2 aa181-323 completely blocked proteolytic processing of itself, as it was detected by both anti-c-*myc* and anti-HA antibodies (Fig.

4.5B, lane 4). Expression of the mutant nsp2-3Δ241-323 appeared unstable and could not be detected (data not shown). However, when a G1197P mutation was introduced to block the putative cleavage site of nsp2, the precursor nsp2-3Δ241-323 G1197P was readily detected by both anti-c-*myc* and HA antibodies (Fig. 4.5B, lane 7). When the plasmid pNsp2Δ241-323 G1197P or pNsp2-3Δ181-323 G1197P was cotransfected with the substrate plasmid pNsp2Δ1-240, nsp2-3Δ1-240 was efficiently cleaved by nsp2Δ241-323 G1197P (Fig. 4.5B, lane 6), but not by nsp2-3Δ181-323 (Fig. 4.5B, lane 3), consistent with the above results showing that aa241-323 was not essential for the PL2 *trans* activity. Therefore, we conclude that nsp2 aa181-323 plays a crucial role in *cis* cleavage of nsp2.

The nsp2 hypervariable region was not essential for proteolysis. Previously, we showed that PRRSV nsp2 could tolerate deletions in the hypervariable region of nsp2 aa324-813 (90). To evaluate the role of this hypervariable region in the processing of nsp2 protein, we cloned the fragment nsp2-3Δ324-813 from the cDNA clone plasmid pVR-V7-nsp2Δ324-813 (90), and generated the new plasmid pNsp2-3Δ324-813 (Fig. 4.5A). A c-*myc* epitope was attached to the N terminus of nsp2. At 48 h post transfection of the plasmid into CHO cells, a band corresponding to the processed nsp2Δ324-813 was readily detected by the anti-*myc* antibodies (Fig. 4.5C, lane 1), although a small amount (<10%) of intact nsp2-3 precursor could still be observed. When the putative cleavage site was blocked with a G1196P mutation, the processing of the nsp2-3 substrate was blocked (Fig. 4.5C, lane 2 and 5). Interestingly, we detected two isoforms of the precursor nsp2-3Δ324-813, which could be due to posttranslational modifications or degradation. In conclusion, the nsp2 hypervariable region aa324-813 is not essential for the PL2 protease to process its downstream substrate.

Separation of *cis*- and *trans*-cleavage activity of the PL2 protease by site-directed mutagenesis. We tested the role of several conserved amino acids in the PL2 domain for their impact on protease activity. Alignment of arterivirus PL2 proteases (Fig. 4.2B) revealed complete conservation at positions Cys^{55}, Gly^{56}, Trp^{86}, Cys^{111}, His^{124}, Trp^{125}, Cys^{142}, and Cys^{147}. Among these, Cys^{55}-Gly^{56}-His^{124}-Trp^{125} is the putative catalytic motif. We also examined several aspartic acid residues that are commonly involved in the

protease activity of several virus-encoded chymotrypsin-like serine or cysteine proteases (68, 199, 200, 277). The aspartic acid residues at positions 85, 89 and 91 are well conserved among PRRSV isolates but not among arteriviruses (Fig. 4.2B). The effect of amino acid substitutions on proteolysis was tested both as the monocistronic construct pNsp2-3 (referred to as "*cis* condition") and in a co-transfection assay (referred to as "*trans* condition"). After 48h of transfection, the cells were lysed and the proteins were analyzed by immunoprecipitation with mouse anti-c-*myc* monoclonal antibody 9E10 and western blot with rabbit anti-c-*myc* polyclonal antibodies or mouse anti-HA antibodies. The results representing 3 independent experiments, are shown in Fig. 4.6A and B.

Consistent with the findings of mutagenesis of the EAV PL2 domain (30), both C55A and H124C mutations blocked proteolytic activity in either *cis* or *trans* conditions (Fig. 4.6A, lanes 1 and 12; Fig. 4.6B, lanes 1 and 11), suggesting their important role in catalysis. For the other three conserved cysteine residues (Cys^{111}, Cys^{142} and Cys^{147}), mutagenesis results revealed different phenotypes. Replacement of Cys^{111} by alanine (C111A) abolished the processing of nsp2-3 in both situations (Fig. 4.6A, lane 11; Fig. 4.6B, lane 10). In contrast, a C147A substitution appeared more detrimental to proteolysis in *trans* than in *cis* since the mutation only partially inhibited cleavage in *cis* (Fig. 4.6A, lane 14) but completely blocked in *trans* proteolysis (Fig. 4.6B, lane 15). Substitution of cysteine with an alanine residue severely affected the expression level of PL2 C142A (Fig. 4.6B, lane 13 bottom panel). When tested in the co-transfection assay, the PL2 C142A mutant failed to cleave the substrate nsp2-3Δ1-240 (Fig. 4.6B, lane 13). An extended incubation time up to 60 h or increased transfection amount (10μg) of the plasmid pPL2 C142A did not result in processing of substrate (data not shown).

We also tested the importance of the residues following the Cys^{55}-His^{124} dyad. As reported previously (213), the catalytic residue Cys^{55} is always followed by the small amino acid Gly^{56}, not the bulky hydrophobic residue Trp, as is characteristic of papain-like proteases. In EAV, a reversion of Gly to the canonical Trp completely inactivates EAV PL2 protease activity (213). Consistent with that, a G56W reversion also prevented the proteolysis of PRRSV nsp2/3 in both *cis* and *trans* conditions (Fig. 4.6A and B, lane 3). Conversely, a G56A replacement did not affect the processing of nsp2 in the *cis*

condition (Fig. 4.6A, lane 2) but partially impaired the PL2 protease activity in *trans* (Fig. 4.6B, lane 2). This suggests that an amino acid with a small side chain at position 56 is essential for optimal enzymatic activity for the PL2 protease *trans*-activity.

Next, we examined the role of the residue Trp^{125} that always follows the catalytic His^{124} in arteriviruses (Fig. 4.2B). A W125G substitution abrogated proteolytic activity in both *cis* and *trans* conditions (Fig. 4.6A, lane 13; Fig. 4.6B, lane 12). The same substitution for the conserved residue Trp^{86} did not affect the processing of nsp2 in the *cis* condition (Fig. 4.6A, lane 6), but interestingly partially impeded the protease activity in the *trans* condition (Fig. 4.6B, lane 5), suggesting the mutational effect is selective. Thus, these data suggests that the Trp^{125} is much more important for protease activity than the residue Trp^{86}.

Aspartic acid usually is the key catalytic residue in viral trypsin-like serine or cysteine proteases (68, 199, 200, 220, 277). The PL2 domain contains several aspartic acid residues that are highly conserved among PRRSV strains (Fig. 4.2B) and we hypothesized that some or all might be required in its catalytic motif (Cys-Asp-His). To test the hypothesis, we made conserved substitutions at positions 85, 89 and 91 to either asparagine or glutamate. The mutation of Asp^{91} to either asparagine or glutamic acid did not impair efficient cleavage of nsp2 in both *cis* and *trans* conditions (Fig. 4.6A lane 9 and 10; Fig. 4.6B, lane 8 and 9). The replacement of Asp^{85} to either asparagine or glutamic acid did not affect the processing of nsp2 in the *cis* condition (Fig. 4.6A, lane 4 and 5), but the D85N mutation partially impaired the proteolytic cleavage of the substrate in the *trans* condition (Fig. 4.6B, lane 4). Substitution of Asp^{89} by asparagine significantly impaired the substrate cleavage particularly in the *trans* (Fig. 4.6B, lane 6). Interestingly, a D89E mutation did not have an effect on nsp2 processing in *cis* condition (Fig. 4.6A, lane 8), but did impair the *trans*-cleavage activity of the PL2 protease (Fig. 4.6B, lane 7), suggesting an acidic amino acid is preferential for catalytic activity at this position.

Overall, we observed that mutations at several positions (G56A, D85N, W86G, D89N, D89E) resulted efficient cleavage in *cis* condition, but not in *trans* condition. The proteolysis of nsp2/3 in *cis* condition involves two possible mechanisms: *cis*- and *trans*-

cleavages in contrast to only one mechanism (*trans*-cleavage) in *trans* condition. The fact that mutations impaired the *trans*-cleavage in *trans* condition implied that the same mutation would also affect the PL2 *trans*-cleavage activity in *cis* condition. Since the nsp2 protein carrying the same mutations was efficiently processed in *cis* condition, this suggested that the PL2 protease most likely possessed *cis*-cleavage activity, which was used for nsp2 processing in *cis* condition. Therefore, we conclude that the PL2 protease possesses both *cis*- and *trans*-cleavage activities that could be distinguished by point mutations, which caused a specific loss of *trans* function but not *cis* activity

The *trans*-cleavage activity of the PL2 protease was essential for viral viability. The data above suggest that the *trans*-cleavage activity of the PL2 protease is more sensitive to mutations. To test whether the *trans*-cleavage activity of the PL2 protease plays an important role in the viral replication cycle, we introduced the same mutations into PRRSV strain VR-2332 cDNA clone pVR-V7 by site-directed mutagenesis. The plasmids containing the full-length PRRSV genome were linearized and transcribed *in vitro*. The full-length RNA transcripts were transfected into MARC-145 cells that support PRRSV entry and replication. Virus-induced CPE, characterized by cell rounding, clustering and detachment, was monitored daily. For mutants that did not result in visible CPE, we also tested for extracellular or intracellular viral RNA by RT-PCR after 3 passages of cell supernatants to new cell monolayers and 5 to 6 days subsequent to incubation. We observed that mutations that blocked cleavage of nsp2 in both *cis* and *trans* conditions were lethal to the virus since viable virus was not produced (Fig. 4.6C) and we failed to detect viral RNA by RT-PCR against ORF7 at passage 3 (data not shown). Mutations that partially blocked the processing of nsp2 in *trans* but did not alter the cleavage in the *cis* condition were also lethal to the virus (G56A, D85N, D89N and D89E). Mutations that did not affect efficient cleavage of nsp2 in CHO cells did not affect viral viability (D85E, D91N and D91E). The mutants V7-D91N and V7-D91E readily induced typical CPE similar to parental virus VR-V7 at 5-6 days after transfection. The mutant virus V7-D85E induced CPE at passage 1 but not post-transfection. We conclude from these results that a functional and efficient PL2 protease *trans*-cleavage activity is critical for viral viability in cell culture.

Identification of the PL2 cleavage site. In experiments described above, only one predominant band was detected following cleavage of the nsp2-3 substrate by the PL2 protease, suggesting a single cleavage site was recognized. Previously, two possible nsp2|3 cleavage sites (981G|G and 1196G|G) were proposed (3, 277). In order to differentiate the relative cleavage position, we synthesized a rabbit peptide antibody (V) against PRRSV VR-2332 strain nsp2 region aa1078-1094. The results demonstrated that the antibody V could recognize both nsp2 and nsp2-3 precursor as shown in Fig. 4.7B, suggesting the cleavage site is downstream of nsp2 aa1078-1094. Thus, we ruled out 981G|G as the potential cleavage site *in vitro*.

Alignment of the region surrounding the residues 1196G|G from 56 PRRSV strains suggests that the 1196G|G dipeptide is highly conserved (Fig. 4.7C). We next performed a series of amino acid substitutions from Lys^{1193} to Pro^{1199}. As shown in Fig. 4.7D, all positions were tolerant of an alanine substitution, except at position Gly^{1197} (Fig. 4.7D, lane 11). When substitutions with proline were introduced, the S1195P mutation only partially affected processing (Fig. 4.7D, lane 7). In contrast, the G1196P, G1197P or G1198P substitutions completely abolished cleavage of the substrate (Fig. 4.7D, lanes 10, 13 and 16), suggesting residues at the position 1996G|G|G were important for cleavage. Since a mutation from glycine to proline could potentially change the tertiary structure of a sequence, substitution to serine was tested in all these three positions. The results revealed that Gly^{1196} was sensitive to serine substitution with only partial cleavage observed (Fig. 4.7D, lane 9), and the G1197S mutation totally blocked the proteolysis (Fig. 4.7D, lane 12). In contrast, a serine mutation at Gly^{1198} did not affect processing (Fig. 4.7D, lane 15). Thus, the $G^{1196}|G^{1197}$ dipeptide was most susceptible to mutations that impaired PL2 protease processing.

The consequences of the mutations at 1196G|G|G were tested in the PRRSV reverse genetics system as described above. Titers for viable viruses were determined on MARC-145 cells. Mutations (G1196P, G1197S, G1197P and G1198P) that totally abolished nsp2 processing *in vitro* were lethal to the virus as neither titers or transcripts could be detected (data not shown) at passage three. Mutations (G1196A, G1198A and G1198S) that did not impair efficient cleavage of nsp2 *in vitro* did not affect viral viability (Fig. 4.7E), and

CPE was readily observed after 4-5 days post-transfection (data not shown). Introduction of mutations such as G1196S and G1197A that resulted in partial processing *in vitro* were detrimental to the virus. Viable virus could not be recovered through three continuous blind passages on MARC-145 cells, and no transcripts for the viral nucleocapsid gene was detected by RT-PCR at passage 3 (data not shown). Therefore, efficient processing of nsp2 appeared essential for productive production of infectious progeny in MARC-145 cells.

Discussion

We previously reported that deletion of the PRRSV nsp2 PL2 domain is lethal to the virus (90). Here, we further characterized the PL2 domain and we provided evidence that the N-terminus of nsp2 encodes a *cis* and *trans* active enzyme that is responsible for cleavage of nsp2 from the nsp2-3 precursor. Mutagenesis studies suggested that the processing most likely took place at the scissile bond of Gly^{1196}-Gly^{1197} and efficient cleavage was critical to ensure successful production of viral progeny. We also showed that the downstream flanking sequence of the PL2 protease core domain was crucial for catalysis. Furthermore, we provided evidence that in addition to the putative catalytic Cys^{55}-His^{124} dyad and the conserved cysteine residues (Cys^{111}, Cys^{142} and Cys^{147}), the aspartic acid residues (Asp^{85}, Asp^{89}) plays an important role in *trans*-cleavage activity and are critical for viral replication.

Several of our results for the PRRSV PL2 domain are consistent with that of the EAV PL2 protease. The PL2 proteases from both EAV and PRRSV show *trans* activity and are responsible for processing the nsp2-3 junction site with a substrate preference for the G|G dipeptide. Also, the putative Cys^{55}-His^{124} catalytic motif is critical for the PL2 protease activity in both viruses.

However, differences exist between the EAV PL2 and PRRSV PL2 proteases. Although both EAV nsp2 and PRRSV nsp2 have a similar domain organization in that a large middle region separates the N terminal protease and downstream substrate site, the PRRSV nsp2 middle hypervariable region is not critical for downstream processing and deletion of the region aa324-726 does not affect viral viability (90). In contrast, deletion of EAV nsp2 middle region blocks the cleavage *in vitro* (213). The proteases display

different susceptibilities to point mutations that affect *cis* versus *trans* cleavage. In EAV, point mutations in the PL2 domain give the same cleavage pattern in both conditions (213), whereas mutations in PRRSV PL2 domain (G56A, D85N, W86G, D89N and D89E) differentially affected the *cis* versus *trans*-cleavage activity. The Asp^{85}, Asp^{89}, and Asp^{91} residues are well conserved among PRRSV strains. In EAV, conserved substitutions of aspartic acid to asparagine or glutamic acid do not affect the processing in either the *cis* or *trans* condition (213). However, similar mutations in the PRRSV PL2 domain (Asp^{89}) affected *trans* processing but not *cis* processing. The inefficient processing of the D89N mutation *in trans* is not due to poor expression of the mutant (Fig. 4.6B, lane 6) and the control PL2 construct processed the substrate well (Fig. 4.6B, lane 15). The phenomenon of differential effects on *cis* vs. *trans* processing is not unique for the proteinases encoded by positive-stranded RNA viruses. Our data for the PRRSV PL2 protease very much resembles the case for poliovirus 2A protease in which site-directed mutagenesis could also separate *cis* and *trans* protease function (270). It is not clear how the D85N and D89N mutations impaired PRRSV PL2 *trans* activity but not *cis*-activity. Considering the role aspartate residues play in the viral encoded chymotrypsin-like serine or serine-like proteases and the different mechanisms by which the PL2 protease may access its substrate (e.g. polyprotein folding to oblige enzyme-substrate interaction in *cis* versus normal enzyme-substrate binding in *trans*) (199, 200, 220), the aspartate and other residues (e.g. G^{56}, D^{85}, D^{89} and W^{86}) most likely play a structural role for substrate binding rather than a direct involvement of catalysis. Resolving the crystal structure of the PL2 domain may eventually shed some insight concerning the catalytic mechanism.

We introduced site-directed mutations into the PRRSV infectious cDNA clone to test the importance of specific amino acid residues to the *trans* function of the PL2 protease in viral replication. The mutations that impaired the *trans*-cleavage activity but not *cis*-cleavage activity were surprisingly detrimental to the virus. Neither viable virus nor viral RNA was detected after several blind passages. Similar results are also found in poliovirus 2A mutants lacking *trans* function only (269). There are several possible explanations for the defective phenotype. First, the PL2 protease may be involved in

cleavage of a downstream replicase polyprotein in addition to processing of the nsp2|3 junction site. The EAV nsp2 has been shown to be a cofactor for nsp4, coding for a 3C-like serine protease (245). Therefore, PRRSV nsp2 may also assume an additional role that requires the *trans*-cleavage activity of the PL2 protease. Second, the PL2 protease may be multifunctional and exerts its *trans*-cleavage activity against host proteins required for anti-viral responses. In fact, many virus-encoded proteases are actively involved in suppressing host innate anti-viral immunity, including the hepatitis C virus NS3/4A protease that also cleaves the interferon promoter stimulator-1 (IPS-1), toll-like receptor 3 adaptor protein TRIF, and mitochondrial antiviral signaling protein (MAVS) to ablate interferon alpha/beta signaling (124, 125, 132). Other examples are the $2A^{pro}$ proteases from rhinoviruses and enteroviruses, which have also evolved to assume dual functions of primary processing of the viral polyprotein by *cis*-cleavage of its own N terminus and specific inhibition of host cell protein synthesis by *trans*-cleavage of host cell translation initiation factor eIF-4G, thus effectively halting cap-dependent translation of host mRNAs (89, 115). PRRSV represses interferon production (1, 155) as minimal amounts of interferon alpha and beta are produced during virus infection in pigs and in the supporting cell line MARC-145. Recently, it is revealed that PRRSV interferes with the RIG-1 signaling pathway and suppresses the activation of IRF3 (135). It is conceivable that ablation of the PRRSV PL2 *trans* cleavage activity may impair its ability to block intracellular innate immunity which renders the virus susceptible to host anti-viral responses. Lastly, it is also possible that the PL2 protease interacts with a host or viral factor during viral replication, as occurs for the 2A protein of poliovirus virus that binds to the 5' untranslated region of poliovirus RNA (136), and the mutations could potentially affect protein-protein/RNA interactions.

Site-directed mutagenesis showed the PL2 core domain downstream flanking sequence aa181-240 was critical for *trans*-cleavage activity and the nsp2 aa181-323 was important for *cis*-cleavage activity and protein stability. The importance of this region is also supported by previous data showing that deletion of either nsp2 aa181-323 or aa241-323 is lethal to PRRSV (90). Alignment of the nsp2 region aa181-323 shows it to be highly divergent with less than 10% amino acid identity between PRRSV North

American and European strains, but relatively conserved within PRRSV genotypes (75, 92, 192). However, regardless of the dramatic genetic variability, this region is rich in cysteine and histidine residues in both PRRSV genotypes. Although the molecular significance of this is unclear, the cysteine residues may play a role in inter- or intra-molecular interactions, or are involved in formation of a zinc binding structure. Such interactions could be critical for protease catalysis or to maintain a favorable structure for substrate binding, as observed for other virally encoded cysteine or serine proteases (199, 200, 277).

Protease-mediated replicase polyprotein maturation constitutes a very critical part of the replication cycle for positive stranded RNA viruses, which occurs in a highly delicate and orchestrated order. The mature subunits have been shown to be largely involved in the assembly of viral replication complexes. Correct identification of the cleavage site is a prerequisite for studying the function of a protein. Our site-directed mutagenesis study yielded results consistent with the previous prediction that the arterivirus PL2 proteases prefer a G|G dipeptide (39). The dipeptide $Gly^{1196}|Gly^{1197}$ was most susceptible to mutations as even a conservative G1197A substitution significantly impaired cleavage efficiency. A structurally less dramatic G1196S substitution partially blocked cleavage while a G1197S mutation completely abolished proteolytic processing. Meanwhile, the residue Gly^{1198} appeared unimportant for cleavage since neither a G1198A nor a G1198S mutation affected proteolysis by the PL2 protease. This was as expected because the Gly^{1198} is not completely conserved among PRRSV strains and is often substituted by an alanine residue. It appears that the $G^{1196}|G^{1197}$ dipeptide is spatially and structurally preferred in that the replacement of Gly^{1196} by serine did not cause the protease to cleave the $Gly^{1197}|Gly^{1198}$ dipeptide. Therefore, substrate recognition by PL2 protease may be not only sequence specific, but also structurally tuned. This might explain why PL2 did not, *in vitro,* recognize other conserved dipeptides ($G^{647}|G^{648}$, $G^{981}|G^{982}$, $G^{828}|G^{829}|G^{830}$) among PRRSV strains. Certainly, we cannot rule out the possibility that the PL2 protease may recognize and cleave these additional sites in PRRSV susceptible macrophages, perhaps with the help of host or viral cofactors.

In summary, we have identified PRRSV nsp2 PL2 domain as an active protease, which possessed both *trans* and *cis* cleavage activity that had a substrate recognition site of the $Gly^{1196}|Gly^{1197}$ dipeptide. The protease was likely found to use a Cys-Asp-His motif for its *trans*-cleavage activity. Importantly, *trans* and *cis* cleavage activity of the PL2 protease could be distinguished by aspartic acid residue mutations and played an important role in the PRRSV replication cycle. These findings establish the PL2 protease as a new therapeutic target for the development of anti-viral drugs against PRRSV infection.

Acknowledgements

This research was supported by a USDA NRI-CSREES grant (No. 2006-01598).

Table 4.1 Primers used in this study. Forward primers are indicated by a slash (/) or symbol (F) after the designator, reverse primers are preceded by a slash or symbol (R). Genome positions are based on GenBank Submission U87392 (VR-2332).

Primer	Genome Position	Sequence
Construction of nsp2, PL2 and their mutants		
HA-Flag Linker U100/	HA-FLAG	5′ CTGGCGGCCGCTCGAGCATGCATCTAGATACCCA TACGATGTTCCAGATTACGCTTATCCTTACGACGT CCCAGACTATGCCTGTACAGATTACAAGGAT
/HA-Flag Linker L100	HA-FLAG	5′ TAGCATTTAGGTGACACTATAGAATAGGGCCCTT ATCACTTGTCATCATCGTCCTTATAGTCCTTATCG TCGTCATCCTTGTAATCTGTACAGGCATAGT
Nsp2CP2 1U37/	1373-1387	5′ AGCT***AAGCTT***GCCACC**ATGGTG**GCGACTGCTACAGTC
/Nsp2PL2 941L60 (XhoI)		5′ ATG***CTCGAG***TTATCACAGATCCTCTTCTGAGATGA GTTTTTGTTCCAAGGACTTTTGAGT
/VR-5583L35	5558-5583	5′ CTA***TCTAGA***AGACCCAAGCTGGGACGGGGTAAACA
VR-2058U43 (BamHI)/	2055-2074	5′ CTC***GGATCC***GCCACC**ATG**GGATGTTCCCAGAACAA AACCAACC
Nsp2 47U77 (HindIII)/	1475-1500	5′ CCC***GGATCC***GCCACC**ATGGGAG**AACAAAAACTCAT CTCAGAAGAGGATCTGTACTCCCCGCCTGCCGAAGGGA ATTG
/VR-1784L60 (XhoI)	1786-1800	5′ ATG***CTCGAG***TTATCACAGATCCTCTTCTGAGATGA GTTTTTGTTCGGAACCAAGACCGCC
/VR-1859L60 (XhoI)	1862-1876	5′ ATG***CTCGAG***TTATCACAGATCCTCTTCTGAGATG AGTTTTTGTTCGCTAGGCAGGTGCAT
/VR-2039L60 (XhoI)	2042-2056	5′ ATG***CTCGAG***TTATCACAGATCCTCTTCTGAGATG AGTTTTTGTTCACAGCAGCAGTCCTC
VR-1475U47 (HindIII)/	1475-1499	5′ AGCT***AAGCTT***GCCACC**ATGGTG**TACTCTCCGCCT GCCGAAGGGAATT
PL2 1U37/	1373-1387	5′ AGCT***GGATCC***GCCACC**ATGGTG**GCGACTGCTACAGTC
pcDNA 726U25/		5′ CAACGGGACTTTCCAAAATGTCGTA
/pcDNA 1066L22		5′ ACGGGGGAGGGGCAAACAACAG
POK12 19U25/		5′ CTCCCCGCGCGTTGGCCGATTCATT
/POK 354L23		5′ AGCAGCCGGATCCGAGCTCTCCC
Site-directed mutagenesis of the PL2 protease domain and the potential cleavage site		
C55A F	1482-1519	5′ CGCCTGCCGAAGGGAATGCTGGTTGGCACTGCATTTC
C55A R	1482-1519	5′ GAAATGCAGTGCCAACCAGCATTCCCTTCGGCAGGCG
G56W F	1487-1520	5′ GCCGAAGGGAATTGTTGGTGGCACTGCATTTCCG
G56W R	1487-1520	5′ CGGAAATGCAGTGCCACCAACAATTCCCTTCGGC
G56A F	1489-1519	5′ CGAAGGGAATTGTGCTTGGCACTGCATTTC
G56A R	1489-1519	5′ GAAATGCAGTGCCAAGCACAATTCCCTTCG
D85E F	1571-1603	5′ AGAGTGAGACCTCCAGATGAATGGGCTACTGAC
D85E R	1571-1603	5′ GTCAGTAGCCCATTCATCTGGAGGTCTCACTCT
D85N F	1572-1604	5′ GAGTGAGACCTCCAGATAACTGGGCTACTGACG
D85N R	1572-1604	5′ CGTCAGTAGCCCAGTTATCTGGAGGTCTCACTC
W86G F	1578-1606	5′ GACCTCCAGATGACGGGGCTACTGACGAG
W86G R	1578-1606	5′ CTCGTCAGTAGCCCCGTCATCTGGAGGTC

D89E F	1586-1620	5′ GATGACTGGGCTACTGAAGAGGATCTTGTGAATGC
D89E R	1586-1620	5′ GCATTCACAAGATCCTCTTCAGTAGCCCAGTCATC
D89N F	1580-1612	5′ CCTCCAGATGACTGGGCTACTAACGAGGATCTT
D89N R	1580-1612	5′ AAGATCCTCGTTAGTAGCCCAGTCATCTGGAGG
D91E F	1593-1625	5′ GGGCTACTGACGAGGAGCTTGTGAATGCCATCC
D91E R	1593-1625	5′ GGATGGCATTCACAAGCTCCTCGTCAGTAGCCC
D91N F	1590-1624	5′ ACTGGGCTACTGACGAGAATCTTGTGAATGCCATC
D91N R	1590-1624	5′ GATGGCATTCACAAGATTCTCGTCAGTAGCCCAGT
C111A F	1652-1684	5′ GACAGGAACGGTGCTGCTACTAGCGCCAAGTAC
C111A R	1652-1684	5′ GTACTTGGCGCTAGTAGCAGCACCGTTCCTGTC
H124C F	1688-1725	5′ CTTAAGCTGGAAGGTGAGTGTTGGACTGTCACTGTGAC
H124C R	1688-1725	5′ GTCACAGTGACAGTCCAACACTCACCTTCCAGCTTAAG
W125G F	1696-1721	5′ GGAAGGTGAGCATGGGACTGTCACTG
W125G R	1696-1721	5′ CAGTGACAGTCCCATGCTCACCTTCC
C142A F	1743-1778	5′ CTTTGCTCCCTCTTGAAGCTGTTCAGGGCTGTTGTG
C142A R	1743-1778	5′ CACAACAGCCCTGAACAGCTTCAAGAGGGAGCAAAG
C147A F	1763-1789	5′ GTTCAGGGCTGTGCTGGGCACAAGGGC
C147A R	1763-1789	5′ GCCCTTGTGCCCAGCACAGCCCTGAAC
K1193A F	4896-4931	5′ AAATCAGGCAAATTTCCGCGCCTTCAGGGGGAGGCC
K1193A R	4896-4931	5′ GGCCTCCCCCTGAAGGCGCGGAAATTTGCCTGATTT
K1193R F	4896-4931	5′ AAATCAGGCAAATTTCCCGGCCTTCAGGGGGAGGCC
K1193R R	4896-4931	5′ GGCCTCCCCCTGAAGGCCGGGAAATTTGCCTGATTT
P1194T F	4900-4931	5′ CAGGCAAATTTCCAAGACTTCAGGGGGAGGC
P1194T R	4900-4931	5′ GCCTCCCCCTGAAGTCTTGGAAATTTGCCTG
S1195P F	4904-4934	5′ CAAATTTCCAAGCCTCCAGGGGGAGGCCCAC
S1195P R	4904-4934	5′ GTGGGCCTCCCCCTGGAGGCTTGGAAATTTG
S1195A F	4904-4934	5′ CAAATTTCCAAGCCTGCAGGGGGAGGCCCAC
S1195A R	4904-4934	5′ GTGGGCCTCCCCCTGCAGGCTTGGAAATTTG
G1196A F	4911-4935	5′ CCAAGCCTTCAGCGGGAGGCCCACA
G1196A R	4911-4935	5′ TGTGGGCCTCCCGCTGAAGGCTTGG
G1196P F	4901-4934	5′ AGGCAAATTTCCAAGCCTTCACCGGGAGGCCCAC
G1196P R	4901-4934	5′ GTGGGCCTCCCGGTGAAGGCTTGGAAATTTGCCT
G1196S F	4901-4934	5′ AGGCAAATTTCCAAGCCTTCATCGGGAGGCCCAC
G1196S R	4901-4934	5′ GTGGGCCTCCCGATGAAGGCTTGGAAATTTGCCT
G1197A F	4912-4939	5′ CAAGCCTTCAGGGGCAGGCCCACATCTC
G1197A R	4912-4939	5′ GAGATGTGGGCCTGCCCCTGAAGGCTTG
G1197P F	4911-4939	5′ CCAAGCCTTCAGGGCCAGGCCCACATCTC
G1197P R	4911-4939	5′ GAGATGTGGGCCTGGCCCTGAAGGCTTGG
G1197S F	4909-4942	5′ TTCCAAGCCTTCAGGGTCAGGCCCACATCTCATG
G1197S R	4909-4942	5′ CATGAGATGTGGGCCTGACCCTGAAGGCTTGGAA
G1198A F	4916-4942	5′ CCTTCAGGGGGAGCCCCACATCTCATG
G1198A R	4916-4942	5′ CATGAGATGTGGGGCTCCCCCTGAAGG
G1198P F	4911-4941	5′ CCAAGCCTTCAGGGGGACCCCCACATCTCAT
G1198P R	4911-4941	5′ ATGAGATGTGGGGGTCCCCCTGAAGGCTTGG
G1198S F	4910-4942	5′ TCCAAGCCTTCAGGGGGATCCCCACATCTCATG
G1198S R	4910-4942	5′ CATGAGATGTGGGGATCCCCCTGAAGGCTTGGA
P1199A F	4918-4944	5′ TTCAGGGGGAGGCGCACATCTCATGGC
P1199A R	4918-4944	5′ GCCATGAGATGTGCGCCTCCCCCTGAA
Detection of ORF7		
PET71/	14887-14903	5′ GCGCATATGCCAAATAACAAGCGC
/P72	15341-15361	5′ CGCCCTAATTGAATAGGTGAC

Fig. 4.1. The putative cysteine protease PL2 domain mediated efficient processing of nsp2 in CHO cells. (A) Schematic diagrams of constructs used in examining the role of the PL2 domain in the nsp2/3 proteolysis. Three consecutive c-*myc* epitopes were inserted into the position where nsp2 region aa324-434 was deleted, and a HA-FLAG tag was attached to the C-terminus of nsp3 protein. The plasmids were transfected into CHO cells. At 48 hours post transfection, the cells were lysed and immunopreciated with mouse monoclonal antibodies against c-*myc* (9E10) or HA. The immunoprecipitated proteins were separated by SDS-PAGE, and then transferred to nitrocellulose sheets and reacted with selected antibodies. **(B)** Detection of nsp2-3 and nsp2-3 H124C mutant by rabbit anti-c-*myc* antibodies. **(C)** Mutation of the putative catalytic site His^{124} to cysteine abolished the processing of nsp2. The nsp2-3 H124C mutant precursor but not *wt* nsp2-3 protein were detected by anti-HA antibodies. **(D)** Detection of nsp3 protein by mouse anti-FLAG antibodies after immuoprecipitation with anti-HA antibodies. **(E)** Deletion of nsp2 region aa1-240 containing PL2 domain blocked the processing of nsp2. The nsp2 protein could be detected by both anti-c-*myc* and anti-HA antibodies. Molecular weight markers (kDa) are shown at the left of each panel.

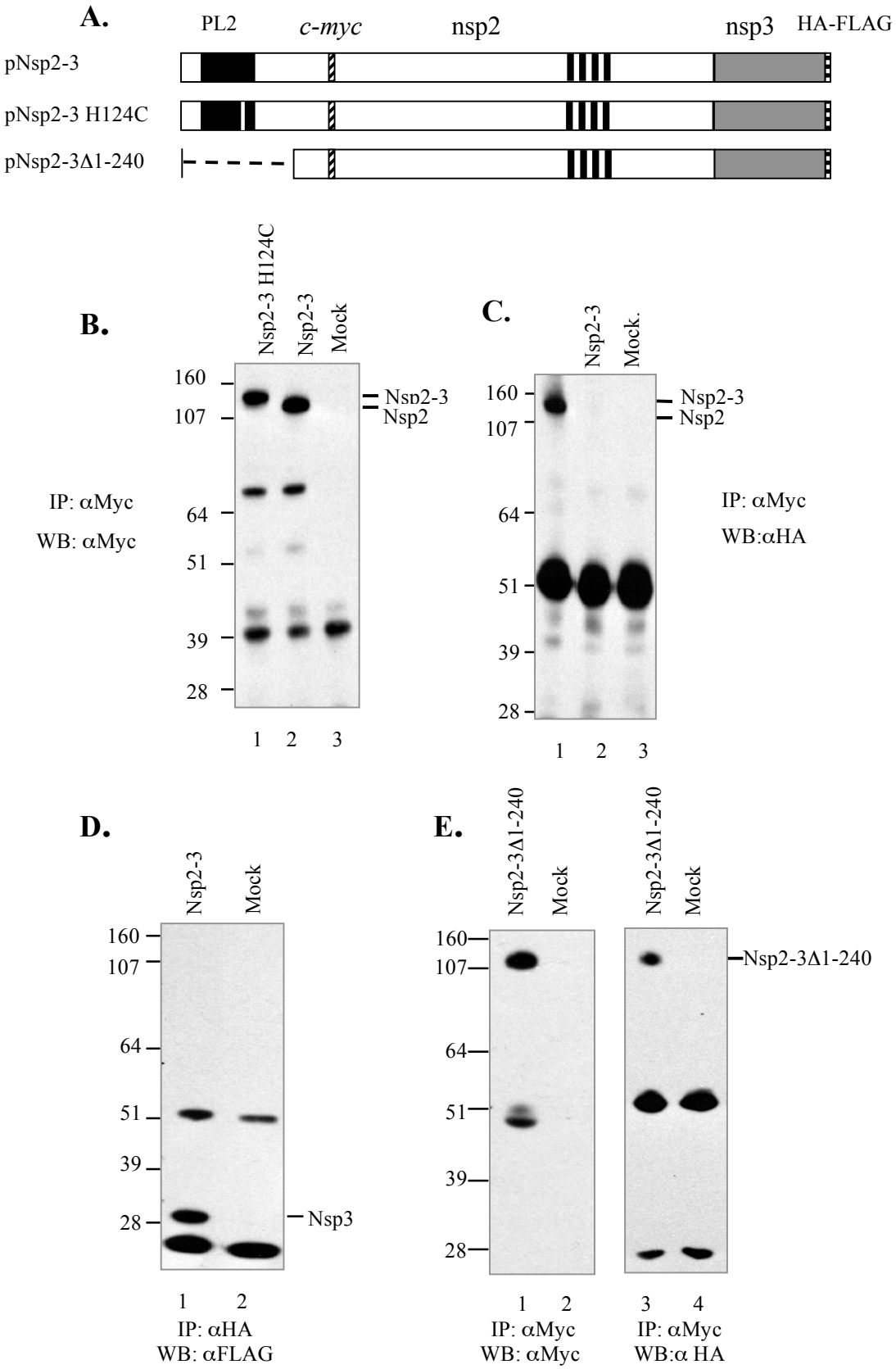
A.
PL2
c-myc
nsp2
nsp3
HA-FLAG
pNsp2-3
pNsp2-3 H124C
pNsp2-3Δ1-240
B.
Nsp2-3 H124C
Nsp2-3
Mock
160
107
64
51
39
28
Nsp2-3
Nsp2
IP: αMyc
WB: αMyc
1 2 3
C.
Nsp2-3
Mock.
160
107
64
51
39
28
Nsp2-3
Nsp2
IP: αMyc
WB:αHA
1 2 3
D.
Nsp2-3
Mock
160
107
64
51
39
28
Nsp3
1 2
IP: αHA
WB: αFLAG
E.
Nsp2-3Δ1-240
Mock
Nsp2-3Δ1-240
Mock
160
107
64
51
39
28
Nsp2-3Δ1-240
1 2
IP: αMyc
WB: αMyc
3 4
IP: αMyc
WB:α HA

Fig. 4.2. Structure of PRRSV nsp2-3 and alignment of arterivirus nsp2 cysteine protease PL2 domains. (A) Diagram of the nsp2-3 protein. The multidomain nsp2 protein contains five different regions: hypervariable region I (HV-I; aa1-47), a putative PL2 cysteine protease core domain (aa47-147), the middle hypervariable region (HV-II; aa147-847), a predicted transmembrane domain (vertical gray bars) (TM; aa876-898, 911-930, 963-979 and 989-1009) and a C-terminal tail with uncertain size. The proposed cleavage sites of nsp2 are shown by black triangles and the positions are annotated. The nsp3 is predicted to be a highly hydrophobic protein with predicted transmembrane domains annotated by vertical bars (TM; aa1203-1223, 1268-1290, 1302-1327 and 1339-1365). **(B)** Comparison of arterivirus PL2 cysteine protease domains. The alignment was generated by using CLUSTALW. Conserved residues investigated in this study are highlighted by boxshade. The nsp2 proteins and their accession numbers are as follows: VR-2332 (AY150564), 16244B (AF046869), CC-1 (EF153486), CH-1a (AY032626), HB-2 (AY262352), JA142 (AY424271), MN184A (DQ176019), P129 (AF494042), AAW81311, ABO93301, ABO99305, EuroPRRSV (AY366525), LV (M96262), RPOA_SHFV (Q68722), RPOA_LDVC (Q06562), RPOA_LDVP (Q83017), CAC42775, Q6V7J0 and NP705.

A.

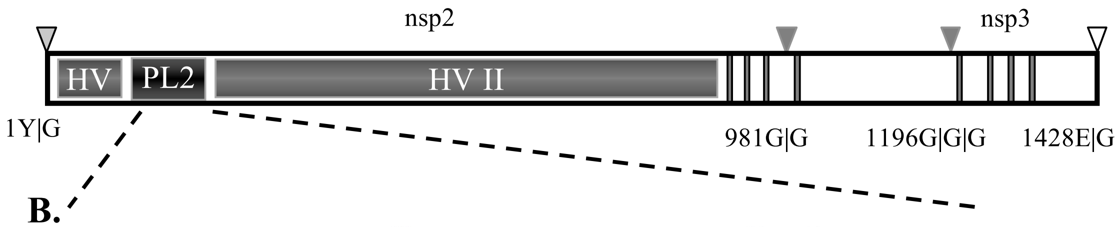

B.

```
                                  55                                86   91
VR-2332_PRRSV      47  YSPPAEGNCGWHCISAIANRMVNSKFETTLPERVRPPDDWATDEDLVNAIQ-ILRLPAAL
16244B_PRRSV       47  YSPPAEGNCGWHCISAIANRMVNSIFETTLPERVRPPDDWATDDDLANAIQ-ILRLPAAL
CC-1_PRRSV         47  YSPPAEGNCGWHCISAIANRMVNSKFETTLPERVRPPDDWATDEDLVNAIQ-ILRLPAAL
CH-1a_PRRSV        47  YSPPAEGNCGWHCISAIANRMVNSNFETTLPERARPLDDWATDEDLVNTIQ-ILRLPAAL
HB-2_PRRSV         47  YSPPAEGNCGWHCISAIVNRMVNSNFETTLPERVRPSDDWATDEDFVNTIQ-ILRLPAAL
JA142_PRRSV        47  YSPPADGNCGWHCISAIANRMVNSKFETTLPERVRPSDDWATDEDLVNTIQ-ILKLPAAL
MN184A_PRRSV       47  YSPPAEGNCGWHCISAIANRMVNSKFETALPERVRSPEDWATDEDLVNTIQ-ILRLPAAL
P129_PRRSV         47  YSPPADGNCGWHCISAITNRMVNSKFETTLPERVRPSDDWATDEDLVNTIQ-ILRLPAAL
AAW81311_PRRSV     35  YSPPTDGSCGWHVLAAIMNRMMNDDFTSPLTQYNRPEDDWASDYDLAQAIQ-CLQLPATV
ABO93301_PRRSV     35  YSPPTDGSCGWHVLAAIMNRMMNGDFTSPLPQYNRPEDDWASDYDLAQAIQ-CLQLPATV
ABO93305_PRRSV     35  YSPPTDGSCGWHVLAAIMNRMINGDFTSPLTQYNRPEDDWASDYDLAQAIQ-CLQLPATV
EuroPRRSV_PRRSV    35  YSPPTDGSCGWHVLAAIMNRMMNDDFTSPLTQYNRPEDDWASDYDLAQAIQ-CLQLPATV
LV_PRRSV           35  YSPPTDGSCGWHVLAAIMNRMINGDFTSPLTQYNRPEDDWASDYDLVQAIQ-CLRLPATV
RPOA_SHFV         284  FIPPPDGGCGVHAFAAIQYHINTGHWPEQKPVVNWAYEAWTTNEDIGHMIC-STETPAAL
RPOA_LDVC           2  YSPPGDGACGLHCISAMLNDIFGDSFTTRLGKCSRDSSEWLSDQDLYQLVM-TANLPATI
RPOA_LDVP           2  YSPPGDGACGLHCISAIINDIFGDALCTKLTNCSRDSSEWLSDQDMYQLVM-TARLPATL
CAC42775_EAV        2  YNPPGDGACGYRCLAFMNGATVVSAGCS--------SDLWCDDELAYRVFQLSPTFTVTI
Q6V7J0_EAV          2  YNPPGDGACGYRCLAYMNGANAVSAGCS--------SDLWCDDELAYRVFQLSPTFTVTI
NP705584_EAV        2  YNPPGDGACGYRCLAFMNGATVVSAGCS--------SDLWCDDELAYRVFQLSPTFTVTI

                            111          124                  142  147
VR-2332_PRRSV     106  DRNGACTSAKYVLKLEGEHWTVTVTPG-MSPSLLPLECVQGCCGHKGG
16244B_PRRSV      106  DRNGACTSAKYVLKLEGEHWTVTVTPG-MSPSLLPLECVQGCCEHKGG
CC-1_PRRSV        106  DGNGACTSAKYVLKLEGEHWTVTVTPG-MFPSLLPLECVQSCCGHKGG
CH-1a_PRRSV       106  DRNGACTSAKYVLRLEGEHWTVSVTPG-MSPSLLPLECVQGCCEHKGG
HB-2_PRRSV        106  DRNGACKSAKYVLKLEGEHWTVSVAPG-MSPSLLPLECVQGCCEHKGG
JA142_PRRSV       106  DRNGACVGAKYVLKLEGEHWTVSVTLG-MSPSLLPLECVQGCCEHKSG
MN184A_PRRSV      106  DRNGACASAKYILKLEGEHWTVSVIPG-MXPSLLPLECVQGCCEHKGN
P129_PRRSV        106  DRNGACAGAKYVLKLEGEHWTVSVTPG-MTPSLLPLECVQGCCEHKSG
AAW81311_PRRSV     94  VRSRACPNAKYLIKLNGVHWEVGVRSG-MAPRSLSRECVVGVCS-EGC
ABO93301_PRRSV     94  VRNRACPNAKYLVRLNGVHWEVEVRSG-MAPRSLSRECVVGVCS-EGC
ABO93305_PRRSV     94  VRNRVCPNAKYLIKLNGVHWEVEVRSG-MAPRSLSRECVVGVCS-EGC
EuroPRRSV_PRRSV    94  VRNRACPNAKYLIKLNGVHWEVEVRSG-MAPRSLSRECVVGVCS-EGC
LV_PRRSV           94  VRNRACPNAKYLIKLNGVHWEVEVRSG-MAPRSLSRECVVGVCS-EGC
RPOA_SHFV         343  ---EPCLHARYVVRLDSDHWVVDHYPN--RPMCFVEACAHGWCS--SL
RPOA_LDVC          61  ---GHCPSAIYKLDCVNQHWTVTKRKGDRAVGRLAPDCLRGVCG-ECE
RPOA_LDVP          61  ---GHCPSATYKLDCVNQHWTVTKRKGDRALGGLSPECVRGVCGGECK
CAC42775_EAV       54  PGGRVCPNAKYAMICDKQHWRVKRAKG--VGLCLDESCFRGICNCQRM
Q6V7J0_EAV         54  PGGRVCPNAKYVMICDKQHWRVKHAKG--VGLCFDENCFRGTCNCQRK
NP705584_EAV       54  PGGRVCPNAKYAMICDKQHWRVKRAKG--VGLCLDESCFRGICNCQRM
```

Fig. 4.3. **The cysteine protease PL2 domain possessed *trans*-cleavage activity. (A).** Diagrams of constructs used in *trans*-cleavage assays. The plasmid pNsp2-3 H124C was co-transfected with either pPL2 or pPL2 H124C into the CHO cells. The plasmids encoding the unmodified nsp2-3 or PL2 served as control. CHO cells were lysed at 48h post transfection and immunoprecipitated by mouse monoclonal antibodies against the c-*myc* epitope. The immunoprecipitated proteins were separated by SDS-PAGE and analyzed by western blot. **(B).** Analysis of protein expression by rabbit anti-c-*myc* antibodies. **(C)**. Analysis of nsp2 expression by anti-HA antibodies after immunoprecipitation by anti-c-*myc* antibodies. **(D)**. Mutation of the *trans*-provided PL2 domain restored the detection of nsp2-3 H124C precursor. The PL2 H124C failed to cleave the nsp2-3 H124C protein when provided in *trans* (lane 2).

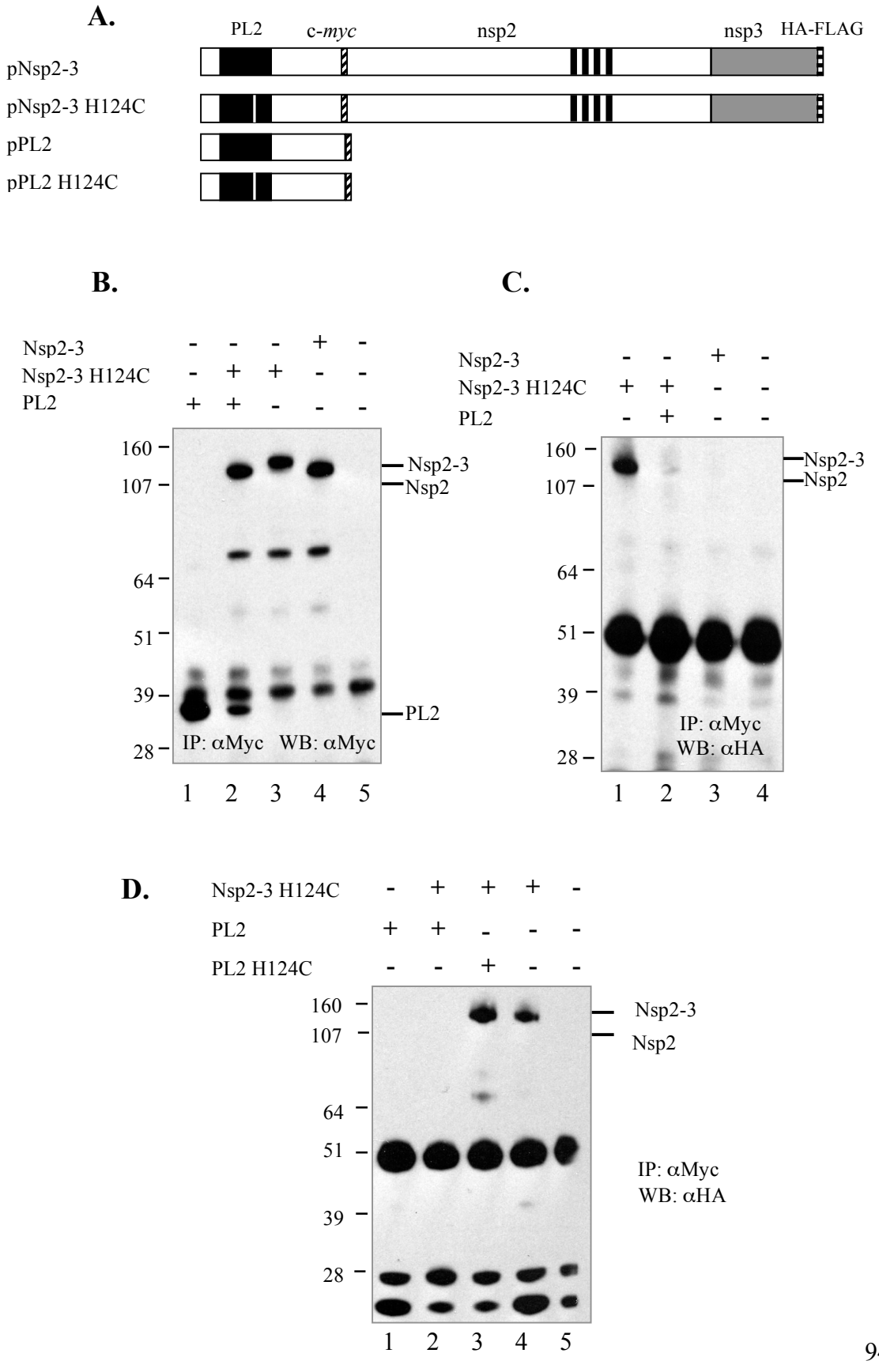
A.
PL2
c-myc
nsp2
nsp3
HA-FLAG
pNsp2-3
pNsp2-3 H124C
pPL2
pPL2 H124C
B.
Nsp2-3
Nsp2-3 H124C
PL2
160
107
64
51
39
28
Nsp2-3
Nsp2
PL2
IP: αMyc WB: αMyc
1 2 3 4 5
C.
Nsp2-3
Nsp2-3 H124C
PL2
160
107
64
51
39
28
Nsp2-3
Nsp2
IP: αMyc
WB: αHA
1 2 3 4
D.
Nsp2-3 H124C
PL2
PL2 H124C
160
107
64
51
39
28
Nsp2-3
Nsp2
IP: αMyc
WB: αHA
1 2 3 4 5

Fig. 4.4. **The nsp2 region aa47-240 was the minimal size required for the PL2 *trans*-cleavage activity**. **(A)** Schematic representation of PL2 deletion mutants. Each of the PL2 mutants was tagged with a c-*myc* epitope at the C-terminus and co-transfected with the substrate plasmid pNsp2-3Δ1-240. The transfected CHO cells were lysed and then subjected to immunoprecipitation and western blot analysis. **(B)** The PL2 mutants were analyzed directly by western blot with rabbit anti-c-*myc* antibodies, as shown in upper panel. The processing of nsp2-3Δ1-240 precursors was analyzed by western blot with rabbit anti-*myc* antibodies after immunoprecipitation with mouse monoclonal antibodies (9E10) against c-*myc*.

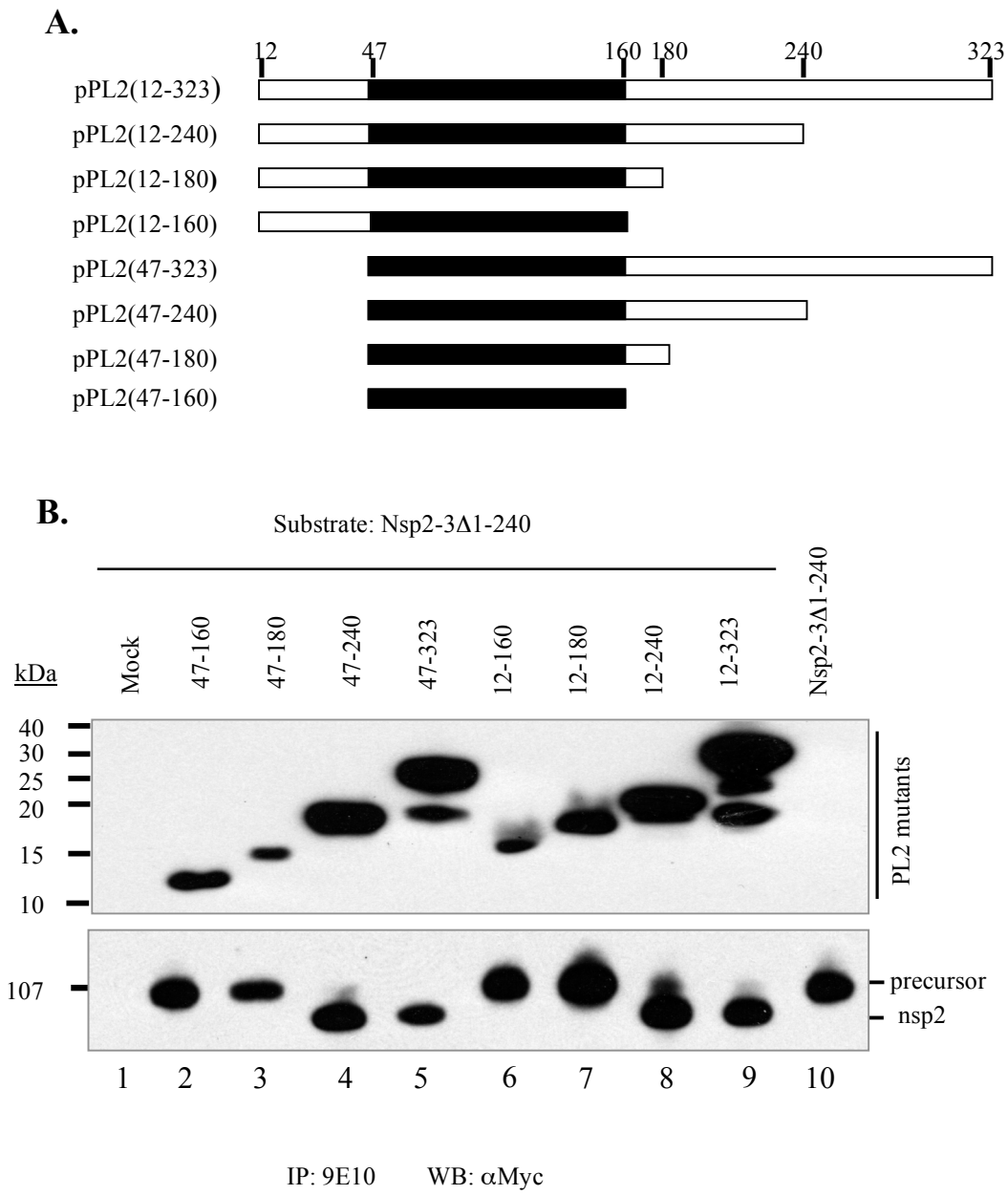
A.
12
47
160
180
240
323
pPL2(12-323)
pPL2(12-240)
pPL2(12-180)
pPL2(12-160)
pPL2(47-323)
pPL2(47-240)
pPL2(47-180)
pPL2(47-160)
B.
Substrate: Nsp2-3Δ1-240
kDa
Mock
47-160
47-180
47-240
47-323
12-160
12-180
12-240
12-323
Nsp2-3Δ1-240
40
30
25
20
15
10
107
PL2 mutants
precursor
nsp2
1
2
3
4
5
6
7
8
9
10
IP: 9E10
WB: αMyc

Fig. 4.5. Nsp2 aa181-323 were essential for nsp2/3 proteolysis under monocistronic condition. (A) Diagram of nsp2 deletion constructs which were tagged with a c-*myc* epitope at the N-terminus of nsp2. **(B)** Deletion of nsp2 aa181-323 blocked processing of nsp2-3. The nsp2-3 precursor was detected by both anti-c-*myc* and HA antibodies after immunoprecipitation by mouse monoclonal antibodies against c-*myc* when nsp2 region aa181-323 was deleted. Deletion of nsp2 aa241-323 resulted in unstable nsp2 which could not be detected by anti-c-*myc* antibodies (not shown). **(C)** The nsp2 hypervariable region aa324-813 was not essential for PL2 mediated downstream cleavage. The nsp2-3 protein was detected with anti-c-*myc* or HA antibodies after immunoprecipitation with c-*myc* antibody 9E10.

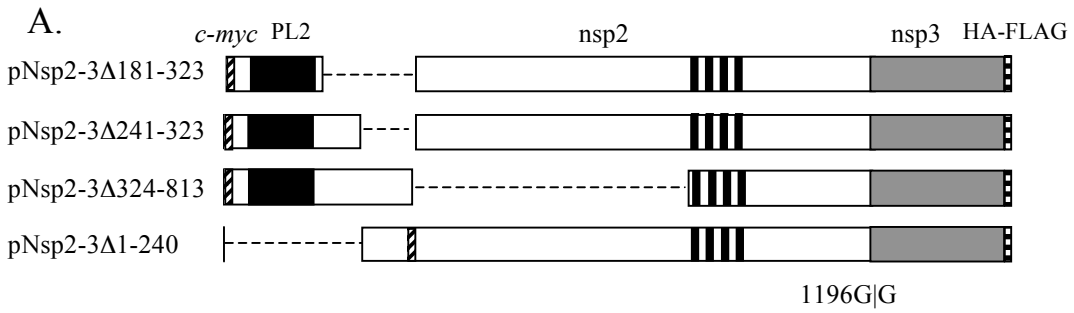
A.
c-myc
PL2
nsp2
nsp3
HA-FLAG
pNsp2-3Δ181-323
pNsp2-3Δ241-323
pNsp2-3Δ324-813
pNsp2-3Δ1-240
1196G|G

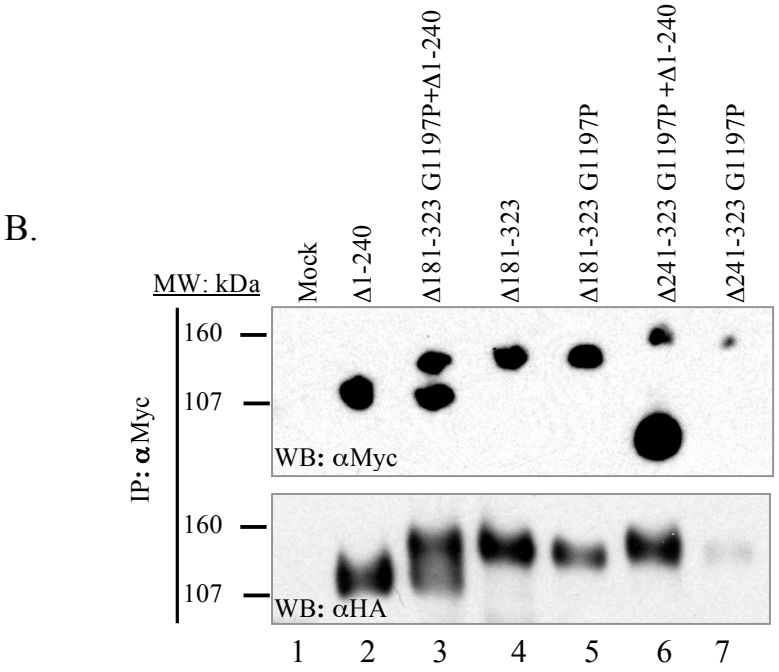
B.
MW: kDa
Mock
Δ1-240
Δ181-323 G1197P+Δ1-240
Δ181-323
Δ181-323 G1197P
Δ241-323 G1197P +Δ1-240
Δ241-323 G1197P
IP: αMyc
160
107
WB: αMyc
160
107
WB: αHA
1 2 3 4 5 6 7

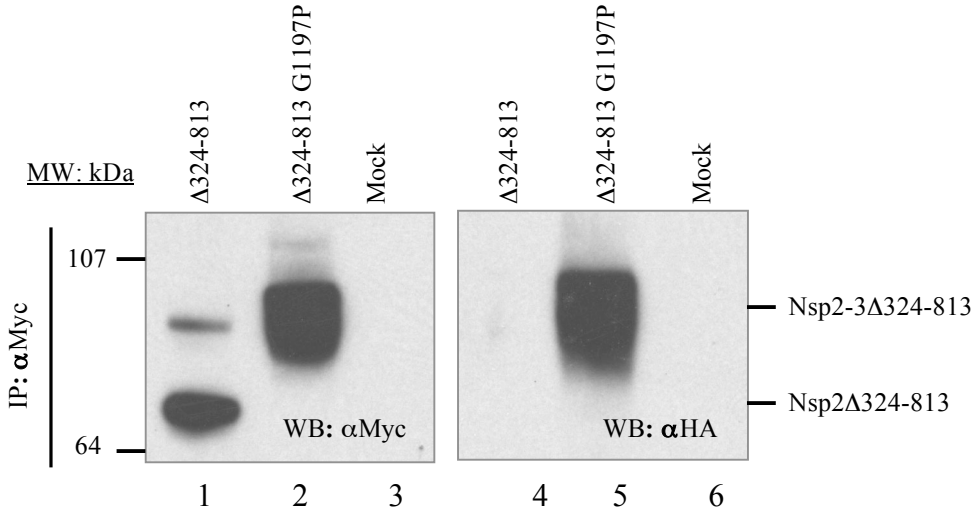
C.
MW: kDa
Δ324-813
Δ324-813 G1197P
Mock
Δ324-813
Δ324-813 G1197P
Mock
IP: αMyc
107
64
WB: αMyc
WB: αHA
Nsp2-3Δ324-813
Nsp2Δ324-813
1 2 3 4 5 6

Fig. 4.6. **Separation of *cis* function from *trans* activity of the PL2 protease by site-directed mutagenesis. (A)** Nsp2-3 mutants were transfected into CHO cells and the protein processing was analyzed with rabbit anti-c-*myc* antibodies or mouse anti-HA antibodies after immunoprecipitation with mouse anti-c-*myc* monoclonal antibodies. **(B)** The PL2 mutants were co-transfected with the substrate plasmid pNsp2-3Δ1-240. Protein expression was analyzed by western blot with rabbit polyclonal antibodies against c-*myc* after immunoprecipitation with anti-c-*myc* monoclonal antibodies. **(C)** Mutations were introduced into the PRRSV strain VR-2332 infectious cDNA clone and tested in MARC-145 cells. The viable viruses were titrated and the nonviable mutants were confirmed by RT-PCR against ORF7 after three blind passages.

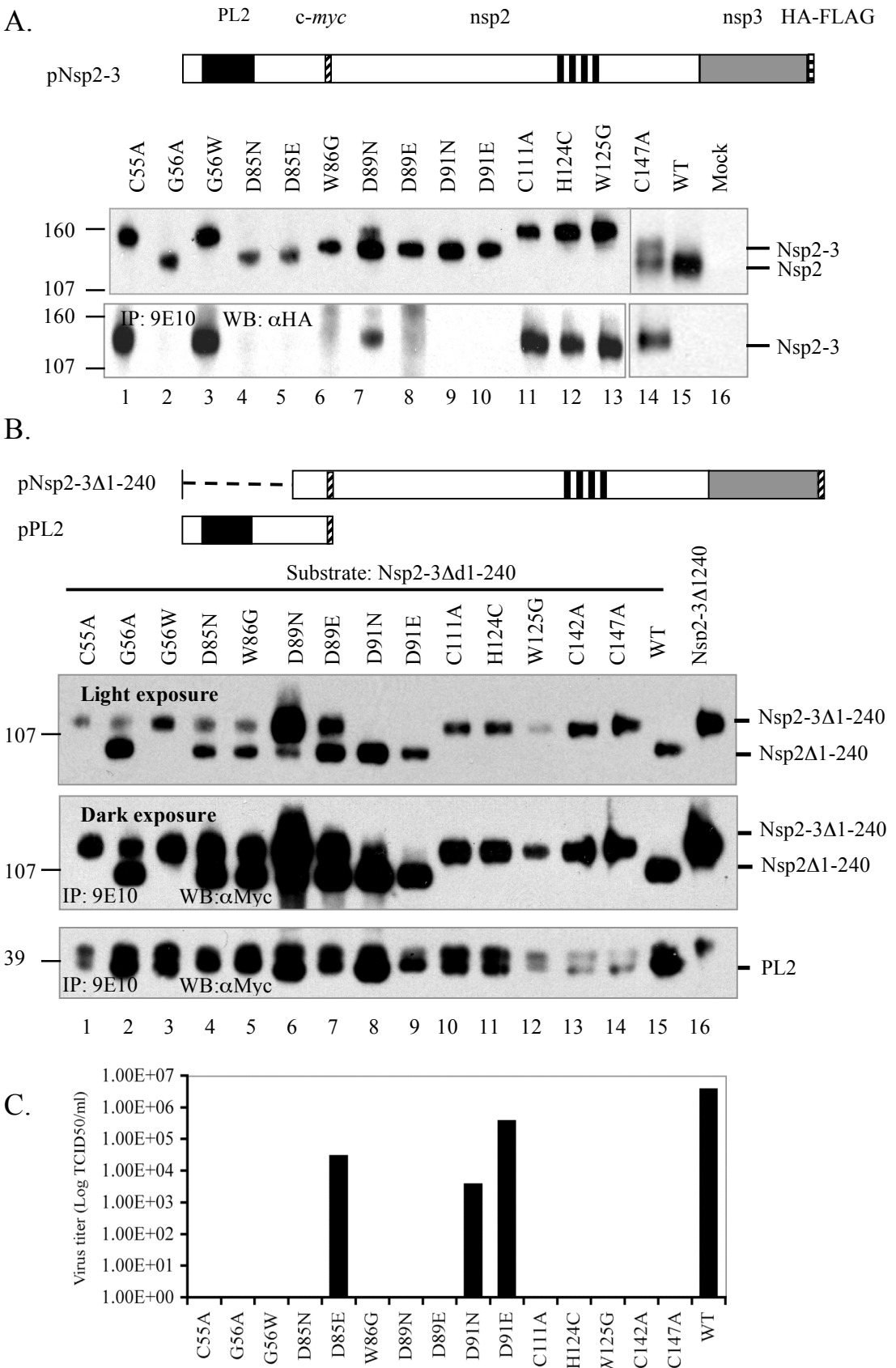
A.
PL2
c-myc
nsp2
nsp3
HA-FLAG
pNsp2-3
C55A
G56A
G56W
D85N
D85E
W86G
D89N
D89E
D91N
D91E
C111A
H124C
W125G
C147A
WT
Mock
160
107
Nsp2-3
Nsp2
IP: 9E10
WB: αHA
Nsp2-3
1 2 3 4 5 6 7 8 9 10 11 12 13 14 15 16
B.
pNsp2-3Δ1-240
pPL2
Substrate: Nsp2-3Δd1-240
Nsp2-3Δ1240
Light exposure
Nsp2-3Δ1-240
Nsp2Δ1-240
Dark exposure
IP: 9E10
WB:αMyc
39
PL2
1 2 3 4 5 6 7 8 9 10 11 12 13 14 15 16
C.
Virus titer (Log TCID50/ml)
1.00E+07
1.00E+06
1.00E+05
1.00E+04
1.00E+03
1.00E+02
1.00E+01
1.00E+00

Fig. 4.7. Site-directed mutagenesis of the putative PL2 cleavage site. (A) Diagram of the construct used in this experiment. The position for the synthesized rabbit peptide antibody V against nsp2 is indicated**. (B)** The peptide antibody V could recognized both the precursor nsp2-3 and processed nsp2 protein. **(C)** Alignment of the region surrounding the putative cleavage site 11996G|G by WebLogo 3 (43)**.** The bits score represents the strength of conservation**. (D)** The processing of the nsp2-3 mutants was analyzed by western blot with anti-c-*myc* or HA antibodies after immunoprecipitation with mouse anti-c-*myc* antibodies**. (E)** Mutations were introduced into the PRRSV strain VR-2332 infectious cDNA clone pVR-V7 and tested in MARC-145 cells. Viable viruses were titrated in MARC-145 cells and the nonviable mutants were confirmed by RT-PCR against ORF7 coding for viral nucleocapsid protein after three blind passages.

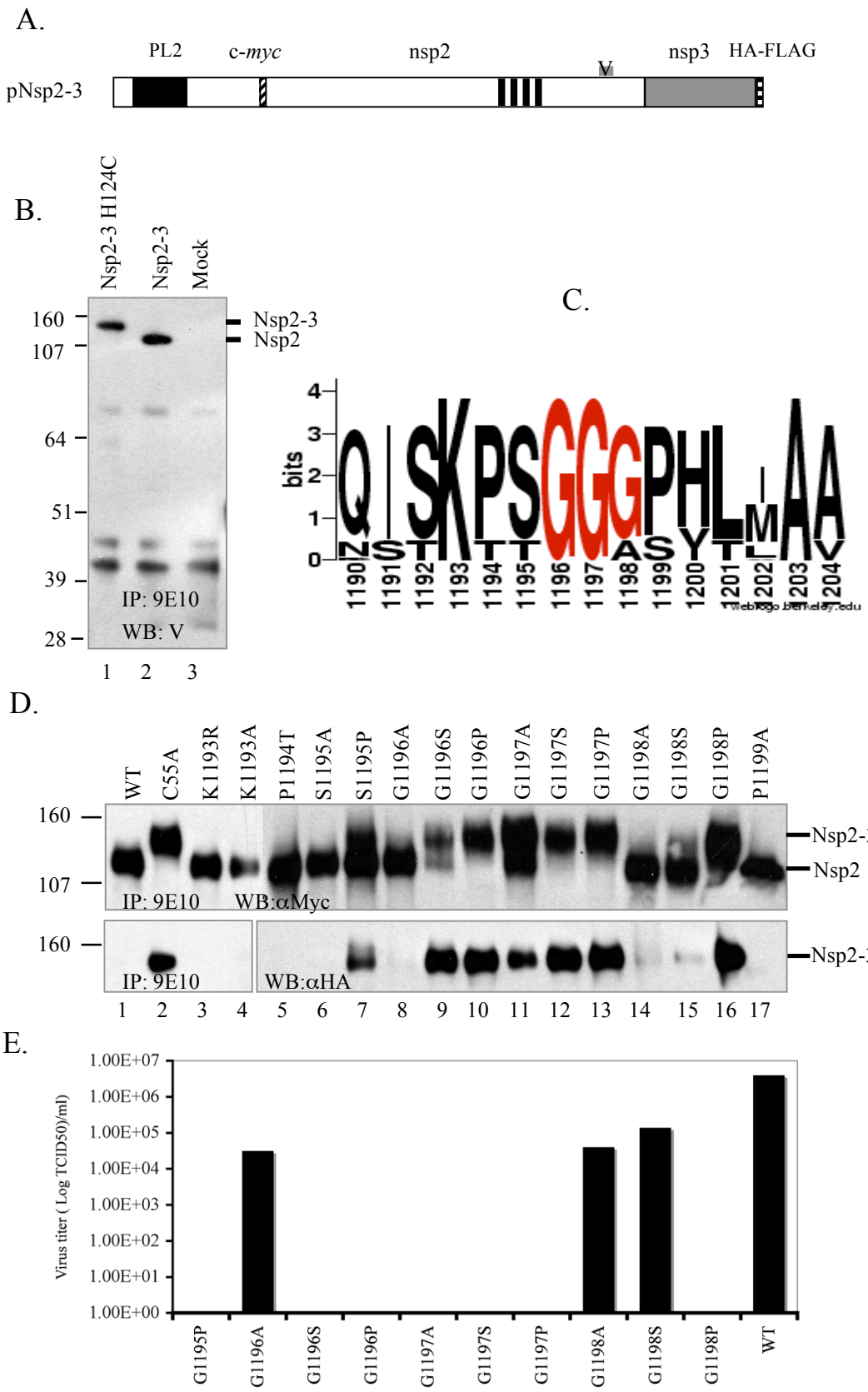
A.
PL2
c-myc
nsp2
nsp3
HA-FLAG
pNsp2-3
V
B.
Nsp2-3 H124C
Nsp2-3
Mock
160
107
64
51
39
28
Nsp2-3
Nsp2
IP: 9E10
WB: V
1 2 3
C.
bits
4
3
2
1
0
1190 1191 1192 1193 1194 1195 1196 1197 1198 1199 1200 1201 1202 1203 1204
D.
WT
C55A
K1193R
K1193A
P1194T
S1195A
S1195P
G1196A
G1196S
G1196P
G1197A
G1197S
G1197P
G1198A
G1198S
G1198P
P1199A
160
107
Nsp2-3
Nsp2
IP: 9E10
WB:αMyc
160
IP: 9E10
WB:αHA
Nsp2-3
1 2 3 4 5 6 7 8 9 10 11 12 13 14 15 16 17
E.
Virus titer (Log TCID50)/ml)
1.00E+07
1.00E+06
1.00E+05
1.00E+04
1.00E+03
1.00E+02
1.00E+01
1.00E+00
G1195P
G1196A
G1196S
G1196P
G1197A
G1197S
G1197P
G1198A
G1198S
G1198P
WT

Chapter V

Proteolytic Processing of Porcine Reproductive and Respiratory Syndrome Virus Nsp2 Replicase Protein

Abstract

In Chapter IV, we showed that PRRSV nsp2 encoded an active PL2 protease that mediated a single cleavage at the nsp2/3 junction in transfected CHO cells. Here, we investigated the proteolytic processing of nsp2 in MARC-145 cells by using recombinant PRRSV expressing epitope-tagged nsp2 protein. We report the presence of nsp2 as six different isoforms during PRRSV infection, termed nsp2a, b, c, d, e and f, which appeared to share the same N-terminus but differed in their respective C-termini based on deletion mutagenesis and antibody probing. The largest nsp2a protein corresponded to the nsp2 product that was previously identified in transfected CHO cells in which the cleavage occurred between residues $G^{1196}|G^{1197}$. Nsp2b and c were processed within or near the TM region, presumably at the conserved sites $G^{981}|G^{982}$ and $G^{828}|G^{829}|G^{830}$, respectively. The C-termini for nsp2d, e and f were mapped within the nsp2 middle hypervariable region, but no conserved cleavage sites could be predicted, suggesting likely involvement of host proteases. The nsp2 species emerged almost simultaneously in the early stage of PRRSV infection. Pulse-chase analysis revealed that all six nsp2 species were stable and had low turnover rates. Deletion and site-directed mutagenesis suggested that nsp2d, e and f were not essential for viral replication in cell culture. Lastly, we identified heat shock 70kDa protein 5 (HSPA5) as a cellular component strongly associated with nsp2. Further *in vitro* analysis revealed that antibodies to the cysteine protease PL2 domain co-immunoprecipitated HSPA5.

Introduction

Replicase polyprotein maturation is a highly precisely regulated process and plays a very important role in the replication cycle of positive-stranded RNA viruses, the products of which are critical for downstream assembly of viral replication complexes and are often antagonists of host anti-viral responses. The proteolytic cleavages are usually carried out by virus-encoded proteases, with occasional action by cellular proteases (24, 68, 73). Porcine reproductive and respiratory syndrome virus (PRRSV) is a positive-stranded RNA virus with a genome size of about 15.4kb and is a member of the family *Arteriviridae* in the order *Nidovirales* (3, 29, 152, 162). PRRSV encodes replicase polyproteins at its 5'end, occupied by two large open reading frames: ORF1a and ORF1b (152, 162, 208). ORF1a generates polyprotein pp1a while ORF1b is translated through a frame-shift mechanism to produce pp1ab (208). At least 12 functional nonstructural protein (nsp) subunits have been predicted during the proteolysis of ppla and pp1ab (277). The processing is thought to be mediated by four virus-encoded proteases: two papain-like cysteine proteases (PCPα and PCPβ), a cysteine proteinase (PL2) and a picornavirus 3C-like serine proteinase ($3CL^{pro}$) (60, 210, 277).

The nsp1 protein of PRRSV is cotranslationally processed *in vitro* into nsp1α and nsp1β by solely *cis*-active PCPα and PCPβ, respectively (60, 210). Nsp2 is a large multidomain protein located immediately adjacent to nsp1 and contains a N-terminal PL2 cysteine protease, a 500-700aa middle hypervariable region with unknown function and a putative near C-terminal transmembrane domain (92, 213). In Chapter IV, we demonstrated that the PL2 cysteine protease of PRRSV was both *cis* and *trans* active and mediated the processing of nsp2 into one predominant product in transfected CHO cells (91). Biochemical probing and site-directed mutagenesis suggested that the glycine dyad at nsp2 position 1196 was sensitive to point mutations and most likely served as the scissile bond for the PL2 protease (91), consistent with a previous report that the related equine arteritis virus (EAV) nsp2 PL2 protease prefers a G|G dipeptide for its cleavage site (214). The function of PRRSV nsp2 in the virus replication cycle is not clear yet, while EAV nsp2 is involved in the generation of double-membrane vesicles together with nsp3 and serves as a cofactor for the nsp4 encoded enzyme (209, 245). The 3C-like serine

protease encoded by nsp4 of PRRSV is predicted to cleave the remainder of ORF1a and ORF1b like its counterpart EAV 3CLpro (212, 214, 233, 234, 277).

In this report, we extended our previous findings and examined the processing of nsp2 in PRRSV-infected MARC-145 cells by using recombinant viruses expressing foreign epitope-tagged nsp2. The nsp2 protein was found to exist as several different isoforms with apparently different C-termini. Total proteolysis of PRRSV nsp2 was thought to involve both the PL2 protease and other unknown viral or cellular proteases. The processing was demonstrated to be rapid and the cleaved products were relatively stable. In addition, the cellular protein HSPA5 was found to interact with the nsp2 protein and could be specifically co-immunoprecipitated by anti-nsp2 antibodies.

Materials and Methods

Plasmids and Antibodies. The plasmids used in this study, including pNsp2-3, pNsp2-3 C55A, pNsp2-3 G1197P, and pPL2, were described previously (91). Nsp2 coding regions aa12-813, aa12-980 and aa12-1196 were amplified from the plasmid pNsp2-3 and cloned into the site between BamHI and XbaI of the plasmid pcDNA/HA-FLAG to generate new plasmids pNSP2 (12-813), pNSP2 (12-981) and pNSP2 (12-1196), respectively. The HSPA5 gene tagged with a c-*myc* epitope at the N-terminus was amplified with primers and cloned into vector pcDNA3 to generate the plasmid pHSPA5-*myc*.

Antibodies used in this report include anti-c-*myc* monoclonal antibody (9E10) (Developmental Studies Hybridoma Bank at the University of Iowa), rabbit polyclonal anti-c-*myc* antibodies (Abcam), mouse anti-HA antibodies (Covance), mouse anti-FLAG antibodies (M2, Sigma), HRP conjugated anti-mouse IgG or anti-rabbit IgG secondary antibodies (Southern biotechnology, Inc) and rabbit anti-HSPA5 antibody (Santa Cruz Biotechnology). The mouse monoclonal antibody YF07 to the PL2 cysteine protease domain was from Dr. Ying Fang (South Dakota State University), and D3A4 and E5F8 from Dr. Hanchun Yang (China Agricultural University). The rabbit polyclonal antibody V was raised against a peptide containing PRRSV strain VR-2332 nsp2 aa1078-1094 (SEKPIAFAQLDEKKITA) (Covance).

Construction of PRRSV deletion mutants. The plasmid pV7-nsp2Δ324-434-GFP was reported previously (90). To generate c-*myc* epitope recombinant virus, the GFP gene was replaced by 3 c-*myc* epitopes (EQKLISEEDL) to generate plasmid pV7-nsp2Δ324-434-*myc* (pV7-*myc*) by overlapping PCR as described before (90). To generate HA-c-*myc* double tagged virus pV7-HA-*myc*, an influenza A virus hemagglutinin (HA) epitope tag (YPYDVPDYA) replaced nsp2 aa12-24 in the plasmid pV7-*myc*. A similar strategy was used to create nsp2 deletion viruses based on the plasmid pV7-*myc* and the new plasmids were designated as pV7-*myc*-nsp2Δ543-632, pV7-*myc*-nsp2Δ633-726 and pV7-*myc*-nsp2Δ727-813, respectively.

Transient expression. MARC-145 (ATCC) and CHO cells (Invitrogen) were maintained in EMEM (SAFC Biosciences) supplemented with 10% fetal bovine serum (FBS) at 37 °C with 5% CO_2. CHO cells were transiently transfected by using Lipofectamine™ 2000 (Invitrogen) as described (91). RNA transfection of MARC-145 cells was performed as described previously (90).

Viral growth assays. MARC-145 cells in T-25 flasks were infected with 0.1 MOI of either parental or mutant viruses at passage 3. After 1 h of attachment at room temperature with gentle mixing, unbound viruses were removed and the monolayers were washed three times with serum-free EMEM and replaced with 7 ml complete medium. Samples were collected from medium at different time points after infection and titrated by viral plaque assay on MARC-145 cells (90).

Immunoprecipitation and western blot. Transfected CHO cells or infected MARC-145 cells were rinsed twice with cold PBS (0.14M NaCl, 2.7mM KCl, 10mM Na_2HPO_4, 1.5mM KH_2PO_4), and lysed with RIPA buffer (50mM Tris-HCl pH 7.4, 1% NP-40, 0.5% Na-deoxycholate, 150mM NaCl, 1mM EDTA and cocktail protease inhibitors (Sigma)) on a platform shaker for 30 min at 4°C. The cell debris was removed by centrifugation at 13, 000 rpm for 20 min. The supernatants were precleared by Protein G or A agarose, and then incubated with selected antibodies as well as Protein G PLUS-agarose (Santa Cruz Biotechnology) or Protein A agarose (Roche) at 4°C overnight. The immunocomplexes were washed twice with cold RIPA buffer, once with 0.1% SDS in RIPA buffer and once with PBS. After heating for 5 min at 100°C, the proteins were

separated by SDS-PAGE and then electrophoretically transferred onto a nitrocellulose membrane. For western blotting, the membrane was blocked with 5% milk powder in PBST (0.14M NaCl, 2.7mM KCl, 10mM Na_2HPO_4, 1.5mM KH_2PO_4, 0.1% Tween-20) for 1 h, and then incubated with the appropriate primary antibodies diluted in PBST-5% milk overnight at 4°C. After washing three times for 30 min with PBST, the blot was incubated with an appropriate diluted secondary antibody in PBST for 1 h. The membrane was again washed and then developed with the ECL Western Blotting Analysis System (Pierce).

Radiolabeling and pulse-chase analysis of the nsp2 protein. MARC-145 cells in 60 mm peri dishes were infected with V7-*myc* at passage 3 with a MOI of 0.1 and incubated in 5 ml EMEM with 10% FBS, 37°C. For pulse-chase analysis, at 12-18 hours postinfection, MARC-145 cells were washed with Dulbecco's modified essential medium (DMEM) deficient in methionine and cysteine (Met/Cys) and starved for 30 min. The cells were then labeled with 4 ml of DMEM with 100 μCi/ml ^{35}S-Met/Cys. After 5-6 hours of labeling, MARC-145 cells were washed twice with DMEM, then incubated with 5 ml DMEM with 10% FBS. At indicated times (0, 15, 30, 60, 120, 180, 240 min), one dish was removed from the incubator; the cells were washed with cold PBS and then lysed in RIPA buffer. The cell lysates were cleared by centrifugation and immunoprecipitated using suitable antibodies.

Tandem affinity purification and mass spectrometry. MARC-145 cells were infected with PRRSV recombinant virus V7-*myc* (passage 3) at 0.1 MOI and then incubated in EMEM with 10% FBS, 37°C. The cells were harvested at 36 hours postinfection and lysed in RIPA buffer. Nsp2-associated complexes were purified by two rounds of immunoprecipitation with mouse monoclonal antibodies to c-*myc* and rabbit polyclonal antibody V. The complexes were washed twice with RIPA buffer, once with RIPA buffer with 0.1% SDS and once with PBS, and eluted by boiling in SDS-PAGE loading buffer with 5% 2-mercapathanol. The complexes were separated by SDS-PAGE on 4-12% Nupage gel (Invitrogen) and visualized by Coomassie blue or SYPRO® Ruby (Invitrogen). SYPRO® Ruby-stained bands were excised, trypsin digested, extracted and

analyzed by liquid chromatography and tandem mass spectrometry (LC-MS/MS) at the University of Minnesota Mass Spectrometry Center.

Results

Construction and recovery of *c-myc* and *HA-tagged* PRRSV. The purpose of generating foreign epitope-tagged recombinant virus was to facilitate the analysis of nsp2 processing by utilizing high quality commercial antibodies. We previously showed that the nsp2 regions including aa12-35 and aa324-813 are not essential for virus replication and that the recombinant PRRSV with a GFP gene in place of nsp2 aa324-434 is viable (90). It is therefore possible to generate foreign epitope-tagged recombinant virus without affecting viral replication.

To generate a c-*myc* tagged virus, the GFP gene of previous PRRSV infectious clone plasmid pV7-nsp2Δ324-434-GFP was replaced with 3 consecutive c-*myc* epitopes to generate the new plasmid pV7-nsp2Δ323-434-*myc* (pV7-*myc*) (Fig. 5.1A). To generate a double-tagged virus, two copies of HA epitopes were inserted to the position where nsp2 aa12-24 was deleted and the new plasmid was designated pV7-nsp2Δ12-24-HA-nsp2Δ323-434-*myc* (pV7-HA-*myc*) (Fig. 5.1A). The plasmids were linearized and *in vitro* transcribed. The RNA transcripts were transfected into MARC-145 cells. Virus-induced cytopathic effect (CPE) was readily detected 4-5 days post transfection, characterized by cell rounding, clustering and detachment (data not shown).

Next, we examined the growth properties of the two mutant viruses. As shown in Fig. 5.1B, the two mutant viruses displayed indistinguishable growth kinetics in MARC-145 cells at passage 3 compared to the parental virus VR-V7, suggesting that insertion of one to two small foreign epitopes into the nsp2 region does not affect viral growth. The mutant V7-*myc* was stable after 10 passages as confirmed by nsp2-coding region sequence analysis. Immunostaining with c-*myc* antibodies revealed a typical perinuclear localization pattern (Fig. 5.1C), similar to that of *wt* strain VR-2332. We failed to detect nsp2 of V7-HA-*myc* by immunofluorescence assay with anti-HA antibodies, perhaps because the HA epitope is inaccessible for antibody binding under native conditions.

Identification of nsp2 products. To detect nsp2-associated products, MARC-145 cells were infected with 0.1 MOI of V7-*myc* at passage 3. The cells were lysed at 24-36

hours post infection using RIPA buffer and cleared by centrifugation. Following immunoprecipitation with mouse monoclonal antibodies 9E10 against the c-*myc* epitope and separation by SDS-PAGE, the nsp2 protein was probed with mouse monoclonal antibody E5F8, recognizing nsp2 region aa77-87 (261). Six specific products were detected with estimated sizes of 120, 100, 80, 51 and 41-43 kDa, and we designated these products nsp2a, b, c, d, e and f, respectively (Fig. 5.2A, lane 1). A similar processing pattern was also observed in double-tagged V7-HA-*myc* infected MARC-145 cells probed with anti-HA antibodies after immunoprecipitation with c-*myc* antibody 9E10 (Fig. 5.2B, lane 2). Since the HA epitope was placed immediately downstream of the cleavage site for nsp1 and the antibody E5F8 recognition site is very near the N-terminus of nsp2 (Fig. 5.1A), these data suggest that these products most likely share a similar N terminus.

Mapping of the C-termini of the nsp2 isoforms. To differentiate the C-termini of the nsp2 products, we initially attempted to use antibody probing to distinguish the nsp2 isoforms. Mouse monoclonal antibody D3A4 recognizes nsp2 peptide aa545-557 (261) and reacted with nsp2 segments a, b, c and d, but not e and f (Fig 5.2A, lane 3). Since the proteins had been initially precipitated with anti-c-*myc* mAb recognizing the epitope located just before nsp2 aa434, the antibody recognition pattern signified that the C-terminus of nsp2 e and f is located between nsp2 aa434-aa545 (Fig 5.2A, lane 3).

The fact that nsp2d reacted with the antibody D3A4 suggests that nsp2d is cleaved after residue 545. To further map the cleavage site, deletion mutagenesis was carried out (Fig. 5.3A). Three nsp2 deletion mutants (V7-*myc*-nsp2Δ541-632, V7-*myc*-nsp2Δ633-726, and V7-*myc*-nsp2Δ727-813) were generated based on V7-*myc* (Fig. 5.3A). The mutants were viable and showed comparable titers to V7-*myc* and parental virus VR-V7 (data not shown). Using these mutants in similar analyses as described above, nsp2d could be distinguished from nsp2c and e by the deletion of nsp2 hypervariable region 541-632, as no nsp2d product was detected after the region was deleted (Fig. 5.3B), suggesting the cleavage site of nsp2d is located between nsp2 aa543 and aa632.

In contrast to nsp2d, detection of nsp2c was not affected by deletion of nsp2 aa541-632, or aa633-726 or aa727-813 (Fig. 5.3B). Thus, the cleavage site of nsp2c must lie

downstream of the Gly^{813} residue. Nsp2b and c could not be differentiated by deletion mutagenesis since further deletion of the putative transmembrane domain (aa 876 to 898, 911 to 930, 963 to 979, and 989 to 1009 or its upstream flanking sequence (814-845) is lethal to the virus (90). To judge the relative size of nsp2b and nsp2c, peptides coding for nsp2 aa12-813 and nsp2 aa12-980 were *in vitro* expressed in CHO cells by cloning the respective fragment into pcDNA3/HA-FLAG. As shown in Fig. 5.3C, nsp2c and nsp2b showed comparable migration rates as nsp2 (12-813) (82 kDa) and nsp2 (12-981) (100.3 kDa), respectively. The cleavage sites for nsp2c and nsp2b should therefore be close to respective residues 813 and 981.

To differentiate nsp2a and b, rabbit peptide antibody V was raised against nsp2 region aa1078-1094. As shown in Fig. 5.2C, antibody V detected nsp2a but not other nsp2 species, consistent with the previous result that antibody V recognized the processed nsp2 in CHO cells (91). As shown in Fig. 3C, the nsp2a had a similar migration rate to nsp2 processed from nsp2-3 that was cleaved at the site 1196G|G in CHO cells, as demonstrated by site-directed mutagenesis (91), but migrated faster than the nsp2-3 C55A precursor. In addition, nsp2a had a similar migration rate to the polypeptide coding nsp2 aa12-1196 (123.6 kDa). Therefore, we conclude that nsp2a is the equivalent to the nsp2 product processed in CHO cells.

Nsp2 d, e and f were not essential for viral replication in cell culture. The experiments described above localized the cleavage sites of nsp2d, e and f within the middle hypervariable region of nsp2. The deletion mutagenesis in this study, when combined with a previous report (90), demonstrated that deletion of either nsp2aa 324-525 containing putative cleavage sites for nsp2e and f or 543-632 containing the putative cleavage site for nsp2d did not affect viral replication in cell culture. In addition, a 400aa deletion (aa324-726) of the nsp2 hypervariable region that contains the proposed cleavage sites of nsp2d, e and f generated viable virus that acquired comparable growth kinetics to parental virus VR-V7 (90). The data thus indicate that nsp2d, e and f are not essential for viral replication in cell culture.

We showed that the cleavage of nsp2a most likely occurs at the site $G^{1196}|G^{1197}$ (91). By using reverse genetics, we also showed that the mutations that blocked the cleavage at

this site are lethal to the virus (91). Thus, the proteolytic generation of nsp2a is critical for viral replication. The cleavage sites that generate nsp2b and c were mapped to the region around the transmembrane (TM) domains. Previously, we showed that the TM region and its upstream sequence (aa814-845) are essential for viral viability (90), suggesting nsp2b and c may be important for viral replication.

Accumulation, stability and turnover of the nsp2 isoforms. To study when and how the nsp2 species emerge during PRRSV infection, the virus V7-myc was used to infect MARC-145 cells at a low MOI of 0.1. As shown in Fig. 5.4, the nsp2 proteins appeared almost simultaneously in the early stage of PRRSV infection from 6 to 12h, especially for the larger nsp2 isoforms, and accumulated to peak levels at 36-42 h post infection. To investigate the processing kinetics of nsp2, radioimmunoprecipitation assays were carried out with anti-c-*myc* antibody 9E10 and rabbit peptide antibody V. Consistent with the results described above, the same nsp2 species were recognized in the radioimmunoprecipitation assay by anti-c-*myc* antibodies (Fig. 5.5A). As expected, the antibody V immunoprecipitated nsp2a (Fig. 5.5C). Interestingly, two products with estimated sizes of 70-80 kDa and 14 kDa respectively were markedly co-immunoprecipitated by both anti-*myc* and V antibodies, and appeared to be either of host or viral origin. A specific band with molecular weight of about 39kDa could only be immunoprecipitated by V antibody, the origin of which is not clear. In addition, the large protein band precipitated by 9E10 antibody only in mock-infected cells was of unknown origin (Fig. 5.5A).

The stability of nsp2-associated products was analyzed by pulse-chase assay in MARC-145 cells. Cells were infected with V7-*myc* virus at a MOI of 0.1 and metabolically labeled with [35S]-methionine/cysteine for 5 h. The nsp2 species accumulated to a maximal level after a pulse for 5-6 h (Fig. 5.5B). After a 5 h pulse with [^{35}S] methionine/cysteine, the incorporated label was chased for various periods (up to 240 min). The cleavage of nsp2 from polyprotein pp1a occurred rapidly and no precursor proteins were detected (Fig. 5.5B and C). The protein amount and ratio among different nsp2 isoforms appeared be relatively constant (Fig. 5.5B), suggesting the isoforms are stable and the protein turnover is slow.

Coimmunoprecipitation of heat shock 70 kDa protein 5 with the nsp2 replicase protein. The results from he radioimmunoprecipitation assays revealed that a protein band with apparent molecular weight of 70-80 kDa was strongly co-immunoprecipitated with nsp2 by either anti-c-*myc* antibodies or antibody V against nsp2 but was not detected by previous western blot analyses (Fig. 5.5B and D). In order to identify the protein, we performed two rounds of immunoprecipitation with anti-c-*myc* antibody 9E10 and peptide antibody V, respectively. The immunocomplexes were eluted and resolved by SDS-PAGE (Fig. 5.6A). The 70-80 kDa specific band was visualized, excised, digested with trypsin, extracted and subjected to mass spectrometry analysis by LC-MS/MS. The recovered peptides were highly matched to heat shock 70 kDa protein 5 (HSPA5 or GRP78) (Fig. 5.6B). Coverage was about 32% and a total of 19 unique peptides of HSPA5 were recovered (Fig. 5.6B). Identity as HSPA5 was further confirmed by western blot with rabbit anti-HSPA5 specific antibodies (Fig. 5.6C).

Coimmunoprecipitation of HSPA5 with the PL2 cysteine protease domain. The experiments described above suggest there is an interaction between HSPA5 and nsp2. Since the nsp2 middle region is highly variable, we hypothesized that the conserved PL2 protease domain of nsp2 might interact with HSPA5. To test this hypothesis, cDNA coding for the HSPA5 protein was amplified from MARC-145 cells and cloned into the vector pcDNA3 to generate pHSPA5-*myc* in which a c-*myc* epitope was attached to the N-terminus of HSPA5 (Fig. 5.7A). Coimmunoprecipitation of coexpressed PL2 and HSPA5 was performed by using PL2 protease specific mAb YF07 to immunoprecipitate PL2. As shown in Fig. 5.7B, HSPA5 was pulled down in the presence of PL2 (Fig. 5.7B, lane 1), suggesting the specific interaction between HSPA5 and the PL2 cysteine protease domain.

Discussion

Cleavage site of PRRSV nsp2 isoforms. In this report, we examined the proteolytic processing of PRRSV nsp2 in virus-infected MARC-145 cells, and revealed the presence of different isoforms of nsp2, which appeared share the same N-terminus but differed in their C-termini. Previously, several candidate cleavage sites (e.g. $G^{828}|G^{829}|G^{830}$, $G^{981}|G^{982}$ and $G^{1196}|G^{1197}$) for the processing of PRRSV nsp2 were proposed based on knowledge

of EAV PL2, a PRRSV PL2 counterpart which prefers a G|G dipeptide as its substrate, and by comparative sequence alignment (3, 92, 277). Our previous studies from *in vitro* transfection assays in CHO cells revealed that the PL2 protease processed nsp2 into one predominant product (91). Similar to the cleavage property of the EAV PL2 protease, we showed the conserved $G^{1196}|G^{1197}$ dipeptide of PRRSV nsp2 was highly susceptible to point mutations and most likely served as the cleavage site (91). In this report, we identified several nsp2 species with apparently different C-termini in PRRSV-infected MARC-145 cells. We showed that nsp2a was recognized by rabbit peptide antibody V (Fig. 5.2B) and had a similar migration rate as the nsp2 protein processed in CHO cells (Fig. 5.3C) (91). Nsp2-3 C55A, representing the unprocessed precursor from transfected CHO cells, had a slower migration rate than that of nsp2a (Fig. 5.3C). Furthermore, mutations at $G^{1196}|G^{1197}$ that blocked the processing of nsp2 were lethal to PRRSV in MARC-145 cells as demonstrated by reverse genetics (91). Thus, we conclude that nsp2a is the equivalent to the nsp2 protein that is processed from the nsp2-3 precursor in CHO cells, and the PL2 protease recognizes the same substrate site ($G^{1196}|G^{1197}$) in both CHO cells and MARC-145 cells.

The $G^{981}|G^{982}$ dipeptide is also highly conserved between PRRSV strains (92). Nsp2b possessed a similar gel migration rate as the polypeptide coding for nsp2 aa12-980 tagged with a 10aa c-*myc* epitope expressed in CHO cells (Fig. 5.3C). We performed site-directed mutagenesis of the residue Gly^{982} in the infectious clone. Results showed that either G982A or G982P was lethal to the virus (data not shown). Combining the cleavage nature of nsp2a at $G^{1196}|G^{1197}$ (15), we postulate the $G^{981}|G^{982}$ dipeptide may be the potential cleavage site for generating nsp2b.

Similarly, we showed nsp2c is processed after the residue Gly^{813} and had a gel migration pattern similar to nsp2 aa12-813 tagged with a c-*myc* epitope expressed in CHO cells (Fig. 5.3C). Considering the PL2 protease is highly selective for G|G dipeptide, $G^{828}|G^{829}|G^{830}$ may be the site for nsp2c cleavage. Indirect evidence supporting this hypothesis comes from previous deletion mutagenesis studies, which showed that deletion of nsp2aa727-813 does not affect viral viability while deletion of nsp2 aa727-845 is lethal to PRRSV (90). Thus, the region aa813-845, which includes $G^{828}|G^{829}|G^{830}$,

appears crucial for viral replication. Thus, diminishing nsp2c processing might have affected viral replication. It should be noted that $G^{828}|G^{829}|G^{830}$ is only highly conserved in North American strains (92). Therefore, the generation of nsp2c may be type or strain specific, reminiscent of the situation of hepatitis C virus in which the internal cleavage of HCV NS3 only takes place in group 2a strains (114).

We could not identify conserved residues among PRRSV strains that could serve as potential cleavage sites to generate nsp2d, e and f. The fact that the cleavage events for nsp2d, e and f take place in the hypervariable region of nsp2 suggests that the processing of these nsp2 isoforms may involve proteases of cell host origin. This should not be surprising, as a similar situation was also observed in CHO cells in which the same nsp2 protein was partially processed in the middle hypervariable region by an unknown cellular protease (91). Certainly, we could not rule out the possibility that the PL2 protease recognizes residues other than G|G dipeptide for cleavage, or that other viral proteases may be involved in nsp2 processing.

Regulation and implication of PRRSV nsp2 isoform processing. The different processing pattern of nsp2 in CHO cells and PRRSV-infected MARC-145 cells raises several questions: (i) are all the processing events PL2 protease specific? (ii) How is the processing of nsp2 regulated? (iii) What are the potential functions of the nsp2 isoforms? For the first question, we have tried to investigate the processing of nsp2 in MARC-145 cells by transiently transfecting the plasmids encoding nsp2 protein and its mutants but failed due to low transfection efficiency of this cell line and perhaps potential toxicity to the cells. Indirect evidence suggests that the processing of nsp2 may involve an unknown cellular protease, particularly for nsp2d, e and f. (a) The nsp2 region aa324-632 containing the cleavage sites of nsp2d, e and f is highly heterogeneous among PRRSV strains (92). Deletion mutations and extensive point mutations across the potential cleavage sites in field strains have been observed (92, 222). It is unlikely that the virus would choose such highly variable region for its PL2 cleavage substrate from an evolutionary point of view. (b) Among PRRSV strains, no conserved residues in VR-2332 nsp2 aa324-632 could be identified to serve as potential cleavage sites that would satisfy the cleavage properties for the PL2 cysteine protease and other papain-like

proteases. Specifically, PL2 was shown to be highly selective for the G|G dipeptide, and even a G to S mutation at the P1 position or a G to A mutation at the p1' position partially abolished the processing of nsp2 in CHO cells (91). (c) We observed that the same hypervariable region of nsp2 was recognized and cleaved by an unknown cellular protease in transfected CHO cells, although only one cleavage product was seen (91).

Radioimmunoprecipitation experiments revealed that nsp2a, b and c represented the most abundant nsp2 species (Fig. 5.5B and D). In addition, fairly conserved putative cleavage sites could be identified through sequence alignment analysis of various PRRSV strains (92) and mutagenesis studies as discussed above. Thus, these data suggest that the generation of nsp2a, b and c might be PL2 protease specific. The fact that the PL2 protease mainly recognizes the nsp2a cleavage site in CHO cells suggests the processing of other nsp2 species may need additional cofactors of either host or viral origin (91). Cofactor binding may alter the overall folding of the nsp2 precursor so that the cleavage sites would be exposed due to the conformation change, or change the substrate binding specificity. Pulse-chase experiments revealed low turnover rate for the nsp2 products in virally infected MARC-145 cells (Fig. 5.5B and D). We did not observe an obvious change in ratio between isoforms, particular for nsp2a, b, and c, during 4 h of chase (Fig. 5.4B). It is unclear whether the smaller nsp2 species are generated from the larger isoforms or if all isoforms originated from the pp1a polyprotein. Certainly, it may also be possible that the whole processing is fast and, once a balance is reached, the relative ratio would not be changed dramatically. Either way, the processing must be highly regulated.

PRRSV generates different nsp2 species by proteolytic processing during infection of MARC-145 cells. Although varied in mechanisms employed, such as alternative splicing, or translation reinitiation, many viruses encode full-length and truncated versions of the same protein that carry overlapping or distinct functions. The most salient examples are protein pairs $U_L26/U_L26.5$, ICP22/$U_S1.5$ and $U_S3/U_S3.5$ of herpes simplex virus (27, 130, 131, 185). Representative examples from RNA viruses include measles virus V/P, infectious bursal disease virus VP2/VPX and Sendai virus C/C' proteins (28, 45, 79). Therefore, it is reasonable to assume that the nsp2 isoforms may carry different functions in the replication cycle of PRRSV. The benefits for a positive stranded RNA

virus like PRRSV in adopting such a strategy may be to maximize coding capacity, dictate individual protein abundance, regulate protein-protein interactions, or protein trafficking.

The role of HSPA5 in viral replication. HSPA5 (GRP78 or bip) is member of the heat shock 70 kDa protein family and is constitutively expressed in the lumen of the ER (44). This cellular protein is known to be associated with a variety of folding and assembly intermediates of cellular or viral membrane proteins (33, 36, 64, 144). In this report, we showed that HSPA5 strongly coimmunoprecipitated with the nsp2 protein (Fig. 5.5). The observation has several implications as following. (i) Involvement in proteolysis. HSPA5 could play an important part in assisting nsp2 folding for proteolysis by either or both PL2 or host cell proteases. It has been reported that the proteolytic activity of bovine viral diarrhea (BVDV) NS2 protein depends on a cellular cofactor, namely a chaperone protein termed Jiv (J-domain protein interacting with viral protein) or its 90aa fragment Jiv90 (118). It is possible that the interaction of HSPA5 with nsp2 could change the confirmation of nsp2 and expose additional cleavage sites for the PL2 protease. (ii) Regulation in viral replication. Production of viral progeny depends on the successful recruitment of host cellular components for their own replication, protein synthesis, and virion assembly. A massive amount of proteins are synthesized in a relatively short time during viral replication, whereby protein folding can become a limiting step (144). Assembly of viral replication complexes on intracellular membranes involves large numbers of viral and/or host proteins. Recruitment of HSPA5 may facilitate the folding of the PRRSV macromolecular complex. (iii) Immune evasion. Sequestration of molecular chaperones may lead to unfolded protein responses or ER stress (97), leaving many host proteins incorrectly folded. The unfolded proteins, including those involved in host anti-viral responses, are sent to ubiquitin-proteosomal system (UPS) for degradation (97, 112, 113). In addition, ER stress can cause host translation attenuation (97, 112, 113). Future work may be directed toward dissecting the detailed interaction of PRRSV nsp2 and HSPA5, and defining the role of HSPA5 in the PRRSV replication cycle.

In summary, we report the presence of nsp2 isoforms with apparently different C-termini in PRRSV-infected MARC-145 cells and the interaction of a host chaperone HSPA5. These findings indicate that PRRSV nsp2 is increasingly emerging as a multifunctional protein that may have a profound impact on viral replication and viral pathogenesis.

Acknowledgements

We thank Dr. Bruce Witthuhn at the University of Minnesota Mass Spectrometry Center for the technical help in the mass spectrometry analysis. We also thank Dr. Ying Fang and Dr. Hanchun Yang for providing monoclonal antibodies to PRRSV nsp2. This study was funded by a USDA grant (No. 2006-01598).

Table 5.1 Primers used in this study. Forward primers are indicated by a slash (/) after the designator, reverse primers are preceded by a slash. Genome positions are based on GenBank Submission U87392 (VR-2332).

Primers	Genome Position	Sequence
Construction of pV7-myc and pV7-HA-myc		
VR-1051U27/	1051-1077	5' TCGCCATGCTAACCAATTTGGCTATC
/VR-2430L24	2407-2430	5' TTGGCATGAGCCCATATTCTTCTC
/VR-1859L33	1827-1859	5' ATGCTCGAGTTATCAGCTAGGCAGGTGCATCAC
VR-1824U24/	1824-1847	5' TTGACCGGCTGGCTGAGGTGATGC
/VR-3349L26	3324-3349	5' GCGTAGCAGGGTCATCAAGCTTAGTC
dVR-67U22/	2167-2187	5' CGCCCGCCACGCGTAATCGACA
/Nsp2Δ324-434-*myc* 2306L64	c-*myc*	5' GATCTTCTTCTGAAATCAACTTTTGTTCCAGAT CTTCTTCAGAGATGAGTTTCTGCTCGCTAGC
Nsp2Δ324-434-*myc* 2344U64/	c-*myc*	5' ACAAAAGTTGATTTCAGAAGAAGATCTGGAACA GAAGCTCATCTCTGAGGAAGATCTGCCTAGG
Nsp2Δ324-434-*myc* 2387U43/	c-*myc*	5' TCTGAGGAAGATCTGCCTAGGCCAAAAGTT CAGCCTCGAAAAA
VR-HA2 1387U65/	*HA*	5' TCCAGATTACGCTTACCCATACGATGTCCCTGA TTACGCAGTTCGTGAAACCCGGCAGGCCAAG
/VR-HA2 1350L65	*HA*	5' GACATCGTATGGGTAAGCGTAATCTGGAACA TCGTATGGGTAACAAGAGCGTGCTTTTCTTGCTC
Construction of nsp2 truncation mutants and cloning of HSPA5		
Nsp2 PL2 1U37/	1373-1387	5' AGCT***AAGCTT***GCCACC**ATGGTG**GCGACTGCTACAGTC
/VR-3755L33	3732-3755	5' TAC***TCTAGA***AGAGCCGGCGCCACCTGTGCCTGCC
/VR-4258L31	4237-4258	5' CTA***TCTAGA***GCCCAGTAACCTGCCAAGAATGG
/VR-4898L33	4875-4898	5' CCC***TCTAGA***TGAAGGCTTGGAAATTTGCCTGATT
/VR-5583L35	5558-5583	5' CTA***TCTAGA***AGACCCAAGCTGGGACGGGGTAAACAA
HSPA5 1U74/	HSPA5	5' CCC***AAGCTT***GCCACCATGGGAGAACAAAAACTCATCTC AGAAGAGGATCTGAAGCTCTCCCTGGTGGCCGCGAT
/HSPA5 1988L38	HSPA5	5' ATG***CTCGAG***TTACTACAACTCATCTTTTTCTGCTGTAT

Fig. 5.1. Characterization of foreign epitope tagged PRRSV. **(A)** Diagram of nsp2-3 and construction of recombinant PRRSV expressing c-*myc* or c-*myc* and HA tagged nsp2. Nsp2 contains a N-terminal small hypervariable region (HV-I), a PL2 protease domain, a middle hypervariable region (HV-II), a putative transmembrane domain (black vertical bars) and a size unknown C-terminal domain. The predicted cleavage sites of nsp2 are shown as gray triangles and the cleavage site of nsp1|nsp2 and nsp3|nsp4 are shown as black and white triangles, respectively. The sizes of the predicted products are also indicated. Three consecutive c-*myc* epitopes were inserted in place of nsp2 aa324-434, based on strain VR-2332 full-length cDNA clone pVR-V7, to generated mutant pV7-*myc*. In the bottom construct, a HA epitope replaced nsp2 aa12-24 of pV7-*myc* to generate double tagged mutant pV7-HA-*myc*. **(B)** Growth kinetics of mutants V7-*myc*, V7-HA-*myc* and parental virus VR-V7 at passage 3. The viruses were used to infect MARC-145 cells in T25 flasks with an MOI of 0.1. The virus-infected cell supernatants were collected every 12 hours and titrated by viral plaque assay. **(C)** Immunostaining of nsp2 protein. At 20 h post infection, the nsp2 protein in V7-*myc* infected MARC-145 cells was labeled using monoclonal antibody 9E10 to c-*myc* epitope and an Alexa-568 conjugated secondary antibody (red) (Molecular Probes). Nuclei were stained with DAPI (blue). The fields were merged using Photoshop.

A.

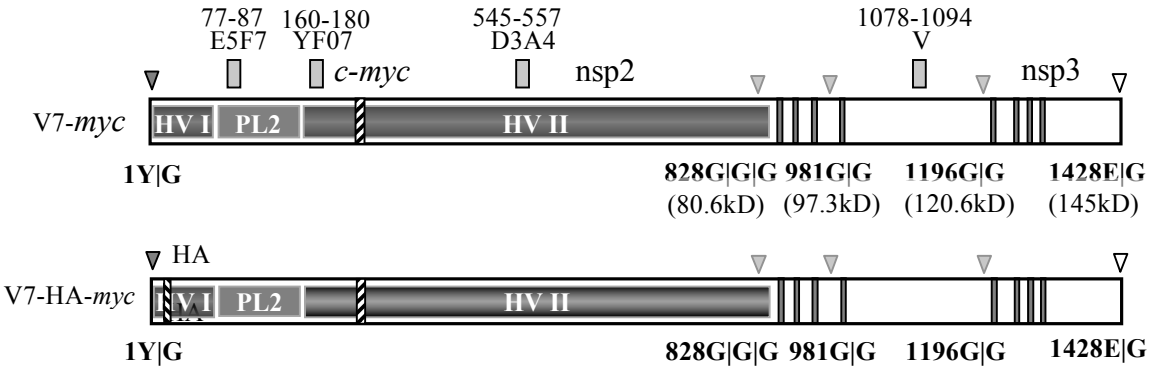
77-87
E5F7
160-180
YF07
c-myc
545-557
D3A4
nsp2
1078-1094
V
nsp3
V7-myc
HV I
PL2
HV II
1Y|G
828G|G|G
(80.6kD)
981G|G
(97.3kD)
1196G|G
(120.6kD)
1428E|G
(145kD)
HA
V7-HA-myc
HV I
PL2
HV II
1Y|G
828G|G|G
981G|G
1196G|G
1428E|G

B.

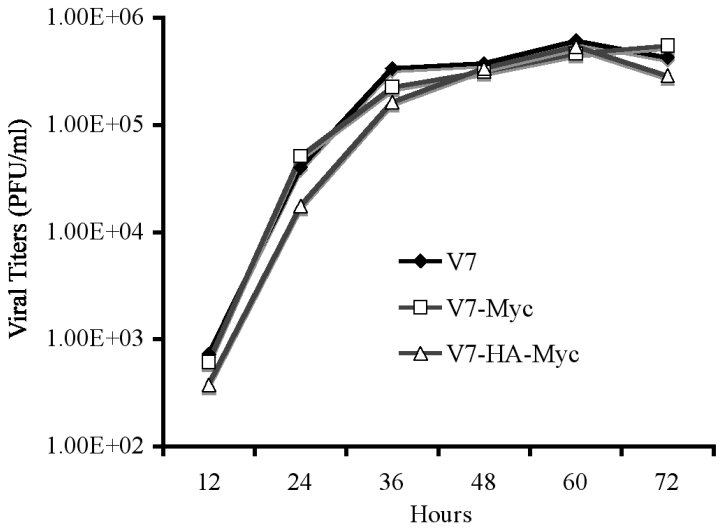
1.00E+06
1.00E+05
1.00E+04
1.00E+03
1.00E+02
Viral Titers (PFU/ml)
12
24
36
48
60
72
Hours
V7
V7-Myc
V7-HA-Myc

C.

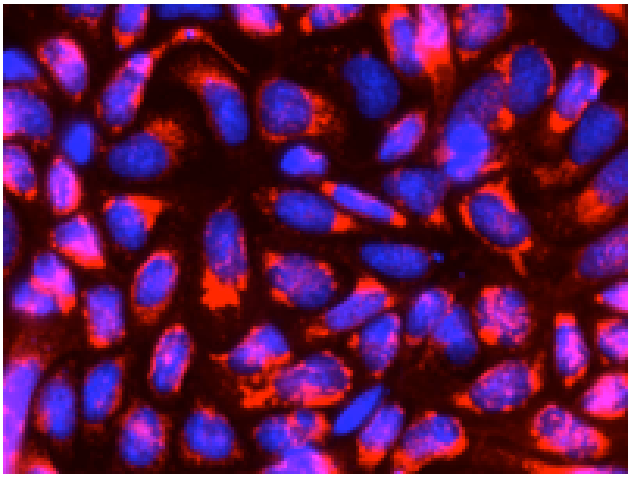

Fig. 5.2. Identification of nsp2 products in PRRSV-infected MARC-145 cells. (A) MARC-145 cells were mock infected or infected with 0.1 MOI of V7-*myc* at passage 3. At 24-36 hours post infection, the cells were lysed and nsp2 proteins were immunoprecipitated by mouse monoclonal antibody 9E10 recognizing the c-*myc* epitope. The samples were analyzed by reducing SDS-PAGE on a 4-12% polyacrylamide gel followed by immunoblot with nsp2 specific antibody E5F8 or D3A4. **(B)** Analysis of nsp2 associated products in V7-HA-*myc* infected MARC-145 cells. The nsp2 products were first immunoprecipitated by c-*myc* antibody 9E10, separated by SDS-PAGE and then analyzed by mouse monoclonal antibody to the HA epitope. **(C)** V7-*myc* infected cell lysates were immunoprecipitated by c-*myc* antibody 9E10 or rabbit antibody V recognizing a peptide near the C terminus of nsp2, separated by SDS-PAGE and then analyzed by western blot with antibody V or rabbit anti-c-*myc* polyclonal antibodies.

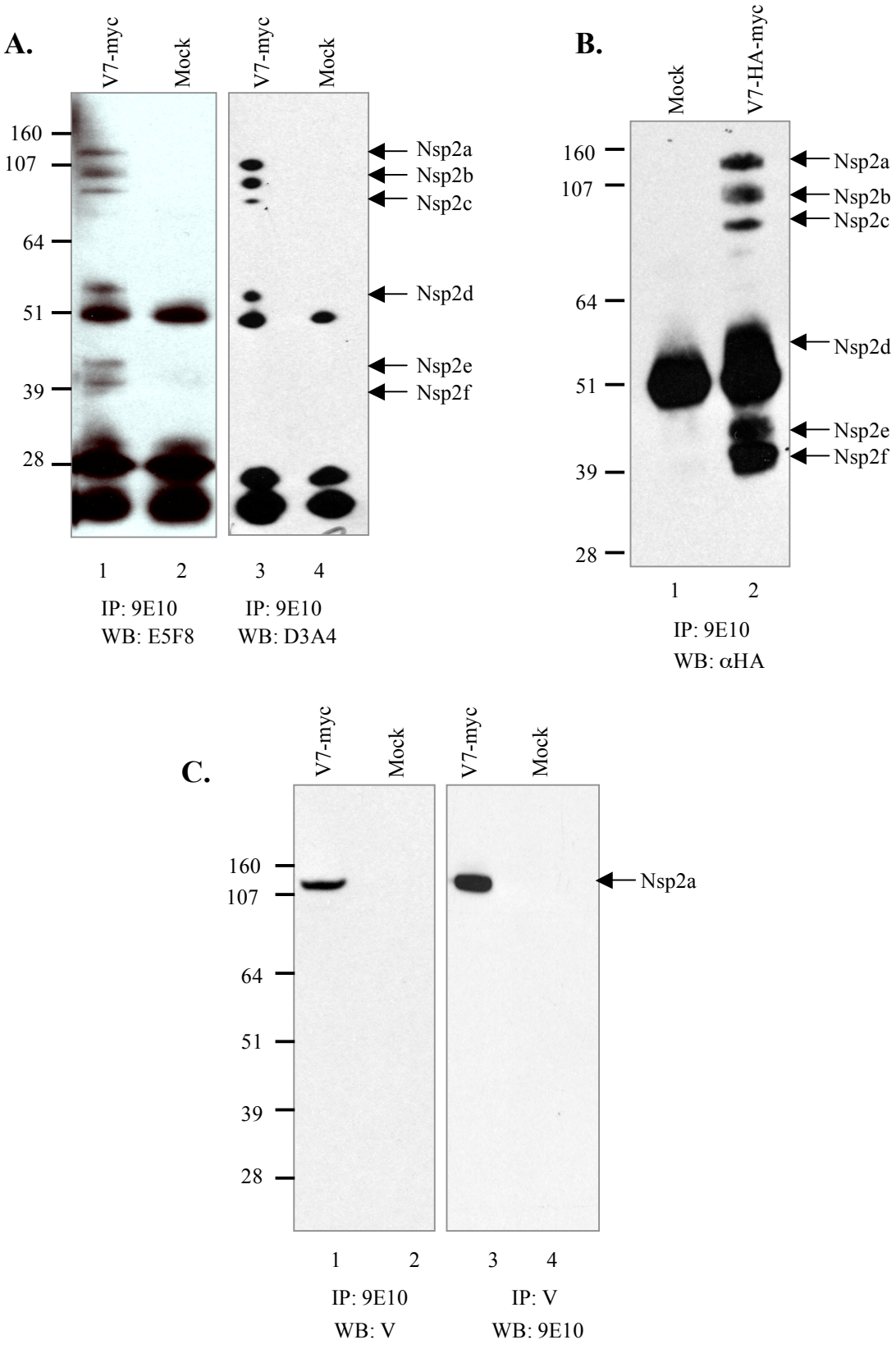
A.
V7-myc
Mock
V7-myc
Mock
160
107
64
51
39
28
Nsp2a
Nsp2b
Nsp2c
Nsp2d
Nsp2e
Nsp2f
1
2
3
4
IP: 9E10
WB: E5F8
IP: 9E10
WB: D3A4
B.
Mock
V7-HA-myc
160
107
64
51
39
28
Nsp2a
Nsp2b
Nsp2c
Nsp2d
Nsp2e
Nsp2f
1
2
IP: 9E10
WB: αHA
C.
V7-myc
Mock
V7-myc
Mock
160
107
64
51
39
28
Nsp2a
1
2
3
4
IP: 9E10
WB: V
IP: V
WB: 9E10

Fig. 5.3. Mapping of the relative positions of the nsp2 isoforms. (A) V7-*myc* nsp2 regions aa541-632, aa633-726 or aa727-813 were deleted to generate new full-length infectious cDNA clone mutants pV7-*myc*-nsp2Δ543-632, pV7-*myc*-nsp2Δ633-726 and pV7-*myc*-nsp2Δ727-813, respectively. The polypeptides corresponding to nsp2 aa12-813, aa12-981 and aa12-1196 were cloned into pcDNA3 to generate plasmid constructs pNsp2 (12-813), pNsp2 (12-981) and pNsp2 (12-1196). The HA-FLAG epitope was attached to the C-terminus of each polypeptide. The predicted molecular weights for the corresponding polypeptides were indicated. (B) MARC-145 cells were infected with nsp2 deletion mutants V7-*myc*-nsp2Δ543-632, V7-*myc*-nsp2Δ633-726 and V7-*myc*-nsp2Δ727-813. At 24-36 hours post infections, the cells were lysed and immunoprecipitated with monoclonal antibody 9E10 to c-*myc*, separated by SDS-PAGE on 4-12% Nupage gel followed by western blot with rabbit polyclonal antibodies to c-*myc*. (C) CHO cells were transfected with plasmids expressing nsp2-3, nsp2-3 C55A or nsp2 truncation mutants. The cells were lysed after 48 hours of transfection and immunoprecipitated with monoclonal antibody 9E10 to *myc* and analyzed by western blot with rabbit polyclonal antibody to c-*myc*. The nsp2 proteins immunoprecipitated from V7-*myc* infected MARC-145 cells served as control.

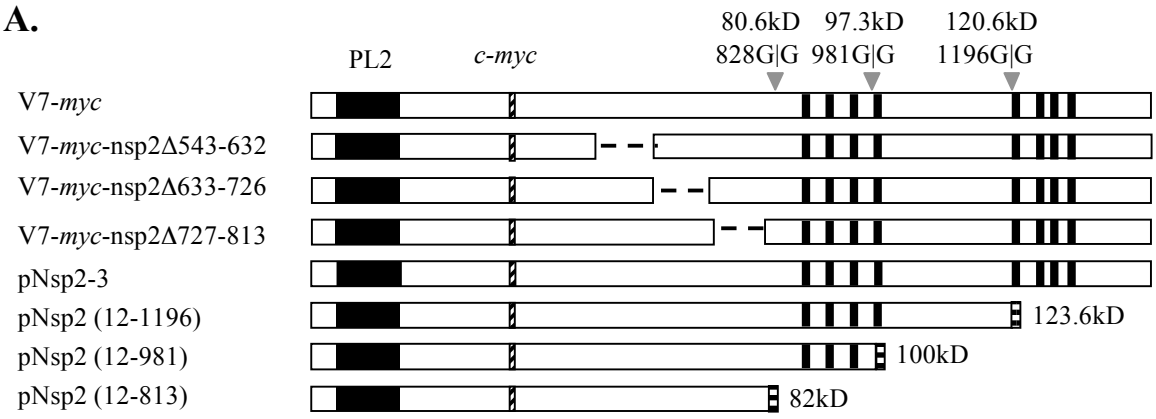
A.
80.6kD
828G|G
97.3kD
981G|G
120.6kD
1196G|G
PL2
c-myc
V7-myc
V7-myc-nsp2Δ543-632
V7-myc-nsp2Δ633-726
V7-myc-nsp2Δ727-813
pNsp2-3
pNsp2 (12-1196)
123.6kD
pNsp2 (12-981)
100kD
pNsp2 (12-813)
82kD

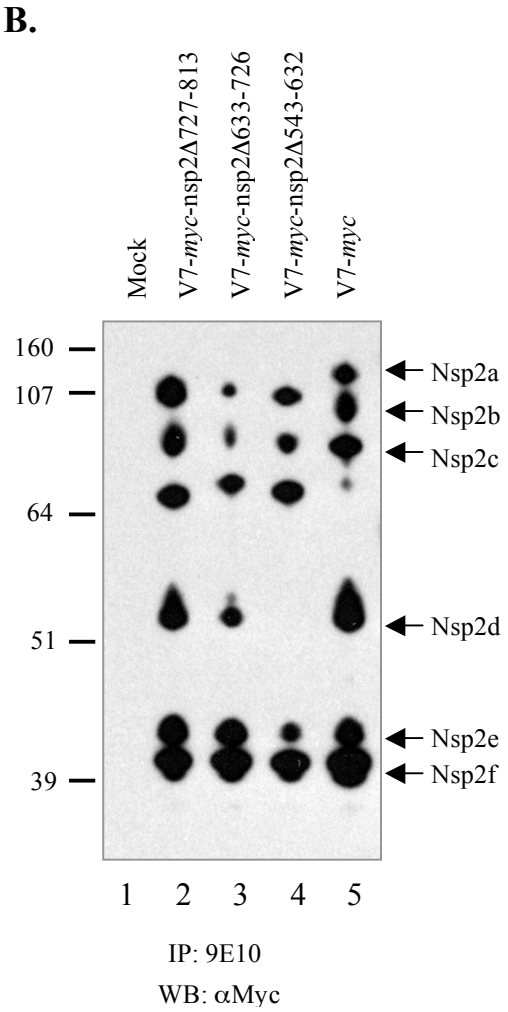
B.
Mock
V7-myc-nsp2Δ727-813
V7-myc-nsp2Δ633-726
V7-myc-nsp2Δ543-632
V7-myc
160
107
64
51
39
Nsp2a
Nsp2b
Nsp2c
Nsp2d
Nsp2e
Nsp2f
1 2 3 4 5
IP: 9E10
WB: αMyc

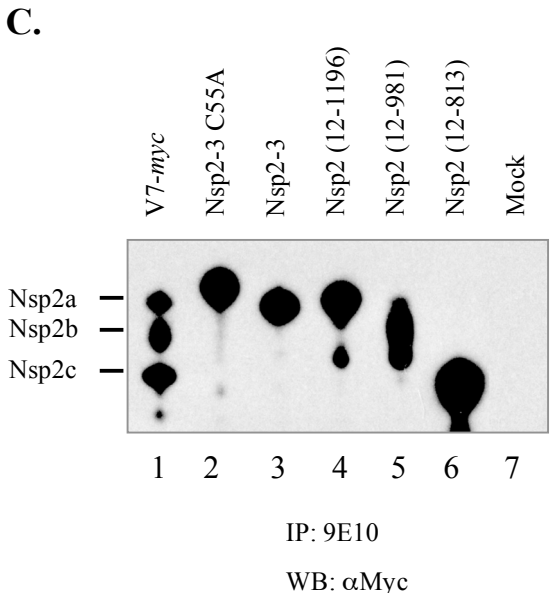
C.
V7-myc
Nsp2-3 C55A
Nsp2-3
Nsp2 (12-1196)
Nsp2 (12-981)
Nsp2 (12-813)
Mock
Nsp2a
Nsp2b
Nsp2c
1 2 3 4 5 6 7
IP: 9E10
WB: αMyc

Fig. 5.4. Accumulation of the nsp2 isoforms during virus infection. MARC-145 cells in 60 mm petri dishes were infected with 0.1 MOI of V7-*myc*. At different time points after infection as indicated, the cells were lysed and immunoprecipitated with monoclonal antibody 9E10 to c-*myc* epitope, separated by SDS-PAGE on 4-12% Nupage gel with 5% β-mercaptoethanol followed by western blot with rabbit polyclonal antibodies to c-*myc*.

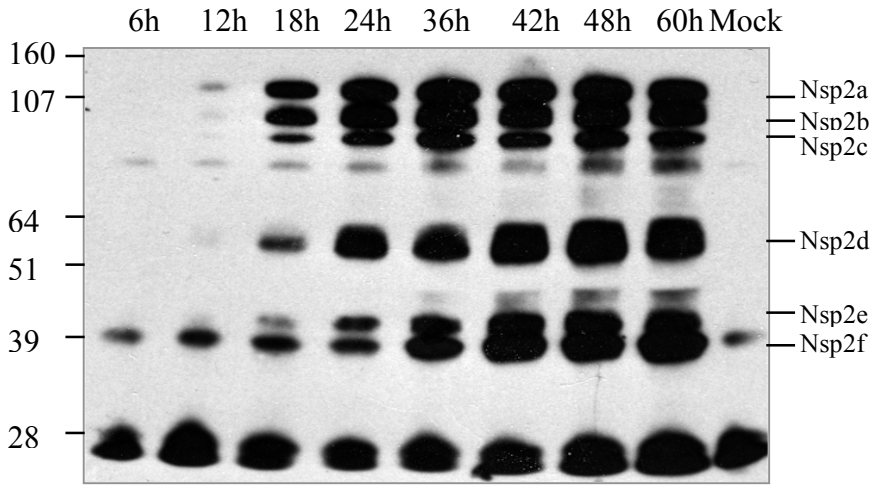

IP: 9E10 WB: αMyc

Fig. 5.5. Pulse-chase analysis of the nsp2 isoforms. MARC-145 cells in 60 mm petri dishes were infected with V7-*myc* at an MOI of 0.1. At 20 hours post infection, the cells were labeled with [^{35}S]-methionine/cysteine. Cells were lysed and immunoprecipitated with (A) c-*myc* antibody 9E10 or (C) rabbit peptide antibody V. For pulse chase analysis, the cells were pulsed for 5 hours and then chased up to 4 hours. Nsp2 proteins were immunoprecipitated with (B) 9E10 monoclonal antibody or (D) rabbit peptide antibody V. The proteins were separated by 4-12% SDS-PAGE with 10% DTT. The gel was dried and the radiolabeled nsp2 proteins were detected by autoradiography.

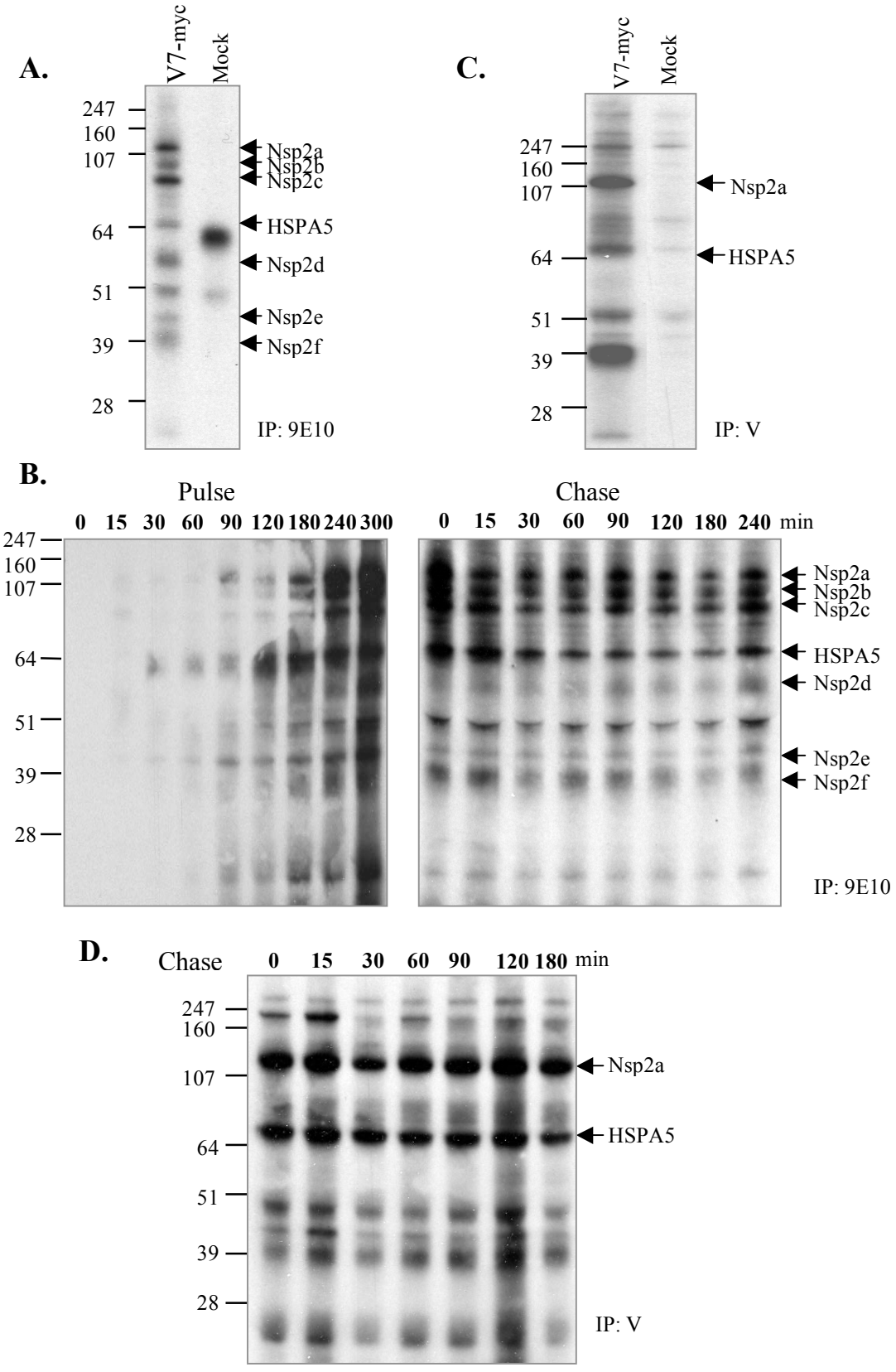
A.
V7-myc
Mock
247
160
107
64
51
39
28
Nsp2a
Nsp2b
Nsp2c
HSPA5
Nsp2d
Nsp2e
Nsp2f
IP: 9E10
C.
V7-myc
Mock
247
160
107
64
51
39
28
Nsp2a
HSPA5
IP: V
B.
Pulse
0 15 30 60 90 120 180 240 300
Chase
0 15 30 60 90 120 180 240 min
247
160
107
64
51
39
28
Nsp2a
Nsp2b
Nsp2c
HSPA5
Nsp2d
Nsp2e
Nsp2f
IP: 9E10
D.
Chase
0 15 30 60 90 120 180 min
247
160
107
64
51
39
28
Nsp2a
HSPA5
IP: V

Fig. 5.6. Coimmunoprecipitation of HSPA5 with nsp2. (A) MARC-145 cells were infected with 0.1 MOI of V7-*myc*. At 24-36 hours post infection, the cells were lysed and treated with two rounds of immunoprecipitation with anti-c-*myc* 9E10 monoclonal antibody and rabbit peptide antibody V, respectively. The proteins were resolved on 4-12% NuPage reducing gel and stained with Coomassie blue. (B) The separated proteins were stained with SYPRO Ruby, excised, digested with trypsin, extracted and subjected to LC-MS/MS analysis. The HSPA5 amino acid sequence is shown, with the recovered sequences highlighted in yellow. (C) Immunoblot analysis of the immunoprecipitated proteins with rabbit polyclonal antibody to HSPA5.

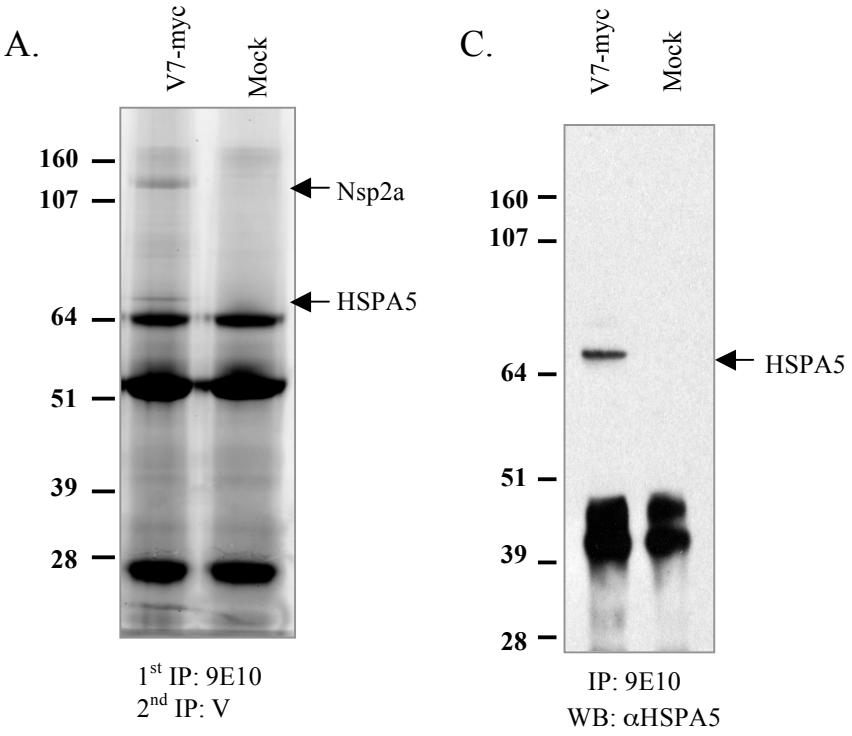

B.

MKLSLVAAML LLLSAARAEE EDKKEDVGTV VGIDLGTTYS CVGVFKNGRV
EIIANDQGNR ITPSYVAFTP EGERLIGDAA KNQLTSNPEN TVFDAKRLIG
RTWNDPSVQQ DIKFLPFKVV EKKTKPYIQV DIGGGQTKTF APEEISAMVL
TKMKETAEAY LGKKVTHAVV TVPAYFNDAQ RQATKDAGTI AGLNVMRIIN
EPTAAAIAYG LDKREGEKNI LVFDLGGGTF DVSLLTIDNG VFEVVATNGD
THLGGEDFDQ RVMEHFIKLY KKKTGKDVRK DNRAVQKLRR EVEKAKRALS
SQHQARIEIE SFYEGEDFSE TLTRAKFEEL NMDLFRSTMK PVQKVLEDSD
LKKSDIDEIV LVGGSTRIPK IQQLVKEFFN GKEPSRGINP DEAVAYGAAV
QAGVLSGDQD TGDLVLLDVC PLTLGIETVG GVMTKLIPRN TVVPTKKSQI
FSTASDNQPT VTIKVYEGER PLTKDNHLLG TFDLTGIPPA PRGVPQIEVT
FEIDVNGILR VTAEDKGTGN KNKITITNDQ NRLTPEEIER MVNDAEKFAE
EDKKLKERID TRNELESYAY SLKNQIGDKE KLGGKLSSED KETMEKAVEE
KIEWLESHQD ADIEDFKAKK KELEEIVQPI ISKLYGSAGP PPTGEEDTAE
KDEL

Fig. 5.7. Coimmunoprecipitation of HSPA with the PL2 cysteine protease domain. (A) The PL2 domain corresponding to nsp2 aa12-323 and the HSPA5 coding region were cloned separately into pcDNA3. A c-*myc* epitope was attached to the C-terminus of PL2 and N terminus of the HSPA5 protein. (B) CHO cells were transfected with plasmids expressing PL2 and HSPA5, or HSPA5 alone. Cells were lysed and PL2-HSPA5 complexes were coimmunoprecipitated by using mouse monoclonal antibody YF07 to the PL2 cysteine protease domain or c-*myc* antibody 9E10. Samples were separated by SDS-PAGE on 4-12% NuPage reducing gel followed by immunoblotting with rabbit anti-*myc* antibodies.

A.

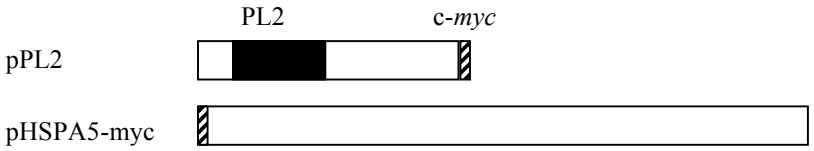
PL2
c-*myc*
pPL2
pHSPA5-myc

B.

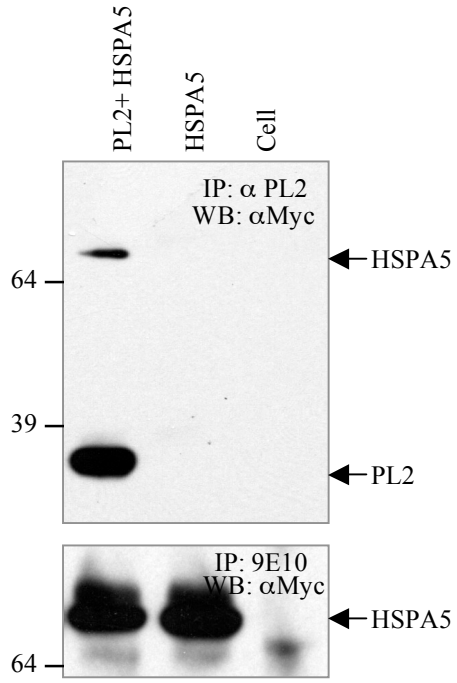
PL2+ HSPA5
HSPA5
Cell
IP: α PL2
WB: αMyc
HSPA5
64
39
PL2
IP: 9E10
WB: αMyc
HSPA5
64

Chapter VI
Major Conclusions and Discussion

Replication of positive-stranded RNA viruses involves translation of viral replicase polyproteins that are proteolytically processed into nonstructural protein subunits, which direct assembly of viral replication complexes and antagonize host anti-viral responses. This dissertation focused on understanding the biology of the multidomain nsp2 replicase protein of PRRSV. We showed that PRRSV nsp2 undergoes rapid evolution in field strains and further identified nsp2 hypervariable regions as nonessential elements for viral replication in cell culture through reverse genetics. We also characterized the N-terminal cysteine protease PL2 domain and provided evidence that the PL2 encodes an active enzyme possessing both *cis* and *trans* activity with a preference for the $G^{1196}|G^{1197}$ dipeptide. Importantly, we showed that the *cis* and *trans* proteolytic activity could be differentiated by point mutations. Mutagenesis studies revealed that the PL2 protease may employ Cys^{55}-Asp^{89}-His^{124} as the catalytic triad and that the *trans*-cleavage activity of the PL2 protease played an essential role in the PRRSV replication cycle. Lastly, we showed the presence of several nsp2 species in PRRSV infected MARC-145 cells and that nsp2 interacted with a host cell factor HSPA5, implying a multifunctional role for nsp2 in PRRSV replication. Several salient points from this research could be summarized as discussed in the following paragraphs.

PRRSV nsp2 is highly heterogeneous and is undergoing rapid evolution

The interesting feature of PRRSV nsp2 genetic variation was noted 10 years ago when the full-length genome sequences of North American (NA) and European (EU) PRRSV, represented by strain VR-2332 and LV, respectively, became available (3, 152, 162). PRRSV of the two genotypes cause similar clinical symptoms but appear to undergo divergent evolution, particularly in the nsp2 region. The nsp2 of PRRSV strain LV is 392 bases shorter than that of strain VR-2332, and the two genotypes share only limited similarity at amino acid level (≤ 45%) (3, 162). Several years later, genetic variation was also observed within genotypes in field strains, characterized by small deletions or insertions and point mutations (75, 80, 192, 206). In an effort to understand

the significance of nsp2 genetic variation, we monitored the evolution in field strains. In parallel to previous findings, we showed in Chapter II that PRRSV nsp2 protein is undergoing unprecedented evolution in that: (i) MN184 strain nsp2 proteins contain three discontinuous deletions with a total size of 131 aa, leading to the shortest PRRSV genome identified to date. The size variation significantly exceeds previously reported deletions that have been maintained at or less than 30aa within genotypes prior to the year 2000. In addition, the dramatic size variation also diminishes the length difference between NA and EU counterparts. (ii) The PRRSV NA lineage MN184 nsp2 also underwent point mutations, sharing only 70% similarity with NA strains and even lower when compared to EU strains (≤ 30%). The findings have led to several questions: (1) how does PRRSV nsp2 carry out a presumably similar function in all PRRSV strains despite such diverse sequences? (2) Is there any correlation between genetic variation and viral virulence? (3) Why does a nonstructural protein of PRRSV need to mutate so vigorously? It is understandable that viral glycoproteins undergo genetic variation because they are exposed to the adaptive immune system and face selective pressure from the host and environment, and thus the mutations help escape host neutralization. It is rare to see a replicase protein undergoing dramatic mutations. Therefore, what is the significance of that? Does it link to viral fitness *in vivo*? If so, how? (4) What are the roles of the conserved putative cysteine protease domain and transmembrane domain in the PRRSV replication cycle?

The hypervariable regions in nsp2 are nonessential for PRRSV replication in cell culture

In an effort to address the above questions, we have successfully developed a reverse genetics system based on PRRSV strain VR-2332 as described in Chapter III. Using deletion mutagenesis approach, we established that the nsp2 hypervariable regions aa12-35 and nsp2 aa324-813 were not essential for viral replication while the putative cysteine protease domain and its downstream flanking sequence as well as the predicted transmembrane domains were indispensable for viral growth in MARC-145 cells. As expected, small deletions did not affect viral growth and the mutants displayed growth kinetics similar to parental virus VR-V7 (Fig. 3.4C). However, a 400aa deletion of the

nsp2 middle segment resulted in a defective phenotype in that the mutant virus could not develop visible plaques (Fig. 3.5A). Although viral growth, release and spreading were shown to be normal, the mutant virus displayed inefficient lysis of MARC-145 cells (Fig. 3.5B and C). Only partial lysis occurred by 5-6 days post infection, while the parental virus infection led to complete detachment of cells at 60-70 hours post infection (Fig. 3.5C). Therefore, it appears that the hypervariable region does play a role in the viral replication cycle and is linked somehow to the viral cytolytic activity. The hypervariable regions of nsp2 are rich in B cell epitopes (48, 168, 261) and induce strong immune responses in PRRSV-infected pigs, which could be detected as early as one week after viral infection (48, 105, 158, 168). An immunological role for nsp2 to serve as an immune decoy has been proposed (75, 206). To test the hypothesis, future work should compare the replication of the different deletion mutants in animal trials. It will be of interest to know how the mutants replicate in pigs and how the viral infection of pigs by these mutants affects host immune parameters. A full investigation of the infection properties *in vivo* will definitely give insight into the role of the hypervariable region of PRRSV nsp2 in viral pathogenesis.

Certainly, other possibilities concerning the role of the nsp2 hypervariable region in the replication cycle of PRRSV should also be considered as follows. (i) *Regulation of protein translation at mRNA level*. Dramatic mutations and deletions could potentially change the structure of the viral mRNA, which may enhance or reduce translation efficiency at the protein level. (ii) *Regulation of protein folding*. Mutations in a genetically flexible region could potentially affect overall protein folding, the consequence of which may be two-fold. (a) It may affect cleavage efficiency of the PL2 protease on its downstream substrate(s). Since *cis*-cleavage is obliged by polyprotein folding, as shown in Chapter IV, the deletion of nsp2 hypervariable region aa324-813 affected the processing efficiency of nsp2 at the site $G^{1196}|G^{1197}$. We have identified several other nsp2 isoforms as described in Chapter V, and thus deletion or mutation may also affect the proteolytic cleavage efficiency of these isoforms. (b) Effect on protein function. Conformational change may have a profound effect on protein function. PRRSV nsp2 has been implicated in the induction of double membrane vesicles where

viral RNA replication takes place, as exemplified by its counterpart EAV nsp2 (209). Thus, nsp2 topology alteration may further affect protein functions, such as correct trafficking and protein-protein/RNA interactions.

Taken together, hypermutations in the nsp2 middle region may have a profound effect on nsp2 processing or function at multiple levels. This fact may reveal a new strategy for a virus to regulate gene expression and protein function as well as viral pathogenesis.

The N-terminus of PRRSV nsp2 encodes an unusual cysteine protease

The fact that deletion of the putative cysteine protease is lethal to PRRSV as described in Chapter III led to the hypothesis that the nsp2 N-terminus encodes a functional protease. Using *in vitro* assays as described in Chapter IV, we provided necessary evidence that the PL2 domain does encode an active protease, which possesses both *cis* and *trans*-cleavage activity *in vitro*. The most significant finding is that the *cis* and *trans*-cleavage activity of the PL2 protease could be distinguished by point mutations, which makes it possible to study the individual functions separately. Reverse genetics revealed that mutations that caused a specific loss of *trans* function but not *cis* activity are detrimental to the virus, suggesting the *trans*-cleavage activity of the PL2 protease plays an important in role in the PRRSV replication cycle. As discussed in Chapter IV, one of the implications is that the *trans*-activity of the PL2 protease plays an active role in suppressing host innate immune responses. Inevitably, almost all of the proteases from positive-stranded RNA viruses assume multiple roles (199, 200, 220). The papain-like protease of coronaviruses has multiple functions including deubiquitinating the ubiquitin-conjugated proteins and inducing degradation of IRF-3 factor in addition to proteolytic processing (129, 196). The NS3 protease of hepatitis C virus targets several molecules in interferon signaling pathway including TRIF and MAVS (124, 125). The 2A, L^{pro} and 3C protease from picornaviruses cleave translation initiation factor eIF4FG, poly (A) binding protein, TATA box binding protein and other cellular factors (15, 115, 136, 199), therefore effectively inhibiting cap-dependent translation of host proteins. As reported earlier, PRRSV is a repressor of interferon signaling, and strongly inhibits the production of interferon alpha and beta as well as IL-1, IL-6 and TNFα during viral

infection (1, 160). It was reported recently that PRRSV particularly interferes with the RIG-1 signaling pathway and suppresses the activation of IRF3 (135). By analogy with the proteases from other RNA viruses described above, it is reasonable to hypothesize that the PL2 protease is actively involved in viral anti-host responses. Elucidation of the role of the PL2 protease in anti-interferon signaling will certainly provide valuable information for understanding viral pathogenesis.

Aspartic acid is an important component of the catalytic triad (His-Asp-Ser/Cys) of virally encoded serine or serine-like proteases (199, 200, 220, 277), including NS3 proteases from *Flaviviridae,* alpha virus capsid protein, 2A and 3C proteases from *Picornaviridae*, and nidovirus 3C-like proteases, all of which adopt chymotrypsin-like folding. Normally, papain-like proteases do not employ aspartic acid as a catalytic component (199, 200, 220, 277). PRRSV PL2 is a hybrid protease and carries features of both papain-like and chymotrypsin-like proteases (213). In the studies described in Chapter IV, we showed that the D89N mutation in the PL2 domain resulted in almost total loss of *trans* activity. The inactivation of the PL2 protease activity is selective since a similar replacement of Asp^{91}, another conserved Asp residue, did not affect efficient cleavage of the substrate (Fig. 4.6A and B). In addition, the D85N substitution is also not so detrimental, resulting in only a partial block in nsp2 cleavage (Fig. 4.6A and B). Thus, these data suggest an important role for Asp^{89} in the catalytic cleavage of nsp2, indicating the PRRSV PL2 protease may employ Cys^{55}-Asp^{89}-His^{124} as the catalytic triad, resembling the feature of chymotrypsin-like proteases. This is also reminiscent of the situation for the SARS coronavirus papain-like protease. Crystal structure analysis and mutagenesis studies identified D287 residue together with Cys112 and His273 as the catalytic triad (93, 190). D287 is situated in a classic triad formation within hydrogen bond distance (2.7A), and plays a very important role in catalysis (190). Although the exact role of aspartic acids in PL2 *trans*-cleavage activity is not known at present, resolving the crystal structure would certainly provide insights into the mechanism of the enzyme-substrate interaction and reveal how Asp residues contribute to enzymatic activity.

The third important feature concerns the role of the PL2 flanking sequence (aa180-323) in proteolysis. Deletion of nsp2 aa180-323 abolished both *cis* and *trans* activity of the PL2 protease, consistent with the result that deletion of the same flanking sequence is lethal to PRRSV as described in Chapter III. The result is quite surprising since nsp2 aa180-323 region is highly divergent between Type I and Type II PRRSV strains (Chapter II). Although it is not clear how the C-terminal region contributes to the proteolytic activity of the PL2 protease, it is conceivable that several functions could be related to this domain as follows. (i) Mediating the interaction with the substrate molecules, (ii) Maintenance of the overall folding of the enzyme or (iii) A non-proteolytic function. This resembles the situation for alphavirus nsp2 protease in which it was found that the 210aa C-terminal extension region is also critical for nsp2 protease activity (95).

PRRSV nsp2 exists as different isoforms and interacts with heat shock 70kDa protein 5

In Chapter V, we examined the proteolytic processing of PRRSV nsp2 protein in virus-infected MARC-145 cells. We revealed the presence of different isoforms of nsp2, which appeared to have the same N-terminus but differed in their C-termini. One question remaining to be answered is whether the PL2 protease mediates all of the nsp2 processing. In Chapter IV, we showed that the PL2 protease mediated a seemingly single cleavage at the site 1196G|G in transfected CHO cells. The protease displayed an absolute preference for Gly at the P1' position and a small amino acid (Gly, Ala but not Ser) at the P1 position as tested by site-directed mutagenesis both *in vitro* and *in vivo* (Fig. 4.7D and E). Based on this substrate recognition nature, we propose that the conserved $G^{828}|G^{829}$ and $G^{981}|G^{982}$ could potentially serve as the cleavage sites for nsp2c and b, respectively, in PRRSV-infected MARC-145 cells. The evidence supporting this hypothesis also includes the facts that the *in vitro* expressed polypeptides corresponding to nsp2 region aa12-813 and aa 12-981 had similar masses to respective nsp2c and b, and that the nsp2c was cleaved downstream of the residue Gly^{813} and nsp2b was processed before Pro^{1076} (Fig. 5.3 and Fig. 5.2). As described in Chapter II and III, four transmembrane-spanning helices (aa876-898, 911-930, 963-979, 989-1009) have been

predicted in this region. Since the nsp2c is much smaller than the peptide coding for nsp2 aa12-981 (Fig. 5.3C), the only possible cleavage site for nsp2c would lie in the region either before the transmembrane domain (aa814-875) or between the transmembrane helices (aa899-910, 931-962), while the cleavage site for nsp2b will be within the region (aa931-962, 980-988, 1010-1087). Alignment of these small regions suggests the highly conserved $G^{828}|G^{829}$ and $G^{981}|G^{982}$ would satisfy the PL2 substrate recognition characteristics and most likely serve as the cleavage sites of nsp2c and b, respectively.

The cleavage sites for nsp2d, e and f have been mapped to the nsp2 region aa434-632 (Fig. 5.2 and 5.3). We propose the involvement of (a) cellular protease(s) based on the following facts. (i) The nsp2 region aa434-632 is highly heterogeneous among PRRSV strains (75, 80, 92, 192, 222). Mutations and deletions were both observed, which makes it less likely to be a viral protease substrate. (ii) No conserved residues that satisfy the cleavage criteria of PL2 protease could be identified among PRRSV strains. (iii) We observed that the nsp2 hypervariable region was cleaved by a cellular protease in transfected CHO cells in Chapter IV. Together, we can conclude that the processing of PRRSV nsp2 in infected MARC-145 cells involves both the PL2 protease and one or more host cell proteases, or other unidentified PRRSV proteases.

The second essential question that must be addressed in the future regards the potential function of the nsp2 isoforms and their role in viral replication. DNA viruses such as herpesviruses generate full-length and truncated versions of the same viral protein through translation reinitiation or mRNA splicing (130, 131, 185). Examples are $U_L26/U_L26.5$, a22/$U_S1.5$ and $U_S3/U_S3.5$, from herpes simplex virus (130, 131, 185). For instance, both U_S3 and $U_S3.5U$ serve as kinase in phosphorylating some viral or cellular proteins, but they differ with respect to their function in blocking apoptosis and in virion maturation and egress (185). For RNA viruses, proteolytic processing of viral replicase proteins may sometimes generate nonstructural protein intermediates (220, 277). For example, the highly regulated processing of alphavirus nonstructural proteins leads to different intermediates that possess discrete functions in viral replication (49, 207, 220, 244). For arterivirus, it was recently reported that EAV nsp7 contains an internal cleavage site for nsp4 encoded 3C-like serine protease and thus the nsp7 has two different

isoforms (227). Mutation studies with the infectious clone demonstrated that both isoforms are critical for viral replication (227). The PRRSV nsp2 isoforms may fit a similar fate, assuming different important roles in viral replication cycle. By using reverse genetics and other approaches, the function and importance of the individual isoform may be tested in the future.

Lastly, we identified the host cell molecular chaperone HSPA5 as an nsp2 co-immunoprecipitate. As a protein chaperone, HSPA5 is actively involved in protein folding in the ER (44, 113). HSPA5 has also been reported to be involved in viral replication processes of many viruses (64, 144) and implications for viral protein-HSPA5 interaction have been discussed in detail in Chapter V. Future work is needed to further dissect the detailed interaction between nsp2 and HSPA5. It will also be interesting to know whether the interaction assists in the processing of nsp2 and what the roles HSPA5 plays in PRRSV replication.

Model for the multifunctionality of PRRSV nsp2

Based on the data obtained in this thesis and the emerging knowledge from other positive-stranded RNA viruses discussed above, we propose a model for the function of nsp2 in the PRRSV replication cycle (Fig. 6.1). Upon PRRSV entry and translation of ORF1a and/or ORF1ab, the replicase precursor nsp2-3 is rapidly processed in *cis* by the PL2 protease to generate nsp2 a, b and c while the generation of nsp2d, e and f involves cellular proteases. The whole process is highly regulated and involves host or viral cofactors. The abundance, function, structure and trafficking of PRRSV nsp2 may be regulated by the hypervariations in the middle region of nsp2 through affecting proteolytic cleavage efficiency, protein folding, viral RNA structure and so on. The hypermutations in nsp2 may also shape host immune responses by generating antigenic and immunogenic epitopes. To antagonize host antiviral responses, on one hand, the nsp2 proteins may interact with and sequester host proteins such as protein chaperone HSPA5, leading to in ER stress which in turn results in unfolded protein responses (UPR) and thereby attenuates host protein translation as a feedback (97, 113). Once the ER stress is over its threshold, it may lead to apoptosis of PRRSV-infected cells (112). On the other hand, it is possible that the nsp2 proteins may interact with proteins involved in host

innate immunity in a way such as mediating host protein cleavage through its *trans*-cleavage activity. To serve a replication purpose, the nsp2 proteins recruit host protein chaperones to assist the folding of macromolecular proteins in viral replication complexes, or may modify the intracellular membranes just as its arterivirus counterpart EAV nsp2 (209), or may interact with different molecules via different isoforms of nsp2 to carry out distinct functions. Future work based on this model may be directed at investigating the following essential questions. (i) What are the roles for the hypervariable region in the proteolytic processing of the nsp2 isoforms? Do mutations affect specific functions of individual nsp2 isoforms such as protein-protein interactions or protein trafficking? (ii) What is the role of the hypervariable region in viral pathogenesis in pigs? Does it affect the immune parameters? (iii) What is the role for the PL2 *trans*-cleavage activity in viral anti-host responses? (iv) What are the roles for HSPA5 in PRRSV replication? (v) what are the additional nsp2 cleavage sites? (vi) What are the functions of the nsp2 isoforms in viral replication? Addressing these questions will most assuredly add further insight into the role of nsp2 protein in PRRSV replication cycle and viral pathogenesis in swine.

Fig 6.1 Proposed model for the function of PRRSV nsp2

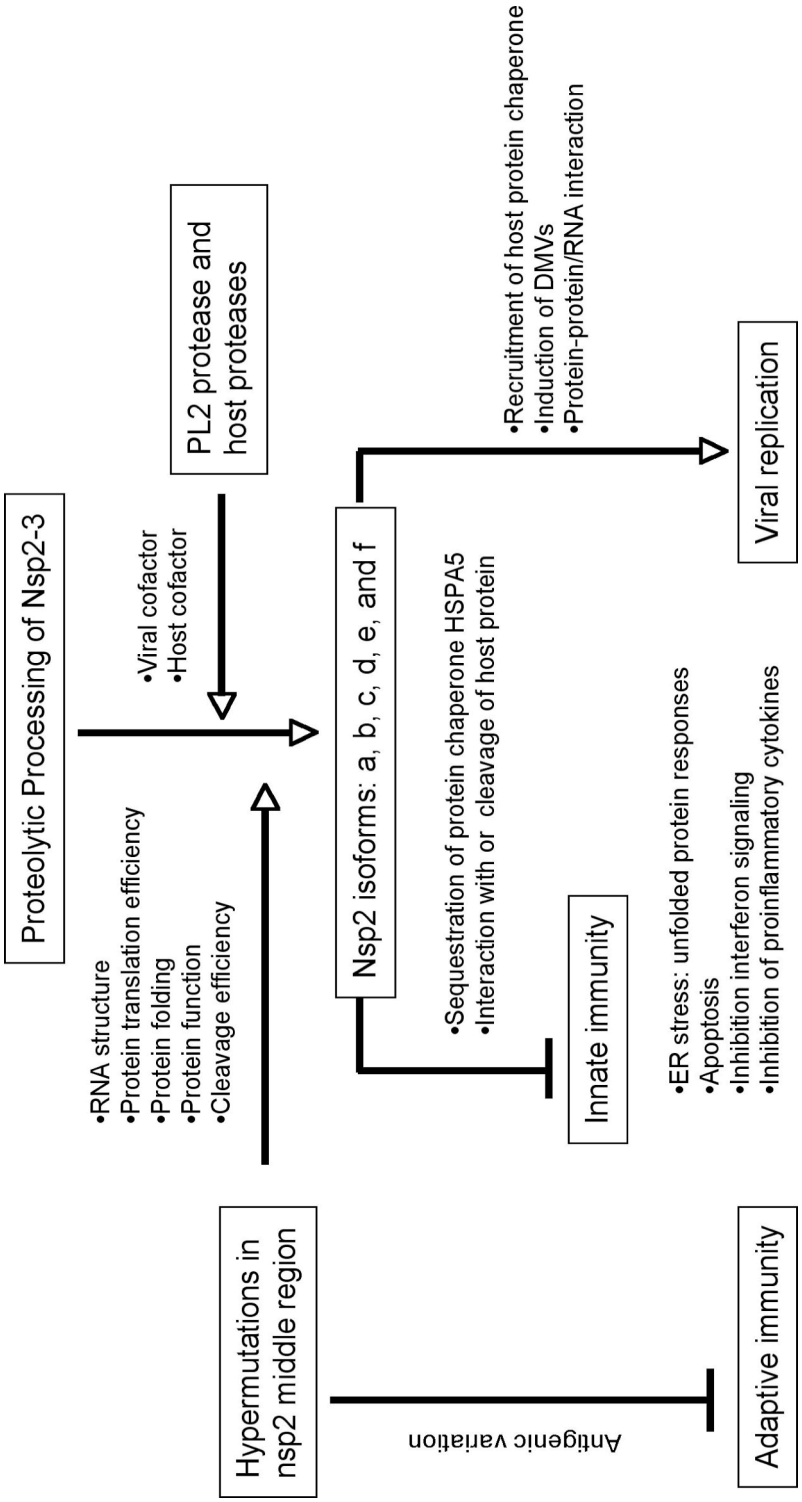

References

1. **Albina, E., C. Carrat, and B. Charley**. 1998. Interferon-alpha response to swine arterivirus (PoAV), the porcine reproductive and respiratory syndrome virus. J. Interferon. Cytokine. Res. **18**:485-490.
2. **Allende, R., W. W. Laegreid, G. F. Kutish, J. A. Galeota, R. W. Wills, and F. A. Osorio**. 2000. Porcine reproductive and respiratory syndrome virus: description of persistence in individual pigs upon experimental infection. J. Virol. **74**:10834-10837.
3. **Allende, R., T. L. Lewis, Z. Lu, D. L. Rock, G. F. Kutish, A. Ali, A. R. Doster, and F. A. Osorio**. 1999. North American and European porcine reproductive and respiratory syndrome viruses differ in non-structural protein coding regions. J. Gen. Virol. **80**:307-315.
4. **Arias, C. F., F. Preugschat, and J. H. Strauss**. 1993. Dengue 2 virus NS2B and NS3 form a stable complex that can cleave NS3 within the helicase domain. Virology. **193**:888-899.
5. **Bairoch, A., P. Bucher, and K. Hofmann**. 1997. The PROSITE database, its status in 1997. Nucleic. Acids. Res. **25**:217-221.
6. **Baker, S. C., K. Yokomori, S. Dong, R. Carlisle, A. E. Gorbalenya, E. V. Koonin, and M. M. Lai**. 1993. Identification of the catalytic sites of a papain-like cysteine proteinase of murine coronavirus. J. Virol. **67**:6056-6063.
7. **Balasuriya, U. B., J. C. Dobbe, H. W. Heidner, V. L. Smalley, A. Navarrette, E. J. Snijder, and N. J. MacLachlan**. 2004. Characterization of the neutralization determinants of equine arteritis virus using recombinant chimeric viruses and site-specific mutagenesis of an infectious cDNA clone. Virology. **321**:235-246.
8. **Barfoed, A. M., M. Blixenkrone-Moller, M. H. Jensen, A. Botner, and S. Kamstrup**. 2004. DNA vaccination of pigs with open reading frame 1-7 of PRRS virus. Vaccine. **22**:3628-3641.
9. **Barretto, N., D. Jukneliene, K. Ratia, Z. Chen, A. D. Mesecar, and S. C. Baker**. 2005. The papain-like protease of severe acute respiratory syndrome coronavirus has deubiquitinating activity. J. Virol. **79**:15189-15198.
10. **Batista, L., S. A. Dee, K. D. Rossow, J. Deen, and C. Pijoan**. 2002. Assessing the duration of persistence and shedding of porcine reproductive and respiratory syndrome virus in a large population of breeding-age gilts. Can. J. Vet. Res **66**:196-200.
11. **Batista, L., C. Pijoan, S. Dee, M. Olin, T. Molitor, H. S. Joo, Z. Xiao, and M. Murtaugh**. 2004. Virological and immunological responses to porcine reproductive and respiratory syndrome virus in a large population of gilts. Can. J. Vet. Res. **68**:267-273.
12. **Bautista, E. M., S. M. Goyal, I. J. Yoon, H. S. Joo, and J. E. Collins**. 1993. Comparison of porcine alveolar macrophages and CL 2621 for the detection of porcine reproductive and respiratory syndrome (PRRS) virus and anti-PRRS antibody. J. Vet. Diagn. Invest. **5**:163-165.
13. **Bautista, E. M., and T. W. Molitor**. 1997. Cell-mediated immunity to porcine reproductive and respiratory syndrome virus in swine. Viral. Immunol. **10**:83-94.

14. **Beerens, N., B. Selisko, S. Ricagno, I. Imbert, L. van der Zanden, E. J. Snijder, and B. Canard**. 2007. De novo initiation of RNA synthesis by the arterivirus RNA-dependent RNA polymerase. J. Virol. **81**:8384-8395.
15. **Belsham, G. J., G. M. McInerney, and N. Ross-Smith**. 2000. Foot-and-mouth disease virus 3C protease induces cleavage of translation initiation factors eIF4A and eIF4G within infected cells. J. Virol. **74**:272-280.
16. **Bendtsen, J. D., H. Nielsen, G. von Heijne, and S. Brunak**. 2004. Improved prediction of signal peptides: SignalP 3.0. J. Mol. Biol. **340**:783-795.
17. **Benfield, D. A., E. Nelson, J. E. Collins, L. Harris, S. M. Goyal, D. Robison, W. T. Christianson, R. B. Morrison, D. Gorcyca, and D. Chladek**. 1992. Characterization of swine infertility and respiratory syndrome (SIRS) virus (isolate ATCC VR-2332). J. Vet. Diagn. Invest. **4**:127-133.
18. **Bonilla, P. J., S. A. Hughes, and S. R. Weiss**. 1997. Characterization of a second cleavage site and demonstration of activity in trans by the papain-like proteinase of the murine coronavirus mouse hepatitis virus strain A59. J. Virol. **71**:900-909.
19. **Bosch, B. J., C. A. de Haan, and P. J. Rottier**. 2004. Coronavirus spike glycoprotein, extended at the carboxy terminus with green fluorescent protein, is assembly competent. J. Virol. **78**:7369-7378.
20. **Botner, A., J. Nielsen, M. B. Oleksiewicz, and T. Storgaard**. 1999. Heterologous challenge with porcine reproductive and respiratory syndrome (PRRS) vaccine virus: no evidence of reactivation of previous European-type PRRS virus infection. Vet. Microbiol. **68**:187-195.
21. **Brierley, I**. 1995. Ribosomal frameshifting viral RNAs. J. Gen. Virol. **76**:1885-1892.
22. **Brockway, S. M., and M. R. Denison**. 2005. Mutagenesis of the murine hepatitis virus nsp1-coding region identifies residues important for protein processing, viral RNA synthesis, and viral replication. Virology. **340**:209-223.
23. **Butkiewicz, N. J., N. Yao, J. Wright-Minogue, R. Zhang, L. Ramanathan, J. Y. Lau, Z. Hong, and B. Dasmahapatra**. 2000. Hepatitis C NS3 protease: restoration of NS4A cofactor activity by N-biotinylation of mutated NS4A using synthetic peptides. Biochem. Biophys. Res. Commun. **267**:278-282.
24. **Cahour, A., B. Falgout, and C. J. Lai**. 1992. Cleavage of the dengue virus polyprotein at the NS3/NS4A and NS4B/NS5 junctions is mediated by viral protease NS2B-NS3, whereas NS4A/NS4B may be processed by a cellular protease. J. Virol. **66**:1535-1542.
25. **Calvert, J. G., D. E. Slade, S. L. Shields, R. Jolie, R. M. Mannan, R. G. Ankenbauer, and S. K. Welch**. 2007. CD163 expression confers susceptibility to porcine reproductive and respiratory syndrome viruses. J. Virol. **81**:7371-7379.
26. **Cano, J. P., S. A. Dee, M. P. Murtaugh, and C. Pijoan**. 2007. Impact of a modified-live porcine reproductive and respiratory syndrome virus vaccine intervention on a population of pigs infected with a heterologous isolate. Vaccine. **25**:4382-4391.
27. **Carter, K. L., and B. Roizman**. 1996. The promoter and transcriptional unit of a novel herpes simplex virus 1 alpha gene are contained in, and encode a protein in frame with, the open reading frame of the alpha 22 gene. J. Virol. **70**:172-178.

28. **Caston, J. R., J. L. Martinez-Torrecuadrada, A. Maraver, E. Lombardo, J. F. Rodriguez, J. I. Casal, and J. L. Carrascosa**. 2001. C terminus of infectious bursal disease virus major capsid protein VP2 is involved in definition of the T number for capsid assembly. J. Virol. **75**:10815-10828.
29. **Cavanagh, D**. 1997. Nidovirales: a new order comprising Coronaviridae and Arteriviridae. Arch. Virol. **142**:629-633.
30. **Chambers, T. J., A. Grakoui, and C. M. Rice**. 1991. Processing of the yellow fever virus nonstructural polyprotein: a catalytically active NS3 proteinase domain and NS2B are required for cleavages at dibasic sites. J. Virol. **65**:6042-6050.
31. **Chappell, K. J., M. J. Stoermer, D. P. Fairlie, and P. R. Young**. 2008. Mutagenesis of the West Nile virus NS2B cofactor domain reveals two regions essential for protease activity. J. Gen. Virol. **89**:1010-1014.
32. **Chen, P., M. Jiang, T. Hu, Q. Liu, X. S. Chen, and D. Guo**. 2007. Biochemical characterization of exoribonuclease encoded by SARS coronavirus. J. Biochem. Mol. Biol. **40**:649-655.
33. **Cho, D. Y., G. H. Yang, C. J. Ryu, and H. J. Hong**. 2003. Molecular chaperone GRP78/BiP interacts with the large surface protein of hepatitis B virus in vitro and in vivo. J. Virol. **77**:2784-2788.
34. **Choi, C., W. S. Cho, B. Kim, and C. Chae**. 2002. Expression of Interferon-gamma and tumour necrosis factor-alpha in pigs experimentally infected with Porcine Reproductive and Respiratory Syndrome Virus (PRRSV). J. Comp. Pathol. **127**:106-113.
35. **Choi, Y. J., S. I. Yun, S. Y. Kang, and Y. M. Lee**. 2006. Identification of 5' and 3' cis-acting elements of the porcine reproductive and respiratory syndrome virus: acquisition of novel 5' AU-rich sequences restored replication of a 5'-proximal 7-nucleotide deletion mutant. J. Virol. **80**:723-736.
36. **Choukhi, A., S. Ung, C. Wychowski, and J. Dubuisson**. 1998. Involvement of endoplasmic reticulum chaperones in the folding of hepatitis C virus glycoproteins. J. Virol. **72**:3851-3858.
37. **Christianson, W. T., J. E. Collins, D. A. Benfield, L. Harris, D. E. Gorcyca, D. W. Chladek, R. B. Morrison, and H. S. Joo**. 1992. Experimental reproduction of swine infertility and respiratory syndrome in pregnant sows. Am. J. Vet. Res. **53**:485-488.
38. **Christopher-Hennings, J., E. A. Nelson, J. K. Nelson, R. J. Hines, S. L. Swenson, H. T. Hill, J. J. Zimmerman, J. B. Katz, M. J. Yaeger, C. C. Chase, and a. et**. 1995. Detection of porcine reproductive and respiratory syndrome virus in boar semen by PCR. J. Clin. Microbiol. **33**:1730-1734.
39. **Clamp, M., J. Cuff, S. M. Searle, and G. J. Barton**. 2004. The Jalview Java alignment editor. Bioinformatics. **20**:426-427.
40. **Clarke, B. E., and D. V. Sangar**. 1988. Processing and assembly of foot-and-mouth disease virus proteins using subgenomic RNA. J. Gen. Virol. **69**:2313-2325.
41. **Collins, J. E., D. A. Benfield, W. T. Christianson, L. Harris, J. C. Hennings, D. P. Shaw, S. M. Goyal, S. McCullough, R. B. Morrison, H. S. Joo, and a. et**. 1992. Isolation of swine infertility and respiratory syndrome virus (isolate ATCC

VR-2332) in North America and experimental reproduction of the disease in gnotobiotic pigs. J. Vet. Diagn. Invest. **4**:117-126.

42. **Conzelmann, K. K., N. Visser, P. Van Woensel, and H. J. Thiel**. 1993. Molecular characterization of porcine reproductive and respiratory syndrome virus, a member of the arterivirus group. Virology. **193**:329-339.
43. **Crooks, G. E., G. Hon, J. M. Chandonia, and S. E. Brenner**. 2004. WebLogo: a sequence logo generator. Genome. Res. **14**:1188-1190.
44. **Daugaard, M., M. Rohde, and M. Jaattela**. 2007. The heat shock protein 70 family: Highly homologous proteins with overlapping and distinct functions. FEBS. Lett. **581**:3702-3710.
45. **de Breyne, S., R. Stalder, and J. Curran**. 2005. Intracellular processing of the Sendai virus C' protein leads to the generation of a Y protein module: structure-functional implications. FEBS. Lett. **579**:5685-5690.
46. **de Groot, R. J., W. R. Hardy, Y. Shirako, and J. H. Strauss**. 1990. Cleavage-site preferences of Sindbis virus polyproteins containing the non-structural proteinase. Evidence for temporal regulation of polyprotein processing in vivo. EMBO. J. **9**:2631-2638.
47. **de Haan, C. A., B. J. Haijema, D. Boss, F. W. Heuts, and P. J. Rottier**. 2005. Coronaviruses as vectors: stability of foreign gene expression. J. Virol. **79**:12742-12751.
48. **de Lima, M., A. K. Pattnaik, E. F. Flores, and F. A. Osorio**. 2006. Serologic marker candidates identified among B-cell linear epitopes of Nsp2 and structural proteins of a North American strain of porcine reproductive and respiratory syndrome virus. Virology. **353**:410-421.
49. **De, I., S. G. Sawicki, and D. L. Sawicki**. 1996. Sindbis virus RNA-negative mutants that fail to convert from minus-strand to plus-strand synthesis: role of the nsP2 protein. J. Virol. **70**:2706-2719.
50. **Dea, S., R. Bilodeau, R. Athanassious, R. Sauvageau, and G. P. Martineau**. 1992. Swine reproductive and respiratory syndrome in Quebec: Isolation of an enveloped virus serologically-related to Lelystad virus. Can. Vet. J. **33**:801-808.
51. **Dea, S., C. A. Gagnon, H. Mardassi, and G. Milane**. 1996. Antigenic variability among North American and European strains of porcine reproductive and respiratory syndrome virus as defined by monoclonal antibodies to the matrix protein. J. Clin. Microbiol. **34**:1488-1493.
52. **Dea, S., C. A. Gagnon, H. Mardassi, B. Pirzadeh, and D. Rogan**. 2000. Current knowledge on the structural proteins of porcine reproductive and respiratory syndrome (PRRS) virus: comparison of the North American and European isolates. Arch. Virol. **145**:659-688.
53. **Dea, S., N. Sawyer, R. Alain, and R. Athanassious**. 1995. Ultrastructural characteristics and morphogenesis of porcine reproductive and respiratory syndrome virus propagated in the highly permissive MARC-145 cell clone. Adv. Exp. Med. Biol. **380**:95-98.
54. **Decroly, E., I. Imbert, B. Coutard, M. Bouvet, B. Selisko, K. Alvarez, A. E. Gorbalenya, E. J. Snijder, and B. Canard**. 2008. Coronavirus nonstructural

protein 16 is a cap-0 binding enzyme possessing (nucleoside-2'O)-methyltransferase activity. J. Virol. **82**:8071-8084.

55. **Dee, S., J. Deen, K. Rossow, C. Wiese, S. Otake, H. S. Joo, and C. Pijoan**. 2002. Mechanical transmission of porcine reproductive and respiratory syndrome virus throughout a coordinated sequence of events during cold weather. Can. J. Vet. Res. **66**:232-239.
56. **Delputte, P. L., S. Costers, and H. J. Nauwynck**. 2005. Analysis of porcine reproductive and respiratory syndrome virus attachment and internalization: distinctive roles for heparan sulphate and sialoadhesin. J. Gen. Virol. **86**:1441-1445.
57. **Delputte, P. L., and H. J. Nauwynck**. 2004. Porcine arterivirus infection of alveolar macrophages is mediated by sialic acid on the virus. J. Virol. **78**:8094-8101.
58. **Delputte, P. L., and H. J. Nauwynck**. 2006. Porcine arterivirus entry in macrophages: heparan sulfate-mediated attachment, sialoadhesin-mediated internalization, and a cell-specific factor mediating virus disassembly and genome release. Adv. Exp. Med. Biol. **581**:247-252.
59. **Delputte, P. L., W. Van Breedam, I. Delrue, C. Oetke, P. R. Crocker, and H. J. Nauwynck**. 2007. Porcine arterivirus attachment to the macrophage-specific receptor sialoadhesin is dependent on the sialic acid-binding activity of the N-terminal immunoglobulin domain of sialoadhesin. J. Virol. **81**:9546-9550.
60. **den Boon, J. A., K. S. Faaberg, J. J. Meulenberg, A. L. Wassenaar, P. G. Plagemann, A. E. Gorbalenya, and E. J. Snijder**. 1995. Processing and evolution of the N-terminal region of the arterivirus replicase ORF1a protein: identification of two papainlike cysteine proteases. J. Virol. **69**:4500-4505.
61. **Diaz, I., L. Darwich, G. Pappaterra, J. Pujols, and E. Mateu**. 2005. Immune responses of pigs after experimental infection with a European strain of Porcine reproductive and respiratory syndrome virus. J. Gen. Virol. **86**:1943-1951.
62. **Diaz, I., L. Darwich, G. Pappaterra, J. Pujols, and E. Mateu**. 2006. Different European-type vaccines against porcine reproductive and respiratory syndrome virus have different immunological properties and confer different protection to pigs. Virology. **351**:249-259.
63. **Ding, M. X., and M. J. Schlesinger**. 1989. Evidence that Sindbis virus NSP2 is an autoprotease which processes the virus nonstructural polyprotein. Virology. **171**:280-284.
64. **Doms, R. W., R. A. Lamb, J. K. Rose, and A. Helenius**. 1993. Folding and assembly of viral membrane proteins. Virology. **193**:545-562.
65. **Done, S. H., and D. J. Paton**. 1995. Porcine reproductive and respiratory syndrome: clinical disease, pathology and immunosuppression. Vet. Rec. **136**:32-35.
66. **Done, S. H., D. J. Paton, and M. E. White**. 1996. Porcine reproductive and respiratory syndrome (PRRS): a review, with emphasis on pathological, virological and diagnostic aspects. Br. Vet. J. **152**:153-174.
67. **Dong, S., and S. C. Baker**. 1994. Determinants of the p28 cleavage site recognized by the first papain-like cysteine proteinase of murine coronavirus. Virology. **204**:541-549.

68. **Dougherty, W. G., and B. L. Semler**. 1993. Expression of virus-encoded proteinases: functional and structural similarities with cellular enzymes. Microbiol. Rev. **57**:781-822.
69. **Dunn, B. M., M. M. Goodenow, A. Gustchina, and A. Wlodawer**. 2002. Retroviral proteases. Genome. Biol. **3**:REVIEWS3006.
70. **Elazhary, Y., J. Weber, H. Bikour, M. Morin, and C. Girard**. 1991. 'Mystery swine disease' in Canada. Vet. Rec. **129(22)**:495-496.
71. **Failla, C., L. Tomei, and R. De Francesco**. 1994. Both NS3 and NS4A are required for proteolytic processing of hepatitis C virus nonstructural proteins. J. Virol. **68**:3753-3760.
72. **Failla, C., L. Tomei, and R. De Francesco**. 1995. An amino-terminal domain of the hepatitis C virus NS3 protease is essential for interaction with NS4A. J. Virol. **69**:1769-1777.
73. **Falgout, B., and L. Markoff**. 1995. Evidence that flavivirus NS1-NS2A cleavage is mediated by a membrane-bound host protease in the endoplasmic reticulum. J. Virol. **69**:7232-7243.
74. **Falgout, B., M. Pethel, Y. M. Zhang, and C. J. Lai**. 1991. Both nonstructural proteins NS2B and NS3 are required for the proteolytic processing of dengue virus nonstructural proteins. J. Virol. **65**:2467-2475.
75. **Fang, Y., D. Y. Kim, S. Ropp, P. Steen, J. Christopher-Hennings, E. A. Nelson, and R. R. Rowland**. 2004. Heterogeneity in Nsp2 of European-like porcine reproductive and respiratory syndrome viruses isolated in the United States. Virus. Res. **100**:229-235.
76. **Fang, Y., R. R. Rowland, M. Roof, J. K. Lunney, J. Christopher-Hennings, and E. A. Nelson**. 2006. A full-length cDNA infectious clone of North American type 1 porcine reproductive and respiratory syndrome virus: expression of green fluorescent protein in the Nsp2 region. J. Virol. **80**:11447-11455.
77. **Fang, Y., P. Schneider, W. P. Zhang, K. S. Faaberg, E. A. Nelson, and R. R. Rowland**. 2007. Diversity and evolution of a newly emerged North American Type 1 porcine arterivirus: analysis of isolates collected between 1999 and 2004. Arch. Virol. **152**:1009-1017.
78. **Feng, W., S. M. Laster, M. Tompkins, T. Brown, J. S. Xu, C. Altier, W. Gomez, D. Benfield, and M. B. McCaw**. 2001. In utero infection by porcine reproductive and respiratory syndrome virus is sufficient to increase susceptibility of piglets to challenge by Streptococcus suis type II. J. Virol. **75**:4889-4895.
79. **Fontana, J. M., B. Bankamp, W. J. Bellini, and P. A. Rota**. 2008. Regulation of interferon signaling by the C and V proteins from attenuated and wild-type strains of measles virus. Virology. **374**:71-81.
80. **Gao, Z. Q., X. Guo, and H. C. Yang**. 2004. Genomic characterization of two Chinese isolates of porcine respiratory and reproductive syndrome virus. Arch. Virol. **149**:1341-1351.
81. **Gomez de Cedron, M., N. Ehsani, M. L. Mikkola, J. A. Garcia, and L. Kaariainen**. 1999. RNA helicase activity of Semliki Forest virus replicase protein NSP2. FEBS. Lett. **448**:19-22.

82. **Gonin, P., H. Mardassi, C. A. Gagnon, B. Massie, and S. Dea**. 1998. A nonstructural and antigenic glycoprotein is encoded by ORF3 of the IAF-Klop strain of porcine reproductive and respiratory syndrome virus. Arch. Virol. **143**:1927-1940.
83. **Gonin, P., B. Pirzadeh, C. A. Gagnon, and S. Dea**. 1999. Seroneutralization of porcine reproductive and respiratory syndrome virus correlates with antibody response to the GP5 major envelope glycoprotein. J. Vet. Diagn. Invest. **11**:20-26.
84. **Gorbalenya, A. E., L. Enjuanes, J. Ziebuhr, and E. J. Snijder**. 2006. Nidovirales: evolving the largest RNA virus genome. Virus. Res. **117**:17-37.
85. **Gosert, R., A. Kanjanahaluethai, D. Egger, K. Bienz, and S. C. Baker**. 2002. RNA replication of mouse hepatitis virus takes place at double-membrane vesicles. J. Virol. **76**:3697-3708.
86. **Gradil, C., C. Dubuc, and M. D. Eaglesome**. 1996. Porcine reproductive and respiratory syndrome virus: seminal transmission. Vet. Rec. **138**:521-522.
87. **Graham, R. L., A. C. Sims, S. M. Brockway, R. S. Baric, and M. R. Denison**. 2005. The nsp2 replicase proteins of murine hepatitis virus and severe acute respiratory syndrome coronavirus are dispensable for viral replication. J. Virol. **79**:13399-13411.
88. **Groot Bramel-Verheije, M. H., P. J. Rottier, and J. J. Meulenberg**. 2000. Expression of a foreign epitope by porcine reproductive and respiratory syndrome virus. Virology. **278**:380-389.
89. **Haghighat, A., Y. Svitkin, I. Novoa, E. Kuechler, T. Skern, and N. Sonenberg**. 1996. The eIF4G-eIF4E complex is the target for direct cleavage by the rhinovirus 2A proteinase. J. Virol. **70**:8444-8450.
90. **Han, J., G. Liu, Y. Wang, and K. S. Faaberg**. 2007. Identification of nonessential regions of the nsp2 replicase protein of porcine reproductive and respiratory syndrome virus strain VR-2332 for replication in cell culture. J. Virol. **81**:9878-9890.
91. **Han, J., M. S. Rutherford, and K. S. Faaberg**. 2008. Characterization of the protease activity of the PL2 cysteine protease domain encoded in the N-terminus of porcine reproductive and respiratory syndrome virus nsp2 replicase protein. Chapter IV.
92. **Han, J., Y. Wang, and K. S. Faaberg**. 2006. Complete genome analysis of RFLP 184 isolates of porcine reproductive and respiratory syndrome virus. Virus. Res. **122**:175-182.
93. **Harcourt, B. H., D. Jukneliene, A. Kanjanahaluethai, J. Bechill, K. M. Severson, C. M. Smith, P. A. Rota, and S. C. Baker**. 2004. Identification of severe acute respiratory syndrome coronavirus replicase products and characterization of papain-like protease activity. J. Virol. **78**:13600-13612.
94. **Hardy, W. R., and J. H. Strauss**. 1988. Processing the nonstructural polyproteins of Sindbis virus: study of the kinetics in vivo by using monospecific antibodies. J. Virol. **62**:998-1007.
95. **Hardy, W. R., and J. H. Strauss**. 1989. Processing the nonstructural polyproteins of sindbis virus: nonstructural proteinase is in the C-terminal half of nsP2 and functions both in cis and in trans. J. Virol. **63**:4653-4664.

96. **Harmon, S. A., W. Updike, X. Y. Jia, D. F. Summers, and E. Ehrenfeld**. 1992. Polyprotein processing in cis and in trans by hepatitis A virus 3C protease cloned and expressed in Escherichia coli. J. Virol. **66**:5242-5247.
97. **He, B**. 2006. Viruses, endoplasmic reticulum stress, and interferon responses. Cell. Death. Differ. **13**:393-403.
98. **Herold, J., A. E. Gorbalenya, V. Thiel, B. Schelle, and S. G. Siddell**. 1998. Proteolytic processing at the amino terminus of human coronavirus 229E gene 1-encoded polyproteins: identification of a papain-like proteinase and its substrate. J. Virol. **72**:910-918.
99. **H, H**. 1990. Overview and history of mystery swine disease (swine infertility respiratory syndrome). Proc. Mystery. Swine. Disease. Committee. Meeting.
100. **Hooper, C. C., W. G. Van Alstine, G. W. Stevenson, and C. L. Kanitz**. 1994. Mice and rats (laboratory and feral) are not a reservoir for PRRS virus. J. Vet. Diagn. Invest. **6**:13-15.
101. **Indik, S., L. Valicek, D. Klein, and J. Klanova**. 2000. Variations in the major envelope glycoprotein GP5 of Czech strains of porcine reproductive and respiratory syndrome virus. J. Gen. Virol. **81**:2497-2502.
102. **Ivanov, K. A., T. Hertzig, M. Rozanov, S. Bayer, V. Thiel, A. E. Gorbalenya, and J. Ziebuhr**. 2004. Major genetic marker of nidoviruses encodes a replicative endoribonuclease. Proc. Natl. Acad. Sci. U S A. **101**:12694-12699.
103. **Ivanov, K. A., V. Thiel, J. C. Dobbe, Y. van der Meer, E. J. Snijder, and J. Ziebuhr**. 2004. Multiple enzymatic activities associated with severe acute respiratory syndrome coronavirus helicase. J. Virol. **78**:5619-5632.
104. **Johnson, C. L., D. M. Owen, and M. J. Gale**. 2007. Functional and therapeutic analysis of hepatitis C virus NS3.4A protease control of antiviral immune defense. J. Biol. Chem. **282**:10792-10803.
105. **Johnson, C. R., W. Yu, and M. P. Murtaugh**. 2007. Cross-reactive antibody responses to nsp1 and nsp2 of Porcine reproductive and respiratory syndrome virus. J. Gen. Virol. **88**:1184-1195.
106. **Johnson, K. L., and L. A. Ball**. 1997. Replication of flock house virus RNAs from primary transcripts made in cells by RNA polymerase II. J. Virol. **71**:3323-3327.
107. **Jore, J., B. De Geus, R. J. Jackson, P. H. Pouwels, and B. E. Enger-Valk**. 1988. Poliovirus protein 3CD is the active protease for processing of the precursor protein P1 in vitro. J. Gen. Virol. **69**:1627-1636.
108. **Kanjanahaluethai, A., D. Jukneliene, and S. C. Baker**. 2003. Identification of the murine coronavirus MP1 cleavage site recognized by papain-like proteinase 2. J. Virol. **77**:7376-7382.
109. **Kapur, V., M. R. Elam, T. M. Pawlovich, and M. P. Murtaugh**. 1996. Genetic variation in porcine reproductive and respiratory syndrome virus isolates in the midwestern United States. J. Gen. Virol. **77**:1271-1276.
110. **Keffaber, K. K**. 1989. Reproductive failure of unkown etiology. Am. Assoc. Swine. Prac. Newsl. **1**:1:10.
111. **Kim, H. S., J. Kwang, I. J. Yoon, H. S. Joo, and M. L. Frey**. 1993. Enhanced replication of porcine reproductive and respiratory syndrome (PRRS) virus in a homogeneous subpopulation of MA-104 cell line. Arch. Virol. **133**:477-483.

112. **Kim, R., M. Emi, K. Tanabe, and S. Murakami**. 2006. Role of the unfolded protein response in cell death. Apoptosis. **11**:5-13.
113. **Kleizen, B., and I. Braakman**. 2004. Protein folding and quality control in the endoplasmic reticulum. Curr. Opin. Cell. Biol. **16**:343-349.
114. **Kou, Y. H., M. F. Chang, Y. M. Wang, T. M. Hung, and S. C. Chang**. 2007. Differential requirements of NS4A for internal NS3 cleavage and polyprotein processing of hepatitis C virus. J. Virol. **81**:7999-8008.
115. **Krausslich, H. G., M. J. Nicklin, H. Toyoda, D. Etchison, and E. Wimmer**. 1987. Poliovirus proteinase 2A induces cleavage of eucaryotic initiation factor 4F polypeptide p220. J. Virol. **61**:2711-2718.
116. **Kreutz, L. C., and M. R. Ackermann**. 1996. Porcine reproductive and respiratory syndrome virus enters cells through a low pH-dependent endocytic pathway. Virus. Res. **42**:137-147.
117. **Kristensen, C. S., A. Botner, H. Takai, J. P. Nielsen, and S. E. Jorsal**. 2004. Experimental airborne transmission of PRRS virus. Vet. Microbiol. **99**:197-202.
118. **Lackner, T., H. J. Thiel, and N. Tautz**. 2006. Dissection of a viral autoprotease elucidates a function of a cellular chaperone in proteolysis. Proc. Natl. Acad. Sci. U S A. **103**:1510-1515.
119. **Lager, K. M., and W. L. Mengeling**. 1995. Pathogenesis of in utero infection in porcine fetuses with porcine reproductive and respiratory syndrome virus. Can. J. Vet. Res. **59**:187-192.
120. **Lager, K. M., W. L. Mengeling, and S. L. Brockmeier**. 1999. Evaluation of protective immunity in gilts inoculated with the NADC-8 isolate of porcine reproductive and respiratory syndrome virus (PRRSV) and challenge-exposed with an antigenically distinct PRRSV isolate. Am. J. Vet. Res. **60**:1022-1027.
121. **Lamontagne, L., C. Page, R. Larochelle, and R. Magar**. 2003. Porcine reproductive and respiratory syndrome virus persistence in blood, spleen, lymph nodes, and tonsils of experimentally infected pigs depends on the level of CD8high T cells. Viral. Immunol. **16**:395-406.
122. **Lemm, J. A., and C. M. Rice**. 1993. Roles of nonstructural polyproteins and cleavage products in regulating Sindbis virus RNA replication and transcription. J. Virol. **67**:1916-1926.
123. **Lemm, J. A., T. Rumenapf, E. G. Strauss, J. H. Strauss, and C. M. Rice**. 1994. Polypeptide requirements for assembly of functional Sindbis virus replication complexes: a model for the temporal regulation of minus- and plus-strand RNA synthesis. EMBO. J. **13**:2925-2934.
124. **Li, K., E. Foy, J. C. Ferreon, M. Nakamura, A. C. Ferreon, M. Ikeda, S. C. Ray, M. J. Gale, and S. M. Lemon**. 2005. Immune evasion by hepatitis C virus NS3/4A protease-mediated cleavage of the Toll-like receptor 3 adaptor protein TRIF. Proc. Natl. Acad. Sci. U S A. **102**:2992-2997.
125. **Li, X. D., L. Sun, R. B. Seth, G. Pineda, and Z. J. Chen**. 2005. Hepatitis C virus protease NS3/4A cleaves mitochondrial antiviral signaling protein off the mitochondria to evade innate immunity. Proc. Natl. Acad. Sci. U S A. **102**:17717-17722.

126. **Lim, K. P., and D. X. Liu**. 1998. Characterization of the two overlapping papain-like proteinase domains encoded in gene 1 of the coronavirus infectious bronchitis virus and determination of the C-terminal cleavage site of an 87-kDa protein. Virology. **245**:303-312.
127. **Lin, C., B. M. Pragai, A. Grakoui, J. Xu, and C. M. Rice**. 1994. Hepatitis C virus NS3 serine proteinase: trans-cleavage requirements and processing kinetics. J. Virol. **68**:8147-8157.
128. **Lin, C. W., H. D. Huang, S. Y. Shiu, W. J. Chen, M. H. Tsai, S. H. Huang, L. Wan, and Y. J. Lin**. 2007. Functional determinants of NS2B for activation of Japanese encephalitis virus NS3 protease. Virus. Res. **127**:88-94.
129. **Lindner, H. A., N. Fotouhi-Ardakani, V. Lytvyn, P. Lachance, T. Sulea, and R. Menard**. 2005. The papain-like protease from the severe acute respiratory syndrome coronavirus is a deubiquitinating enzyme. J. Virol. **79**:15199-15208.
130. **Liu, F. Y., and B. Roizman**. 1991. The promoter, transcriptional unit, and coding sequence of herpes simplex virus 1 family 35 proteins are contained within and in frame with the UL26 open reading frame. J. Virol. **65**:206-212.
131. **Liu, F. Y., and B. Roizman**. 1991. The herpes simplex virus 1 gene encoding a protease also contains within its coding domain the gene encoding the more abundant substrate. J. Virol. **65**:5149-5156.
132. **Loo, Y. M., D. M. Owen, K. Li, A. K. Erickson, C. L. Johnson, P. M. Fish, D. S. Carney, T. Wang, H. Ishida, M. Yoneyama, T. Fujita, T. Saito, W. M. Lee, C. H. Hagedorn, D. T. Lau, S. A. Weinman, S. M. Lemon, and M. J. Gale**. 2006. Viral and therapeutic control of IFN-beta promoter stimulator 1 during hepatitis C virus infection. Proc. Natl. Acad. Sci. U S A. **103**:6001-6006.
133. **Lopez, O. J., M. F. Oliveira, E. A. Garcia, B. J. Kwon, A. Doster, and F. A. Osorio**. 2007. Protection against porcine reproductive and respiratory syndrome virus (PRRSV) infection through passive transfer of PRRSV-neutralizing antibodies is dose dependent. Clin. Vaccine. Immunol. **14**:269-275.
134. **Lopez, O. J., and F. A. Osorio**. 2004. Role of neutralizing antibodies in PRRSV protective immunity. Vet. Immunol. Immunopathol. **102**:155-163.
135. **Luo, R., S. Xiao, Y. Jiang, H. Jin, D. Wang, M. Liu, H. Chen, and L. Fang**. 2008. Porcine reproductive and respiratory syndrome virus (PRRSV) suppresses interferon-beta production by interfering with the RIG-I signaling pathway. Mol. Immunol. **45**:2839-2846.
136. **Macadam, A. J., G. Ferguson, T. Fleming, D. M. Stone, J. W. Almond, and P. D. Minor**. 1994. Role for poliovirus protease 2A in cap independent translation. EMBO. J. **13**:924-927.
137. **Magar, R., R. Larochelle, S. Dea, C. A. Gagnon, E. A. Nelson, J. Christopher-Hennings, and D. A. Benfield**. 1995. Antigenic comparison of Canadian and US isolates of porcine reproductive and respiratory syndrome virus using monoclonal antibodies to the nucleocapsid protein. Can. J. Vet. Res. **59**:232-234.
138. **Mardassi, H., R. Athanassious, S. Mounir, and S. Dea**. 1994. Porcine reproductive and respiratory syndrome virus: morphological, biochemical and serological characteristics of Quebec isolates associated with acute and chronic

outbreaks of porcine reproductive and respiratory syndrome. Can. J. Vet. Res. **58**:55-64.

139. **Mardassi, H., P. Gonin, C. A. Gagnon, B. Massie, and S. Dea**. 1998. A subset of porcine reproductive and respiratory syndrome virus GP3 glycoprotein is released into the culture medium of cells as a non-virion-associated and membrane-free (soluble) form. J. Virol. **72**:6298-6306.
140. **Mardassi, H., B. Massie, and S. Dea**. 1996. Intracellular synthesis, processing, and transport of proteins encoded by ORFs 5 to 7 of porcine reproductive and respiratory syndrome virus. Virology. **221**:98-112.
141. **Mardassi, H., S. Mounir, and S. Dea**. 1994. Identification of major differences in the nucleocapsid protein genes of a Quebec strain and European strains of porcine reproductive and respiratory syndrome virus. J. Gen. Virol. **75**:681-685.
142. **Martelli, P., P. Cordioli, L. G. Alborali, S. Gozio, E. De Angelis, L. Ferrari, G. Lombardi, and P. Borghetti**. 2007. Protection and immune response in pigs intradermally vaccinated against porcine reproductive and respiratory syndrome (PRRS) and subsequently exposed to a heterologous European (Italian cluster) field strain. Vaccine. **25**:3400-3408.
143. **Matthes, N., J. R. Mesters, B. Coutard, B. Canard, E. J. Snijder, R. Moll, and R. Hilgenfeld**. 2006. The non-structural protein Nsp10 of mouse hepatitis virus binds zinc ions and nucleic acids. FEBS. Lett. **580**:4143-4149.
144. **Mayer, M. P**. 2005. Recruitment of Hsp70 chaperones: a crucial part of viral survival strategies. Rev. Physiol. Biochem. Pharmacol. **153**:1-46.
145. **McGuffin, L. J., K. Bryson, and D. T. Jones**. 2000. The PSIPRED protein structure prediction server. Bioinformatics. **16**:404-405.
146. **Meier, W. A., J. Galeota, F. A. Osorio, R. J. Husmann, W. M. Schnitzlein, and F. A. Zuckermann**. 2003. Gradual development of the interferon-gamma response of swine to porcine reproductive and respiratory syndrome virus infection or vaccination. Virology. **309**:18-31.
147. **Meng, X. J**. 2000. Heterogeneity of porcine reproductive and respiratory syndrome virus: implications for current vaccine efficacy and future vaccine development. Vet. Microbiol. **74**:309-329.
148. **Meng, X. J., P. S. Paul, P. G. Halbur, and M. A. Lum**. 1995. Phylogenetic analyses of the putative M (ORF 6) and N (ORF 7) genes of porcine reproductive and respiratory syndrome virus (PRRSV): implication for the existence of two genotypes of PRRSV in the U.S.A. and Europe. Arch. Virol. **140**:745-755.
149. **Mengeling, W. L., K. M. Lager, and A. C. Vorwald**. 1994. Temporal characterization of transplacental infection of porcine fetuses with porcine reproductive and respiratory syndrome virus. Am. J. Vet. Res. **55**:1391-1398.
150. **Meulenberg, J. J., J. N. Bos-de Ruijter, R. van de Graaf, G. Wensvoort, and R. J. Moormann**. 1998. Infectious transcripts from cloned genome-length cDNA of porcine reproductive and respiratory syndrome virus. J. Virol. **72**:380-387.
151. **Meulenberg, J. J., M. M. Hulst, E. J. de Meijer, P. L. Moonen, A. den Besten, E. P. de Kluyver, G. Wensvoort, and R. J. Moormann**. 1993. Lelystad virus, the causative agent of porcine epidemic abortion and respiratory syndrome (PEARS), is related to LDV and EAV. Virology. **192**:62-72.

152. **Meulenberg, J. J., A. Petersen den Besten, E. de Kluyver, A. van Nieuwstadt, G. Wensvoort, and R. J. Moormann**. 1997. Molecular characterization of Lelystad virus. Vet. Microbiol. **55**:197-202.
153. **Meulenberg, J. J., and A. Petersen-den Besten**. 1996. Identification and characterization of a sixth structural protein of Lelystad virus: the glycoprotein GP2 encoded by ORF2 is incorporated in virus particles. Virology. **225**:44-51.
154. **Meulenberg, J. J., A. Petersen-den Besten, E. P. De Kluyver, R. J. Moormann, W. M. Schaaper, and G. Wensvoort**. 1995. Characterization of proteins encoded by ORFs 2 to 7 of Lelystad virus. Virology. **206**:155-163.
155. **Miller, L. C., W. W. Laegreid, J. L. Bono, C. G. Chitko-McKown, and J. M. Fox**. 2004. Interferon type I response in porcine reproductive and respiratory syndrome virus-infected MARC-145 cells. Arch. Virol. **149**:2453-2463.
156. **Minskaia, E., T. Hertzig, A. E. Gorbalenya, V. Campanacci, C. Cambillau, B. Canard, and J. Ziebuhr**. 2006. Discovery of an RNA virus 3'->5' exoribonuclease that is critically involved in coronavirus RNA synthesis. Proc. Natl. Acad. Sci. U S A. **103**:5108-5113.
157. **Molitor, T. W., E. M. Bautista, and C. S. Choi**. 1997. Immunity to PRRSV: double-edged sword. Vet. Microbiol. **55**:265-276.
158. **Mulupuri, P., J. J. Zimmerman, J. Hermann, C. R. Johnson, J. P. Cano, W. Yu, S. A. Dee, and M. P. Murtaugh**. 2008. Antigen-specific B-cell responses to porcine reproductive and respiratory syndrome virus infection. J. Virol. **82**:358-370.
159. **Murtaugh, M. P., K. S. Faaberg, J. Laber, M. Elam, and V. Kapur**. 1998. Genetic variation in the PRRS virus. Adv. Exp. Med. Biol. **440**:787-794.
160. **Murtaugh, M. P., Z. Xiao, and F. Zuckermann**. 2002. Immunological responses of swine to porcine reproductive and respiratory syndrome virus infection. Viral. Immunol. **15**:533-547.
161. **Nauwynck, H. J., X. Duan, H. W. Favoreel, P. Van Oostveldt, and M. B. Pensaert**. 1999. Entry of porcine reproductive and respiratory syndrome virus into porcine alveolar macrophages via receptor-mediated endocytosis. J. Gen. Virol. **80**:297-305.
162. **Nelsen, C. J., M. P. Murtaugh, and K. S. Faaberg**. 1999. Porcine reproductive and respiratory syndrome virus comparison: divergent evolution on two continents. J. Virol. **73**:270-280.
163. **Nelson, E. A., J. Christopher-Hennings, and D. A. Benfield**. 1994. Serum immune responses to the proteins of porcine reproductive and respiratory syndrome (PRRS) virus. J. Vet. Diagn. Invest. **6**:410-415.
164. **Nielsen, H. S., G. Liu, J. Nielsen, M. B. Oleksiewicz, A. Botner, T. Storgaard, and K. S. Faaberg**. 2003. Generation of an infectious clone of VR-2332, a highly virulent North American-type isolate of porcine reproductive and respiratory syndrome virus. J. Virol. **77**:3702-3711.
165. **Nielsen, T. L., J. Nielsen, P. Have, P. Baekbo, R. Hoff-Jorgensen, and A. Botner**. 1997. Examination of virus shedding in semen from vaccinated and from previously infected boars after experimental challenge with porcine reproductive and respiratory syndrome virus. Vet. Microbiol. **54**:101-112.

166. **Nomura-Takigawa, Y., M. Nagano-Fujii, L. Deng, S. Kitazawa, S. Ishido, K. Sada, and H. Hotta**. 2006. Non-structural protein 4A of Hepatitis C virus accumulates on mitochondria and renders the cells prone to undergoing mitochondria-mediated apoptosis. J. Gen. Virol. **87**:1935-1945.
167. **Oleksiewicz, M. B., A. Botner, and P. Normann**. 2001. Semen from boars infected with porcine reproductive and respiratory syndrome virus (PRRSV) contains antibodies against structural as well as nonstructural viral proteins. Vet. Microbiol. **81**:109-125.
168. **Oleksiewicz, M. B., A. Botner, P. Toft, P. Normann, and T. Storgaard**. 2001. Epitope mapping porcine reproductive and respiratory syndrome virus by phage display: the nsp2 fragment of the replicase polyprotein contains a cluster of B-cell epitopes. J. Virol. **75**:3277-3290.
169. **Oleksiewicz, M. B., T. Stadejek, Z. Mackiewicz, M. Porowski, and Z. Pejsak**. 2005. Discriminating between serological responses to European-genotype live vaccine and European-genotype field strains of porcine reproductive and respiratory syndrome virus (PRRSV) by peptide ELISA. J. Virol. Methods. **129**:134-144.
170. **Opriessnig, T., R. B. Baker, and P. G. Halbur**. 2007. Use of an experimental model to test the efficacy of planned exposure to live porcine reproductive and respiratory syndrome virus. Clin. Vaccine. Immunol. **14**:1572-1577.
171. **Osorio, F. A., J. A. Galeota, E. Nelson, B. Brodersen, A. Doster, R. Wills, F. Zuckermann, and W. W. Laegreid**. 2002. Passive transfer of virus-specific antibodies confers protection against reproductive failure induced by a virulent strain of porcine reproductive and respiratory syndrome virus and establishes sterilizing immunity. Virology. **302**:9-20.
172. **Ostrowski, M., J. A. Galeota, A. M. Jar, K. B. Platt, F. A. Osorio, and O. J. Lopez**. 2002. Identification of neutralizing and nonneutralizing epitopes in the porcine reproductive and respiratory syndrome virus GP5 ectodomain. J. Virol. **76**:4241-4250.
173. **Otake, S., S. A. Dee, K. D. Rossow, H. S. Joo, J. Deen, T. W. Molitor, and C. Pijoan**. 2002. Transmission of porcine reproductive and respiratory syndrome virus by needles. Vet. Rec. **150**:114-115.
174. **Otake, S., S. A. Dee, K. D. Rossow, R. D. Moon, and C. Pijoan**. 2002. Mechanical transmission of porcine reproductive and respiratory syndrome virus by mosquitoes, Aedes vexans (Meigen). Can. J. Vet. Res. **66**:191-195.
175. **Parks, G. D., J. C. Baker, and A. C. Palmenberg**. 1989. Proteolytic cleavage of encephalomyocarditis virus capsid region substrates by precursors to the 3C enzyme. J. Virol. **63**:1054-1058.
176. **Pasternak, A. O., W. J. Spaan, and E. J. Snijder**. 2004. Regulation of relative abundance of arterivirus subgenomic mRNAs. J. Virol. **78**:8102-8113.
177. **Pasternak, A. O., W. J. Spaan, and E. J. Snijder**. 2006. Nidovirus transcription: how to make sense.? J. Gen. Virol. **87**:1403-1421.
178. **Pattnaik, A. K., L. A. Ball, A. W. LeGrone, and G. W. Wertz**. 1992. Infectious defective interfering particles of VSV from transcripts of a cDNA clone. Cell. **69**:1011-1020.

179. **Pedersen, K. W., Y. van der Meer, N. Roos, and E. J. Snijder**. 1999. Open reading frame 1a-encoded subunits of the arterivirus replicase induce endoplasmic reticulum-derived double-membrane vesicles which carry the viral replication complex. J. Virol. **73**:2016-2026.
180. **Pirzadeh, B., and S. Dea**. 1997. Monoclonal antibodies to the ORF5 product of porcine reproductive and respiratory syndrome virus define linear neutralizing determinants. J. Gen. Virol. **78**:1867-1873.
181. **Pirzadeh, B., C. A. Gagnon, and S. Dea**. 1998. Genomic and antigenic variations of porcine reproductive and respiratory syndrome virus major envelope GP5 glycoprotein. Can. J. Vet. Res. **62**:170-177.
182. **Plagemann, P. G**. 2001. Complexity of the single linear neutralization epitope of the mouse arterivirus lactate dehydrogenase-elevating virus. Virology. **290**:11-20.
183. **Plagemann, P. G**. 2004. The primary GP5 neutralization epitope of North American isolates of porcine reproductive and respiratory syndrome virus. Vet. Immunol. Immunopathol. **102**:263-275.
184. **Plagemann, P. G., R. R. Rowland, and K. S. Faaberg**. 2002. The primary neutralization epitope of porcine respiratory and reproductive syndrome virus strain VR-2332 is located in the middle of the GP5 ectodomain. Arch. Virol. **147**:2327-2347.
185. **Poon, A. P., L. Benetti, and B. Roizman**. 2006. U(S)3 and U(S)3.5 protein kinases of herpes simplex virus 1 differ with respect to their functions in blocking apoptosis and in virion maturation and egress. J. Virol. **80**:3752-3764.
186. **Posthuma, C. C., D. D. Nedialkova, J. C. Zevenhoven-Dobbe, J. H. Blokhuis, A. E. Gorbalenya, and E. J. Snijder**. 2006. Site-directed mutagenesis of the Nidovirus replicative endoribonuclease NendoU exerts pleiotropic effects on the arterivirus life cycle. J. Virol. **80**:1653-1661.
187. **Prentice, E., J. McAuliffe, X. Lu, K. Subbarao, and M. R. Denison**. 2004. Identification and characterization of severe acute respiratory syndrome coronavirus replicase proteins. J. Virol. **78**:9977-9986.
188. **Rao, J. K., J. W. Erickson, and A. Wlodawer**. 1991. Structural and evolutionary relationships between retroviral and eucaryotic aspartic proteinases. Biochemistry. **30**:4663-4671.
189. **Rapp, F**. 1964. Plaque differentiation and replication of virulent and attenuated strains of measles virus. J. Bacteriol. **88**:1448-1458.
190. **Ratia, K., K. S. Saikatendu, B. D. Santarsiero, N. Barretto, S. C. Baker, R. C. Stevens, and A. D. Mesecar**. 2006. Severe acute respiratory syndrome coronavirus papain-like protease: structure of a viral deubiquitinating enzyme. Proc. Natl. Acad. Sci. U S A. **103**:5717-5722.
191. **Rikkonen, M., J. Peranen, and L. Kaariainen**. 1994. ATPase and GTPase activities associated with Semliki Forest virus nonstructural protein nsP2. J. Virol. **68**:5804-5810.
192. **Ropp, S. L., C. E. Wees, Y. Fang, E. A. Nelson, K. D. Rossow, M. Bien, B. Arndt, S. Preszler, P. Steen, J. Christopher-Hennings, J. E. Collins, D. A. Benfield, and K. S. Faaberg**. 2004. Characterization of emerging European-like

porcine reproductive and respiratory syndrome virus isolates in the United States. J. Virol. **78**:3684-3703.
193. **Rossow, K. D**. 1998. Porcine reproductive and respiratory syndrome. Vet. Pathol. **35**:1-20.
194. **Rost, B., P. Fariselli, and R. Casadio**. 1996. Topology prediction for helical transmembrane proteins at 86% accuracy. Protein. Sci. **5**:1704-1718.
195. **Rost, B., and J. Liu**. 2003. The PredictProtein server. Nucleic. Acids. Res. **31**:3300-3304.
196. **Roth-Cross, J. K., L. Martinez-Sobrido, E. P. Scott, A. Garcia-Sastre, and S. R. Weiss**. 2007. Inhibition of the alpha/beta interferon response by mouse hepatitis virus at multiple levels. J. Virol. **81**:7189-7199.
197. **Rowland, R. R., R. Kervin, C. Kuckleburg, A. Sperlich, and D. A. Benfield**. 1999. The localization of porcine reproductive and respiratory syndrome virus nucleocapsid protein to the nucleolus of infected cells and identification of a potential nucleolar localization signal sequence. Virus. Res. **64**:1-12.
198. **Rowland, R. R., S. Lawson, K. Rossow, and D. A. Benfield**. 2003. Lymphoid tissue tropism of porcine reproductive and respiratory syndrome virus replication during persistent infection of pigs originally exposed to virus in utero. Vet. Microbiol. **96**:219-235.
199. **Ryan, M. D., and M. Flint**. 1997. Virus-encoded proteinases of the picornavirus super-group. J. Gen. Virol. **78**:699-723.
200. **Ryan, M. D., S. Monaghan, and M. Flint**. 1998. Virus-encoded proteinases of the Flaviviridae. J. Gen. Virol. **79**:947-959.
201. **Sawicki, D. L., and S. G. Sawicki**. 1993. A second nonstructural protein functions in the regulation of alphavirus negative-strand RNA synthesis. J. Virol. **67**:3605-3610.
202. **Sawicki, D. L., and S. G. Sawicki**. 1994. Alphavirus positive and negative strand RNA synthesis and the role of polyproteins in formation of viral replication complexes. Arch. Virol. Suppl. **9**:393-405.
203. **Scortti, M., C. Prieto, E. Alvarez, I. Simarro, and J. M. Castro**. 2007. Failure of an inactivated vaccine against porcine reproductive and respiratory syndrome to protect gilts against a heterologous challenge with PRRSV. Vet. Rec. **161**:809-813.
204. **Scortti, M., C. Prieto, I. Simarro, and J. M. Castro**. 2006. Reproductive performance of gilts following vaccination and subsequent heterologous challenge with European strains of porcine reproductive and respiratory syndrome virus. Theriogenology. **66**:1884-1893.
205. **Seybert, A., C. C. Posthuma, L. C. van Dinten, E. J. Snijder, A. E. Gorbalenya, and J. Ziebuhr**. 2005. A complex zinc finger controls the enzymatic activities of nidovirus helicases. J. Virol. **79**:696-704.
206. **Shen, S., J. Kwang, W. Liu, and D. X. Liu**. 2000. Determination of the complete nucleotide sequence of a vaccine strain of porcine reproductive and respiratory syndrome virus and identification of the Nsp2 gene with a unique insertion. Arch. Virol. **145**:871-883.

207. **Shirako, Y., and J. H. Strauss**. 1990. Cleavage between nsP1 and nsP2 initiates the processing pathway of Sindbis virus nonstructural polyprotein P123. Virology. **177**:54-64.
208. **Snijder, E. J., and J. J. Meulenberg**. 1998. The molecular biology of arteriviruses. J. Gen. Virol. **79**:961-979.
209. **Snijder, E. J., H. van Tol, N. Roos, and K. W. Pedersen**. 2001. Non-structural proteins 2 and 3 interact to modify host cell membranes during the formation of the arterivirus replication complex. J. Gen. Virol. **82**:985-994.
210. **Snijder, E. J., A. L. Wassenaar, and W. J. Spaan**. 1992. The 5' end of the equine arteritis virus replicase gene encodes a papainlike cysteine protease. J. Virol. **66**:7040-7048.
211. **Snijder, E. J., A. L. Wassenaar, and W. J. Spaan**. 1993. Proteolytic processing of the N-terminal region of the equine arteritis virus replicase. Adv. Exp. Med. Biol. **342**:227-232.
212. **Snijder, E. J., A. L. Wassenaar, and W. J. Spaan**. 1994. Proteolytic processing of the replicase ORF1a protein of equine arteritis virus. J. Virol. **68**:5755-5764.
213. **Snijder, E. J., A. L. Wassenaar, W. J. Spaan, and A. E. Gorbalenya**. 1995. The arterivirus Nsp2 protease. An unusual cysteine protease with primary structure similarities to both papain-like and chymotrypsin-like proteases. J. Biol. Chem. **270**:16671-16676.
214. **Snijder, E. J., A. L. Wassenaar, L. C. van Dinten, W. J. Spaan, and A. E. Gorbalenya**. 1996. The arterivirus nsp4 protease is the prototype of a novel group of chymotrypsin-like enzymes, the 3C-like serine proteases. J. Biol. Chem. **271**:4864-4871.
215. **Sur, J. H., A. R. Doster, J. S. Christian, J. A. Galeota, R. W. Wills, J. J. Zimmerman, and F. A. Osorio**. 1997. Porcine reproductive and respiratory syndrome virus replicates in testicular germ cells, alters spermatogenesis, and induces germ cell death by apoptosis. J. Virol. **71**:9170-9179.
216. **Takkinen, K**. 1986. Complete nucleotide sequence of the nonstructural protein genes of Semliki Forest virus. Nucleic. Acids. Res. **14**:5667-5682.
217. **Takkinen, K., J. Peranen, and L. Kaariainen**. 1991. Proteolytic processing of Semliki Forest virus-specific non-structural polyprotein. J. Gen. Virol. **72**:1627-1633.
218. **Takkinen, K., J. Peranen, S. Keranen, H. Soderlund, and L. Kaariainen**. 1990. The Semliki-Forest-virus-specific nonstructural protein nsP4 is an autoproteinase. Eur. J. Biochem. **189**:33-38.
219. **Tanji, Y., M. Hijikata, S. Satoh, T. Kaneko, and K. Shimotohno**. 1995. Hepatitis C virus-encoded nonstructural protein NS4A has versatile functions in viral protein processing. J. Virol. **69**:1575-1581.
220. **ten Dam, E., M. Flint, and M. D. Ryan**. 1999. Virus-encoded proteinases of the Togaviridae. J. Gen. Virol. **80**:1879-1888.
221. **Thompson, J. D., T. J. Gibson, F. Plewniak, F. Jeanmougin, and D. G. Higgins**. 1997. The CLUSTAL_X windows interface: flexible strategies for multiple sequence alignment aided by quality analysis tools. Nucleic. Acids. Res. **25**:4876-4882.

222. **Tian, K., X. Yu, T. Zhao, Y. Feng, Z. Cao, C. Wang, Y. Hu, X. Chen, D. Hu, X. Tian, D. Liu, S. Zhang, X. Deng, Y. Ding, L. Yang, Y. Zhang, H. Xiao, M. Qiao, B. Wang, L. Hou, X. Wang, X. Yang, L. Kang, M. Sun, P. Jin, S. Wang, Y. Kitamura, J. Yan, and G. F. Gao**. 2007. Emergence of fatal PRRSV variants: unparalleled outbreaks of atypical PRRS in China and molecular dissection of the unique hallmark. PLoS. ONE. **2**:e526.
223. **Tomei, L., C. Failla, R. L. Vitale, E. Bianchi, and R. De Francesco**. 1996. A central hydrophobic domain of the hepatitis C virus NS4A protein is necessary and sufficient for the activation of the NS3 protease. J. Gen. Virol. **77**:1065-1070.
224. **Tong, G. Z., Y. J. Zhou, X. F. Hao, Z. J. Tian, T. Q. An, and H. J. Qiu**. 2007. Highly pathogenic porcine reproductive and respiratory syndrome, China. Emerg. Infect. Dis. **13**:1434-1436.
225. **Torremorell, M., C. Pijoan, K. Janni, R. Walker, and H. S. Joo**. 1997. Airborne transmission of Actinobacillus pleuropneumoniae and porcine reproductive and respiratory syndrome virus in nursery pigs. Am. J. Vet. Res. **58**:828-832.
226. **Toyoda, H., M. J. Nicklin, M. G. Murray, C. W. Anderson, J. J. Dunn, F. W. Studier, and E. Wimmer**. 1986. A second virus-encoded proteinase involved in proteolytic processing of poliovirus polyprotein. Cell. **45**:761-770.
227. **van Aken, D., J. Zevenhoven-Dobbe, A. E. Gorbalenya, and E. J. Snijder**. 2006. Proteolytic maturation of replicase polyprotein pp1a by the nsp4 main proteinase is essential for equine arteritis virus replication and includes internal cleavage of nsp7. J. Gen. Virol. **87**:3473-3482.
228. **Van Den Born, E., A. P. Gultyaev, and E. J. Snijder**. 2004. Secondary structure and function of the 5'-proximal region of the equine arteritis virus RNA genome. RNA. **10**:424-437.
229. **van den Born, E., C. C. Posthuma, A. P. Gultyaev, and E. J. Snijder**. 2005. Discontinuous subgenomic RNA synthesis in arteriviruses is guided by an RNA hairpin structure located in the genomic leader region. J. Virol. **79**:6312-6324.
230. **van der Linden, I. F., E. M. van der Linde-Bril, J. J. Voermans, P. A. van Rijn, J. M. Pol, R. Martin, and P. J. Steverink**. 2003. Oral transmission of porcine reproductive and respiratory syndrome virus by muscle of experimentally infected pigs. Vet. Microbiol. **97**:45-54.
231. **van der Meer, Y., E. J. Snijder, J. C. Dobbe, S. Schleich, M. R. Denison, W. J. Spaan, and J. K. Locker**. 1999. Localization of mouse hepatitis virus nonstructural proteins and RNA synthesis indicates a role for late endosomes in viral replication. J. Virol. **73**:7641-7657.
232. **van der Meer, Y., H. van Tol, J. K. Locker, and E. J. Snijder**. 1998. ORF1a-encoded replicase subunits are involved in the membrane association of the arterivirus replication complex. J. Virol. **72**:6689-6698.
233. **van Dinten, L. C., S. Rensen, A. E. Gorbalenya, and E. J. Snijder**. 1999. Proteolytic processing of the open reading frame 1b-encoded part of arterivirus replicase is mediated by nsp4 serine protease and Is essential for virus replication. J. Virol. **73**:2027-2037.
234. **van Dinten, L. C., A. L. Wassenaar, A. E. Gorbalenya, W. J. Spaan, and E. J. Snijder**. 1996. Processing of the equine arteritis virus replicase ORF1b protein:

identification of cleavage products containing the putative viral polymerase and helicase domains. J. Virol. **70**:6625-6633.

235. **van Nieuwstadt, A. P., J. J. Meulenberg, A. van Essen-Zanbergen, A. Petersen-den Besten, R. J. Bende, R. J. Moormann, and G. Wensvoort**. 1996. Proteins encoded by open reading frames 3 and 4 of the genome of Lelystad virus (Arteriviridae) are structural proteins of the virion. J. Virol. **70**:4767-4772.
236. **Van Reeth, K., G. Labarque, H. Nauwynck, and M. Pensaert**. 1999. Differential production of proinflammatory cytokines in the pig lung during different respiratory virus infections: correlations with pathogenicity. Res. Vet. Sci. **67**:47-52.
237. **Van Reeth, K., S. Van Gucht, and M. Pensaert**. 2002. In vivo studies on cytokine involvement during acute viral respiratory disease of swine: troublesome but rewarding. Vet. Immunol. Immunopathol. **87**:161-168.
238. **van Vugt, J. J., T. Storgaard, M. B. Oleksiewicz, and A. Botner**. 2001. High frequency RNA recombination in porcine reproductive and respiratory syndrome virus occurs preferentially between parental sequences with high similarity. J. Gen. Virol. **82**:2615-2620.
239. **Vanderheijden, N., P. Delputte, H. Nauwynck, and M. Pensaert**. 2001. Effects of heparin on the entry of porcine reproductive and respiratory syndrome virus into alveolar macrophages. Adv. Exp. Med. Biol. **494**:683-689.
240. **Vanderheijden, N., P. L. Delputte, H. W. Favoreel, J. Vandekerckhove, J. Van Damme, P. A. van Woensel, and H. J. Nauwynck**. 2003. Involvement of sialoadhesin in entry of porcine reproductive and respiratory syndrome virus into porcine alveolar macrophages. J. Virol. **77**:8207-8215.
241. **Verheije, M. H., R. C. Olsthoorn, M. V. Kroese, P. J. Rottier, and J. J. Meulenberg**. 2002. Kissing interaction between 3' noncoding and coding sequences is essential for porcine arterivirus RNA replication. J. Virol. **76**:1521-1526.
242. **Vieira, J., and J. Messing**. 1991. New pUC-derived cloning vectors with different selectable markers and DNA replication origins. Gene. **100**:189-194.
243. **Wagstrom, E. A., C. C. Chang, K. J. Yoon, and J. J. Zimmerman**. 2001. Shedding of porcine reproductive and respiratory syndrome virus in mammary gland secretions of sows. Am. J. Vet. Res. **62**:1876-1880.
244. **Wang, Y. F., S. G. Sawicki, and D. L. Sawicki**. 1994. Alphavirus nsP3 functions to form replication complexes transcribing negative-strand RNA. J. Virol. **68**:6466-6475.
245. **Wassenaar, A. L., W. J. Spaan, A. E. Gorbalenya, and E. J. Snijder**. 1997. Alternative proteolytic processing of the arterivirus replicase ORF1a polyprotein: evidence that NSP2 acts as a cofactor for the NSP4 serine protease. J. Virol. **71**:9313-9322.
246. **Welch, S. K., R. Jolie, D. S. Pearce, W. D. Koertje, E. Fuog, S. L. Shields, D. Yoo, and J. G. Calvert**. 2004. Construction and evaluation of genetically engineered replication-defective porcine reproductive and respiratory syndrome virus vaccine candidates. Vet. Immunol. Immunopathol. **102**:277-290.
247. **Wensvoort, G**. 1993. Lelystad virus and the porcine epidemic abortion and respiratory syndrome. Vet. Res. **24**:117-124.

248. **Wensvoort, G., E. P. de Kluyver, J. M. Pol, F. Wagenaar, R. J. Moormann, M. M. Hulst, R. Bloemraad, A. den Besten, T. Zetstra, and C. Terpstra**. 1992. Lelystad virus, the cause of porcine epidemic abortion and respiratory syndrome: a review of mystery swine disease research at Lelystad. Vet. Microbiol. **33**:185-193.
249. **Wensvoort, G., C. Terpstra, J. M. Pol, E. A. ter Laak, M. Bloemraad, E. P. de Kluyver, C. Kragten, L. van Buiten, A. den Besten, F. Wagenaar, and a. et**. 1991. Mystery swine disease in The Netherlands: the isolation of Lelystad virus. Vet. Q. **13**:121-130.
250. **Wesley, R. D., W. L. Mengeling, K. M. Lager, D. F. Clouser, J. G. Landgraf, and M. L. Frey**. 1998. Differentiation of a porcine reproductive and respiratory syndrome virus vaccine strain from North American field strains by restriction fragment length polymorphism analysis of ORF 5. J. Vet. Diagn. Invest. **10**:140-144.
251. **Wieringa, R., A. A. De Vries, S. M. Post, and P. J. Rottier**. 2003. Intra- and intermolecular disulfide bonds of the GP2b glycoprotein of equine arteritis virus: relevance for virus assembly and infectivity. J. Virol. **77**:12996-13004.
252. **Wieringa, R., A. A. de Vries, and P. J. Rottier**. 2003. Formation of disulfide-linked complexes between the three minor envelope glycoproteins (GP2b, GP3, and GP4) of equine arteritis virus. J. Virol. **77**:6216-6226.
253. **Wieringa, R., A. A. de Vries, J. van der Meulen, G. J. Godeke, J. J. Onderwater, H. van Tol, H. K. Koerten, A. M. Mommaas, E. J. Snijder, and P. J. Rottier**. 2004. Structural protein requirements in equine arteritis virus assembly. J. Virol. **78**:13019-13027.
254. **Wills, R. W., A. R. Doster, J. A. Galeota, J. H. Sur, and F. A. Osorio**. 2003. Duration of infection and proportion of pigs persistently infected with porcine reproductive and respiratory syndrome virus. J. Clin. Microbiol. **41**:58-62.
255. **Wills, R. W., J. J. Zimmerman, K. J. Yoon, S. L. Swenson, L. J. Hoffman, M. J. McGinley, H. T. Hill, and K. B. Platt**. 1997. Porcine reproductive and respiratory syndrome virus: routes of excretion. Vet. Microbiol. **57**:69-81.
256. **Wills, R. W., J. J. Zimmerman, K. J. Yoon, S. L. Swenson, M. J. McGinley, H. T. Hill, K. B. Platt, J. Christopher-Hennings, and E. A. Nelson**. 1997. Porcine reproductive and respiratory syndrome virus: a persistent infection. Vet. Microbiol. **55**:231-240.
257. **Wissink, E. H., M. V. Kroese, H. A. van Wijk, F. A. Rijsewijk, J. J. Meulenberg, and P. J. Rottier**. 2005. Envelope protein requirements for the assembly of infectious virions of porcine reproductive and respiratory syndrome virus. J. Virol. **79**:12495-12506.
258. **Wissink, E. H., H. A. van Wijk, M. V. Kroese, E. Weiland, J. J. Meulenberg, P. J. Rottier, and P. A. van Rijn**. 2003. The major envelope protein, GP5, of a European porcine reproductive and respiratory syndrome virus contains a neutralization epitope in its N-terminal ectodomain. J. Gen. Virol. **84**:1535-1543.
259. **Wu, W. H., Y. Fang, R. Farwell, M. Steffen-Bien, R. R. Rowland, J. Christopher-Hennings, and E. A. Nelson**. 2001. A 10-kDa structural protein of porcine reproductive and respiratory syndrome virus encoded by ORF2b. Virology. **287**:183-191.

260. **Wu, W. H., Y. Fang, R. R. Rowland, S. R. Lawson, J. Christopher-Hennings, K. J. Yoon, and E. A. Nelson**. 2005. The 2b protein as a minor structural component of PRRSV. Virus. Res. **114**:177-181.
261. **Yan, Y., X. Guo, X. Ge, Y. Chen, Z. Cha, and H. Yang**. 2007. Monoclonal antibody and porcine antisera recognized B-cell epitopes of Nsp2 protein of a Chinese strain of porcine reproductive and respiratory syndrome virus. Virus. Res. **126**:207-215.
262. **Yang, L., M. L. Frey, K. J. Yoon, J. J. Zimmerman, and K. B. Platt**. 2000. Categorization of North American porcine reproductive and respiratory syndrome viruses: epitopic profiles of the N, M, GP5 and GP3 proteins and susceptibility to neutralization. Arch. Virol. **145**:1599-1619.
263. **Yoo, D., S. K. Welch, C. Lee, and J. G. Calvert**. 2004. Infectious cDNA clones of porcine reproductive and respiratory syndrome virus and their potential as vaccine vectors. Vet. Immunol. Immunopathol. **102**:143-154.
264. **Yoon, I. J., H. S. Joo, W. T. Christianson, H. S. Kim, J. E. Collins, J. H. Carlson, and S. A. Dee**. 1992. Isolation of a cytopathic virus from weak pigs on farms with a history of swine infertility and respiratory syndrome. J. Vet. Diagn. Invest. **4**:139-143.
265. **Yoon, I. J., H. S. Joo, S. M. Goyal, and T. W. Molitor**. 1994. A modified serum neutralization test for the detection of antibody to porcine reproductive and respiratory syndrome virus in swine sera. J. Vet. Diagn. Invest. **6**:289-292.
266. **Yoon, K. J., J. J. Zimmerman, S. L. Swenson, M. J. McGinley, K. A. Eernisse, A. Brevik, L. L. Rhinehart, M. L. Frey, H. T. Hill, and K. B. Platt**. 1995. Characterization of the humoral immune response to porcine reproductive and respiratory syndrome (PRRS) virus infection. J. Vet. Diagn. Invest. **7**:305-312.
267. **Ypma-Wong, M. F., P. G. Dewalt, V. H. Johnson, J. G. Lamb, and B. L. Semler**. 1988. Protein 3CD is the major poliovirus proteinase responsible for cleavage of the P1 capsid precursor. Virology. **166**:265-270.
268. **Ypma-Wong, M. F., and B. L. Semler**. 1987. In vitro molecular genetics as a tool for determining the differential cleavage specificities of the poliovirus 3C proteinase. Nucleic. Acids. Res. **15**:2069-2088.
269. **Yu, S. F., P. Benton, M. Bovee, J. Sessions, and R. E. Lloyd**. 1995. Defective RNA replication by poliovirus mutants deficient in 2A protease cleavage activity. J. Virol. **69**:247-252.
270. **Yu, S. F., and R. E. Lloyd**. 1991. Identification of essential amino acid residues in the functional activity of poliovirus 2A protease. Virology. **182**:615-625.
271. **Yuan, S., D. Mickelson, M. P. Murtaugh, and K. S. Faaberg**. 2001. Complete genome comparison of porcine reproductive and respiratory syndrome virus parental and attenuated strains. Virus. Res. **79**:189-200.
272. **Yuan, S., M. P. Murtaugh, and K. S. Faaberg**. 2000. Heteroclite subgenomic RNAs are produced in porcine reproductive and respiratory syndrome virus infection. Virology. **275**:158-169.
273. **Yuan, S., M. P. Murtaugh, F. A. Schumann, D. Mickelson, and K. S. Faaberg**. 2004. Characterization of heteroclite subgenomic RNAs associated with PRRSV infection. Virus. Res. **105**:75-87.

274. **Yuan, S., C. J. Nelsen, M. P. Murtaugh, B. J. Schmitt, and K. S. Faaberg**. 1999. Recombination between North American strains of porcine reproductive and respiratory syndrome virus. Virus. Res. **61**:87-98.
275. **Zhou, Y. J., X. F. Hao, Z. J. Tian, G. Z. Tong, D. Yoo, T. Q. An, T. Zhou, G. X. Li, H. J. Qiu, T. C. Wei, and X. F. Yuan**. 2008. Highly virulent porcine reproductive and respiratory syndrome virus emerged in China. Transbound. Emerg. Dis. **55**:152-164.
276. **Ziebuhr, J**. 2005. The coronavirus replicase. Curr. Top. Microbiol. Immunol. **287**:57-94.
277. **Ziebuhr, J., E. J. Snijder, and A. E. Gorbalenya**. 2000. Virus-encoded proteinases and proteolytic processing in the Nidovirales. J. Gen. Virol. **81**:853-879.
278. **Zimmerman, J. J., K. J. Yoon, E. C. Pirtle, R. W. Wills, T. J. Sanderson, and M. J. McGinley**. 1997. Studies of porcine reproductive and respiratory syndrome (PRRS) virus infection in avian species. Vet. Microbiol. **55**:329-336.